NUREG/CR-4164
EGG-2377
November 1985

Data Report for the TPFL Tee/Critical Flow Experiments

James L. Anderson
William A. Owca

F O R M A L R E P O R T

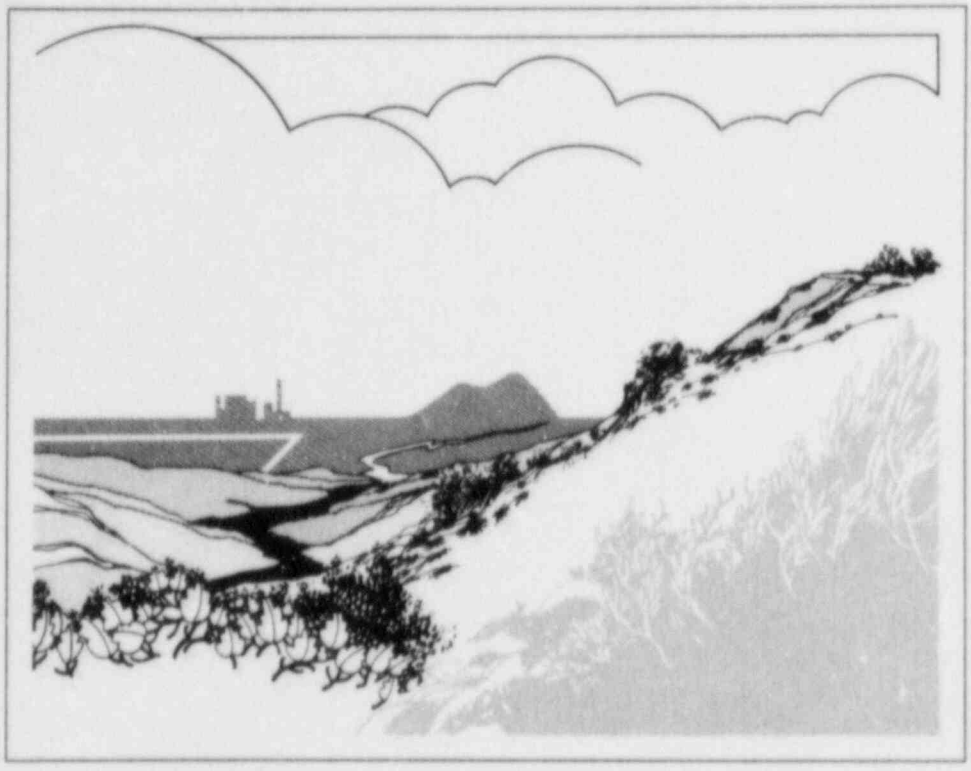

EG&G Idaho

Work performed under DOE Contract No. DE-AC07-76ID01570

for the ***U.S. Nuclear Regulatory Commission***

Idaho National Engineering Laboratory

Managed by the U.S. Department of Energy

Available from

Superintendent of Documents
U.S. Government Printing Office
Post Office Box 37082
Washington, D.C. 20013-7982

and

National Technical Information Service
Springfield, VA 22161

NUREG/CR-4164
EGG-2377
Distribution Category: R2

DATA REPORT FOR THE TPFL TEE/CRITICAL FLOW EXPERIMENTS

James L. Anderson
William A. Owca

Published November 1985

EG&G Idaho, Inc.
Idaho Falls, Idaho 83415

Prepared for the
Division of Accident Evaluation
Office of Nuclear Regulatory Research
U.S. Nuclear Regulatory Commission
Washington, D.C. 20555
Under DOE Contract No. DE-AC07-76IDO1570
FIN No. A6320
and the
Electric Power Research Institute
Under Contract No. RP2299-2

ABSTRACT

A series of experiments have been performed investigating the phenomena of liquid entrainment and vapor pull-through at a tee junction between a horizontal pipe and a small branchline. These experiments were performed under conditions of stratified steam-water flow at 3.4, 4.4, and 6.2 MPa in the 28.4 cm diameter mainline, and critical flow through a nozzle installed in the branchline. Two orientations of the branchline were investigated: horizontal and vertical downflow. This report documents the experimental program, presents the data obtained, and discusses correlations for predicting the levels at which the onset of vapor pull-through and liquid entrainment occur and correlations for predicting the flow quality into the branchline.

SUMMARY

The tee/critical flow experiments[a] were performed in the Two-Phase Flow Loop (TPFL) at the Idaho National Engineering Laboratory (INEL) during the summer of 1984 to investigate the liquid entrainment/vapor pull-through phenomena of a tee with a large mainline-to-branchline diameter ratio, and how these phenomena affect the flow rate in the branchline. Vapor pull-through is a phenomena that occurs when the liquid level is located above the entrance to the branchline and vapor is pulled through from the vapor space above the interface. The pull-through may be accomplished via vortex or vortex-free flow. The liquid entrainment phenomena can occur when the liquid interface level is below the branchline entrance. If the level is high enough, a liquid film in the vicinity of the branchline may flow up to the entrance or, if the vapor velocity in the mainline is large enough, liquid may be entrained from roll waves and carried into the branchline.

The importance of the liquid entrainment/vapor pull-through phenomena, and its effect upon the critical flow rate in the branchline, originates in the concerns of a postulated small break loss of coolant accident (SBLOCA) in a pressurized water reactor (PWR). This type of accident could originate from the rupture of an instrument line or a safety injection line. Although the system conditions are scenario dependent, an expected condition is two-phase natural circulation with resulting low flow rates and a stratified flow of steam and water in horizontal main loop piping. If this stratified condition exists in the vicinity of the broken line, then the existence of the liquid entrainment/vapor pull-through phenomena completely changes the break flow rate in comparison to a single phase flow, thus changing the characteristics of the system transient response thereafter.

The critical flow rate at a break is a function of the two-phase flow quality at the break. This flow quality is, in turn, a function of the liquid entrainment/vapor pull-through rates from the mainline into the branchline. Since the depressurization rate of a PWR system during a SBLOCA, in addition to the total system inventory, is dependent upon the critical break flow rate, the ability to accurately predict entrainment/pull-through rates and timing are important in order for nuclear safety codes to predict system response with acceptable accuracy.

The primary objective of the experimental program was to obtain the flow quality of the steam-water mixture out the branchline of a tee containing high-pressure steam-water stratified flow in the mainline, as a function of the height of the stratified liquid interface level in the mainline. Measurement of the flow quality and total branch flow rate enables evaluation of the rates of liquid entrainment/vapor pull-through. A secondary objective was measurement of the critical flow rate as a function of flow quality in the branchline. These experiments were performed with the branchline in horizontal and vertical downflow orientations (with a 28.4 cm diameter mainline and a 3.4 cm diameter branchline) under conditions of stratified steam-water mixtures at 3.4, 4.4, and 6.2 MPa in the mainline. A nozzle was installed in the branchline to provide a known choking point, thus the emphasis on critical flow. The primary variable was the stratified liquid height in the mainline and its effect upon the flow quality and mass flow rate in the branchline.

Data was acquired for each branchline orientation at each of the three test pressures. A total of 91 test points were obtained, covering a broad range of liquid levels in the mainline. Most of the horizontal test configuration points were transient points in which the level slowly varied from some maximum level to the equilibrium stratified level (determined by the individual flow rates). Many of these points spanned the level range of the onset of vapor pull-through.

Most of the vertical downflow data points are steady-state runs. The mainline liquid level was obtained by adjusting the mainline liquid flow rate while maintaining a constant steam flow rate of 3 kg/s, with the separator level below the mainline. Two to six transient test runs were performed at each pressure for determination of the maximum level at which continuous vapor pull-through occurs.

Results from these experiments confirm the forms of previously proposed correlations for predicting the mainline liquid levels at which vapor pull-through and liquid entrainment occur. However, different values for the constants used in the

a. This report documents the results of an experimental program mutually funded by the U.S. Nuclear Regulatory Commission (Fin. No. A6320) and the Electric Power Research Institute (Contract No. RP2299-2).

correlations are recommended. The data show that the liquid level range over which vapor pull-through and liquid entrainment occur is greater than previously reported.

For the horizontal branchline, it was observed that the mass flow rate into the branchline was a linear function of the mainline liquid level (at a constant mainline pressure); however, the slope of this function changed at a level corresponding to the top of the branchline, possibly indicating that the vapor pull-through phenomena results in different fluid properties in the branchline than does the liquid entrainment phenomena. Another interpretation of this slope change involves the fact that the higher levels were obtained by reducing the mainline steam flow rate. The different steam flow rates may have resulted in different wave patterns in the mainline, thus resulting in different amounts of time-averaged vapor pull-through. Comparison of the branchline void fraction, as a function of the mainline liquid level, for the three test pressures shows equal void fractions for a level corresponding to the top of the mainline. This indicates that the best origin of a coordinate system for predicting the branchline void fraction may be the top of the branchline rather than the pipe bottom or centerline.

Flow quality data presented for the horizontal branchline indicate that the branchline flow quality is an exponential function of the mainline liquid level. A correlation for the flow quality is presented and compared to the data and the only other previously reported correlation for the branchline flow quality. Results from this new correlation are used to predict the branchline void fraction, which compares well to the data.

The data obtained for the horizontal branchline, in which the mainline liquid continually changed during a test run (a transient run), compares quite well to the steady-state data obtained for constant level portions of test runs (comparison is within the tolerance limits of the transient data). This indicates that steady-state data may be used for predicting branchline properties for transient cases in which the level is slowly falling.

For the case of the vertical downflow branchline, the branchline mass flow rate at levels below the onset of vapor pull-through appears to be a linear function of the mainline liquid level. The level at which continuous vapor pull-through begins was observed to occur at about a 50% higher level than that predicted by the correlation developed from previous experiments. This fact is reflected in the recommended new constants for the correlation used to predict the onset level of vapor pull-through in the vertical downflow branchline orientation. An anomaly observed for this configuration was that all steam flow out the branchline occurred when a small nonzero level existed in the mainline upstream of the branchline. This phenomena may have been due to an error in the level measurement or may be due to an effect of vorticity for the steam flow into the branchline, forcing the liquid away from the branchline entrance resulting in the liquid being carried down the mainline. This type of phenomena has been reported[8] for the case of liquid entrainment in a vertical upflow orientation using air/water flows.

The branchline flow quality for the vertical downflow orientation was observed to follow the same type of exponential relationship as was observed for the horizontal orientation. A correlation for predicting the branchline flow quality is proposed and compares favorably to the data. This correlation was used to predict the branchline void fraction which, when compared to the data, compares quite well except at low void fractions (less than 25%).

Further experimental work which could be performed to expand the data base on this subject investigates the effect of having the critical flow orifice located at the pipe wall as opposed to downstream in the branchline. This will help to determine possible evaporation effects at the branchline entrance. Another area that needs to be addressed is the possible vorticity effects for small liquid levels in the mainline with the vertical downflow branchline. Whether this is a real phenomena or an artifact of the measurement system also needs to be resolved.

This report documents the experimental program and the data obtained from the program. The report details the experimental and measurements systems, describes the test conduct and data reduction methods, and presents a detailed uncertainty analysis of the measured and computed parameters. Flow qualities, mass flow rates, void fractions, and pressure drops in the branchline are presented as functions of the mainline stratified liquid level. The data is presented in both graphical and tabular forms. Correlations for predicting the liquid levels for the onset of vapor pull-through and liquid entrainment and the resulting branchline flow quality for all liquid levels between onset of vapor pull-through and the onset of liquid entrainment are also presented.

ACKNOWLEDGMENTS

The authors wish to express their appreciation to Carolee Kearns for the long hours spent in processing and plotting of the data for this report. Additionally, we wish to express our appreciation to the operations staff of the Two-Phase Flow Loop, without whom this experimental program would not have been possible.

CONTENTS

DATA REPORT FOR THE TPFL TEE/CRITICAL FLOW EXPERIMENTS

INTRODUCTION

The tee/critical flow experiments[a] were performed during the summer of 1984 in the Two-Phase Flow Loop (TPFL) at the Idaho National Engineering Laboratory (INEL). These experiments investigated the liquid entrainment/vapor pull-through phenomena of a tee with a large mainline-to-branchline diameter ratio, and how these phenomena affect the flow rate of a two-phase flow into the branchline. The experiments were performed to extend the existing data base on entrainment/pull-through phenomena at a tee (developed exclusively using air and water flows) to include high-pressure saturated steam and water as the working fluids. In addition, the experiments were performed in significantly larger piping sizes to assure scalability of the phenomena to postulated conditions in a nuclear reactor during a small break loss of coolant accident (SBLOCA). Extensive measurements were performed in the mainline and branchline to determine the two-phase conditions including flow rates, flow qualities, and void fractions. The experiments were performed with a 28.4 cm (11.2 in.) diameter mainline (14 in. schedule 160 pipe). A stratified steam-water mixture at 3.4, 4.4, and 6.2 MPa (500, 640, and 900 psia) was established in the mainline. A 1.619 cm (0.6374 in.) nozzle was installed in the 3.4 cm (1.388 in.) branchline to provide a known choking point. The principal experimental variable was the stratified liquid height in the mainline and its effect upon the flow quality and mass flow rate in the branchline. Two sets of experiments were performed with the branchline oriented differently for each experimental set. Branchline orientations were horizontal and vertical downflow. Data from these experiments will be used for development/assessment of codes for predicting the thermal-hydraulic behavior of nuclear reactors during SBLOCAS. This report presents selected data from the experimental program. The entire data set is available on digital magnetic tapes.

a. This report documents the results of an experimental program mutually funded by the U.S. Nuclear Regulatory Commission (Fin. No. A6320) and the Electric Power Research Institute (Contract No. RP2299-2).

Background

The importance of the liquid entrainment/vapor pull-through phenomena and its effect upon the critical flow rate originates in the concerns of a postulated SBLOCA in a pressurized water reactor. This type of accident could result from the rupture of an instrument line or a safety injection line. Although the system conditions are scenario dependent, an expected condition is two-phase natural circulation, with its resulting low flow rates, and a stratified flow condition in the horizontal main loop piping. If this stratified condition exists in the vicinity of the broken line, then the existence of the liquid entrainment/vapor pull-through phenomena would completely change the break flow rate compared to single phase flow, and thus change the characteristics of the system transient response thereafter. These phenomena are illustrated in Figure 1. The case shown is for a horizontal branchline, although the branchline could be on the top or bottom of the mainline. Vapor pull-through is a phenomena which occurs when the liquid level is above the entrance to the branchline and vapor is pulled through the liquid from the vapor space above the interface. The liquid entrainment phenomena can occur when the liquid interface level is below the branchline entrance. If the level is high enough, a liquid film in the vicinity of the branchline may flow up to the entrance or, if the vapor velocity in the mainline is large enough, liquid may be entrained from roll waves and carried into the branchline.

In the case of a broken branchline, the flow at the entrance from the mainline may be critical if the line was sheared off, or subcritical if the branchline was only partially fractured somewhere downstream. In either case, the critical flow rate at the break is a function of two-phase flow quality. This flow quality is, in turn, a function of the liquid entrainment/vapor pull-through rates from the mainline into the branchline. Since the depressurization rate of a pressurized water reactor (PWR) system under a SBLOCA, in addition to the total system inventory, is dependent upon the critical break flow rate, the ability to accurately predict

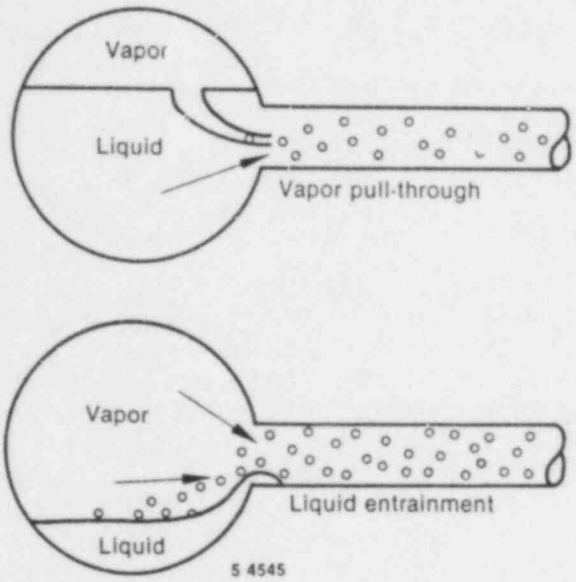

Figure 1. Pictorial view of the vapor pull-through and liquid entrainment phenomena.

entrainment/pull-through rates and timing are important for the nuclear safety codes to predict system response with an acceptable accuracy.

An example of the predictive problems associated with this type of phenomena is provided by a comparison of integral systems experiment code predictions with the Loss-of-Fluid Test facility (LOFT) L3-5 experimental results.[1] This was an experiment which simulated a 10.2 cm diameter break in the cold leg of a PWR. During the period of interest, coolant in the cold leg at the broken line branch was in stratified flow with the liquid level slowly dropping. Figure 2 shows the measured break mass flow rate and system pressure in comparison to predictions of both RELAP5 and TRAC.[2] Both codes significantly overpredicted the critical flow and depressurization rates. The overprediction of the broken line mass flow rate is due to the assumption in the codes that only single-phase flow exists at the break when the mainline liquid level is above (all liquid flow) or below (all steam flow) the branchline entrance. If the level is above the broken line and vapor pull-through occurs, then the actual critical mass flow rate out the break would be greatly reduced.

The TPFL was originally designed and built as a calibration facility[3] for LOFT instrumentation. As such, it was constructed of LOFT size piping (14 in. Schedule 160) to handle steam-water flows at pressures as high as 6.9 MPa (1000 psia). It was decided that for the tee/critical flow experiments a mockup of the LOFT L3-5 tee geometry would be used, including the same size of break nozzle. The reasons for this were two-fold. First, the equipment for this experiment already existed from a previous experimental program.[4] Secondly, data from the tee/critical flow experiments could be used in a direct comparison to the LOFT L3-5 data and an evaluation of the improvement in code predictions resulting from use of the correlations developed as part of this program could be performed.

Experimental Objectives

The objective of this effort was to develop a reliable and accurate experimental data base for critical flow through small breaks in a pipe in which stratified two-phase flow is prevalent. Recent experiments with air-water mixture in small pipes have indicated that liquid entrainment and vapor pull-through significantly influence discharge rates, and that these phenomena are functions of stratified level and break azimuthal location. The objectives of this experimental project were to obtain accurate data on critical discharge rates (steam and water) as functions of break orientation and stratified level. The specific objectives were:

- Establish an experimental data base on critical flow through small breaks for two different break orientations, namely, bottom and side locations.
- Establish a data base relating discharge rates to stratified level and thermal-hydraulic conditions in the mainline.
- Establish an experimentally measured data base relating the discharge rate and level in the mainline to the conditions in the branchline.

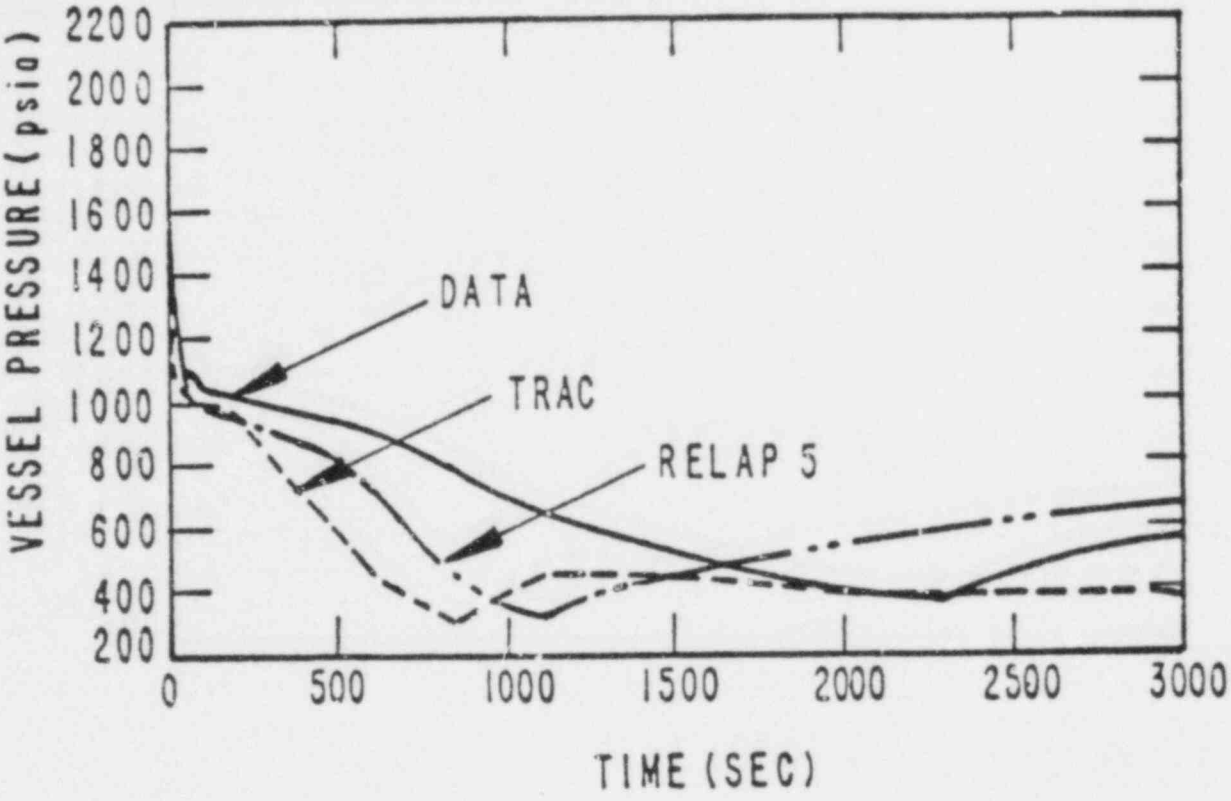

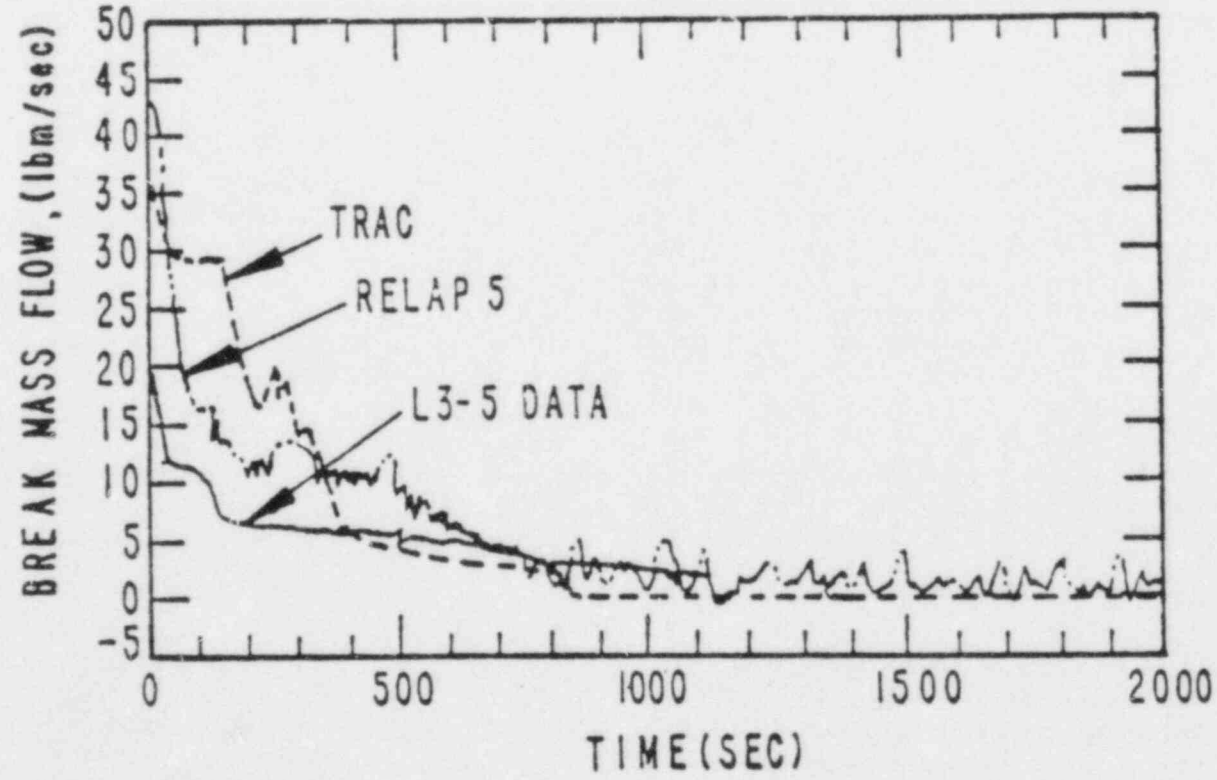

Figure 2. Comparison of calculated and measured behavior for LOFT Test L3-5/L3-5A.

TECHNICAL ASPECTS

In the following sections the technical aspects of the liquid entrainment/vapor pull-through phenomena will be discussed. The discussion includes a summary of previous research on the phenomena, and correlations which have been developed for prediction of the liquid levels at which onset of the entrainment/pull-through phenomena occurs.

Previous Research

The entrainment/pull-through phenomena and its impact on SBLOCA was discussed by Zuber,[5] along with a review and summary of existing experimental work and correlations. At that time no directly applicable experimental work had been performed on the entrainment/pull-through phenomena in horizontal pipes. However, Zuber modified the existing correlations (which had been developed from data obtained from experiments in tanks) for use in the piping configurations of interest in SBLOCA analysis. These correlations predicted the stratified liquid levels between which entrainment or pull-through would occur. No correlations existed for the amount of pull-through or entrainment. Subsequently, entrainment and vapor pull-through were studied by Crowley and Rothe[6] for low pressure air-water stratified flows. They obtained branchline flow rate data for the horizontal, vertical upflow, and vertical downflow configurations in a 7.6 cm mainline pipe along with the effect of a short nozzle as opposed to an orifice at the pipe wall. The Crowley and Rothe data for the liquid levels at which liquid entrainment and vapor pull-through first occur compare favorably (within 10-25%) with predictions from the correlations proposed by Zuber. No data was presented for the branchline void fraction or flow quality as functions of the mainline liquid level.

The vapor pull-through phenomena was also studied by Reimann and Khan[7] for the case of a downflow orientation with stratified air-water flow in a 20.6 cm (8.1 in.) mainline and three different branchline diameters of 0.6, 1.2, and 2.0 cm. These same pipe sizes were used by Reimann and Smoglie[8] to study liquid entrainment from a vertical upflow branch orientation, with a stratified flow in the mainline. Smoglie[25] also studied the entrainment/pull-through phenomena for the horizontal branchline configuration and performed an extensive comparison and analysis of the data from the three branchline orientations. Smoglie concluded that the forms of the correlations proposed by Zuber were correct, but obtained different values for the constants in the correlations. In addition, no effect of branchline diameter on the correlations was determined. Smoglie also presented new correlations for the branchline flow quality as a function of the mainline liquid level.

Saba and Lahey[9] studied the phase separation phenomena of a tee with a horizontal branchline. They were not predominately interested in entrainment/pull-through and reported no observations of the onset of these phenomena; instead, they developed a set of five two-phase conservation equations to describe the flow rates and pressure drops in the tee. These experiments were performed in small diameter pipe with air-water flow.

In all previous research performed on the entrainment/pull-through phenomena, neither the working fluids nor the test section scale has been representative of the expected conditions during a SBLOCA in a PWR. The current experimental program was undertaken to extend the experimental data base to representative fluids (steam/water at pressures anticipated to occur during a SBLOCA) at a significantly larger scale than previous experiments.

Liquid Entrainment

The data of Crowley and Rothe confirmed the correlation for onset of entrainment, derived by Craya, for two incompressible fluids of different densities (Reference 10), and previously verified experimentally by Gariel for liquid withdrawal from a large reservoir (Reference 11). The Craya correlation modified by Zuber for a horizontal piping orientation with a side entry branch is given by,

$$\left[\frac{V_g^2 \rho_g}{g(\rho_f - \rho_g)(D/2 - h_e)}\right]^{1/2} = 3.25\left(\frac{D/2 - h_e}{d}\right)^2 \quad (1)$$

where

V_g = the gas velocity out the branch (m/s)

ρ_g, ρ_f = the phase densities (kg/m^3)

g = gravitational acceleration (equal to 9.8 m/s^2)

D = the mainline inner diameter (m)

d = the branchline inner diameter (m)

h_e = the liquid interface height measured from the pipe bottom at which liquid entrainment begins (m).

Equation (1) can be solved for the interface level h_e/D, and the dependency on branch diameter eliminated by using the gas flow rate, $\dot{m}_g$, resulting in

$$\frac{h_e}{D} = \frac{1}{2} - \frac{1}{D}\left[\frac{\dot{m}_g^2}{6.52\, g\, \rho_g\, (\rho_f - \rho_g)}\right]^{0.2} \quad . \qquad (2)$$

For the steam/water test conditions at 6.2 MPa, Equation (2) results in an entrainment criteria of

$$\frac{h_e}{D} = 0.25 \quad .$$

For the case of a vertical upflow branch orientation, Zuber recommended a modification of a correlation developed by Rouse[12] for liquid entrainment from a tank through a vertical pipe. The correlation is given by

$$\left[\frac{V_g^2\, g}{g\,(\rho_f - \rho_g)\,(D - h_{ve})}\right]^{1/2} = 5.7\left(\frac{D - h_{ve}}{d}\right)^{3/2} \qquad (3)$$

where h_{ve} is the liquid level above which entrainment begins, and all other variables are as defined for Equation (1). Equation (3) can be solved for the onset of liquid entrainment interface level, giving

$$\frac{h_{ve}}{D} = 1 - \frac{1}{D}\left[\frac{\dot{m}_g^2}{20\, g\, d\, \rho_g\, (\rho_f - \rho_g)}\right]^{1/4} \quad . \qquad (4)$$

For the test conditions at 6.2 MPa, Equation (4) results in an interface level for onset of entrainment in a vertical upflow orientation of

$$\frac{h_{ve}}{D} = 0.77 \quad .$$

Vapor Pull-Through

For the case of vapor pull-through, Zuber recommended use of a modification of the correlation developed by Lubin and Hurwitz[13] for draining from the bottom of a tank in vortex free flow. For a vertical downflow branchline, this modified correlation can be written as

$$\left[\frac{V_l^2\, \rho_f}{g\,(\rho_f - \rho_g)\, d}\right]^{1/2} = 3.25\left(\frac{h_{vp}}{d}\right)^{5/2} \qquad (5)$$

where $h_{vp}/d > 1$. Solving Equation (5) for h_{vp}/D (and using the liquid mass flow rate, $\dot{m}_f$, to eliminate the branchline diameter dependency) results in

$$\frac{h_{vp}}{D} = \frac{1}{D}\left[\frac{\dot{m}_f^2}{6.52\, g\, \rho_f\, (\rho_f - \rho_g)}\right]^{0.2} \quad . \qquad (6)$$

Equation (6) can be modified for the case of a horizontal branchline by adding the height of the branch ($h_{vp}/D = 0.5$), giving,

$$\frac{h_p}{D} = \frac{1}{2} + \frac{1}{D}\left[\frac{\dot{m}_f^2}{6.52\, g\, \rho_f\, (\rho_f - \rho_g)}\right]^{0.2} \quad . \qquad (7)$$

For the test conditions at 6.2 MPa, Equation (6) results in a value of $h_{vp}/D = 0.21$ for onset of pull-through in the vertical downflow orientation. For the horizontal orientation, Equation (7) results in $h_p/D = 0.71$.

SYSTEM CONFIGURATION AND INSTRUMENTATION

This section presents the system hardware and measurements used during the tee/critical flow experiments.

Experimental Hardware

The tee/critical flow experiments were performed in the two-phase flow loop (TPFL) at the Thermal Hydraulics Laboratory at the INEL. The facility was configured as shown in Figure 3. Appendix A contains all significant engineering drawings of the facility and test sections. The lengths, areas, and volumes of various system components are provided in Table 1 as an aid in modeling the experimental system.

Inlet steam and water flow rates were measured and controlled using the 5 and 7 cm (2 and 3 in.) reference measurements sections. The reference flow measurements were made using calibrated orifices. Flow control valves were located downstream of the metering sections immediately upstream of the mixing tee. A stratifier insert for the mixing tee was installed to help promote a stable stratified flow in the mainline. The mainline was a 28.4 cm (14 in.), schedule 160, 2-piece piping section between the mixing tee and the steam separator. The critical flow section (branchline) teed off the 28.4 cm (14 in.) mainline at the 12 cm (5 in.) penetration. The critical flow measurements section is shown in Figures 4 and 5 for each of two configurations. Details of the break nozzle are shown in Figure 6.

The branchline terminated at the break flow catch tank, which was used to determine the total break mass flow rate. The catch tank measurement system, shown in Figures 7 and 8, consisted of a sparger injection system and a 5.6 m^3 (1500 gal) cylindrical tank suspended by two load cells. The sparger system was connected to the rigidly supported branchline and suspended at the centerline of the catch tank. A flexible nonload sharing coupling connected the catch tank to the branchline.

The sparger assembly consisted of a 6.6 m (20 ft) section of 10.2 cm (4-in) schedule 40 pipe connected at its center to the branchline. Fifty jet-type nozzles were attached to either side of the 10.2 cm (4-in.) pipe. The nozzles produced violent mixing in the catch tank under flow conditions. Prior to performing data points, the catch tank was filled with cold (296 K, 55°F) industrial water to a level above the sparger assembly. The hot two-phase mixture flowing through the branchline/sparger assembly, during a data point, was condensed by the cold liquid initially in the catch tank. The load cells were used to determine the total mass of liquid in the tank that was differentiated to determine the total break mass flow rate. The steam separator connected to the mainline provided a method of separating the two-phase flow mixture into single phase components. The liquid component was pumped back into the liquid metering section and the steam component was vented to the atmosphere through an exhaust flow orifice meter and a pressure control valve used to control system pressure.

Measurements

A list of all measurements recorded during the tee/critical flow experiments is shown in Table 2. This list consists of measurements of temperature, pressure, differential pressure, density, and mass used to calculate mass flow rates, liquid levels, void fractions, and flow qualities. The measurements list summarizes the measurements in groups made at similar locations in the system. System reference measurements included pressures and temperatures upstream of reference orifices, differential pressures across the orifices, and a differential pressure for loop liquid level. Mainline test section measurements include fluid temperatures, pressures, differential pressures from inlet to outlet, densities, and a differential pressure from top to bottom of the mainline which was used to calculate a liquid level. Branchline measurements include fluid temperatures, pressures, differential pressures across the break orifice and branchline tee, densities, and mass of fluid collected in the catch tank. Test support measurements included liquid levels, metal temperatures, and heat fluxes. The types of measurements made throughout the system are shown in a piping and instrument diagram (P&ID) (see Figure 9). The reported measurement locations and identifiers are shown on P&IDs for the reference measurements in Figure 10 and for the test section measurements in Figure 11.

Video probes were installed in the mainline, upstream of the branchline entrance, and in the branchline, upstream of the critical flow nozzle, for

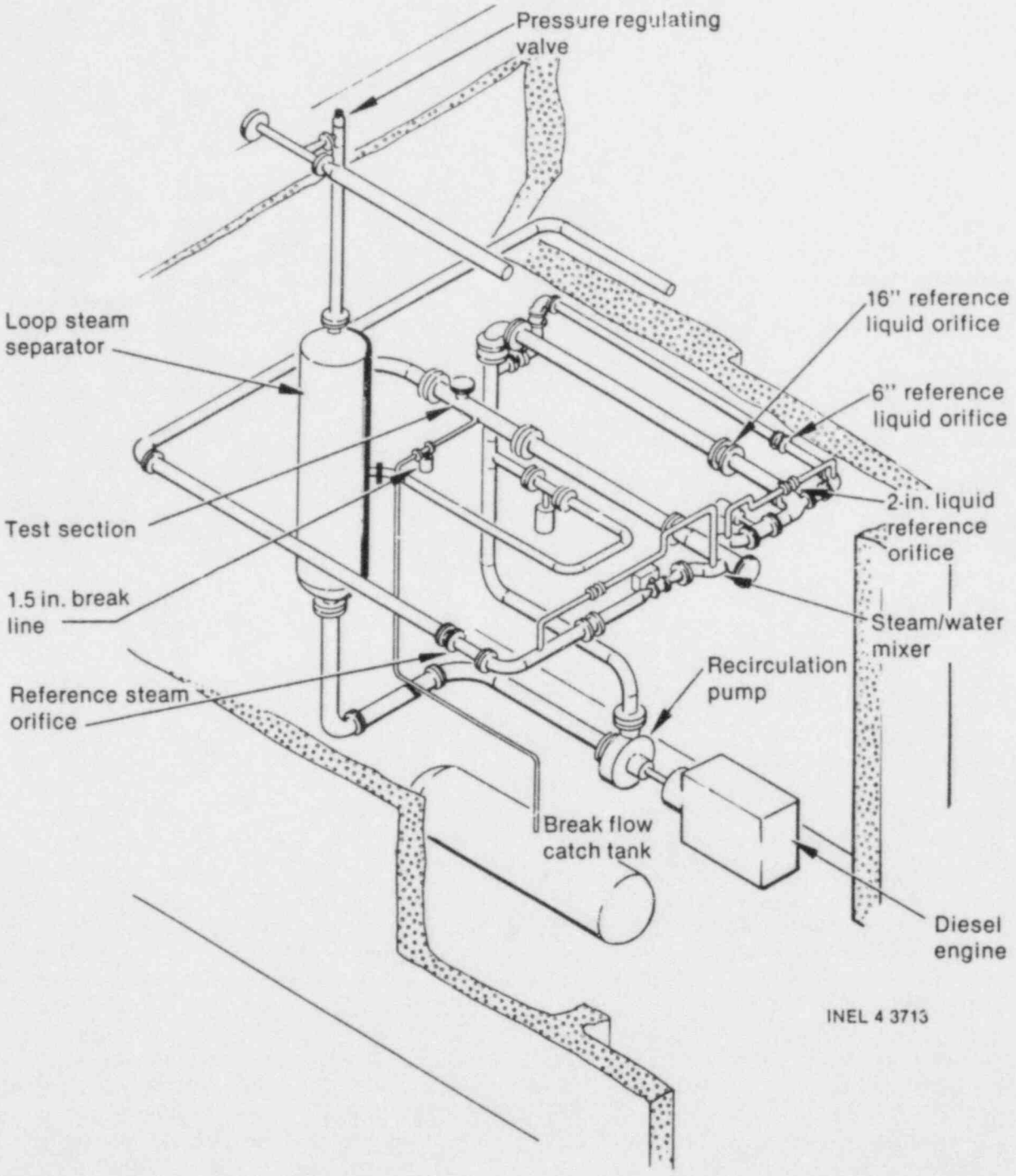

Figure 3. Two phase flow loop as configured for the tee/critical flow experiments.

Table 1. Component lengths, areas, and volumes

Component	Area (m^2)	Length (m)	Volume (m^3)
Mainline—from mixer outlet to branchline	0.0633	5.2	0.33
Mainline—from branchline to loop separator tank	0.0633	2.7	0.17
Branchline—from mainline to beginning of horizontal section (around the elbow)			
Horizontal configuration	9.07E-4	0.297	2.70E-4
Vertical downflow configuration	9.07E-4	0.943	8.56E-4
Branchline—horizontal section to critical flow nozzle	9.07E-4	1.63	1.48E-3
Branchline—critical flow nozzle	2.06E-4	0.054	1.11E-5
Branchline—from nozzle to break valve	3.49E-4	0.86	3.0E-3
Separator tank—bottom to centerline of mainline	1.92	4.7	8.69
Separator tank—centerline of mainline to top (including hemispherical head)	1.92	2.2	4.01
Discharge line—from top of separator tank to measurement orifice	0.0463	1.9	0.088
Discharge line—from orifice to pressure regulating valve	0.0463	1.2	0.056

observation of the flow fields. Videotape was recorded from the video probe output for many of the data points. Unfortunately, the field of view from the probes was limited and the observations are of limited use. These observations will be discussed in the sections on data presentation.

Measurements Uncertainties. The usefulness of data is a direct function of how accurate the data is and how well that accuracy (or, inversely, the uncertainty) is known. In this section, the uncertainties for the basic measurements (temperatures, pressures, differential pressures, and load cells) will be presented. These uncertainties are obtained from a series of uncertainty documents generated by the Water Reactor Research Test Programs (WRRTP) (References 20, 21, 22, 23) primarily to document uncertainties for the Semiscale program. The International Standards Organization's (ISO) draft standard, "Fluid Flow Measurement Uncertainty" (ISO TC30 SC 9), is the basis of the method used in the WRRTP documents. In addition to the basic measurement uncertainties, the uncertainties in all calculated parameters (such as mass flow rates calculated from an orifice) are presented. The method used for combining individual uncertainties for calculated parameters is the root-sum-square (RSS) method originally proposed by Kline and McClintock.[24] All quoted uncertainties are at the 95% confidence level. Derivation of these uncertainties is presented in Appendix J.

The basic measurements are considered to be temperatures, pressures, differential pressures (DP's), and load cells. Quoted uncertainties are from the transducer through the data system and include all uncertainties introduced by the transducer calibration, signal conditioning, and the data

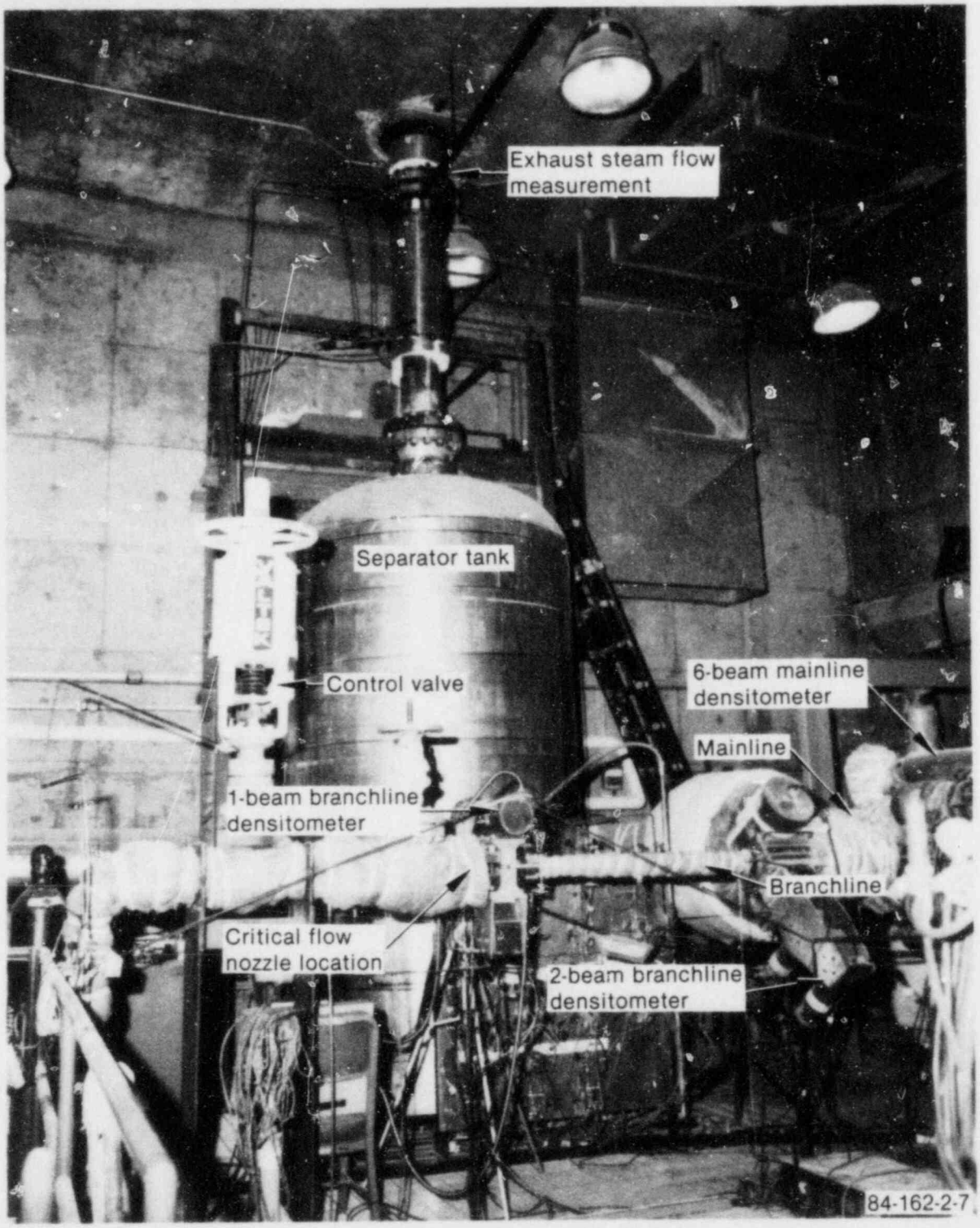

Figure 4. Photograph of the horizontal configuration piping.

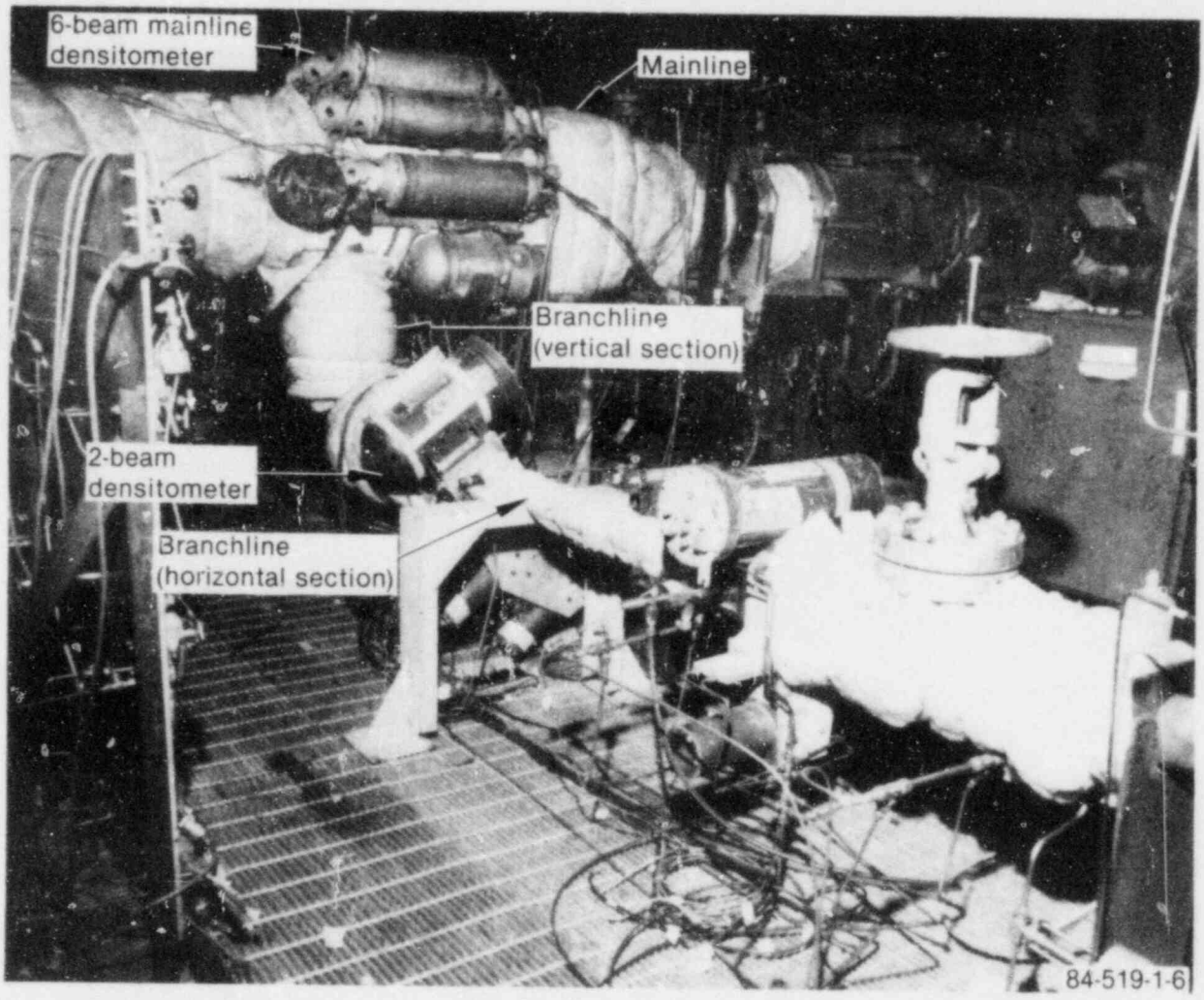

Figure 5. Photograph of the vertical downflow configuration.

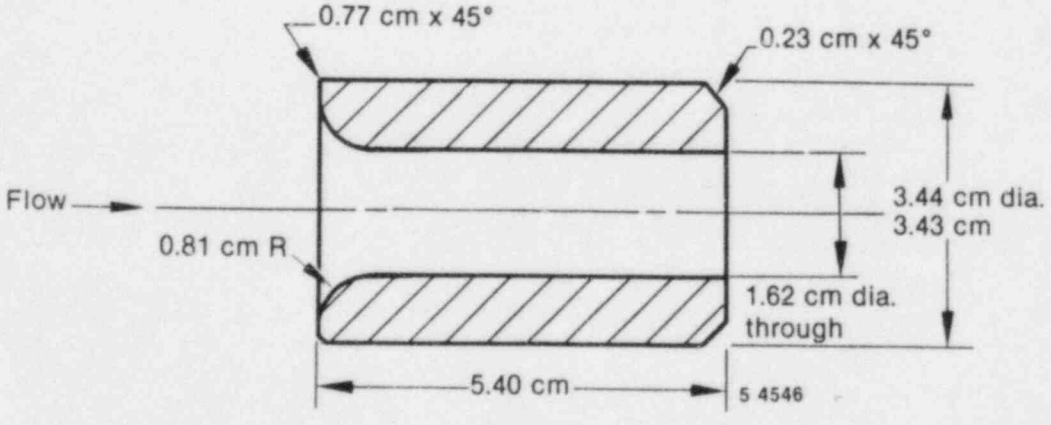

Figure 6. Drawing of the critical flow nozzle.

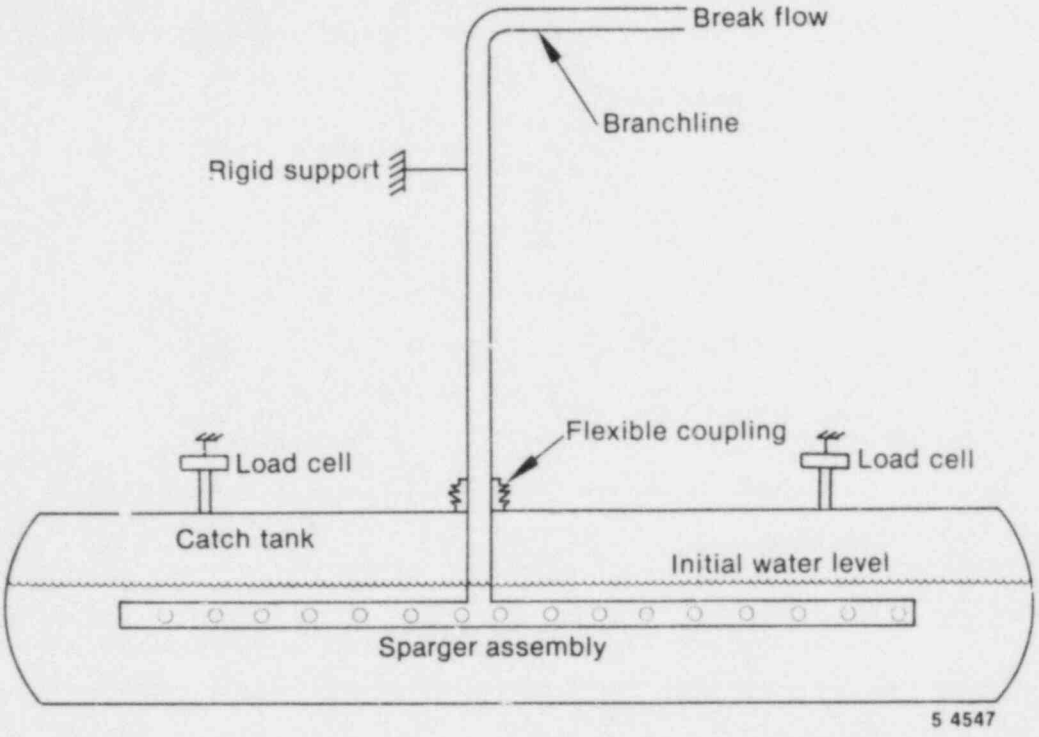

Figure 7. Schematic of the catch tank—sparger system and connection to the branchline.

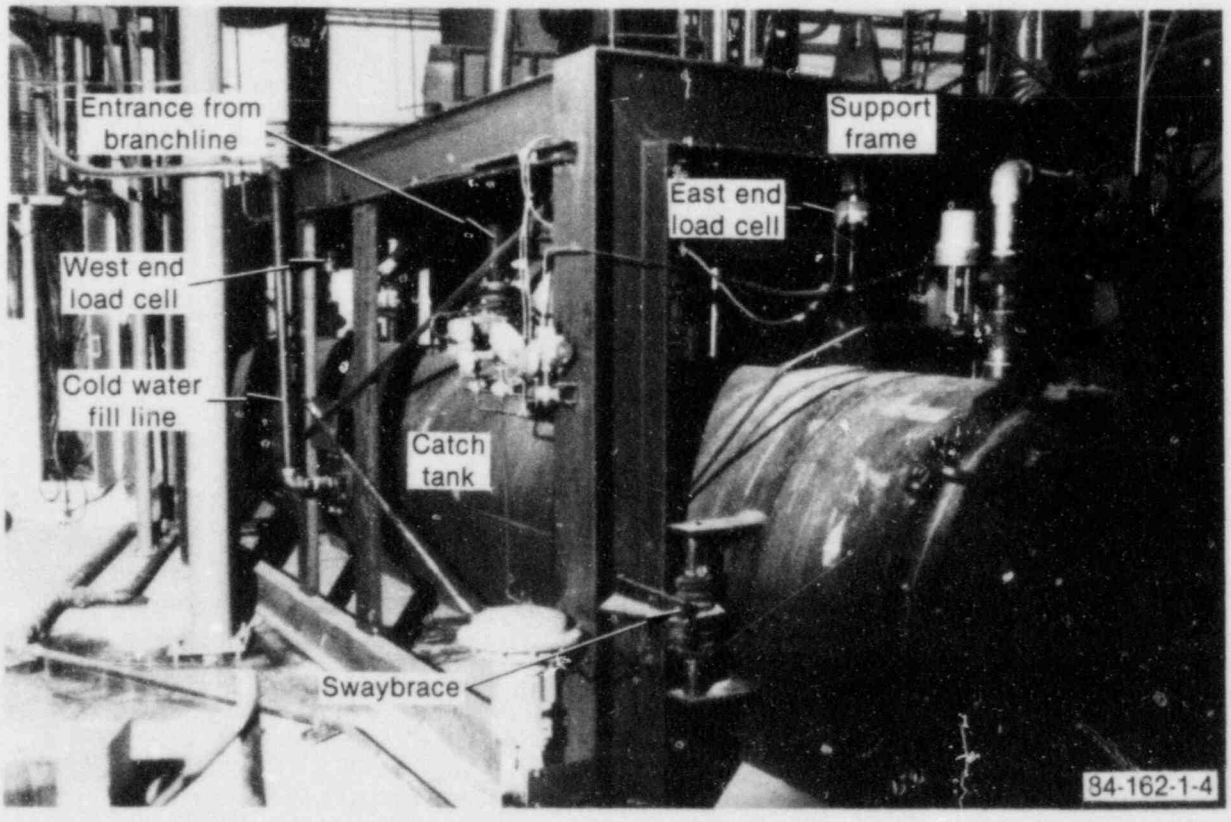

Figure 8. Photograph of the catch tank assembly.

Table 2. Measurements list for two phase flow loop tee/critical flow experiments

Measurement ID	Description	Measurement Range
	REFERENCE MEASUREMENTS	
TE-46S	Fluid temperature upstream of 30 cm reference steam orifice (side mounted)	300-585 K
TE-58S	Fluid temperature upstream of 7 cm reference steam orifice (side mounted)	300-585 K
TE-202	Fluid temperature at steam inlet to mixing tee	300-585 K
TE-106	Fluid temperature upstream of liquid orifice (5 cm reference metering section)	300-585 K
TE-201	Fluid temperature at liquid inlet to mixing tee	300-585 K
TE-FE-63	Fluid temperature at exit of steam separator (upstream of discharge orifice)	300-585 K
TE-MU	Fluid temperature at makeup inlet to steam separator	300-585 K
PT-58	Pressure upstream of 7 cm reference steam orifice	0-10.5 MPa
PE-100	Pressure at steam inlet to mixing tee	0-10.5 MPa
PT-106	Pressure upstream of 5 cm reference liquid orifice	0-6.89 MPa
PE-101	Pressure at liquid inlet to mixing tee	0-6.89 MPa
PE-505	Pressure at exit of steam separator (upstream of discharge orifice)	0-6.89 MPa
FT-58A	Differential pressure across 7 cm reference steam orifice (low range)	0-12.5 kPa
FT-58B	Differential pressure across 7 cm reference steam orifice (high range)	0-172 kPa
FT-106A	Differential pressure across 5 cm reference liquid orifice (low range)	0-12.5 kPa
FT-106B	Differential pressure across 5 cm reference liquid orifice (high range)	0-172 kPa
PDE-100	Differential pressure across steam side of mixing tee (from inlet to mainline)	0-345 kPa
PDE-101	Differential pressure across liquid side of mixing tee (from inlet to mainline)	0-345 kPa

Table 2. (continued)

Measurement ID	Description	Measurement Range
	REFERENCE MEASUREMENTS (continued)	
PDE-500	Differential pressure across discharge reference orifice in steam separator exit line (low range)	0-24.8 kPa
PDE-510	Differential pressure across discharge reference orifice in steam separator exit line (high range)	0-125 kPa
LT-62	Liquid level in upper section of steam separator tank (mainline centerline at LT-62 = 33 cm)	0-366 cm
FT-MUP	Flow turbine in loop make-up line	0.3-3 L/S
	MAINLINE TEST SECTION MEASUREMENTS	
TE-300	Fluid temperature at outlet of mixing tee (3 cm from top)	300-585 K
TE-301	Fluid temperature at entrance to branchline (3 cm from top of mainline)	300-585 K
TE-305	Fluid temperature 0.7 m downstream of branchline in mainline—3 cm from bottom	300-585 K
PE-301	Pressure at outlet of mixing tee in mainline	0-7.0 MPa
PE-302	Pressure at the branchline entrance in the mainline	0-7.0 MPa
PE-305	Pressure in mainline 1 m downstream of branchline	0-17.2 MPa
PDE-310	Differential pressure in mainline from mixer outlet to 2.5 m upstream of branchline	0-25 kPa
PDE-311	Differential pressure in mainline from PDE-310 to 1 m upstream of branchline	0-25 kPa
PDE-312	Differential pressure in mainline from 1 m upstream of branchline to branchline entrance	0-25 kPa
PDE-330	Liquid level in mainline 0.5 m upstream of branchline	0-77 cm
DE-BL-1A	3-beam densitometer at outlet of mixing tee (mainline)—top beam	0-1000 kg/m^3
DE-BL-1B	3-beam densitometer at outlet of mixing tee (mainline)—middle beam	0-1000 kg/m^3
DE-BL-1C	3-beam densitometer at outlet of mixing tee (mainline)—bottom beam	0-1000 kg/m^3

Table 2. (continued)

Measurement ID	Description	Measurement Range
	MAINLINE TEST SECTION MEASUREMENTS (continued)	
DE-1A	6-beam densitometer 0.4 m upstream of branchline entrance—top beam of lower quadrant	0-1000 kg/m^3
DE-1B	6-beam densitometer 0.4 m upstream of branchline entrance—middle beam of lower quadrant	0-1000 kg/m^3
DE-1C	6-beam densitometer 0.4 m upstream of branchline entrance—bottom beam of lower quadrant	0-1000 kg/m^3
DE-2A	6-beam densitometer 0.4 m upstream of branchline entrance—bottom beam of upper quadrant	0-1000 kg/m^3
DE-2B	6-beam densitometer 0.4 m upstream of branchline entrance—middle beam of upper quadrant	0-1000 kg/m^3
DE-2C	6-beam densitometer 0.4 m upstream of branchline entrance—top beam of upper quadrant	0-1000 kg/m^3
	BRANCHLINE TEST SECTION MEASUREMENT	
TE-401	Fluid temperature at inlet of branchline (on centerline)	300-585 K
TE-402	Fluid temperature horizontal piping upstream of critical flow orifice	300-585 K
TE-CTE-1	Fluid temperatures in east end of catch tank—located 45 cm below tank centerline	300-585 K
TE-CTE-2	Fluid temperatures in east end of catch tank—located 22 cm below tank centerline	300-585 K
TE-CTE-3	Fluid temperatures in east end of catch tank—located on tank centerline	300-585 K
TE-CTE-4	Fluid temperatures in east end of catch tank—located 22 cm above tank centerline	300-585 K
TE-CTE-5	Fluid temperatures in east end of catch tank—located 45 cm above tank centerline	300-585 K
TE-CTW-1	Fluid temperature in west end of catch tank—located 22 cm below tank centerline	300-585 K
PE-401	Pressure at inlet of branchline horizontal piping section	0-6.89 MPa
PE-402	Pressure 20 cm upstream of critical flow orifice	0-6.89 MPa

Table 2. (continued)

Measurement ID	Description	Measurement Range
	BRANCHLINE TEST SECTION MEASUREMENTS (continued)	
PE-CT-1	Pressure in catch tank	0-1 MPa
PDE-341	Differential pressure from mainline at the branchline entrance to upstream side of critical flow orifice	0-200 kPa
PDE-450	Differential pressure across critical flow orifice	0-6.89 MPa
DE-3A	Two beam densitometer at inlet to branchline horizontal piping—bottom beam	0-1000 kg/m^3
DE-3B	Two beam densitometer at inlet to branchline horizontal piping—top beam	0-1000 kg/m^3
DE-1-1	Single beam densitometer 30 cm upstream of critical flow orifice (vertical diametrical beam)	0-1000 kg/m^3
LD-LC-1	Catch tank weight (load cell—east end)	0-5000 kg
LD-LC-2	Catch tank weight (load cell—west end)	0-5000 kg
	TEST SUPPORT MEASUREMENTS	
LT-10	Liquid level—Steam Tank No. 1 (process transmitter)	12.5 kPa
LT-18	Liquid level—Steam Tank No. 2 (process transmitter)	12.5 kPa
LT-26	Liquid level—Steam Tank No. 3 (process transmitter)	12.5 kPa
LT-34	Liquid level—Steam Tank No. 4 (process transmitter)	18.7 kPa
LT-30	Experimental liquid level Steam Tank No. 3	—
LT-60	Liquid level—lower section of loop steam separator (process transmitter)	0-742 cm
PE-1	Pressure—Steam Tank No. 1	0-17.24 MPa
PE-2	Pressure—Steam Tank No. 2	0-17.24 MPa
PE-3	Pressure—Steam Tank No. 3	0-17.24 MPa
PE-4	Pressure—Steam Tank No. 4	0-17.24 MPa
TE-14	Temperature—Steam Tank No. 1	300-585 K
TE-22	Temperature—Steam Tank No. 2	300-585 K

Table 2. (continued)

Measurement ID	Description	Measurement Range
	TEST SUPPORT MEASUREMENTS (continued)	
TE-33	Temperature—Steam Tank No. 3	300-585 K
TE-37	Temperature—Steam Tank No. 4	300-585 K
TE-Beam	Tube temperature—densitometer Beam DE-2B	300-585 K
TE-NTC	Temperature north test cell platform	300-585 K
TE-Air	Ambient temperature at differential pressure measurement PDE-330	300-585 K
TE-MT-1	Metal temperature—steam separator inlet	300-585 K
HF-INS	Heat flux—outside of insulation on top	0-10,000 W/M^2
HF-SS	Heat flux—on insulation on steam separator wall, 1 ft above inlet	0-10,000 W/M^2
TE-SS	Surface temperature at HF-SS measurement	300-585 K

NOTE: One optical probe with two light sources was installed upstream of the branchline entrance in the mainline. A second optical probe with two light sources was installed in the branchline upstream of the break orifice.

system. A summary of the basic uncertainties is provided in Table 3. The measurement uncertainty in the fluid temperatures (using type K thermocouples) is considered to be ±2.2 K.[21]

Uncertainties in the pressure and differential pressure measurements are quoted[22] in terms of a percentage of full scale. For the absolute pressure transducer, this value is 0.29% of full scale. For the DP measurements, the value is 0.57% of full scale and does not include the possible effects of a partially voided sense line (which is assumed was corrected for prior to the test point or post-test using the no-flow data averages). For the load cell measurements, the quoted[23] uncertainty is 0.24% of full scale.

Calculated parameters are those parameters which have their basis in one or more basic measurements. Examples are thermodynamic properties (phase densities and enthalpies) and mass flow rates calculated from the measurements at an orifice. The method used in the root-sum-square method is given by

$$\Delta R = \left[\sum_{i=1}^{N} \left(\frac{\partial R}{\partial V_i} \Delta V_i\right)^2\right]^{1/2} \quad (8)$$

where

R = the calculated result

V_i = i^{th} independent variable

$\Delta R, \Delta Vi$ = absolute uncertainty in the result and the independent i^{th} variable, respectively.

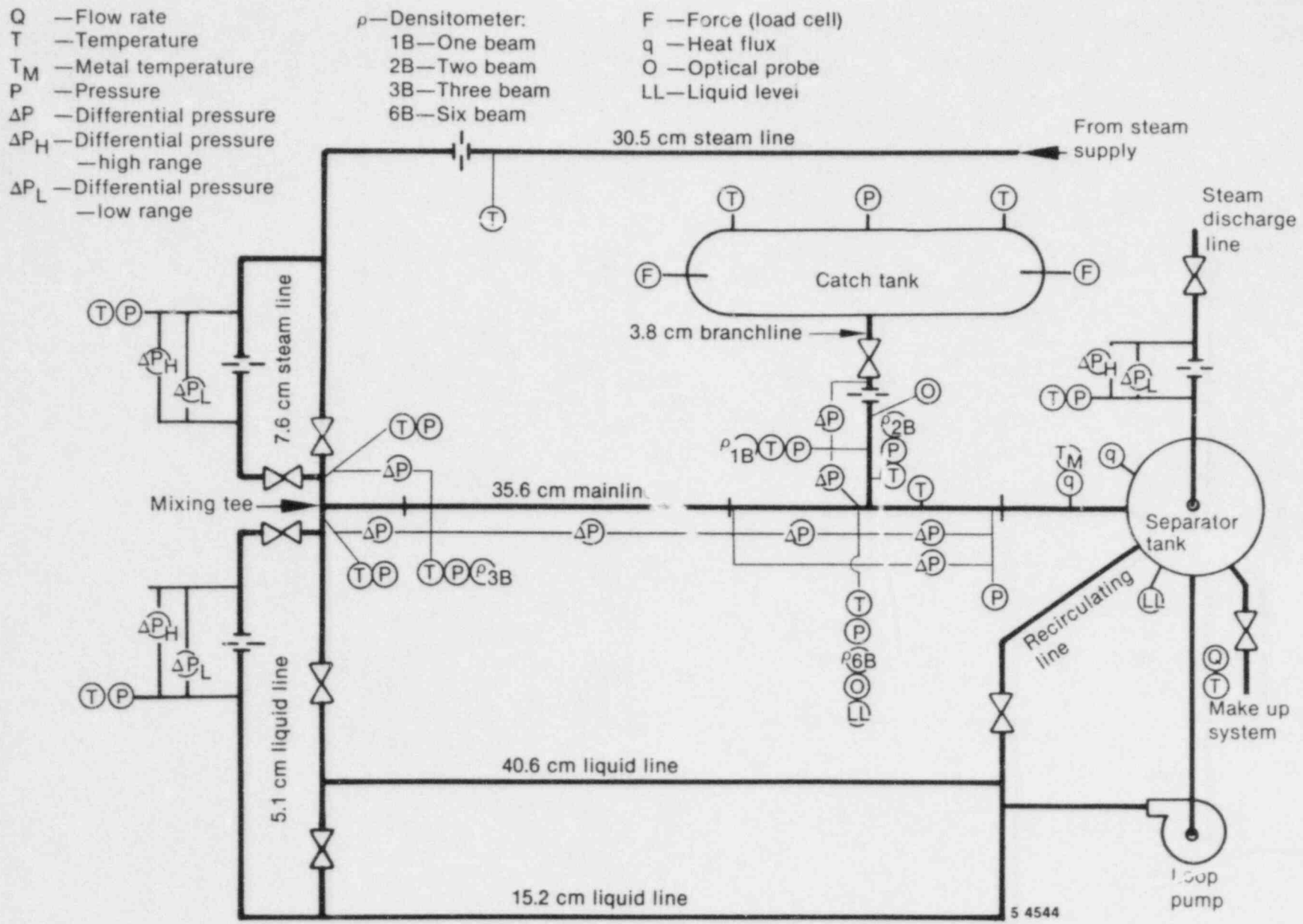

Figure 9. P&ID for TPFL tee/critical flow experiments.

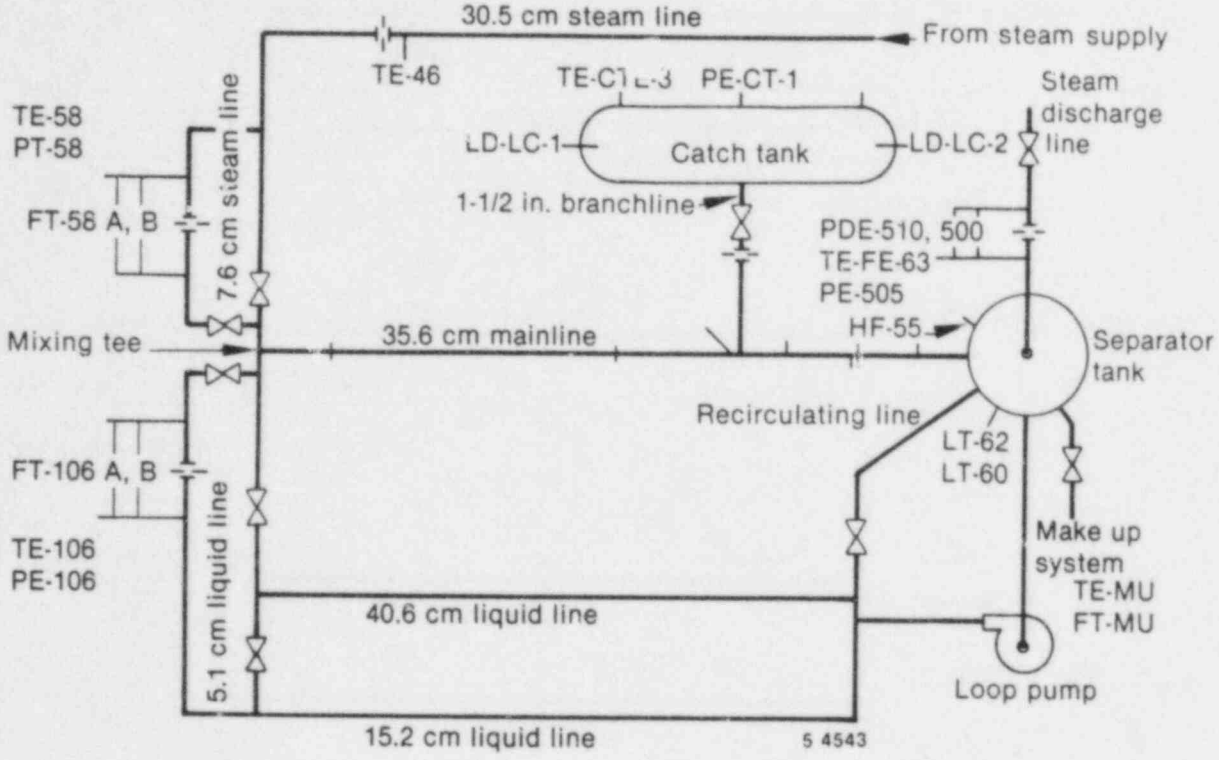

Figure 10. P&ID showing system reference measurements and ID's.

This method was applied to each of the calculated parameters in Appendix J. A summary of the uncertainties in the calculated parameters is provided in Table 4.

Test Point Setup

Both the horizontal and vertical downflow configuration test points were performed in the same manner.[a] Once the system had reached a stationary temperature at the desired pressure and separator tank level, test point setup was initiated. [Prior to this point, the catch tank was filled to the desired initial level with cold (296 K or 55°F) water.] Prior to starting the actual test, a pretest no-flow data average over 60 s was obtained with zero flow in the mainline and branchline. The desired steam and liquid flow rates in the mainline were then established and allowed to reach steady-state (one criteria for steady-state was that the inlet and exhaust steam flow rates were within 0.08 kg/s, the measurement uncertainty, of each other).

Once steady-state was reached, the Data Acquisition System (DAS) was started. Data was acquired for a minimum of 60 s before opening the branchline valve. The test point was continued until the catch tank filled or reached its maximum allowable temperature (365 K), or until the test engineer decided sufficient data had been acquired for that point. At that time, the valve was closed and initial conditions were allowed to reestablish. Sixty seconds after steady-state conditions were again established, the DAS was stopped. Flows were reduced to the minimum required to maintain loop temperature and pressure. The data was then spooled to magnetic tape for permanent storage and DAS was set up for the posttest no-flow data point. All flows in the loop were stopped and the exhaust valve was closed. Sixty seconds of no-flow data were then acquired and a hard copy was made of the data averages for each channel. The pre- and posttest no-flow data averages allowed for correction of differential pressures (DPs) due to drift or change of fluid levels in the sensor lines.

Test Point Flow Rates. The desired condition in the mainline was a stable stratified level with inlet steam and water flows greater than the anticipated individual phasic flow rates out the branch. At the

a. The controlling document for the test program operation was the Experimental Operating Specification (Reference 14).

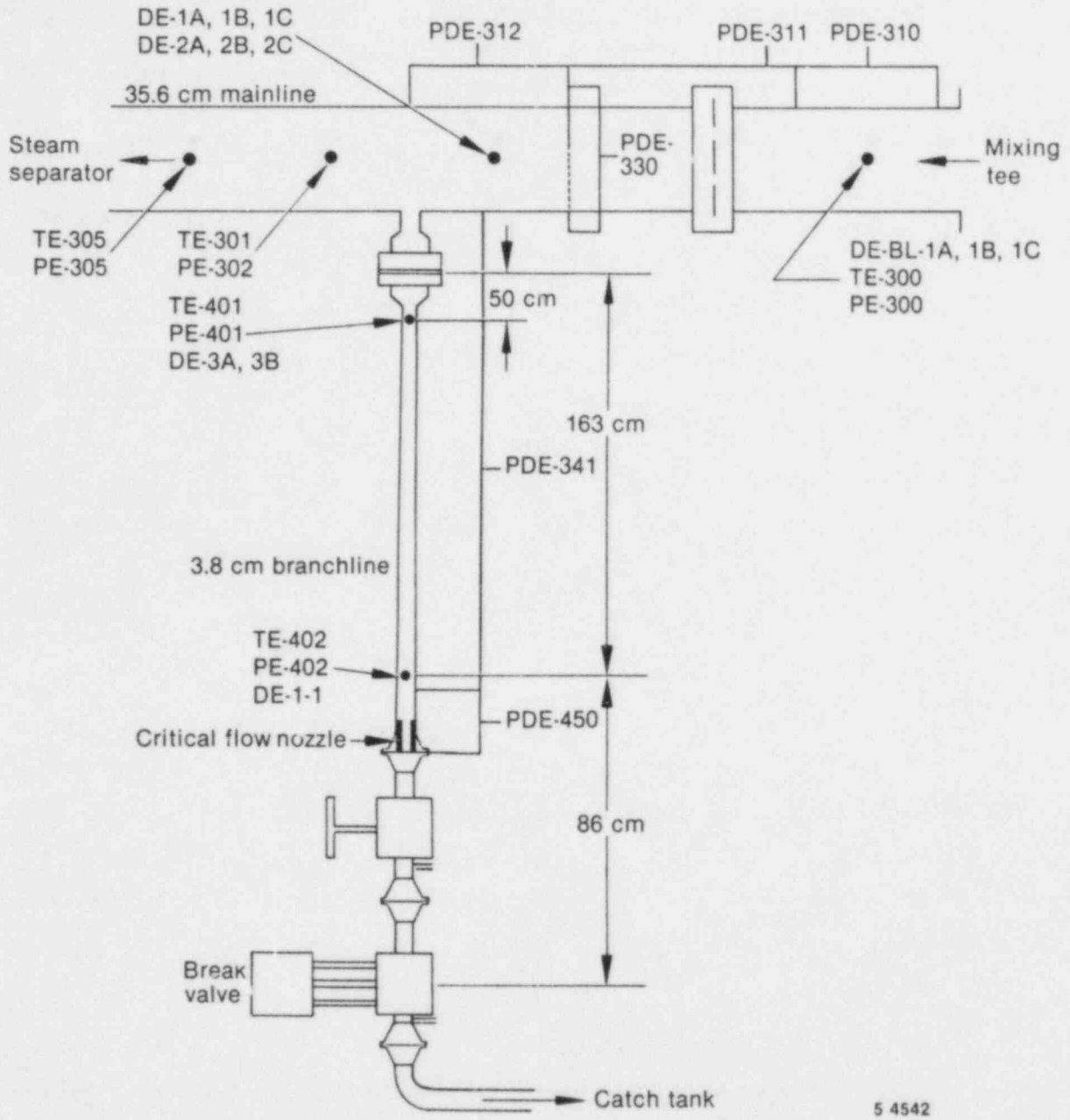

Figure 11. Test section piping sketch, showing measurement locations and ID's.

planned test pressure of 6.2 MPa, the anticipated maximum branchline flow rates (single-phase critical flow) were 1.8 kg/s and 5 kg/s for steam and water, respectively. Since some steam flow out the separator discharge was required for maintaining pressure control, the principle mainline flow rates were chosen as 3 kg/s of steam and 6 kg/s of liquid. The Taitel-Dukler[27] flow regime map predicted wavy-stratified flow for these conditions and observations through the mainline optical probe verified this condition. These flow rates resulted in a mainline liquid level of 19 cm when the separator level was above the mainline and 9 cm when the level was below the mainline (corresponding to the stratified equilibrium level). Since levels outside this range were desired (predominately higher levels for the horizontal configuration and lower levels for the vertical downflow configuration), the flow rates for some test points were adjusted to obtain different initial or final levels. This change in flow was then indicated in the test title as described in the next section.

Table 3. Summary of uncertainties in basic measurements

Measurement Type	Range	Uncertainty (at 95% Confidence Level)
Fluid temperatures	300-585 K	2.2 K
Absolute pressures	0-6.9 MPa	0.02 MPa
Differential pressures	0-12.5 kPa	0.07 kPa
Differential pressures	0-24.8 kPa	0.14 kPa
Differential pressures	0-124.4 kPa	0.71 kPa
Differential pressures	0-172.4 kPa	0.98 kPa
Differential pressures	0-199 kPa	1.1 kPa
Differential pressures	0-6.89 MPa	0.039 MPa
Load cells	0-5000 kg	11 kg
Liquid levels	0-77 cm 0-743 cm	3 cm 15 cm

Table 4. Summary of uncertainties for calculated parameters

Identification	Description	Nominal Uncertainty
MDOT-LIQ, INLET	Inlet liquid flow rate	0.07 kg/s
MDOT-STM, INLET	Inlet steam flow rate	0.047 kg/s
MDOT-LIQ-T/S	Mainline liquid flow rate	0.07 kg/s
MDOT-STM-T/S	Mainline steam flow rate	0.05 kg/s
MDOT-STM-BRANCH	Branchline steam flow rate	0.08 kg/s
MDOT-TOT-BRANCH	Branchline total flow rate from mass balance	0.33 kg/s
MDOT-CT	Branchline total flow rate from catch tank	0.36 kg/s
MDOT-STM, DISCH	Exhaust steam flow rate	0.06 kg/s
STRAT LIQ HT-T/S	Mainline stratified liquid height	1.2 cm
VOID-BRANCH	Branchline void fraction-entrance	0.26

Table 4. (continued)

Identification	Description	Nominal Uncertainty
VOID-BREAK	Branchline void fraction-upstream of break orifice	0.26
BRANCH FLOW QUAL	Branchline flow quality at entrance-from system mass balance	0.10
BREAK FLOW QUAL	Flow quality upstream of critical flow nozzle from catch tank flow rate and steam flow rates	0.10
CT-FLOW QUAL	Branchline flow quality from thermodynamic balance of the catch tank.	0.33

For tests performed at lower pressures, it was desired to maintain the same superficial velocities in the mainline as for the 6.2 MPa tests. Since the liquid density changed little, the liquid mass flow rate was maintained at 6 kg/s and the steam flow rate adjusted to 2.1 kg/s at 4.4 MPa[a] and 1.6 kg/s at 3.45 MPa.

It was originally intended to use the steam separator level to adjust the mainline level. However, system liquid inventory loss out the branchline resulted in a decreasing separator level. This drop in level was to be compensated for through the use of a make-up system. However, there were two problems with this technique: first, the capacity of the available make-up pumps was insufficient to maintain a constant level, and second, the make-up system injects cold (283 K, 50°F) water into the system. The cold water injection cooled down the liquid inventory in the separator, resulting in condensation of steam in the separator that could not be accurately determined as a function of time. Since the branchline steam flow is calculated by the difference between the steam supply rate and that vented from the steam separator, significant condensation in the separator would result in a significant overestimation of the branchline steam flow rate. Thus make-up was used on only four of the test points. As a result, the mainline liquid level dropped as a function of time for all data runs in which the initial separator tank level was above the bottom of the mainline.

a. A mistake was made in the calculation of superficial velocities for 4.4 MPa horizontal configuration data and therefore a steam flow rate of 2.4 kg/s used.

Test Point Identifications. The identification of the test parameters for individual test points, such as presented later in this report, is provided by a unique set of alphanumeric characters. The first set of characters are "TEE", indicating that the data is part of the tee/critical flow experiments. The second set of characters is either "H" or "VD" indicating the configuration as horizontal or vertical downflow. The third set of characters indicates whether the make-up system was used or not used, "MU" or "NMU", respectively. The fourth set of characters are an indication of level in cm, for either the steam separator or mainline. The next one or two sets of characters indicate the steam or liquid mass flow rate (in kg/s) in the mainline (if different from the proposed flow rates); for example, MG = 1.0 for a steam flow rate of 1 kg/s inlet to the mainline. Finally the pressure was indicated if different from 6.2 MPa.

An example of the nomenclature is: TEE-H-NMU-65 (MG = 2.0) (P = 4.4); for a horizontal test point without make-up with a desired separator level of 65 cm (LT-62), a steam mass flow rate of 2.0 kg/s, and a mainline pressure of 4.4 MPa.

DATA PRESENTATION

This section presents a compendium of the data obtained during the tee/critical flow experiments. It would be impractical to attempt to present data for all 80 measurements recorded (plus calculated parameters) for each of the 93 data points performed. Instead, plots of the pertinent portion of data (during branchline flow) for selected measurements and calculated parameters for each of 91 reported data points[a] are presented in Appendices B, C, D, E, F, and G (contained on microfiche and located on the inside back cover of this report). These data are arranged as follows:

Appendix B Horizontal Configuration—6.2 MPa Data

Appendix C Horizontal Configuration—4.4 MPa Data

Appendix D Horizontal Configuration—3.45 MPa Data

Appendix E Vertical Downflow Configuration—6.2 MPa Data

Appendix F Vertical Downflow Configuration—4.4 MPa Data

Appendix G Vertical Downflow Configuration—3.45 MPa Data

Within each Appendix, the figure labels are coded; for example, B.3.12, where the B refers to the Appendix, the .3 refers to the data point (see the list of appendices figures) and the .12 refers to the 12th figure of that data point. A list of the 18 figures for each data point is provided in Table 5.[b]

In addition to the figures in the appendices, plots of specific parameters for selected data points are presented in this section. Data averages for portions of test points in which the mainline stratified liquid level was constant are tabulated in Appendix H, and selected parameters plotted. The horizontal configuration data is presented in the Horizontal-Configuration Data section, with vertical downflow data in the Vertical Downflow Configuration Data section.

During a test point, data was acquired beginning 60 s before opening the branchline valve and continuing until 60 s after closing the branchline valve and reestablishing the initial conditions. Only the data acquired while the valve was open is useful for the investigation of the entrainment/pull-through phenomena and is reported in the appendices. However, these initial and final steady-state conditions are tabulated in Tables H-1 to H-6 for use in evaluating system mass balances. Selected plots of an entire data acquisition period will be presented next, as an example of the data acquired, including the effect of opening and closing the break valve to establish flow in the branchline on the various system parameters.

An overlay of the steam mass flow rates in the test section and outlet of the steam separator for test point TEE-H-NMU-55 (MG = 1.5) is shown in Figure 12. The initial level in the separator tank was at 55 cm on LT-62, which was 8 cm above the top of the 28.4 cm diameter mainline. The difference between these two measured parameters is the steam mass flow rate into the branchline. Notice that the flow rates match within the combined measurement uncertainties for the final, but not for the initial, conditions. The initial difference of 0.12 kg/s (from 0-60 s) is due to condensation effects caused by mixing slightly subcooled liquid with saturated steam in the separator tank. This effect is more pronounced during the initial portion of the test run (prior to opening the break valve) due to the decreased steam flow rate during the pretest point setup. This lower steam flow rate resulted in an initially slightly cooler system (particularly in the separator tank) than the final system condition. However, it was not possible to quantify this effect with any certainty because the major condensation effects were downstream from the reference measurements. The mainline and branchline pressures for the same data point are presented in Figure 13. There is a 0.04 MPa offset between these two measurements. This offset, however, is marginally within the combined measurement uncertainties of twice 0.02 MPa. The perturbation in mainline pressure due to opening

a. The data from two of the test points was inadvertently destroyed during testing.

b. It should be noted that pressure drops along the mainline are not reported. The reason for this is that the data values of the DPs were much smaller than the measurement uncertainties and the signal to noise ratios were much less than 1. This is a result of very low velocity flows which, in turn, result in small frictional pressure drops.

Table 5. List of appendix figures for each test point

1. Mainline pressure (PE-302)
2. Comparison of mainline top temperature (TE-301), bottom temperature (TE-305), and saturation temperature (TSAT-T/S)
3. Comparison of mainline steam mass flow rate (MDOT-STM-T/S) and steam separator discharge mass flow rate (MDOT-STM, DISCH)
4. Mainline liquid mass flow rate (MDOT-LIQ-T/S)
5. Mainline stratified liquid height (STRAT LIQ HT-T/S)
6. Mainline average density (AVE DEN-T/S)
7. Steam separator liquid level (LT-60-COR)
8. Branchline pressure (PE-402)
9. Comparison of branchline temperature (TE-402) and saturation temperature (TSAT-BREAK)
10. Differential pressure from mainline to the branchline upstream of the break orifice (PDE-341), unfiltered data
11. Differential pressure across the branchline simulated break orifice (PDE-450)
12. Steam mass flow rate in the branchline calculated from a system mass balance (MDOT-STM-BRANCH).
13. Comparison of mass flow rate due to a change in steam separator liquid level (MDOT-LIQ-LEVEL) and total mass flow in the branchline (MDOT-TOT-BRANCH)
14. Comparison of void fraction in the branchline entrance (VOID-BRANCH) and immediately upstream of the break orifice (VOID-BREAK)
15. Comparison of flow quality in the branchline calculated from a system mass balance (BRANCH FLOW QUAL), and calculated using the catch tank flow rate (BREAK FLOW QUAL)
16. Comparison of east (LD-LC-2-LO) and west (LD-LC-1-LO) end load cell response
17. Total mass in the catch tank (LD-CT-TOTAL)
18. Comparison of the calculated catch tank mass flow rate (MDOT-CT) and branchline mass flow rate (MDOT-TOT-BRANCH) calculated from a system mass balance

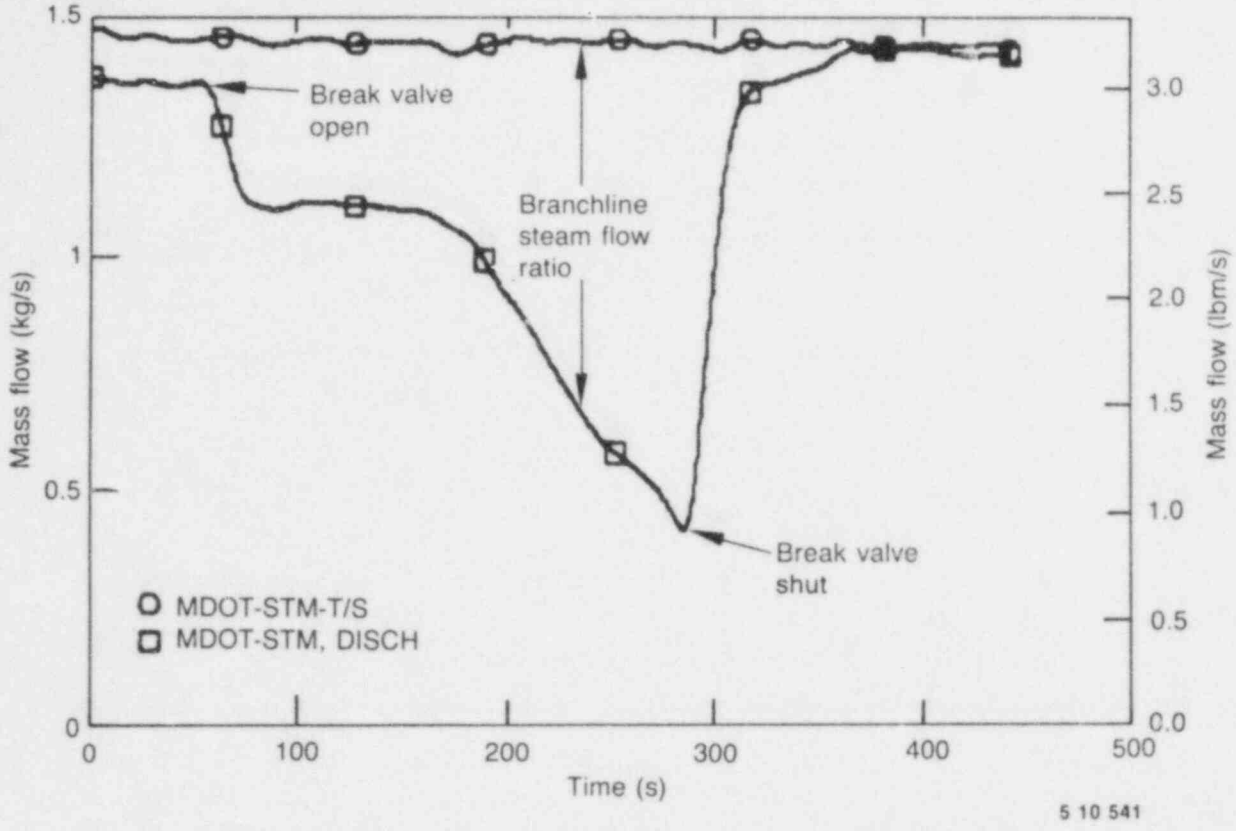

Figure 12. Comparison of mainline steam mass flow rate (MDOT-STM-T/S) and steam separator discharge mass flow rate (MDOT-STM, DISCH) for test point TEE-H-NMU-55 (MG = 1.5).

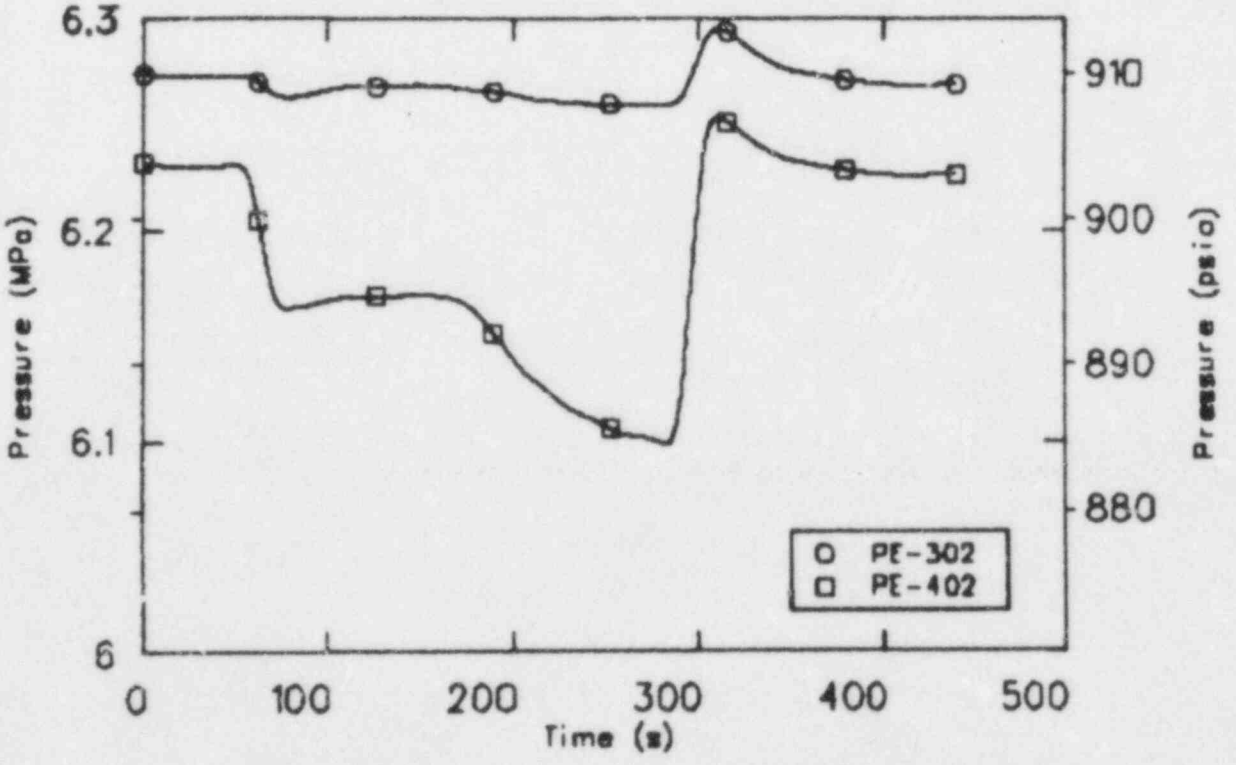

Figure 13. Comparison of mainline pressure (PE-302) and branchline pressure (PE-402) for test point TEE-H-NMU-55 (MG = 1.5).

the branchline valve is noticeable but not overly significant. The differential pressure between these pressure measurements (PDE-341) is the pressure drop from the mainline to branchline and is shown in Figure 14.[a] This data is minimally filtered. Notice the large increase in noise level at about 150 s. This is due to two-phase flow and is an indication of the onset of vapor pull-through. The increase in noise level was used as the primary indication for determination of the onset of vapor pull-through for applicable test points and levels determined from this criteria were tabulated. This data, filtered the same as all other channels, is shown in Figure 15. Notice the point of minimum pressure drop corresponding to a level of about 19 cm. The pressure drop is proportional to the ratio of branchline mass flow rate squared to mixture density. The minimum pressure drop is a result of interaction between decreasing two-phase density and decreasing branchline critical mass flow rate; both are a result of increased vapor flow into the branchline as the mainline liquid level decreases. Once the minimum is reached, continued drop in level causes density to decrease faster than the mass flow rate squared resulting in an increase in the differential pressure.

The mainline stratified liquid level for test point TEE-H-NMU-55 (MG = 1.5) is shown in Figure 16. The liquid level has a small initial increase following the opening of the branchline valve at 60 s. After this, the level remains constant until the steam separator level drops to the mainline level. As liquid continues to be lost from the system out the branchline, mainline level continues to drop until the stratified equilibrium level,[b] corresponding to the mainline superficial phase velocities, is reached or until the branchline valve is closed.

a. A different test point was used for this example. The test point cited in the other figures of this section [TEE-H-NMU-55 (MG = 1.5)] did not exhibit this onset of pull-through behavior since the initial level was below the onset of pull-through level.

b. The stratified equilibrium level is the liquid level in the mainline when the level in the separator tank is below the bottom of the mainline. This level is determined by the flow rates of the steam and water and is usually written as a function of the superficial velocities of the two phases.

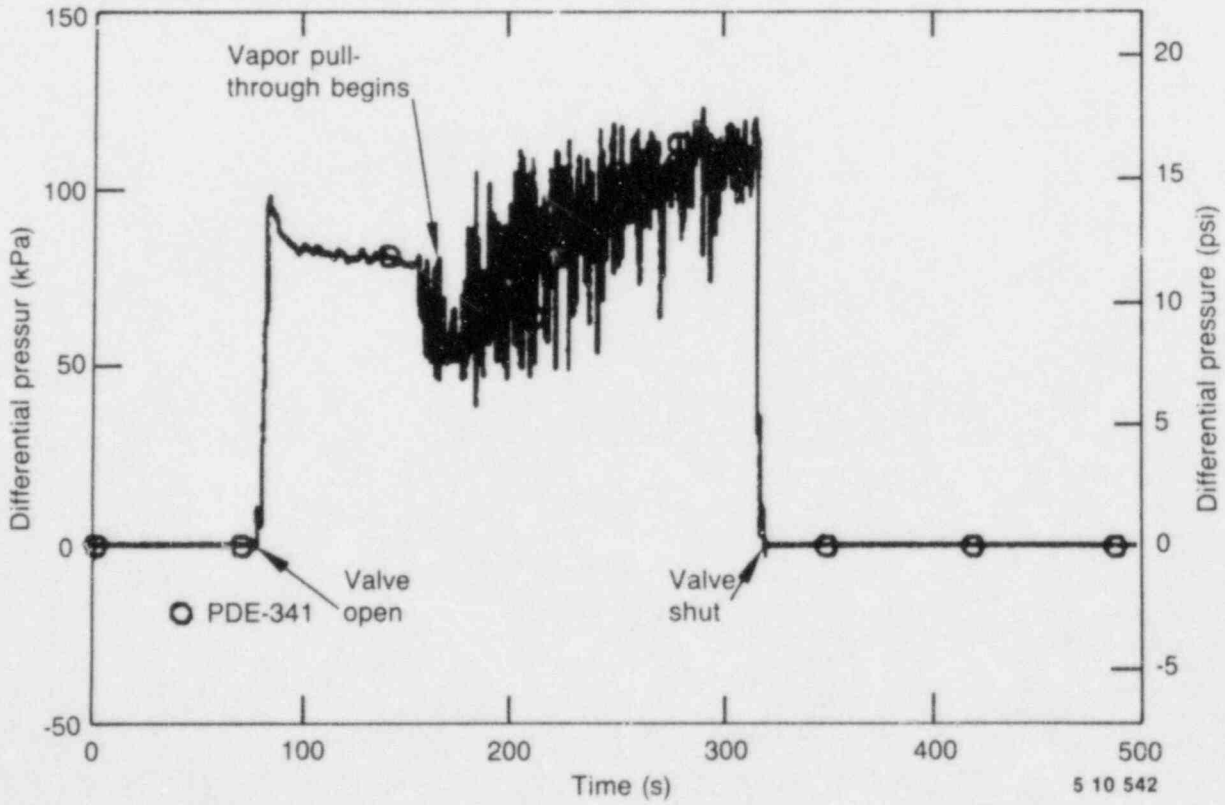

Figure 14. Differential pressure from mainline to branchline (PDE-341), unfiltered, for test point TEE-H-NMU-65 (MG = 0.2).

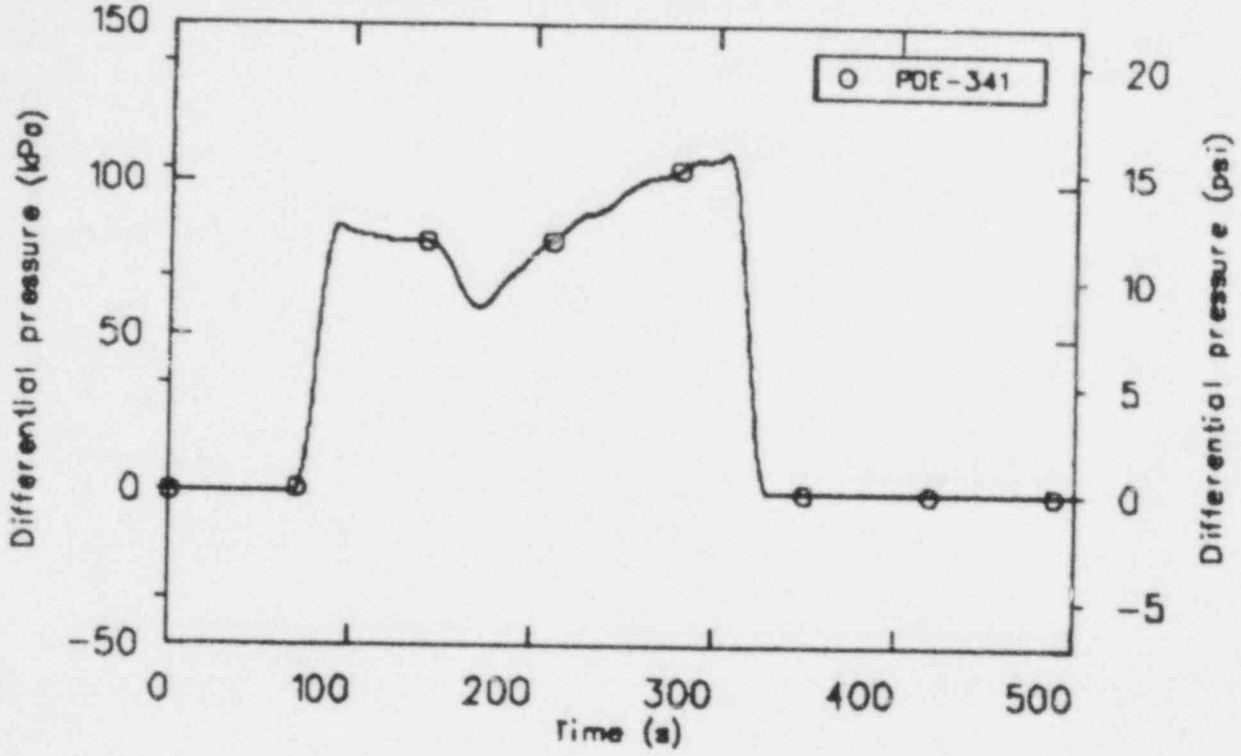

Figure 15. Differential pressure from mainline to branchline (PDE-341), filtered, for test point TEE-H-NMU-65 (MG = 0.2).

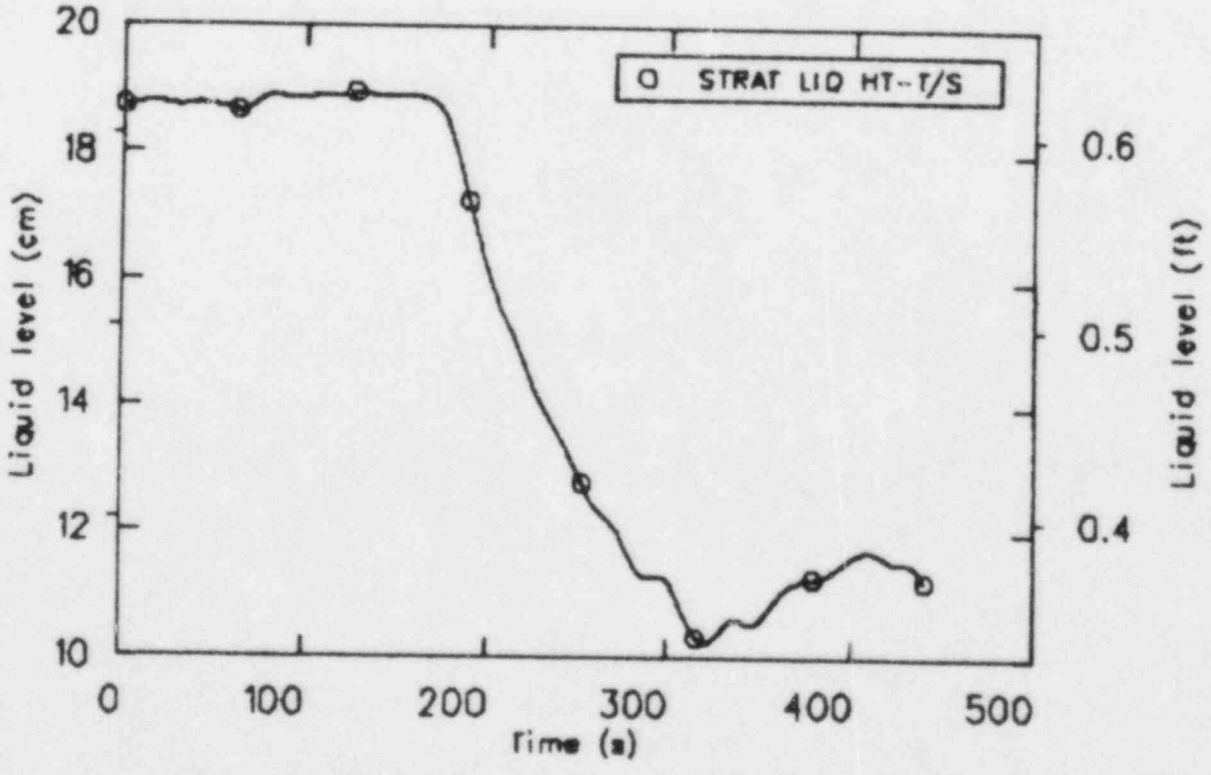

Figure 16. Mainline stratified liquid level (STRAT LIQ HT-T/S) for test point TEE-H-NMU-55 (MG = 1.5).

The total branchline mass flow rate obtained from the system mass balance (using liquid level measurements in the separator tank and mainline) is compared to the branchline mass flow rate measured using the catch tank in Figure 17. For the most part, the comparison is quite good. These two ways of calculating the branchline flow rate provide an independent check on the measurements.

An example of a test point in which make-up was used is TEE-H-MU-14. Figure 18 is an overlay of the mainline and separator steam flow rates for this test point. A comparison of these flows for the final conditions (after the branchline valve closed) indicates that the steam condensation in the separator tank was approximately 13% of the mainline flow rate. The condensation effect is not correctable since condensation occurs downstream of the instrumented test section. A further indication of the magnitude of the problem when using cold liquid make-up is given in Figure 19; branchline flow quality is plotted for two similar test points: with and without make-up. The calculated flow quality, at a given mainline liquid level, for the point with make-up is considerably higher than the point without make-up. This is a result of steam condensation which is not accounted for in the steam mass balance used to obtain the branchline steam flow rate.

Video probes were installed in the mainline upstream of the branchline entrance and in the branchline upstream of the critical flow nozzle. Videotape of the probe data was recorded for many of the data points. The view for all the data points was basically the same. The flow in the mainline was observed to be stratified at all times (with some nonbridging surges in level). The flow in the branchline was observed to be high velocity homogeneous or annular flows, depending on the void fraction.

In the following sections data will be presented and discussed for the horizontal and vertical downflow configurations at pressures of 6.2, 4.4, and 3.45 MPa.

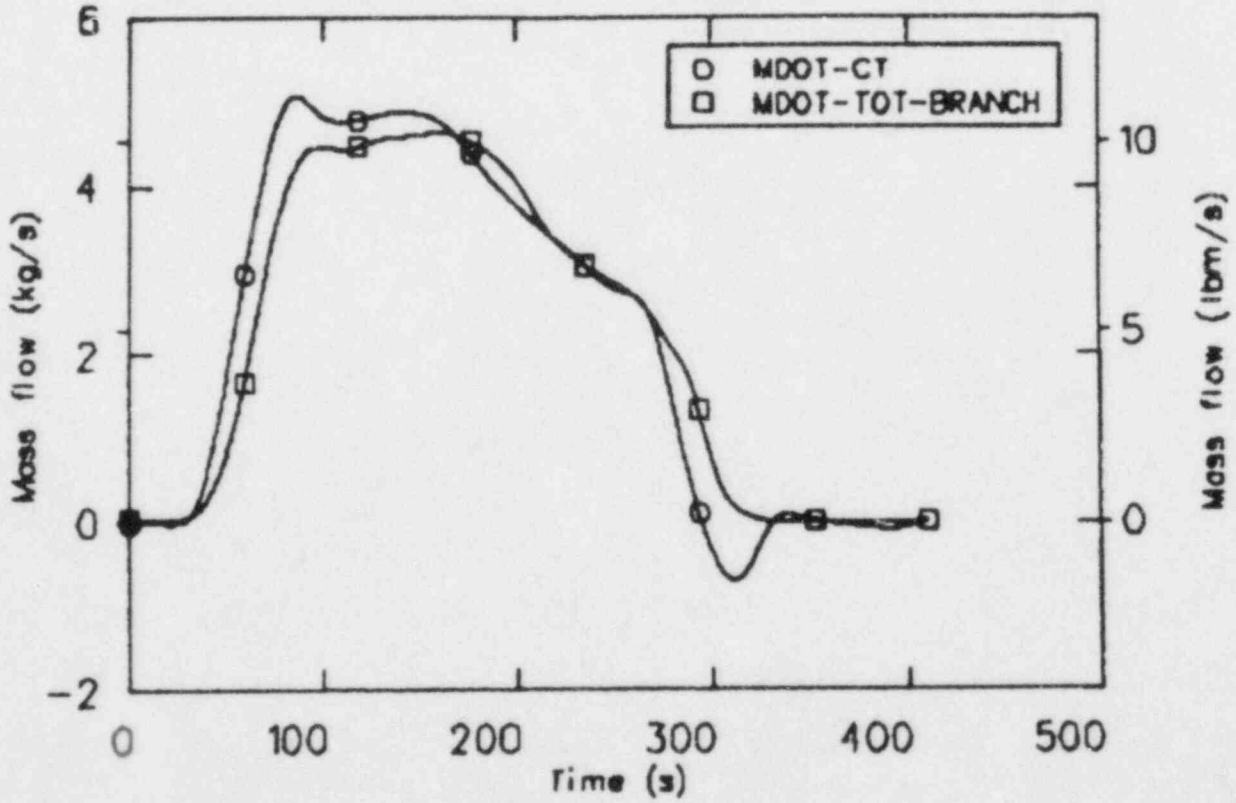

Figure 17. Comparison of the calculated catch tank mass flow rate (MDOT-CT) and branchline mass flow rate (MDOT-TOT-BRANCH) calculated from a system mass balance for test point TEE-H-NMU-55 (MG = 1.5).

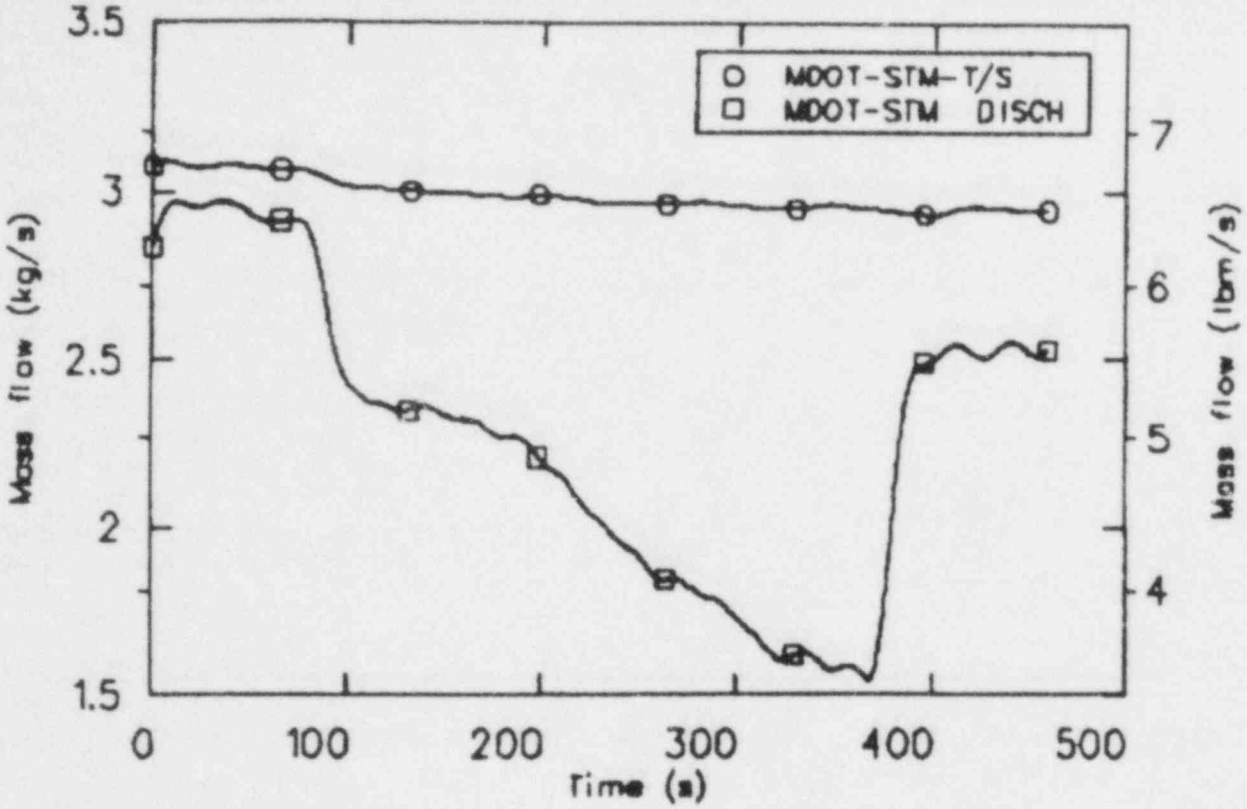

Figure 18. Comparison of mainline steam mass flow rate (MDOT-STM-T/S) and steam separator discharge mass flow rate (MDOT-STM, DISCH) for test point using make-up (TEE-H-MU-14).

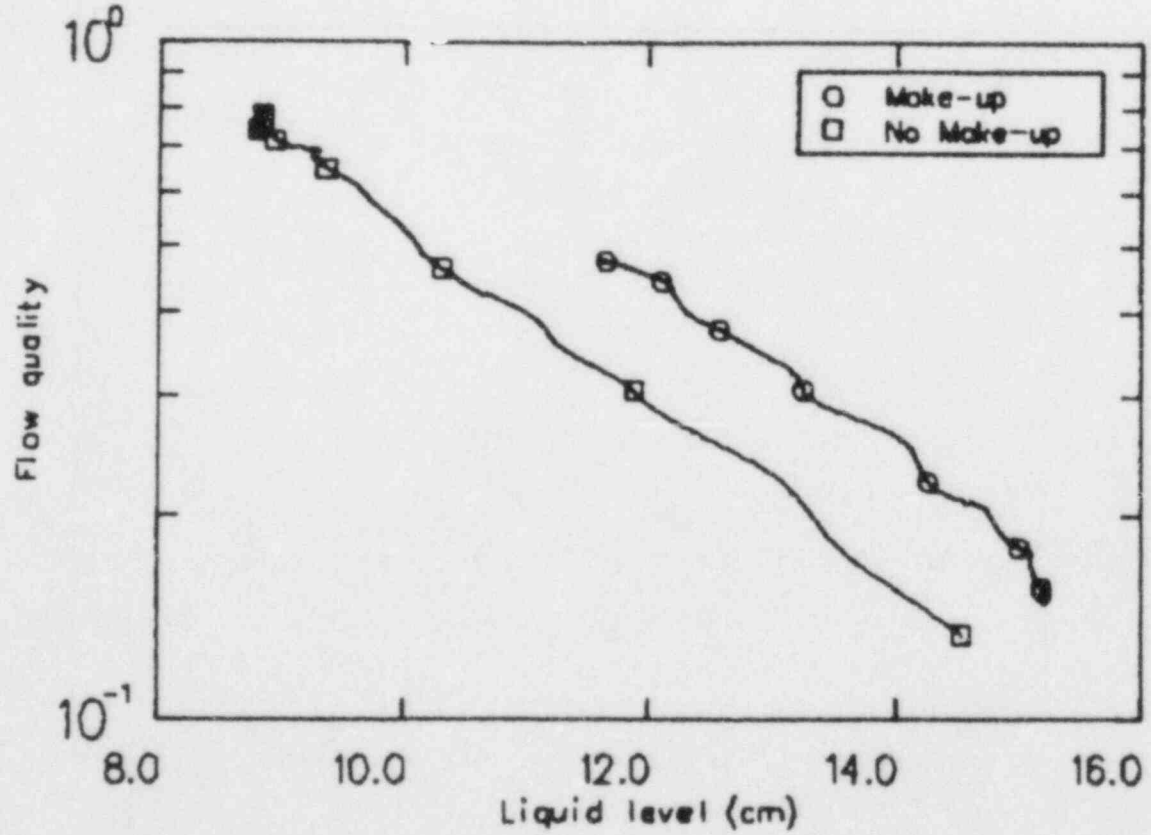

Figure 19. Comparison of branchline flow qualities (BRANCH FLOW QUAL) as functions of the mainline liquid level (STRAT LIQ HT-T/S) for two test points in which make-up was and was not used (TEE-H-MU-14 and TEE-H-NMU-14B).

Horizontal Configuration Data

A total of 48[a] test points were performed in the horizontal configuration (23 at 6.2 MPa, 14 at 4.4 MPa, and 11 at 3.45 MPa). These data are presented in the following three sections. Most of the horizontal configuration test points were transient runs in which the level slowly varied from a maximum initial level to the equilibrium stratified level corresponding to the individual phasic flow rates. Portions of these transient runs had constant levels for greater than 30 s before the level began to drop (while the separator level was above the mainline) and after the equilibrium stratified level was reached. Averaged data for these steady-state segments, with constant mainline liquid levels, are provided in Appendix H, Tables H-7 to H-9, with initial and final conditions provided in Tables H-1 to H-3.

Horizontal—6.2 MPa Data. Data averages for steady-state portions of the horizontal configuration 6.2 MPa data are presented in Table H-7. Selected measurements and computed parameters versus data acquisition time are provided in Appendix B. In this section, the branchline mass flow rate, flow quality, void fraction, and pressure drop as a function of the transient mainline stratified liquid level are presented and discussed.

For horizontal testing, most of the data was acquired at a pressure of 6.2 MPa. This data will be discussed as two subsets of the 6.2 MPa data set. Approximately half of the transient data obtained for the horizontal configuration at 6.2 MPa was for steam flows between 0.2 kg/s and 2.5 kg/s (the steam flow rate of 0.2 kg/s was the minimum steam flow rate which could be reliably controlled). These reduced steam flow data points were performed in an attempt to obtain higher initial mainline liquid levels for determining the level at which vapor pull-through begins and to extend the level range of data. The remainder of data obtained at this pressure and configuration was obtained using a constant steam flow rate of 3 kg/s, and is presented separately. There are two reasons for splitting this data set into two subsets for presentation. First, by splitting the data, the effect of different steam flow rates upon the branchline properties can be discerned. Secondly, too much data exists in the data set to be presented in a single figure. In the remainder of this section, the data subset at reduced steam flow rates and data at a steam flow rate of 3 kg/s is presented. Figures presenting the means for the entire data set are also given. This procedure only applies to the 6.2 MPa horizontal data.

Figure 20 presents the branchline mass flow as a function of mainline liquid level for all test points in which the steam flow rate was reduced from the planned 3 kg/s in order to achieve higher initial levels. For these test points, the mainline steam flow rate varied from 0.2 to 2.5 kg/s (the flow rate was constant during an individual test point). Because of the variance in the data, particularly at the levels corresponding to the level of the branchline, it seems appropriate to present a mean of the data and a tolerance. This was accomplished by calculating the mean and statistical tolerance[b] limits[26] for 0.1 cm intervals, over the entire level span. Results from this procedure are shown in Figure 21. Also shown in Figure 21 are the averaged data from the steady-state portions of the data set points. The averaged data mostly follows the mean and lie within the tolerance limits of the transient data. The tolerance limits for the data in Figure 21 increase with decreasing mass flow rates. This effect may be due to the different steam flow rates used in this data set to achieve the different initial liquid levels.

The data in which the steam flow rate was maintained at 3 kg/s for all the 6.2 MPa data points is presented in Figure 22. For this data the top of the branchline was always uncovered, resulting in the major phenomena of liquid entrainment (at least once the level dropped below the bottom of the branchline to a level of 12.5 cm). The data in Figure 22 covers a range from near the top of the branchline to the onset of liquid entrainment (although this level is not apparent from this figure, it will be from the figure showing flow quality as a function of mainline liquid level). The mean and tolerance limits of the data in Figure 22 is presented in Figure 23. The variance in this data is much smaller than was exhibited for the corresponding branchline flow rates with different mainline steam

a. Forty-eight test points were performed; however, the data tape from one of the 3.45 MPa test points was inadvertently destroyed.

b. The statistical tolerance limits are the standard deviation of the data, from the mean within the 0.1 cm interval, times the tolerance factor (which is a function of the number of data points in the interval). The tolerance factors used were for a 95% probability that 95% of the data would lie within the tolerance limits.

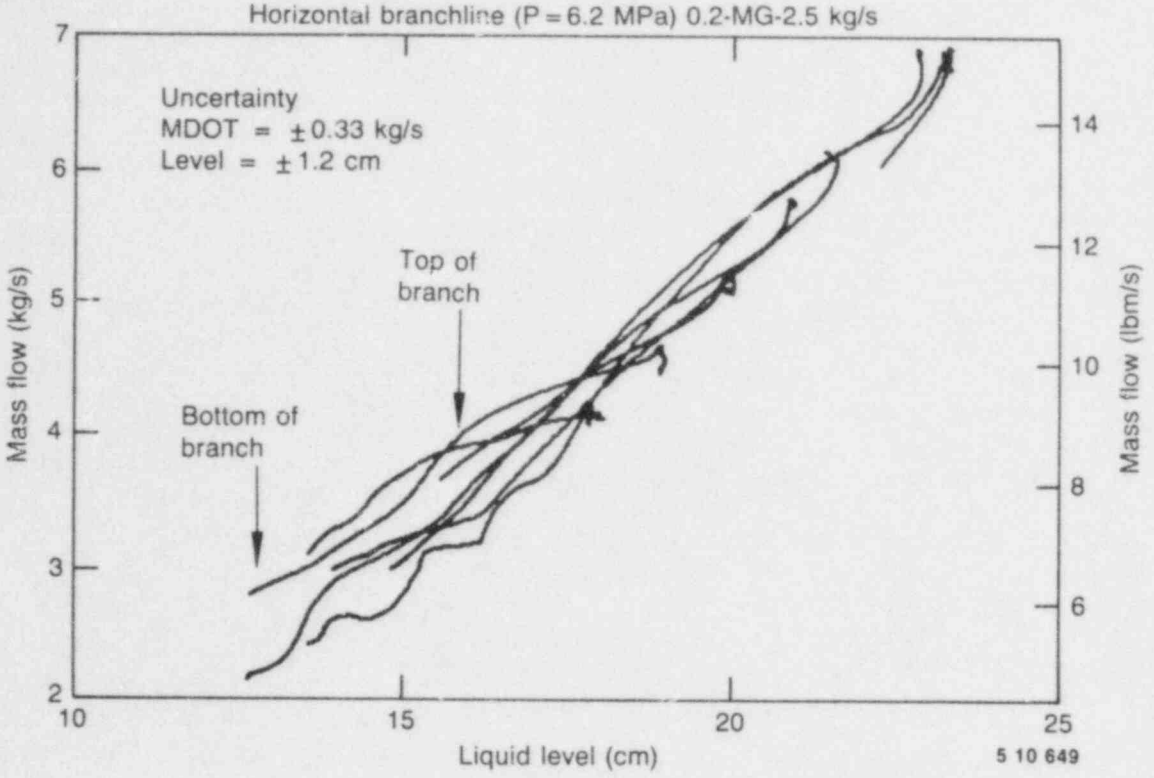

Figure 20. Branchline mass flow rate as a function of mainline stratified liquid level for steam flow rates between 0.2 and 2.5 kg/s of horizontal configuration 6.2 MPa data.

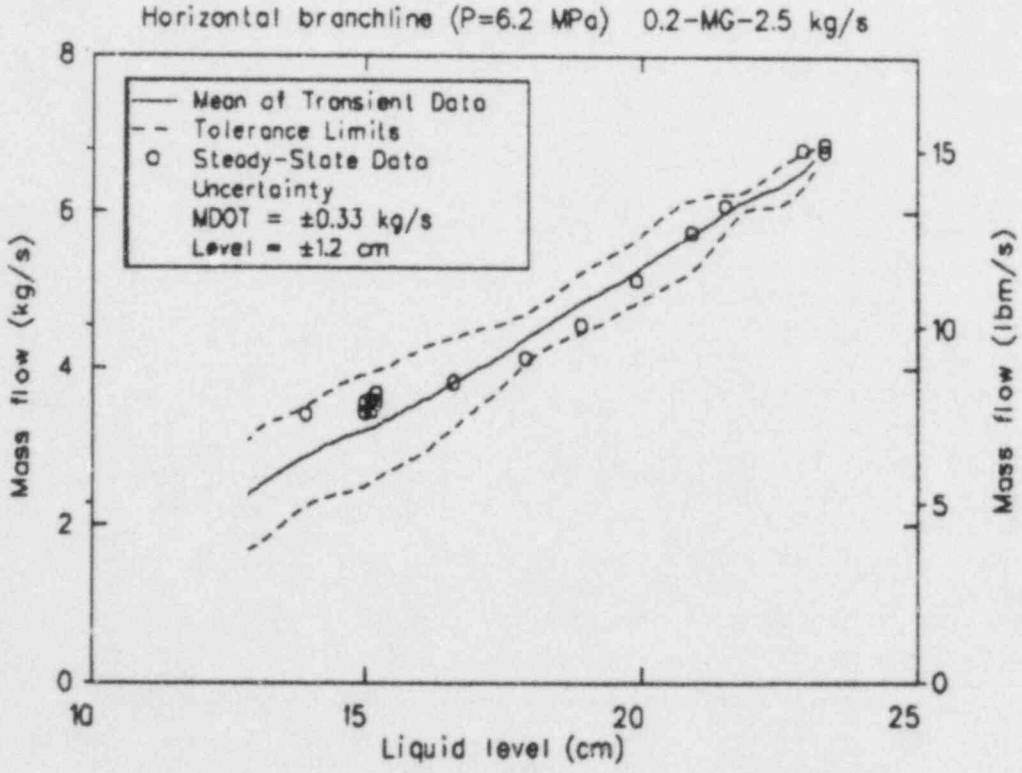

Figure 21. Mean of transient branchline mass flow rate data with steam flow rates between 0.2 and 2.5 kg/s of horizontal configuration 6.2 MPa data.

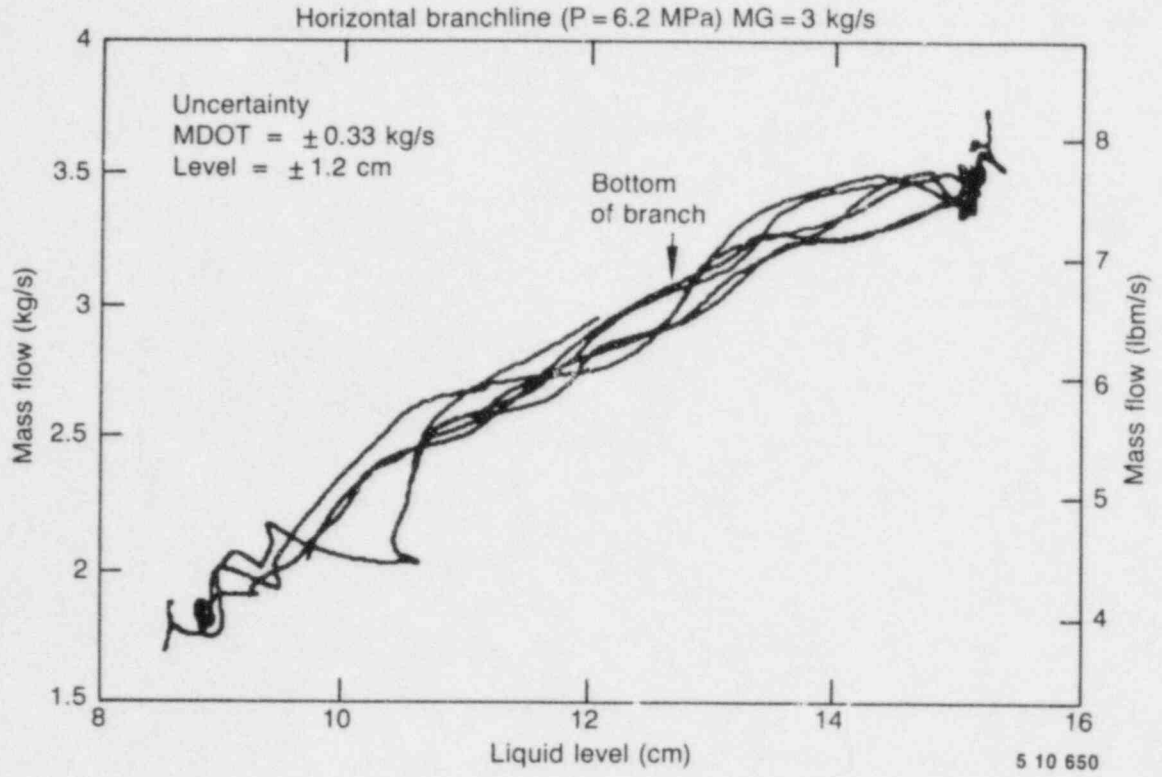

Figure 22. Transient branchline mass flow rate for steam flow rate of 3 kg/s of horizontal configuration 6.2 MPa data.

flow rates. This smaller variance in data indicates that different steam flow rates effect the branchline flow rate, particularly when the mainline level is at the level of the branchline. This effect is probably due to different wave patterns in the mainline as a function of the steam velocity and is perhaps more clearly demonstrated in Figure 24. The mean and tolerance limits of all of the 6.2 MPa horizontal configuration data is compared to the mean of the two data subsets ($0.2 < \dot{m}_G < 2.5$ kg/s and $\dot{m}_G = 3.0$ kg/s), along with the averaged data in Figure 24. The variance in the data at the constant steam flow rate is much smaller than for the data with different steam flow rates.

The branchline flow quality, as a function of mainline liquid level for the transient data in which the steam flow rate was between 0.2 and 2.5 kg/s, is presented in Figure 25. Although there is some variance in the data, it is mostly due to a single data run. The mean of this data and the upper tolerance limit (the lower limit is not meaningful on a log plot) is shown in Figure 26. This figure shows an exponential relationship of flow quality on the liquid level, varying between a minimum flow quality of approximately 0.01 at the onset of vapor pull-through, to a value of 1 at the onset of liquid entrainment. The tolerance limits seem to vary in the same manner. The flow quality at a steam flow rate of 3 kg/s is presented in Figure 27. The variance in this data is again much smaller than for the previous data subset. The mean and upper tolerance limit, along with average data, for this data set is shown in Figure 28. The mean and upper tolerance limit and the averaged data for the entire data set is presented in Figure 29. The data in this figure clearly show an exponential relationship between the branchline flow quality and the mainline liquid level. The steady-state data follow the mean of the transient data and lie within the tolerance limits of the transient data. The upper tolerance limit in Figure 29 is clearly affected by the mainline steam flow rate. Extrapolation of these data to a flow quality of 1 results in an onset of liquid entrainment level of about 7.7 cm.

The branchline void fraction (from the two beam densitometer) for the reduced steam flow rate data subset is given in Figure 30. These data show a much smaller variance than was demonstrated for the mass flow rate and the flow quality and also shows a double tailed exponential relationship on

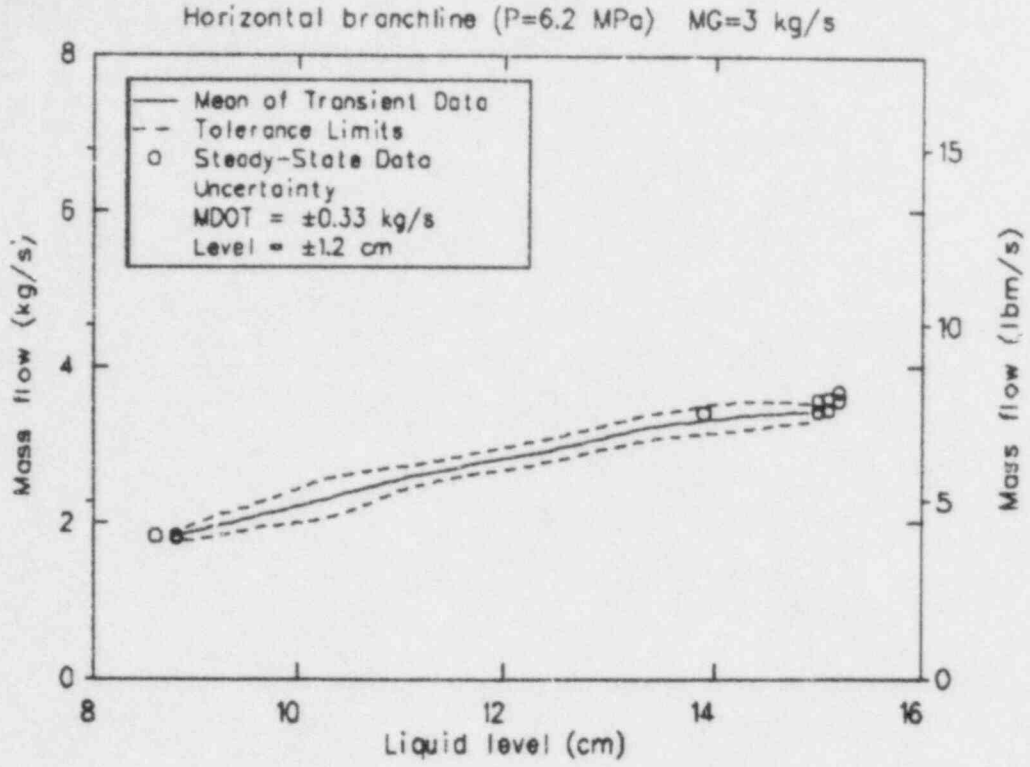

Figure 23. Mean of transient branchline mass flow rate data with steam flow rate of 3 kg/s of horizontal configuration 6.2 MPa data.

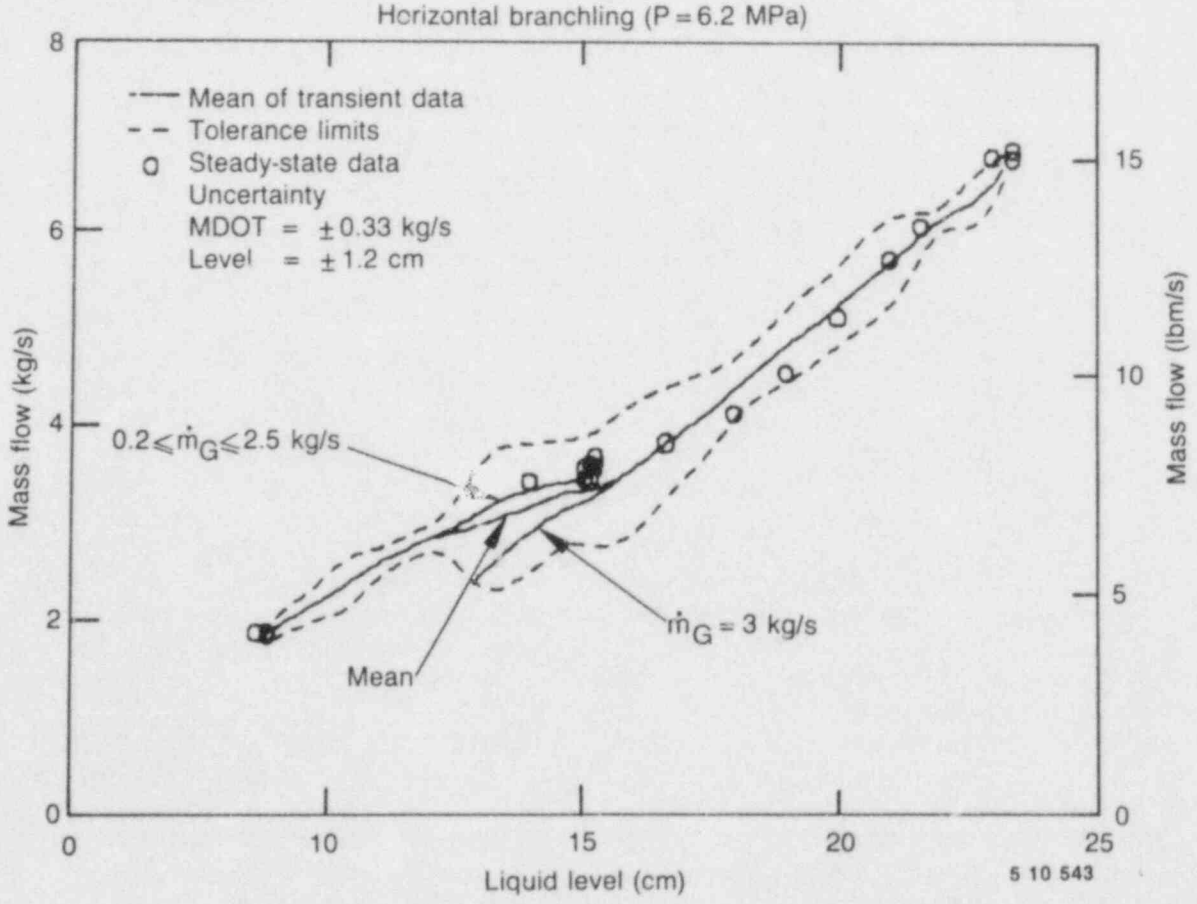

Figure 24. Mean of transient branchline mass flow rate 6.2 MPa data of horizontal configuration.

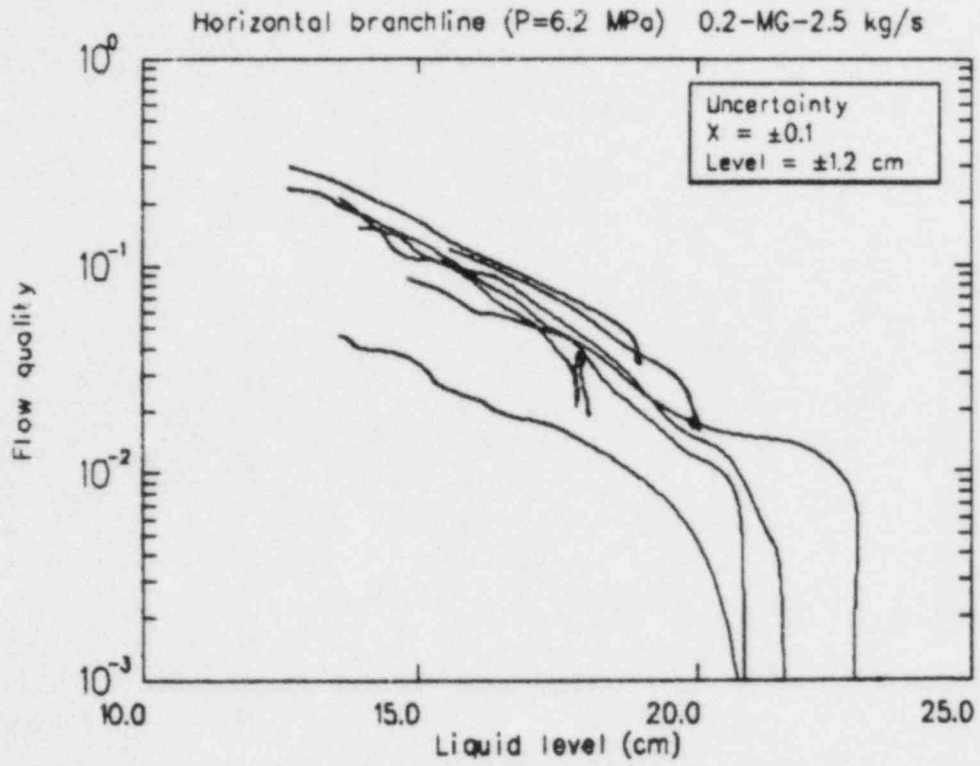

Figure 25. Transient branchline flow quality for steam flow rates of 0.2 to 2.5 kg/s of horizontal configuration 6.2 MPa data.

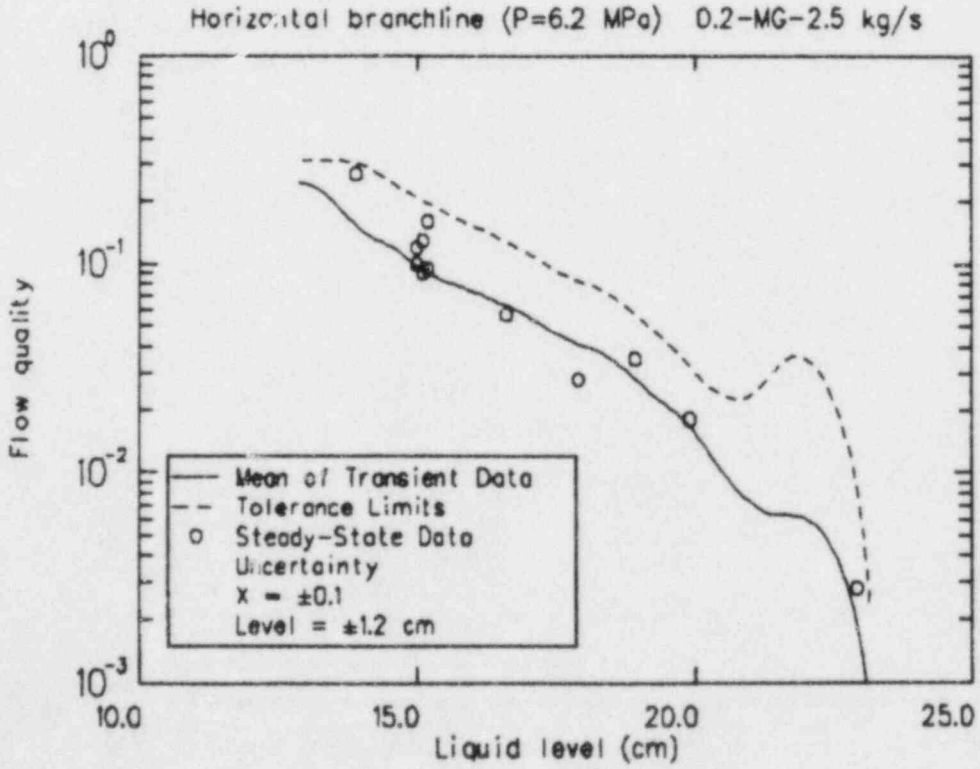

Figure 26. Mean of transient branchline flow quality for steam flow rates of 0.2 to 2.5 kg/s, of horizaontal configuration 6.2 MPa data.

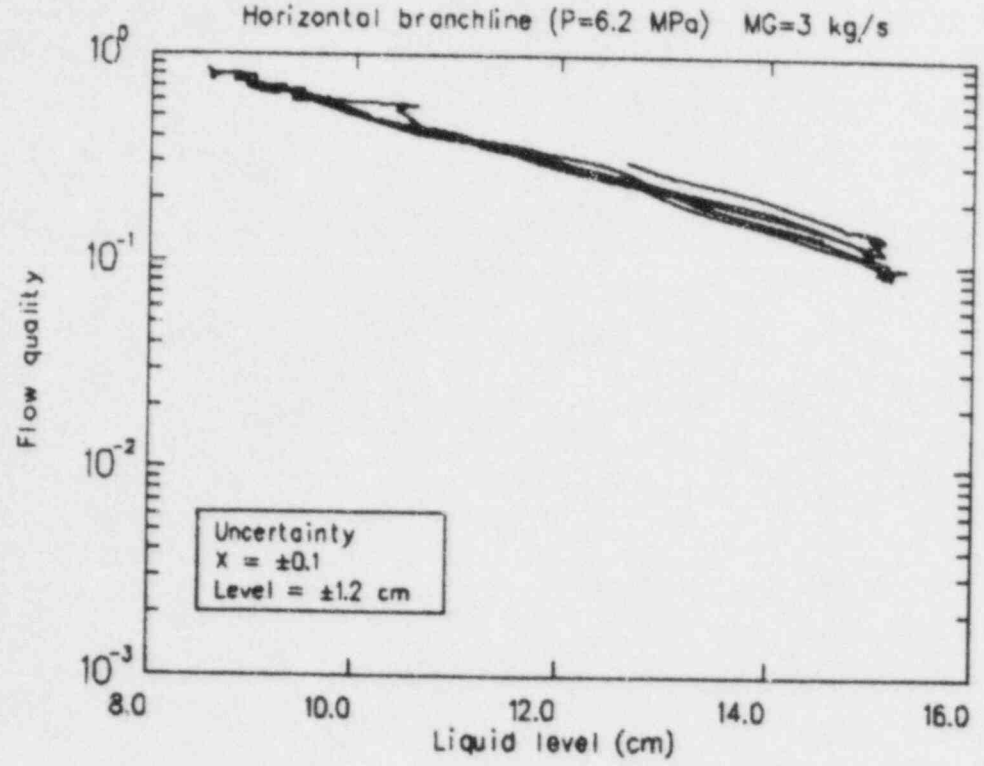

Figure 27. Transient branchline flow quality for steam flow rate of 3 kg/s, of horizontal configuration 6.2 MPa data.

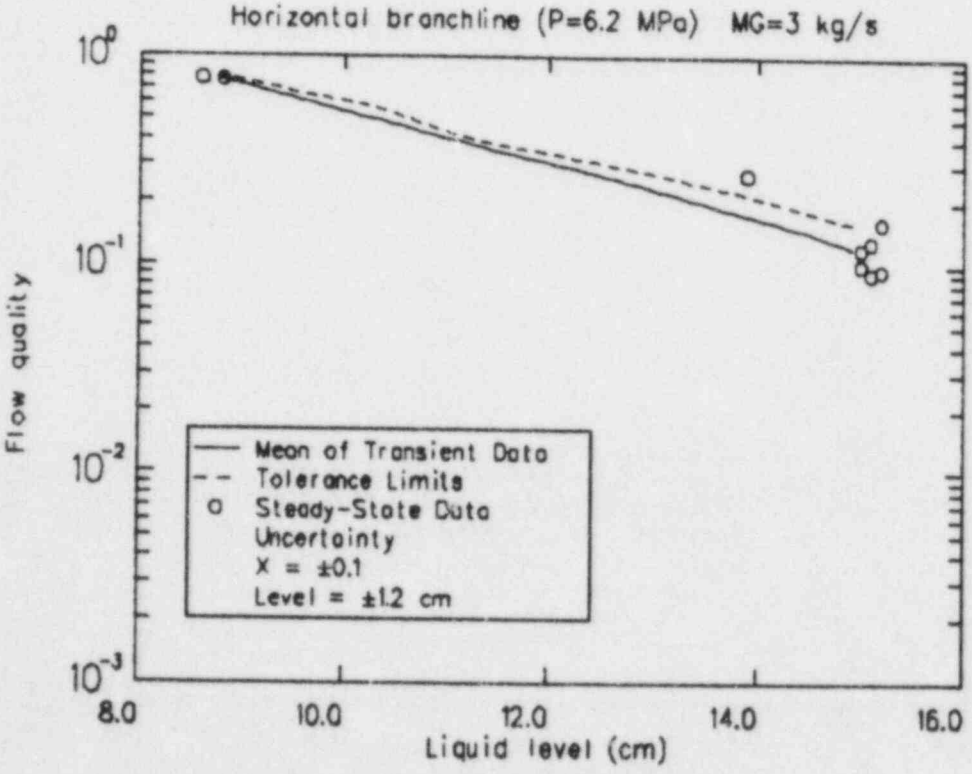

Figure 28. Mean of transient branchline flow quality for steam flow rate of 3 kg/s, of horizontal configuration 6.2 MPa data.

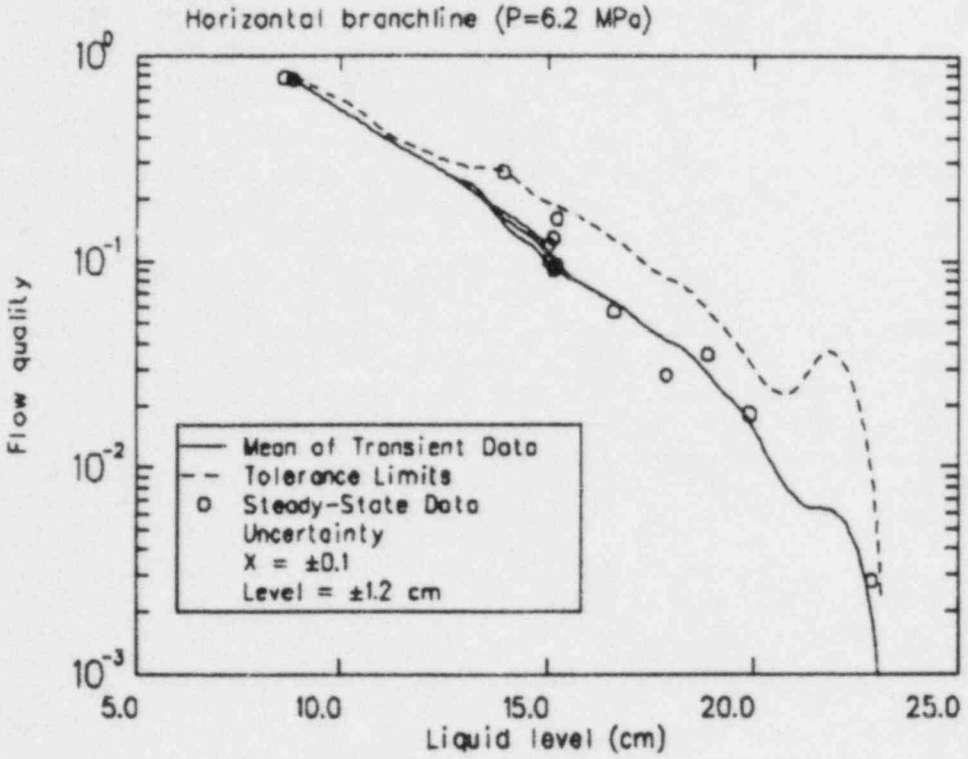

Figure 29. Mean of transient branchline flow quality for all steam flow rates, of horizontal configuration 6.2 MPa data.

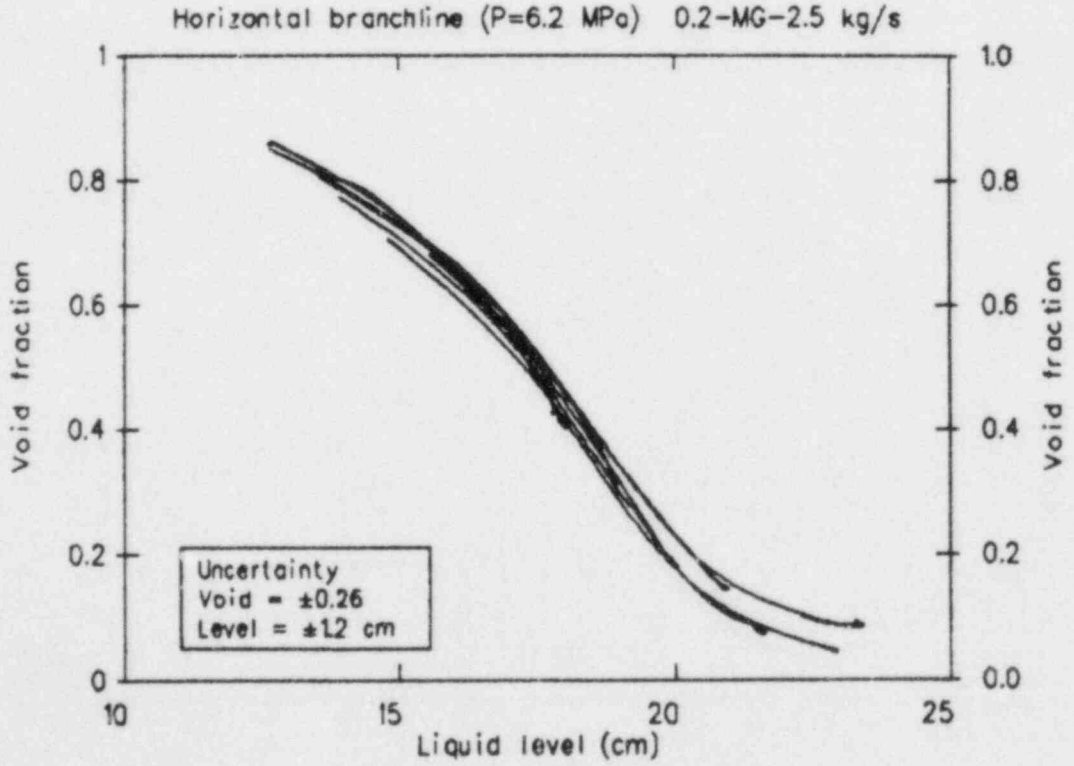

Figure 30. Transient branchline void fraction for steam flow rates of 0.2 to 2.5 kg/s, of horizontal configuration 6.2 MPa data.

liquid level. The mean and tolerance limits, and averaged data, for this data subset is shown in Figure 31. The averaged data fall mostly within the tolerance limits which show an increase at the onset level of vapor pull-through (at about 22 cm). The branchline void fraction for the 3 kg/s data subset is presented in Figure 32, with the mean and tolerance limits and the averaged data for the same data set presented in Figure 33. The mean, tolerance limits, and averaged data for the entire data set and both subsets are presented in Figure 34. The averaged data points lie within the tolerance limits of the transient data. The tolerance limits for the void fraction are greater for the 3 kg/s steam flow points than for the reduced steam flow points—opposite previously observed behavior. No explanation for this fact is offered.

The differential pressure from the mainline to the branchline (PDE-341) for the reduced steam flow rate data subset is presented in Figure 35. This data has a small variance and exhibits the property of decreasing pressure drop with decreasing level, to a minimum at about 19 cm, and then increasing as the level continues to decrease to the level at which liquid entrainment stops. This effect is due to the fact that the two-phase pressure drop is proportional to the ratio of branchline mass flow rate squared to two-phase density. The mean and tolerance limits for these data are shown in Figure 36. The tolerance limits show an increase in the level region at which vapor pull-through occurs (about 22 cm). The transient data for the 3 kg/s steam flow data subset is presented in Figure 37, with the mean and tolerance limits shown in Figure 38. The means for the two subsets and the mean and tolerance limits for the entire 6.2 MPa data set are presented in Figure 39. The tolerance limits increase in the region where the two data subsets overlap (which may be due to the different steam flow rates), however, the mean seems to transition between the two subsets in a continuous manner.

Horizontal—4.4 MPa Data. Data averages for the constant level, steady-state portions of the 4.4 MPa test points are provided in Table H-8. Selected measurements and parameters are presented in Appendix C. The branchline mass flow rate, flow quality, void fraction, and pressure drop as functions of the mainline liquid level are presented for the 10 transient level test points performed at 4.4 MPa.

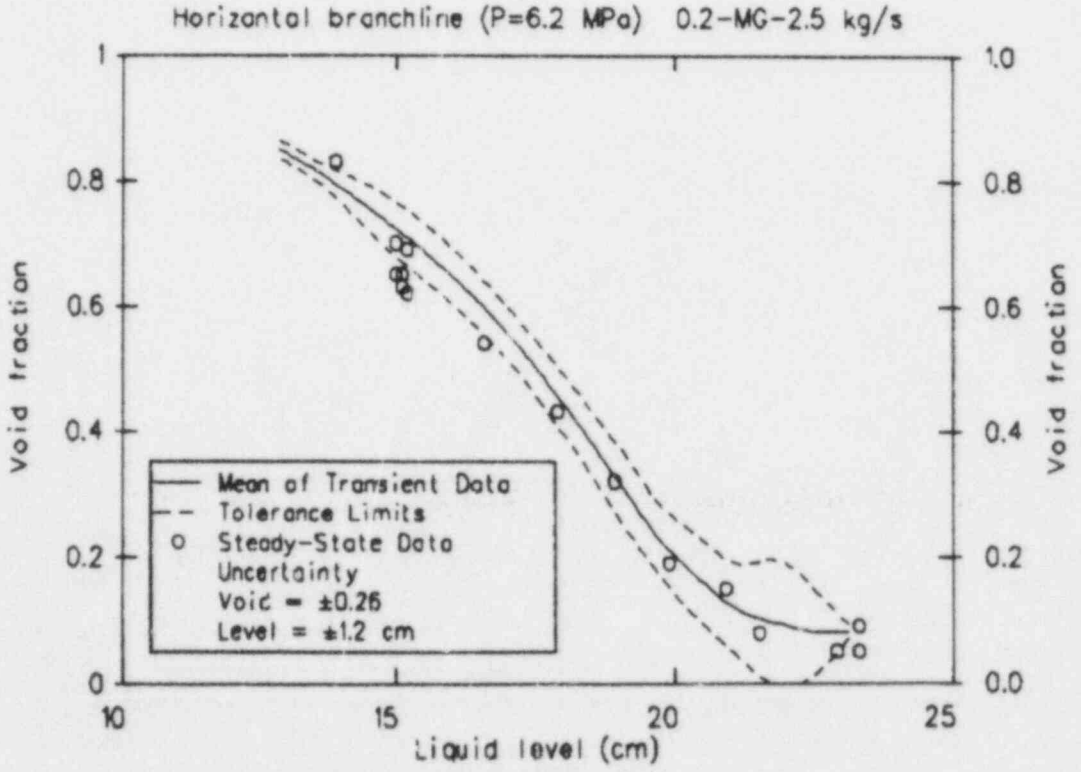

Figure 31. Mean of transient branchline void fraction for steam flow rates of 0.2 to 2.5 kg/s, of horizontal configuration 6.2 MPa data.

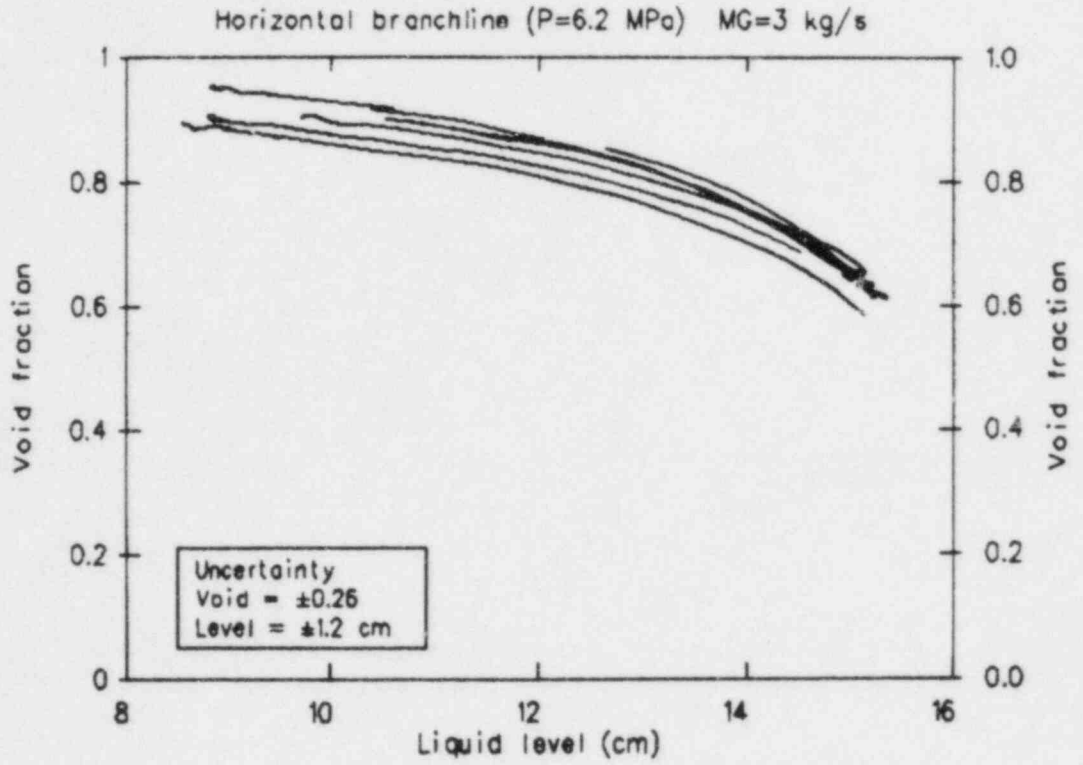

Figure 32. Transient branchline void fraction for steam flow rate of 3 kg/s, of horizontal configuration 6.2 MPa data.

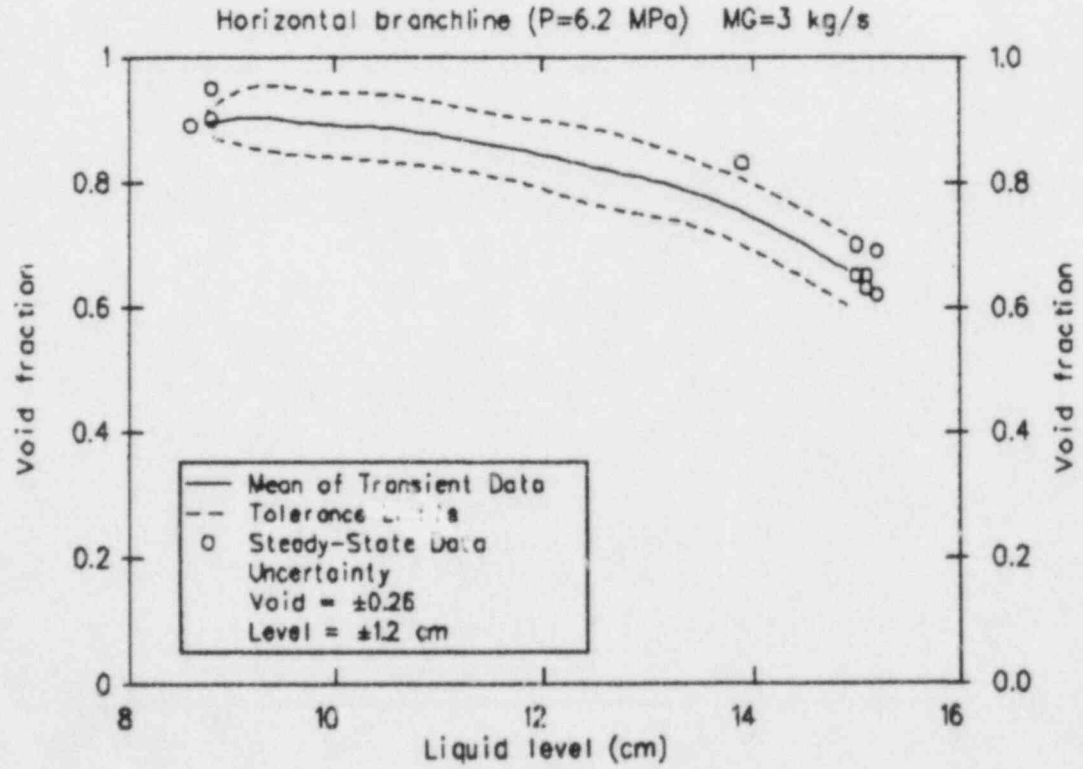

Figure 33. Mean of transient branchline void fraction for steam flow rate of 3 kg/s, of horizontal configuration 6.2 MPa data.

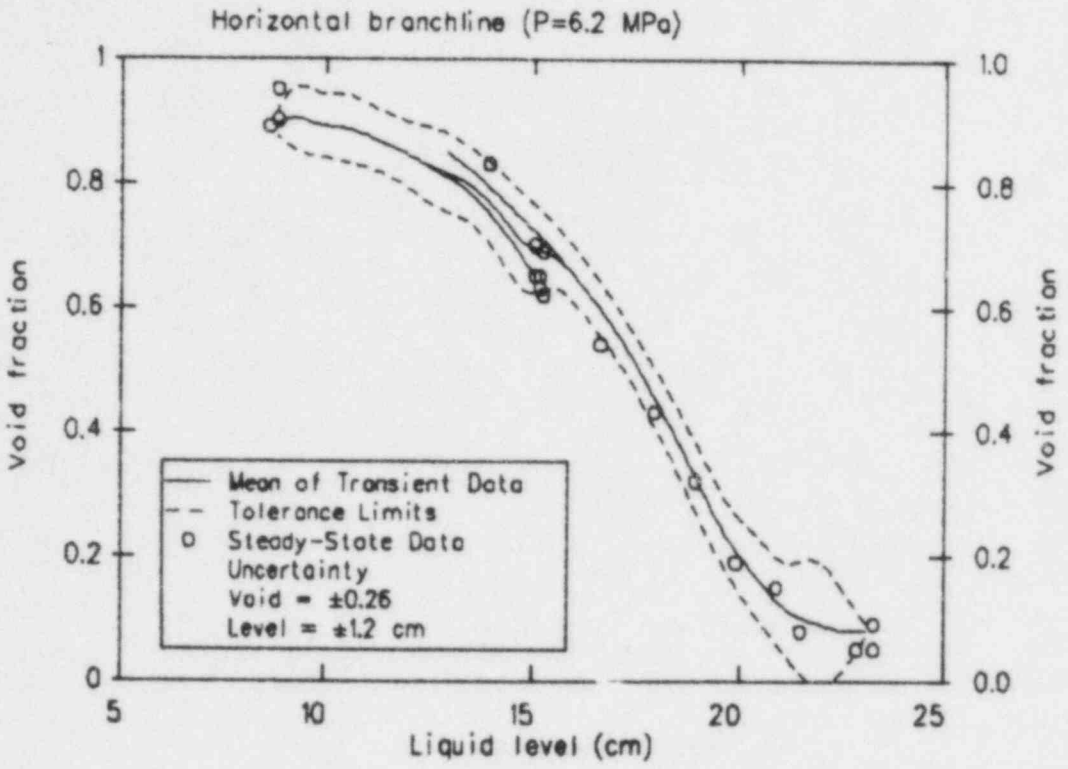

Figure 34. Mean of transient branchline void fraction for all steam flow rates, of horizontal configuration 6.2 MPa data.

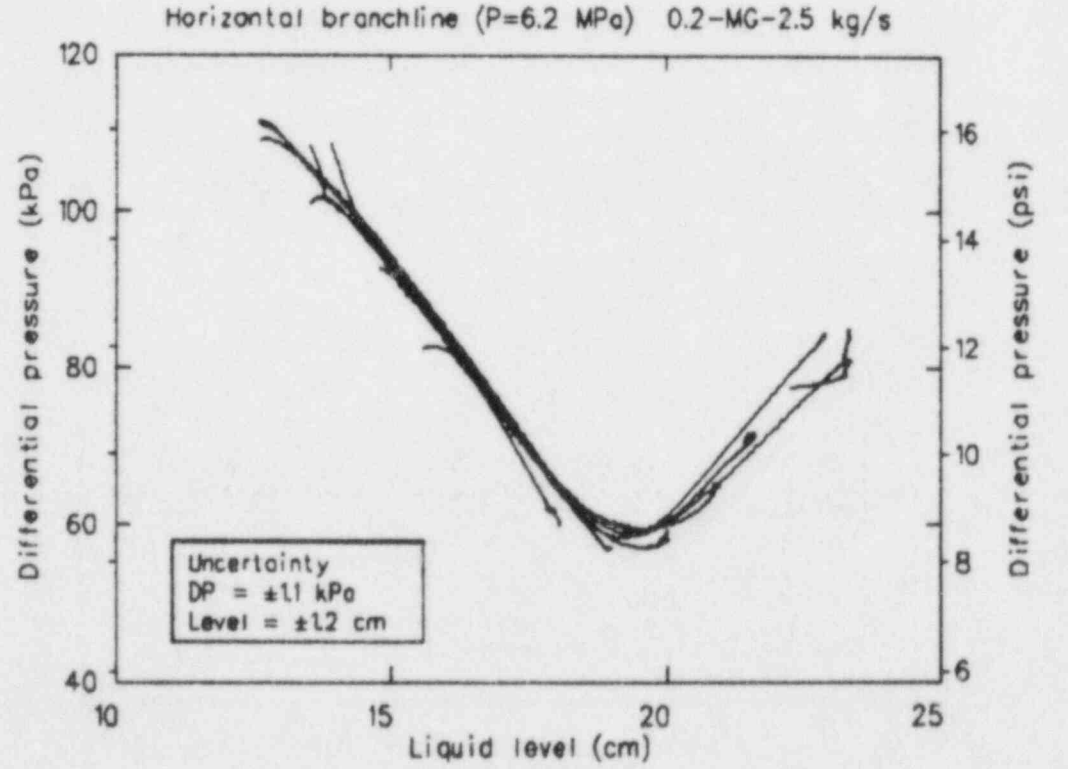

Figure 35. Transient branchline to mainline pressure drop for steam flow rates of 0.2 to 2.5 kg/s, of horizontal configuration 6.2 MPa data.

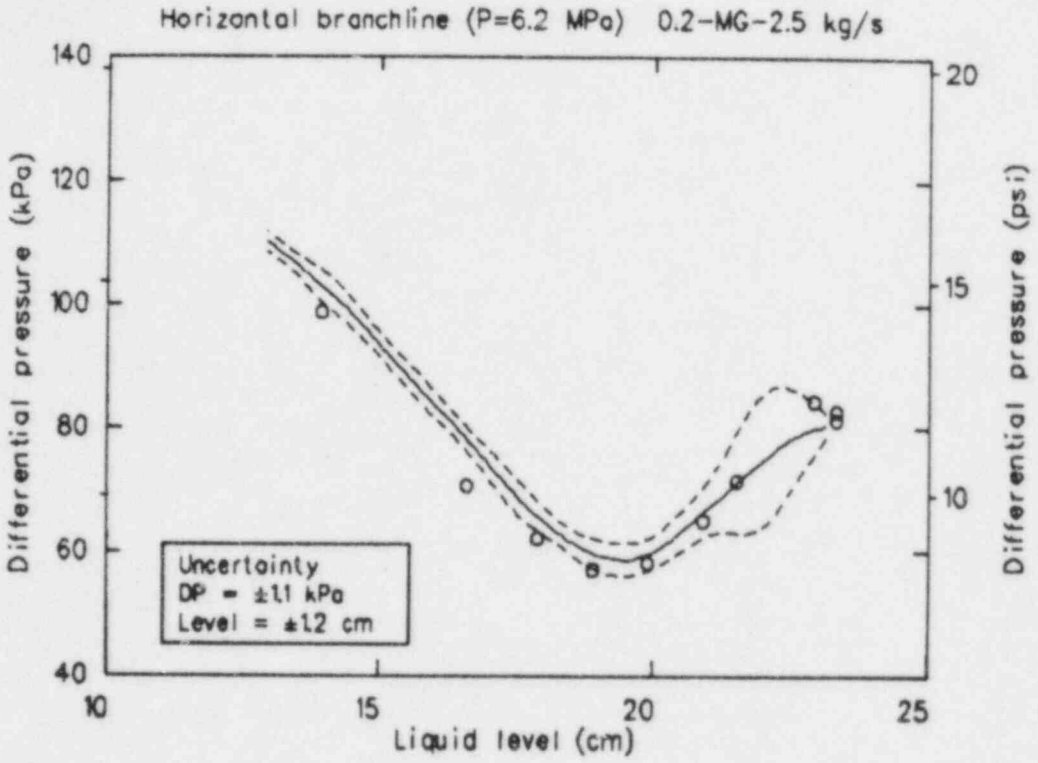

Figure 36. Mean of transient branchline to mainline pressure drop for steam flow rates of 0.2 to 2.5 kg/s, of horizontal configuration 6.2 MPa data.

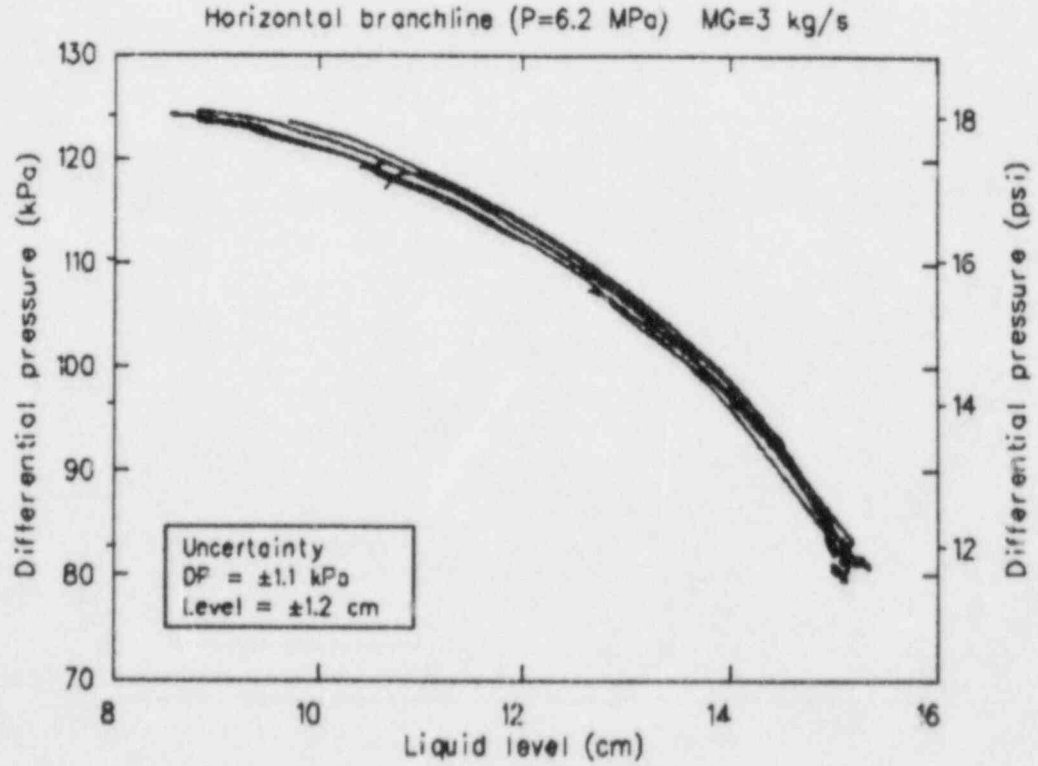

Figure 37. Transient branchline to mainline pressure drop for steam flow rate of 3 kg/s, of horizontal configuration 6.2 MPa data.

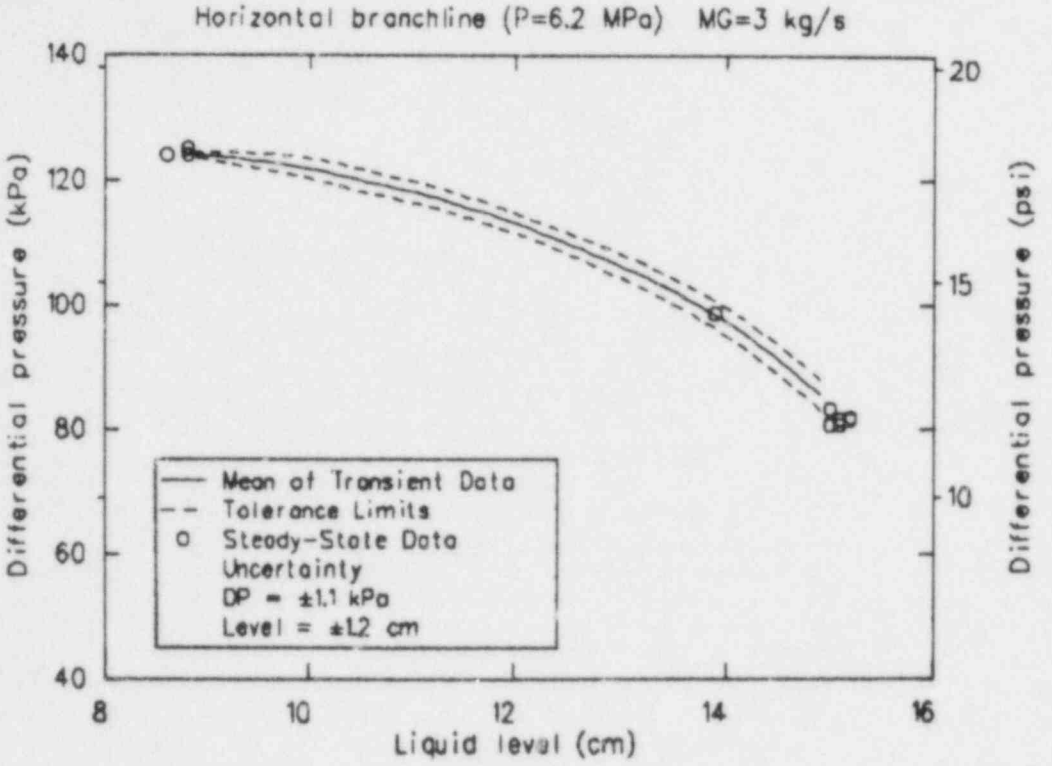

Figure 38. Mean of transient branchline to mainline pressure drop for steam flow rate of 3 kg/s, of horizontal configuration 6.2 MPa data.

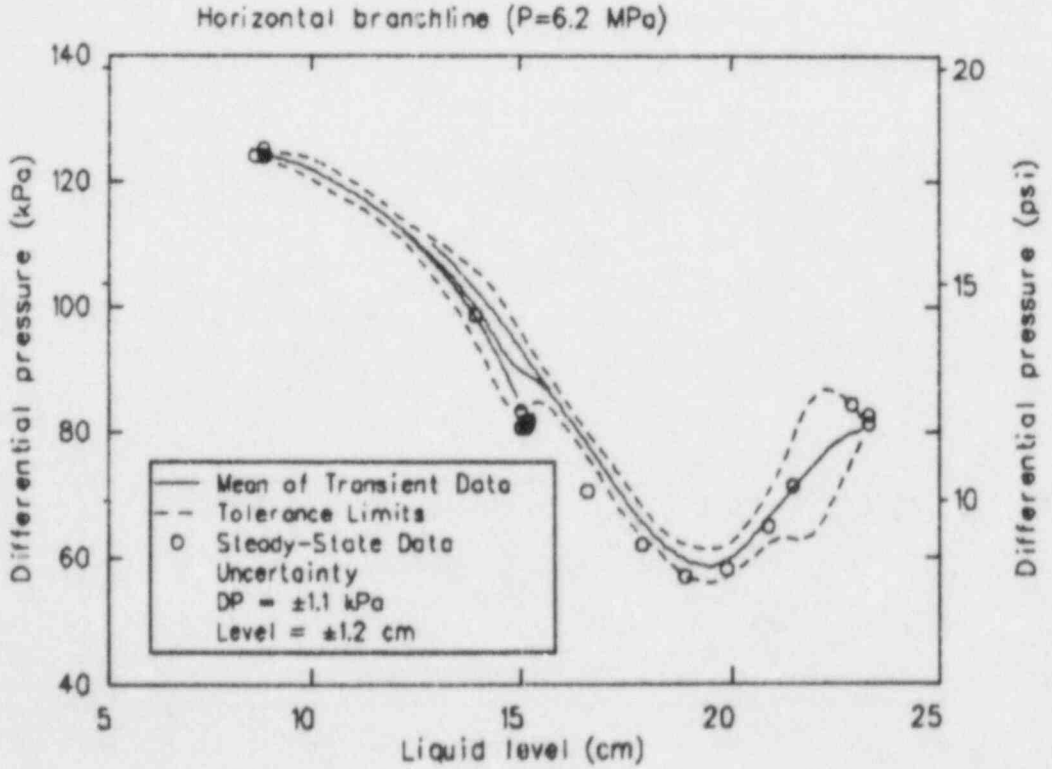

Figure 39. Mean of transient mainline to branchline pressure drop for all steam flow rates, of horizontal configuration 6.2 MPa data.

The branchline mass flow rate as a function of the mainline stratified liquid level for the 10 transient test points is presented in Figure 40, with the mean of the data, the data tolerance limits, and the averaged data presented in Figure 41. The steady-state data follows the mean of the transient data quite closely. The tolerance limits increase for levels above about 15 cm and are probably an effect of the reduced steam flow rates used to obtain these higher levels.

The branchline flow quality as a function of the mainline liquid level for the 10 transient data runs at 4.4 MPa is shown in Figure 42, with the mean, upper tolerance limit, and the steady-state data presented in Figure 43. The tolerance limit for this data is significantly smaller than for the 6.2 MPa data set, and is well within the flow quality measurement uncertainty of 0.1. The sharp increase in flow quality occurs as a result of the beginning of vapor pull-through at a mainline liquid level of approximately 22 cm, as was observed for the 6.2 MPa data set. Extrapolation of the flow quality data to a value of 1 predicts a level of 8 cm for the onset of liquid entrainment. The steady-state data follow the transient mean, and lie within the tolerance limits.

The branchline void fraction as a function of the mainline liquid level is presented in Figure 44, with the mean, tolerance limits, and steady-state data presented in Figure 45. Most of the steady-state data follow the mean and fall within the tolerance limits of the transient data. The tolerance limits tend to increase when the mainline liquid level is within branchline entrance level (between 12.5 and 15.9 cm).

The differential pressure from the mainline to the branchline is presented in Figure 46 as a function of the mainline liquid level for the 10 transient test runs with the mean, tolerance limits, and steady-state data presented in Figure 47. These data show the same relationship to liquid level (a minimum at about 19 cm) as for the 6.2 MPa data set.

Horizontal—3.45 MPa Data. Data averages for the constant level steady-state portions of the 3.45 MPa data runs are provided in Table H-9. Plots of selected measurements and computed parameters are provided in Appendix D. The branchline mass flow rate, flow quality, void fraction, and pressure drop for the nine transient data runs performed at 3.45 MPa are presented and discussed next.

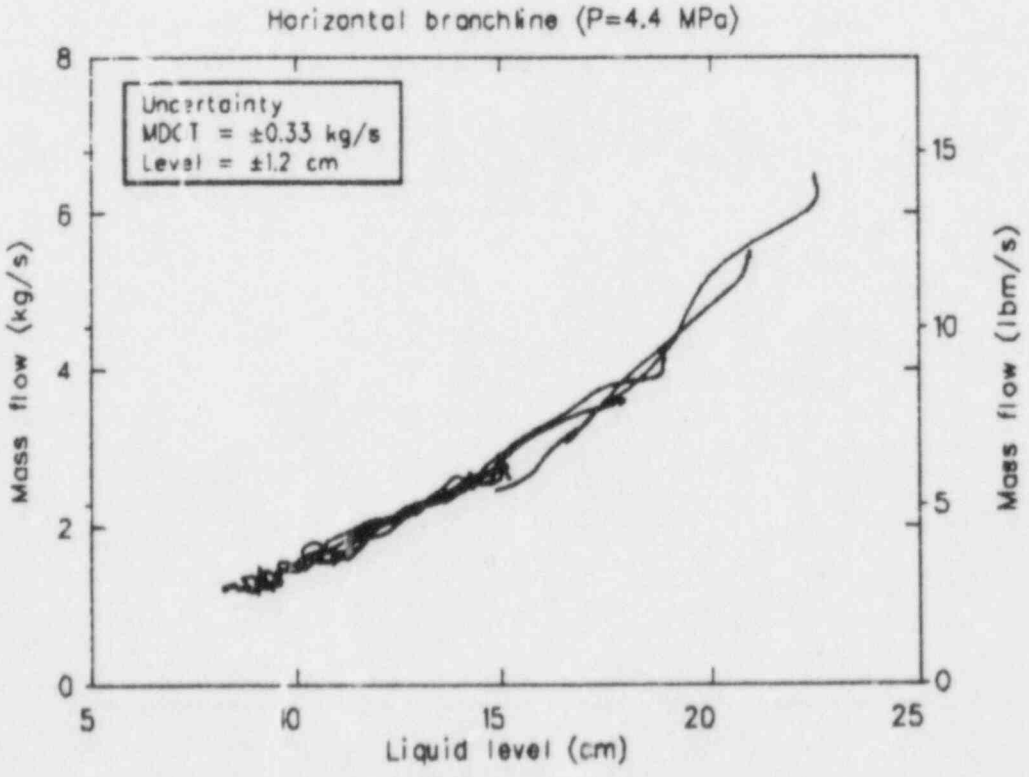

Figure 40. Transient branchline mass flow rates, of horizontal configuration 4.4 MPa data.

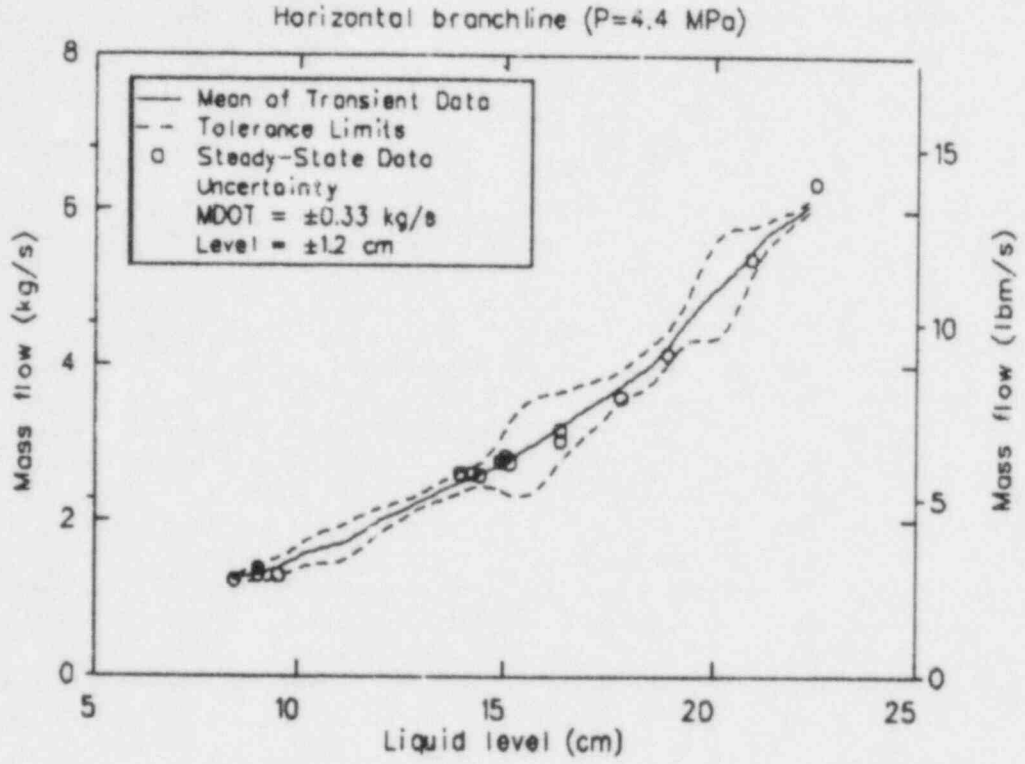

Figure 41. Mean of transient branchline mass flow rates, of horizontal configuration 4.4 MPa data.

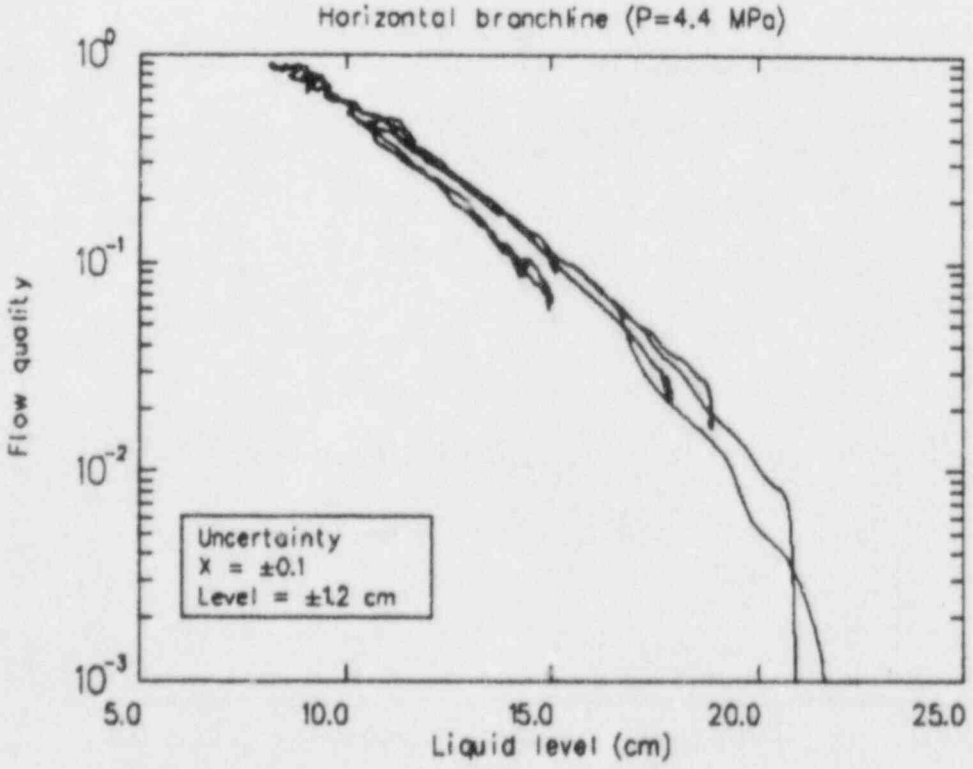

Figure 42. Transient branchline flow quality, of horizontal configuration 4.4 MPa data.

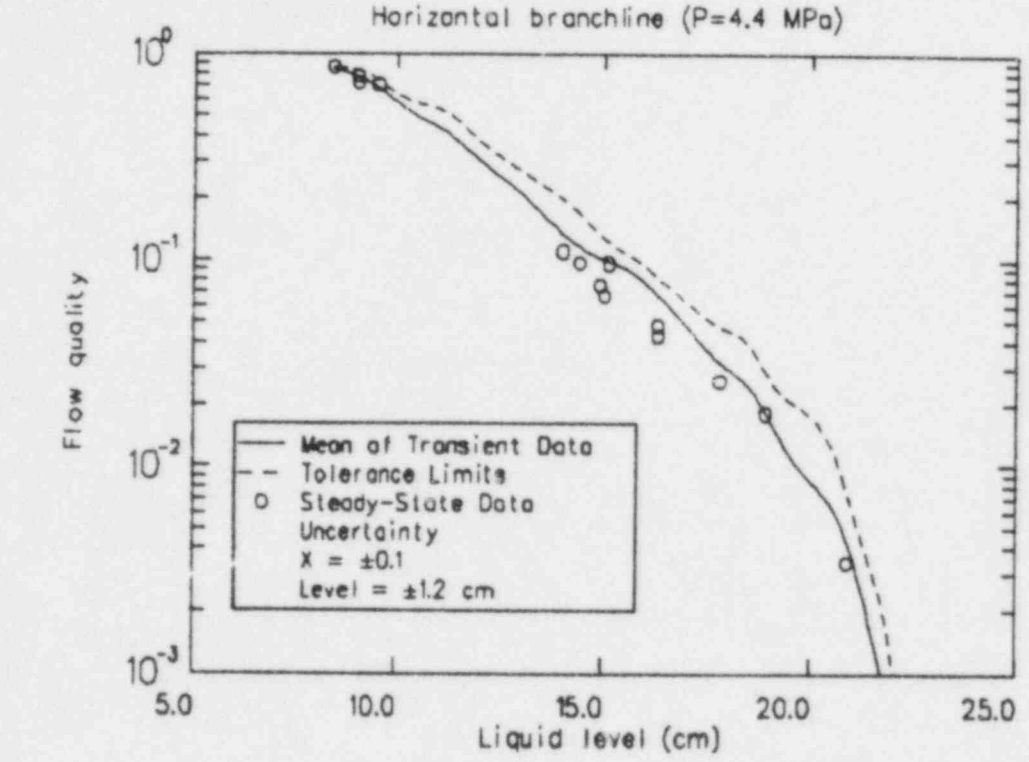

Figure 43. Mean of transient branchline flow quality, of horizontal configuration 4.4 MPa data.

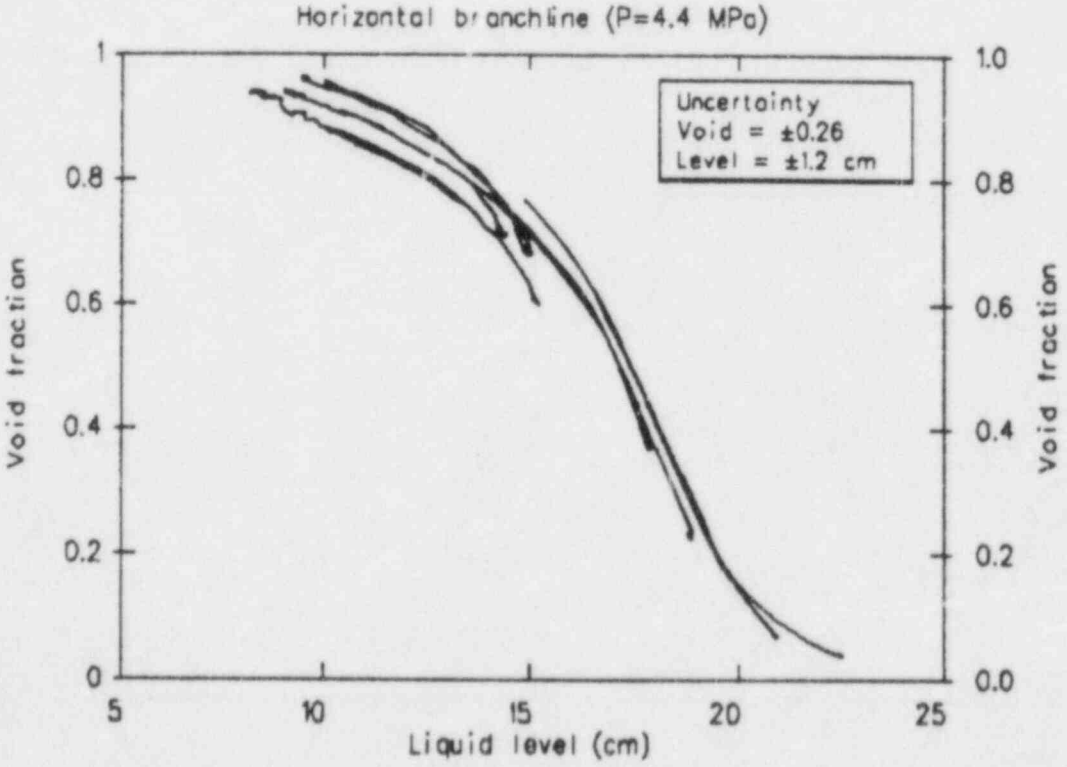

Figure 44. Transient branchline void fraction, of horizontal configuration 4.4 MPa data.

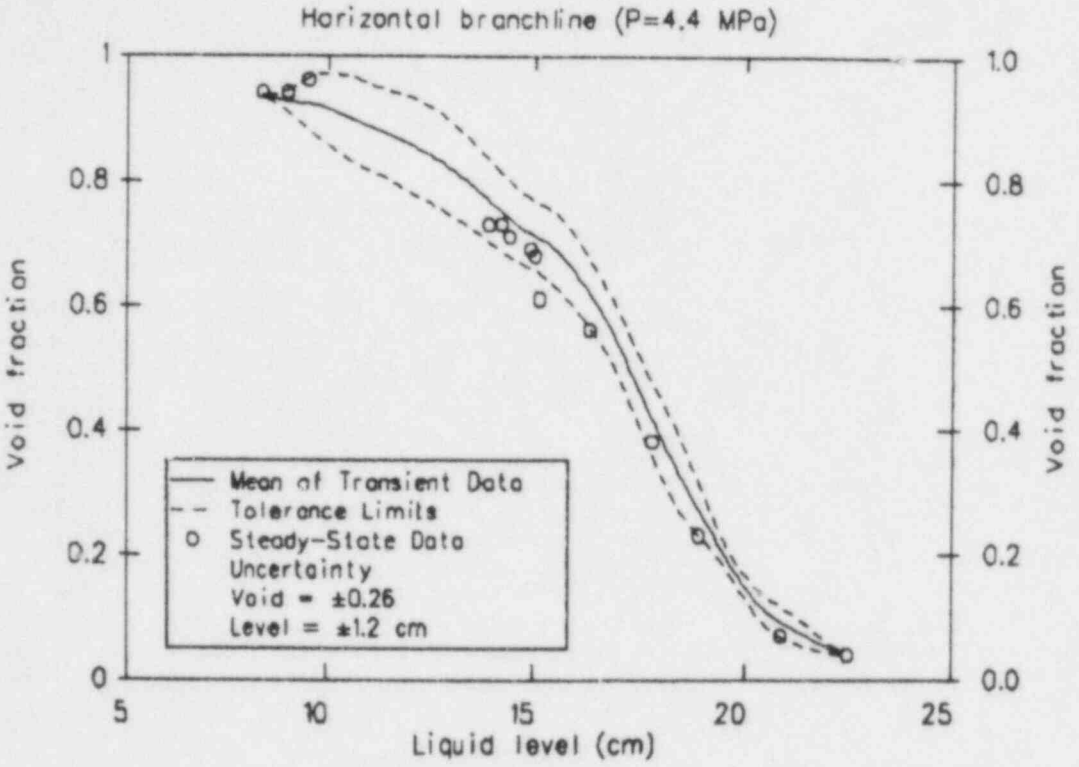

Figure 45. Mean of transient branchline void fraction, of horizontal configuration 4.4 MPa data.

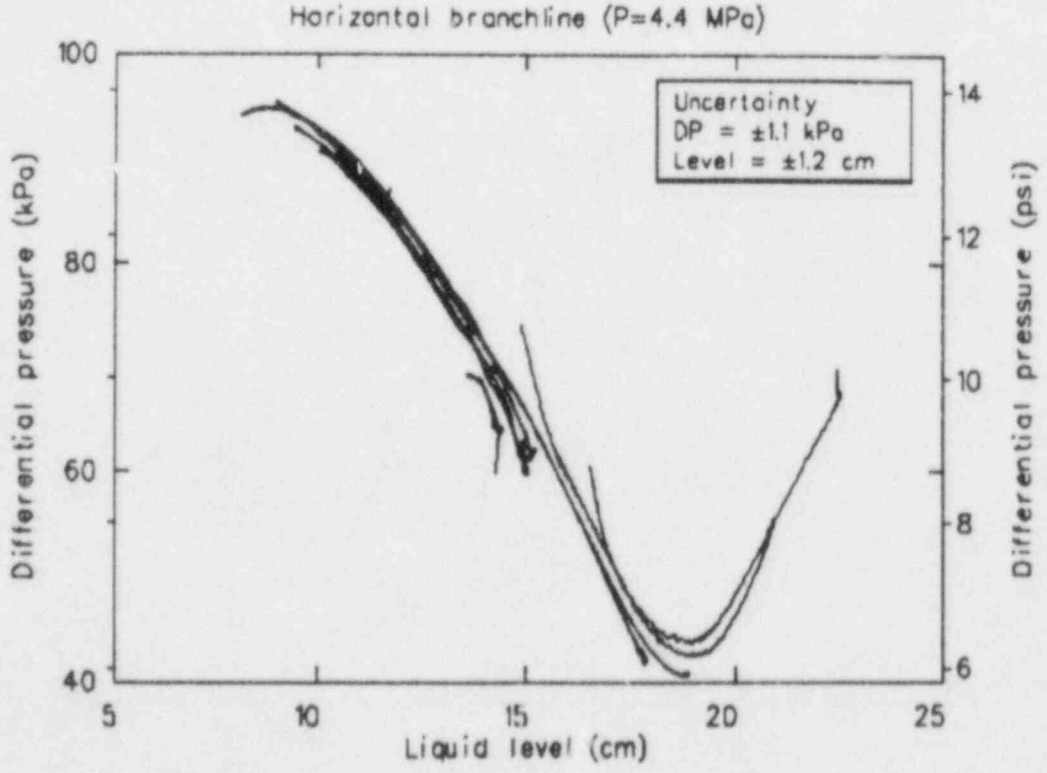

Figure 46. Transient mainline to branchline pressure drop, of horizontal configuration 4.4 MPa data.

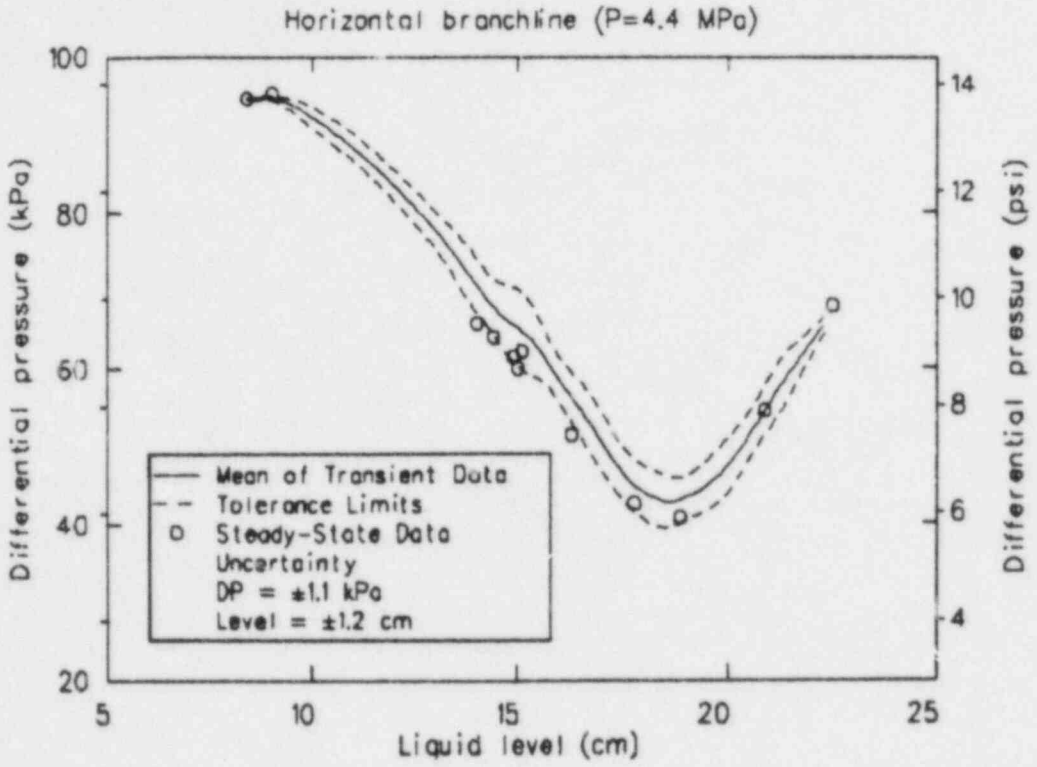

Figure 47. Mean of transient mainline to branchline pressure drop, of horizontal configuration 4.4 MPa data.

The branchline mass flow rate as a function of the mainline stratified liquid level is presented in Figure 48 for the nine transient data points, with the mean, tolerance limits, and averaged data shown in Figure 49. All of the averaged data lie within the tolerance limits, with the maximum tolerance limit ±0.3 kg/s on the branchline centerline.

The branchline flow quality as a function of the mainline liquid level is shown in Figure 50. The mean and upper tolerance limit for these data, along with the averaged data for the steady-state portions of all the data points, is presented in Figure 51. The steady-state data lie within the tolerance limits, with the largest tolerance limit in the vicinity of the vapor pull-through level of approximately 22 cm. Extrapolation of this data to a flow quality of 1 results in an onset of liquid entrainment level of about 7.5 cm.

The branchline void fraction for the nine transient points is shown in Figure 52. The mean and tolerance limits for this data, along with the averaged data, is shown in Figure 53.

The mainline to branchline differential pressure is shown in Figure 54, with the mean, tolerance limits, and averaged data presented in Figure 55. The tolerance limits are largest for levels above the minimum in the pressure drop curve.

Comparison of 6.2, 4.4, and 3.45 MPa Horizontal Data. A comparison of the mean branchline flow rate versus mainline liquid level for the three different pressures is shown in Figure 56. To aid in comparison to other data sets, a second x-axis of nondimensional liquid level (h/D) is provided. As would be expected, there is a direct dependency of the branchline flow rate on pressure. The slope of the data (as a function of liquid level) is essentially the same for all three pressures, with an apparent change in slope for the 6.2 and 3.4 MPa data at a level corresponding to the top of the branchline (15.9 cm). In addition to the mean data for the three pressures, data averages for steady-state portions of all the horizontal data points are included on Figure 56. The trends in the steady-state data match those of the transient means of the data points.

The mean branchline flow quality for the three pressures, as a function of liquid level, is compared in Figure 57. In this case, there appears to be a dependency on pressure for levels above the branchline centerline in which increasing pressure results

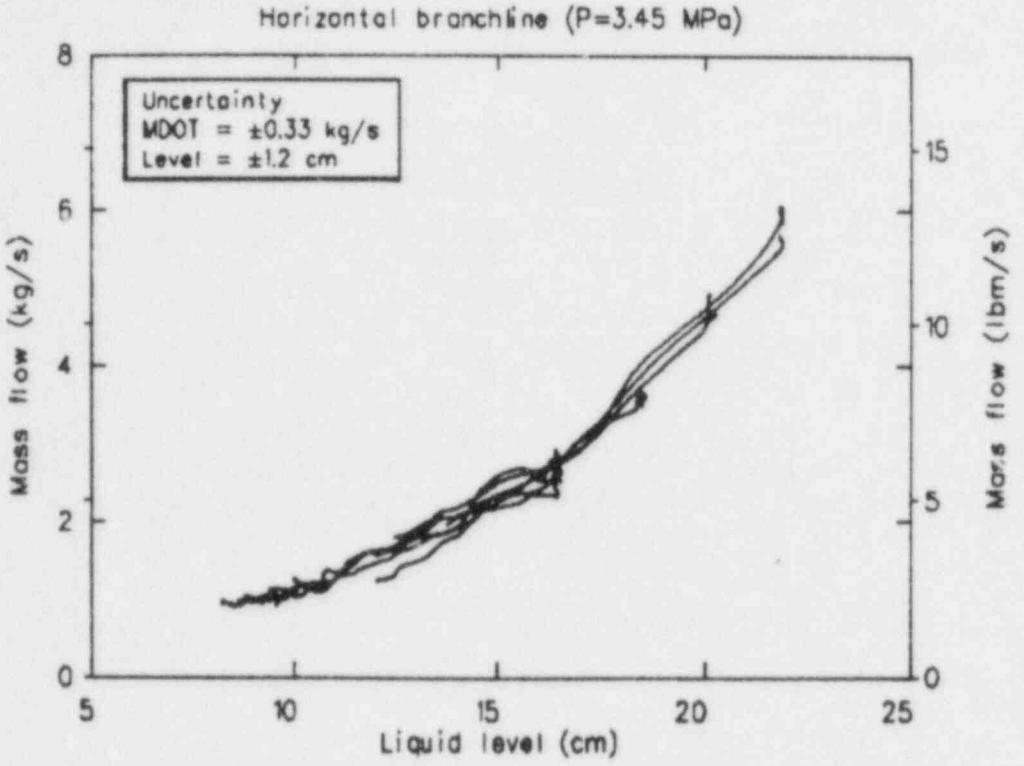

Figure 48. Transient branchline mass flow rates, of horizontal configuration 3.45 MPa data.

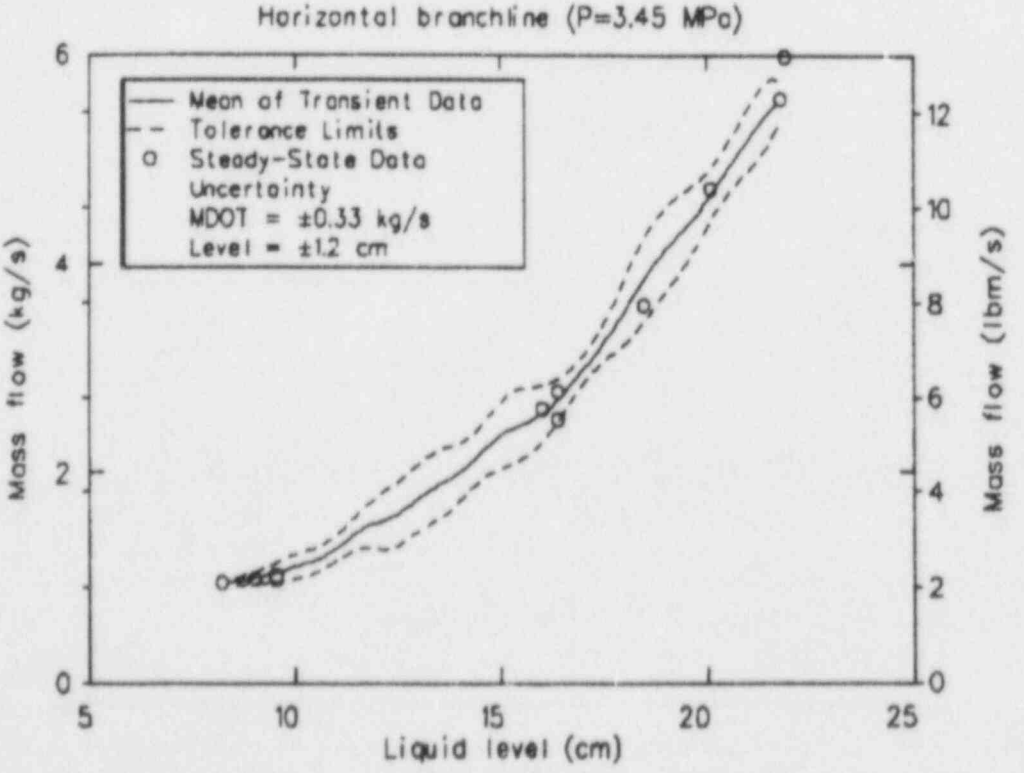

Figure 49. Mean of transient branchline mass flow rates, of horizontal configuration 3.45 MPa data.

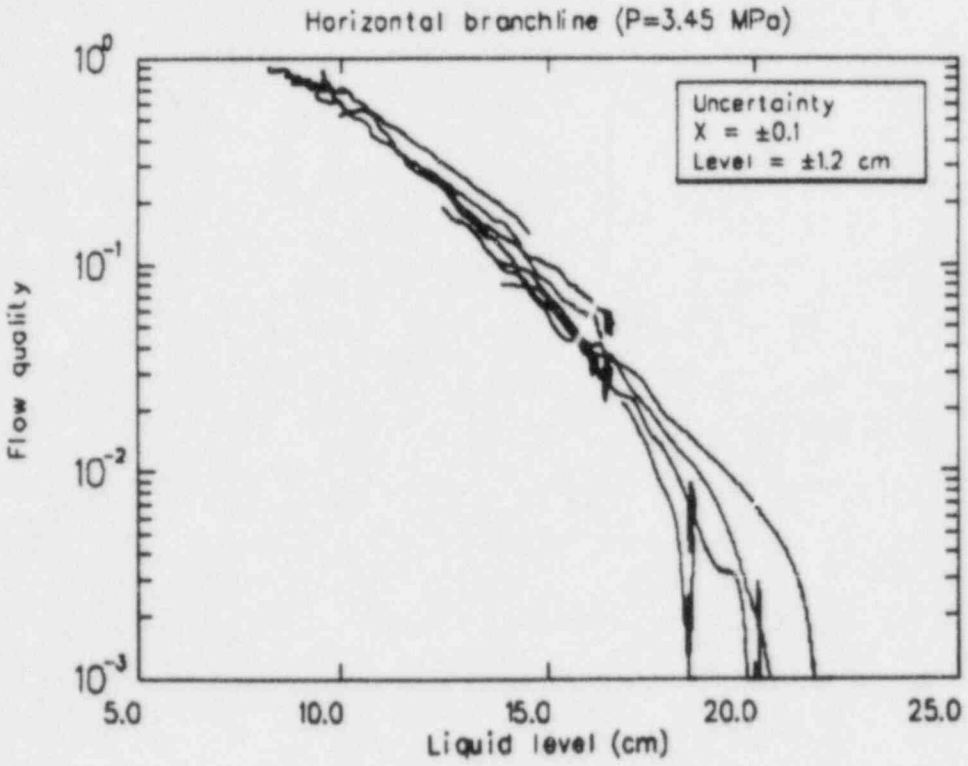

Figure 50. Transient branchline flow quality, of horizontal configuration 3.45 MPa data.

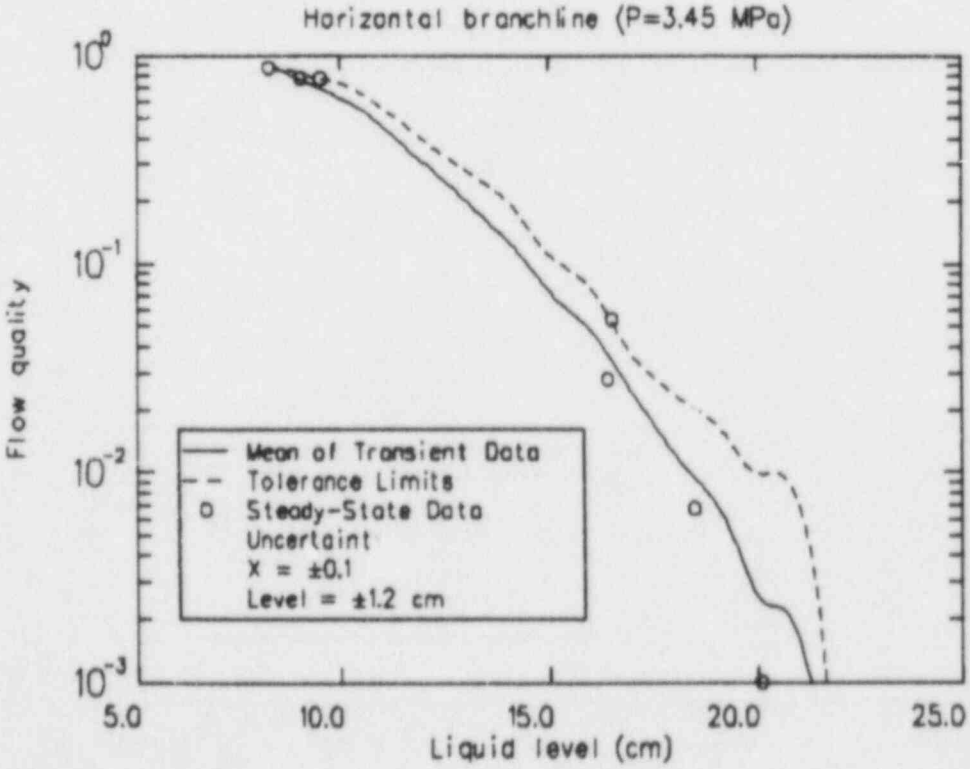

Figure 51. Mean of transient branchline flow quality, of horizontal configuration 3.45 MPa data.

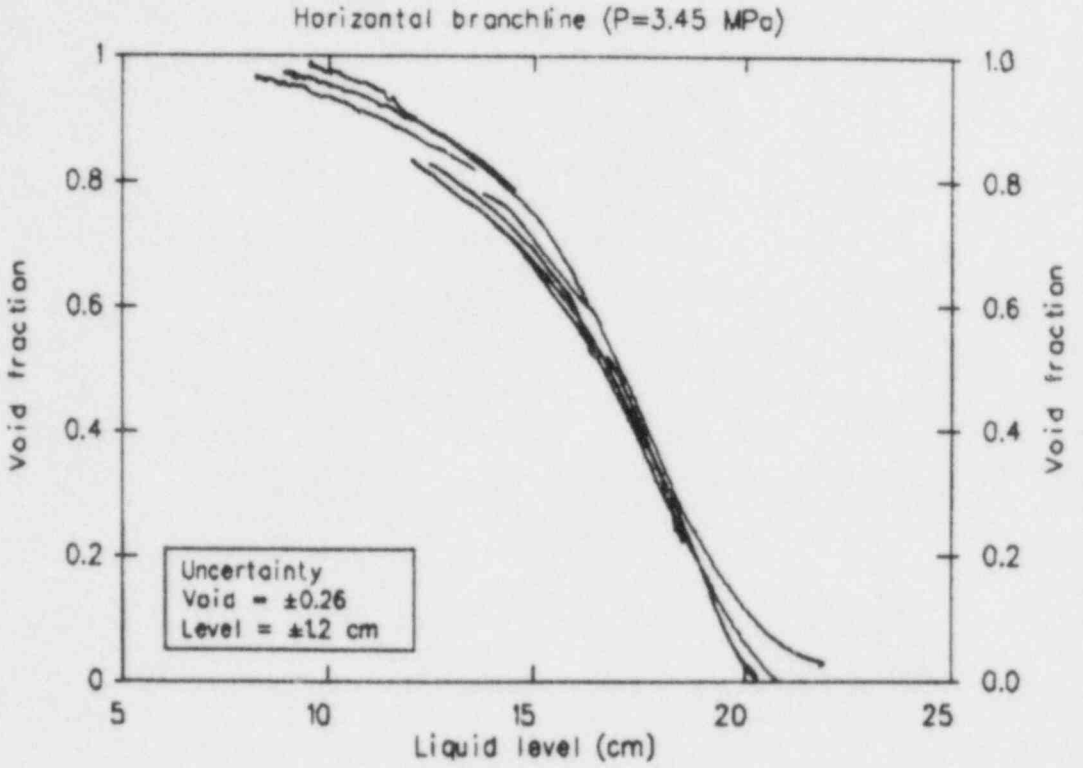

Figure 52. Transient branchline void fraction, of horizontal configuration 3.45 MPa data.

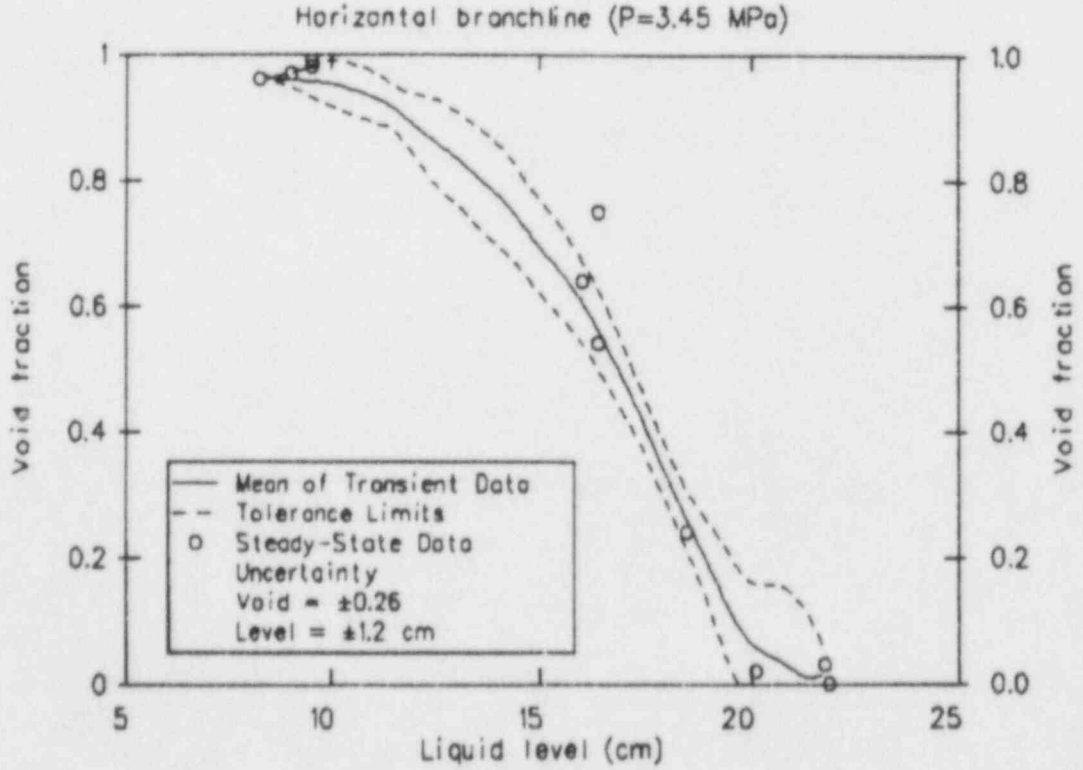

Figure 53. Mean of transient branchline void fraction, of horizontal configuration 3.45 MPa data.

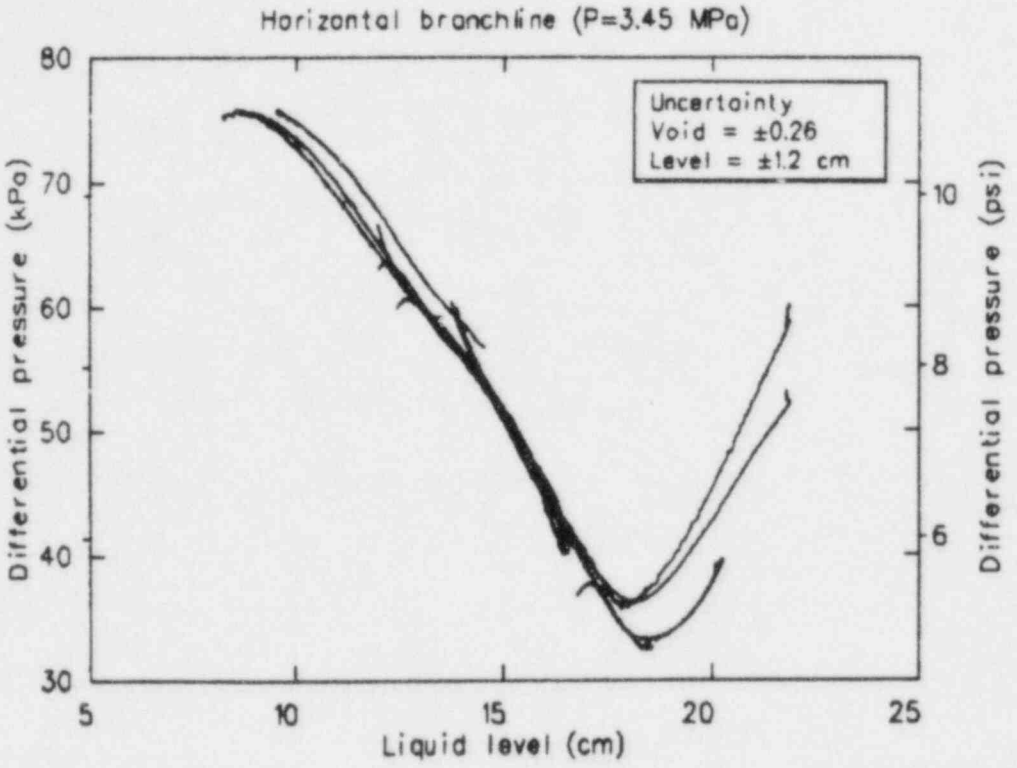

Figure 54. Transient mainline to branchline pressure drop, of horizontal configuration 3.45 MPa data.

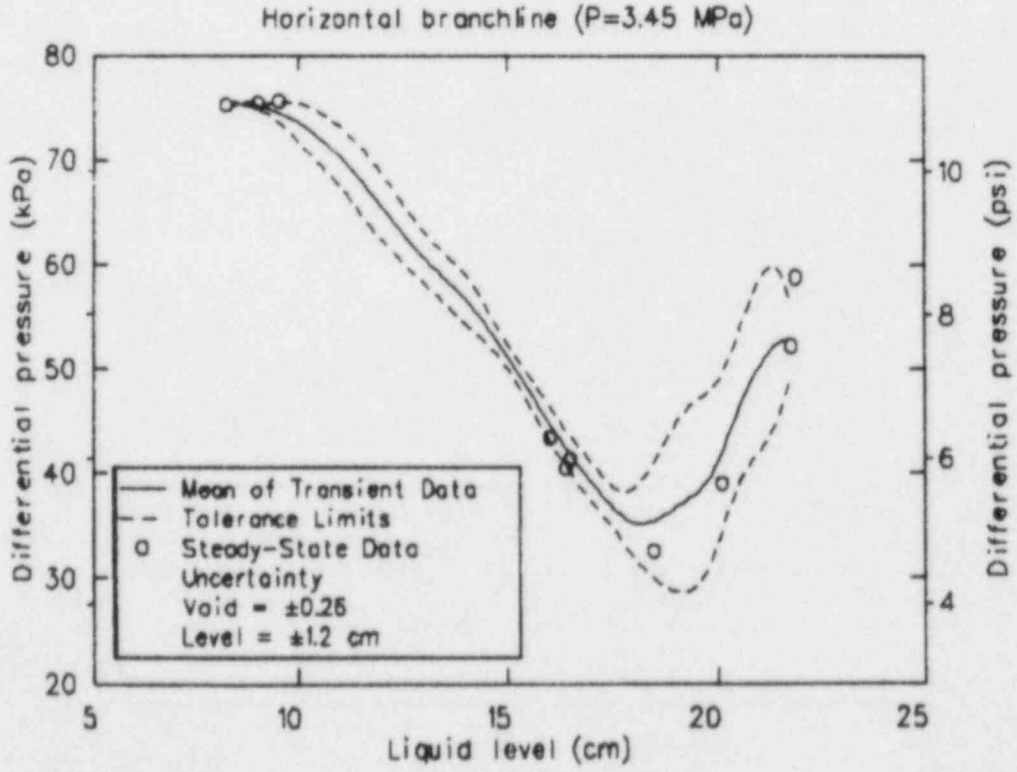

Figure 55. Mean of transient mainline to branchline pressure drop, of horizontal configuration 3.45 MPa data.

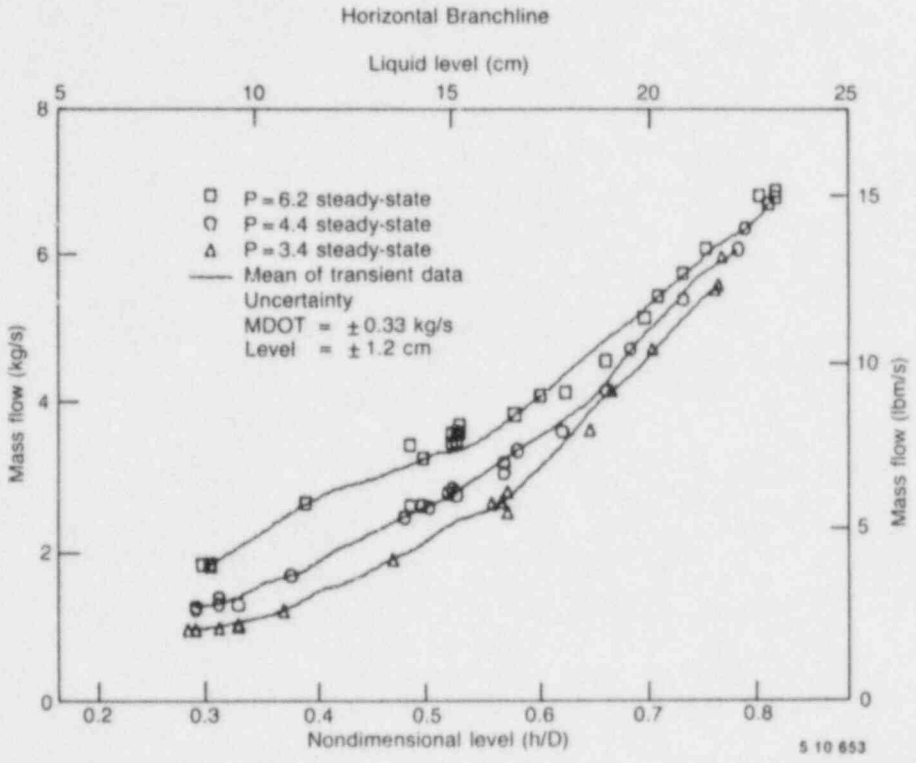

Figure 56. Comparison of steady-state and mean of transient branchline mass flow rate data for the three test pressures of horizontal configuration data.

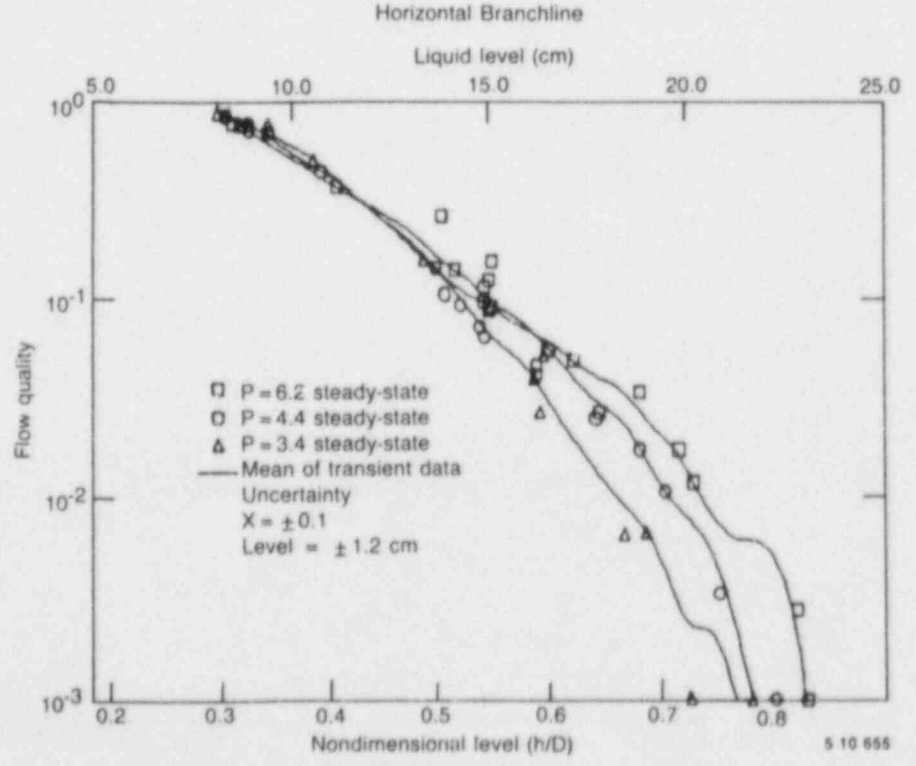

Figure 57. Comparison of steady-state and mean of transient branchline flow quality data for the three test pressures of horizontal configuration data.

in increasing flow quality. The steady-state data, included on Figure 57, has the same trends as the transient data and the magnitude of the flow quality is very close to the transient means. There also appears to be a dependency of the onset of pull-through level on pressure, with increasing pressure resulting in vapor pull-through occurring at higher levels. This type of dependency is predicted by Equation (7).

The mean branchline void fraction versus mainline liquid level for the three different pressures are compared in Figure 58. The major feature of Figure 58 is the equal branchline void fractions observed for the three different pressures at a liquid level corresponding to approximately the top of the branchline. There appears to be a pressure dependency, with decreasing void fraction as the pressure decreases, for levels above the top of the branchline (15.9 cm). For levels below the top of the branchline, this dependency is reversed. This observation is consistent with a pressure dependency for the levels at which vapor pull-through and liquid entrainment occur. Although the reason for equal void fractions for the three pressures at a level of the top of the branchline is not obvious, the steady-state data follows basic trends of the transient data with a slightly larger scatter.

An overlay of the mainline to branchline mean pressure drops for these three pressures is shown in Figure 59. There is an obvious dependency of the magnitude of the pressure drop on mainline pressure, presumably due to the different branchline mass flow rates at the different pressures. The level at which minimum pressure drops occur appears to decrease with decreasing mainline pressure.

Examples of the nonfiltered pressure drop data as a function of the liquid level are shown in Figures 60-62 for the three pressures. The data in these figures span the level range at which vapor pull-through occurs, and in some cases can be used for determining the level for onset of pull-through. The pressure drop data at a mainline pressure of 6.2 MPa is shown in Figure 60. In this case, the level at which pull-through begins is shown as occurring at 22 cm when the magnitude of the pressure drop sharply decreases and the noise level increases. The value tabulated in Table 6 is 22.2 cm, which is the average of the three transient points which spanned this level range. The pressure

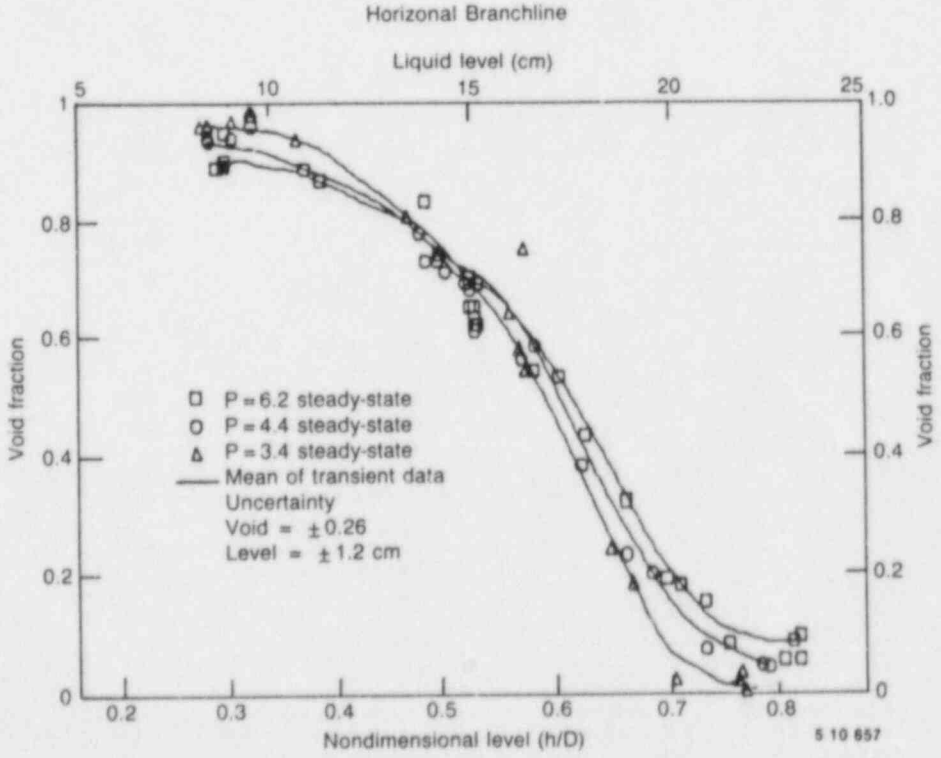

Figure 58. Comparison of steady-state and mean of transient branchline void fraction data for the three test pressures of horizontal configuration data.

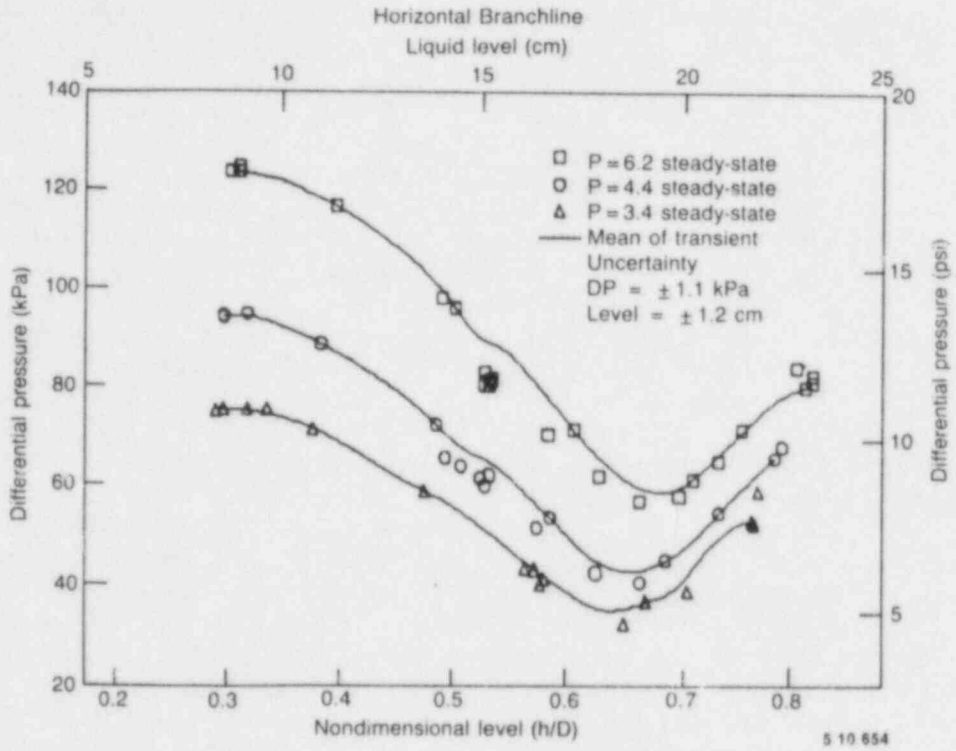

Figure 59. Comparison of steady-state and mean of transient mainline to branchline pressure drop data for the three test pressures of horizontal configuration data.

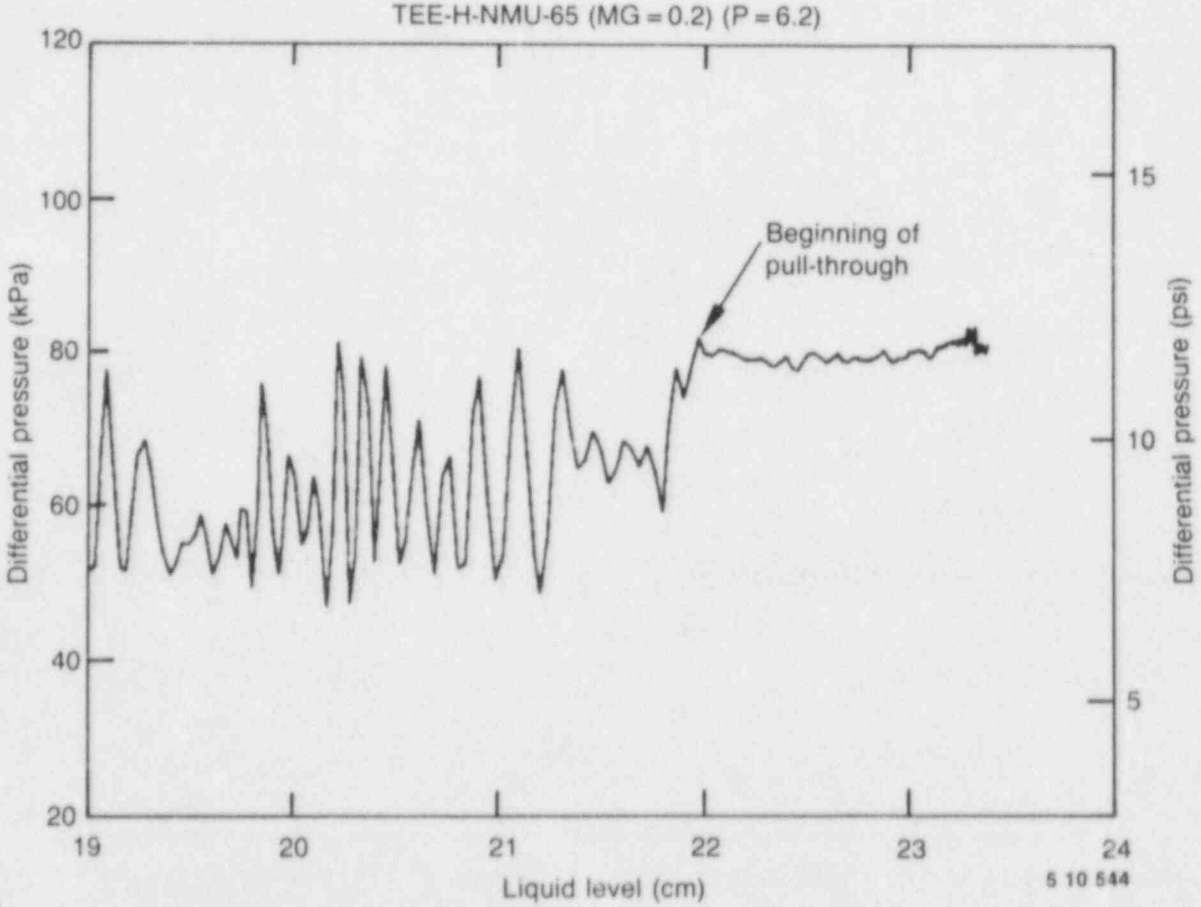

Figure 60. Example of unfiltered mainline to branchline pressure drop data, of horizontal configuration 6.2 MPa data.

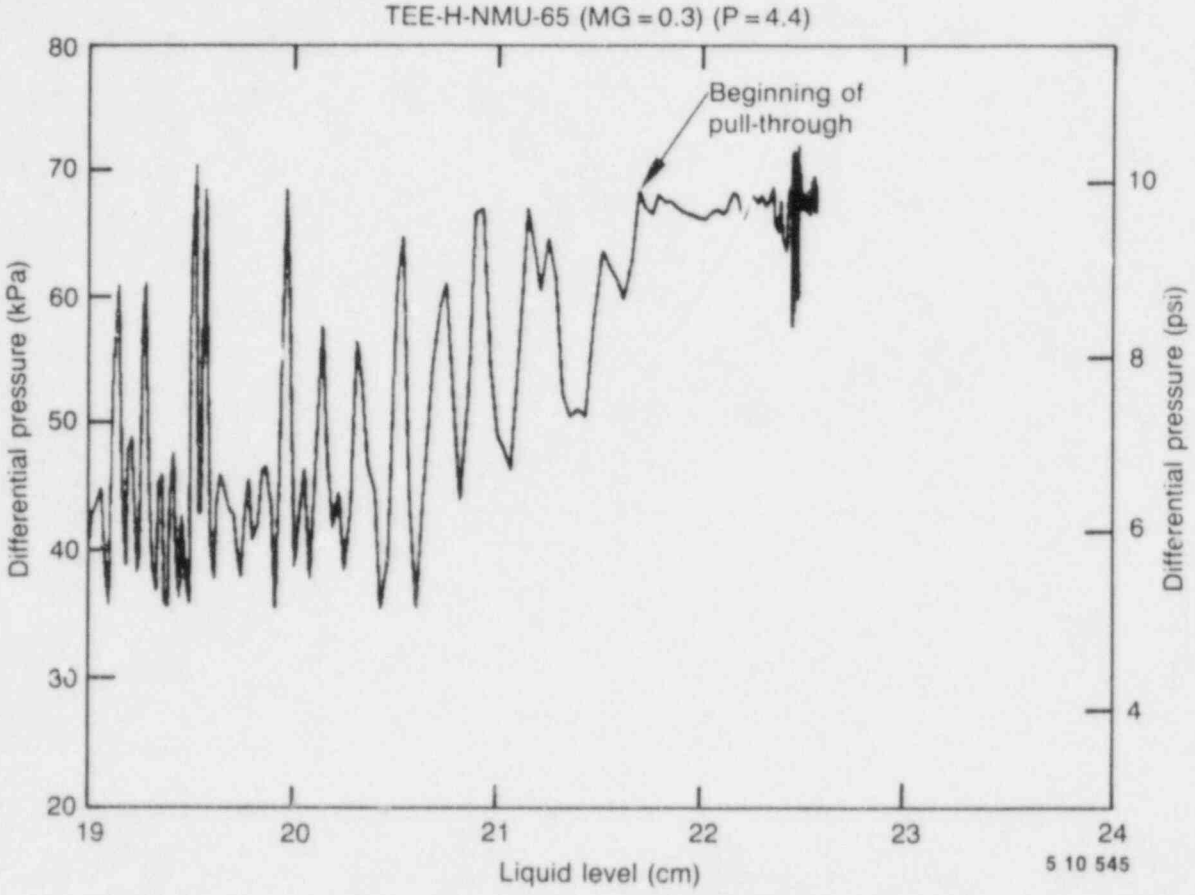

Figure 61. Example of unfiltered mainline to branchline pressure drop data, of horizontal configuration 4.4 MPa data.

drop data at 4.4 MPa is shown in Figure 61. In this case, the level at which pull-through occurs is marked as 21.7 cm. This is the value tabulated in Table 7; this transient run was the only run at 4.4 MPa that covered this level range. The pressure drop data for one of the two transient runs at 3.45 MPa, which covered the pull-through level range, is shown in Figure 62. The level at which pull-through begins is not as clear from the data in this figure due to the noise level before pull-through occurs. A value of 21.5 cm is marked as the most likely value; there is however, some uncertainty in this value (the basic uncertainty in the level measurement is 1.2 cm).

Vertical Downflow Configuration Data

A total of 45[a] data points were performed in the vertical downflow configuration (17 at 6.2 MPa, 13 at 4.4 MPa, and 15 at 3.45 MPa). Performance of these test points found that the transient points were of limited usefulness due to relatively high liquid level remaining in the mainline once the separator level dropped below the bottom of the mainline. This mainline liquid level (the stratified equilibrium level, which is a function of the steam and liquid flow rates) was only slightly lower than the level for onset of vapor pull-through. As a result, the steam mass flow rates out the branchline were small and, apparently, of an intermittent nature. Because of these small branchline steam flow rates, the measured steam flow qualities out the branchline for the transient runs are of little use because the measurement uncertainties result in uncertainties in the flow quality much larger than the measured flow quality. When this fact was recognized, further test points were performed in which the mainline liquid flow rate was reduced, resulting in lower liquid levels in the mainline and higher rates of vapor pull-through into the branchline. Since all of these points were performed with the separator level below the mainline, they are steady-state points. In general, these steady-state points are

a. Forty-five test points were performed; however, the data from one of the 3.45 MPa data points was inadvertently destroyed.

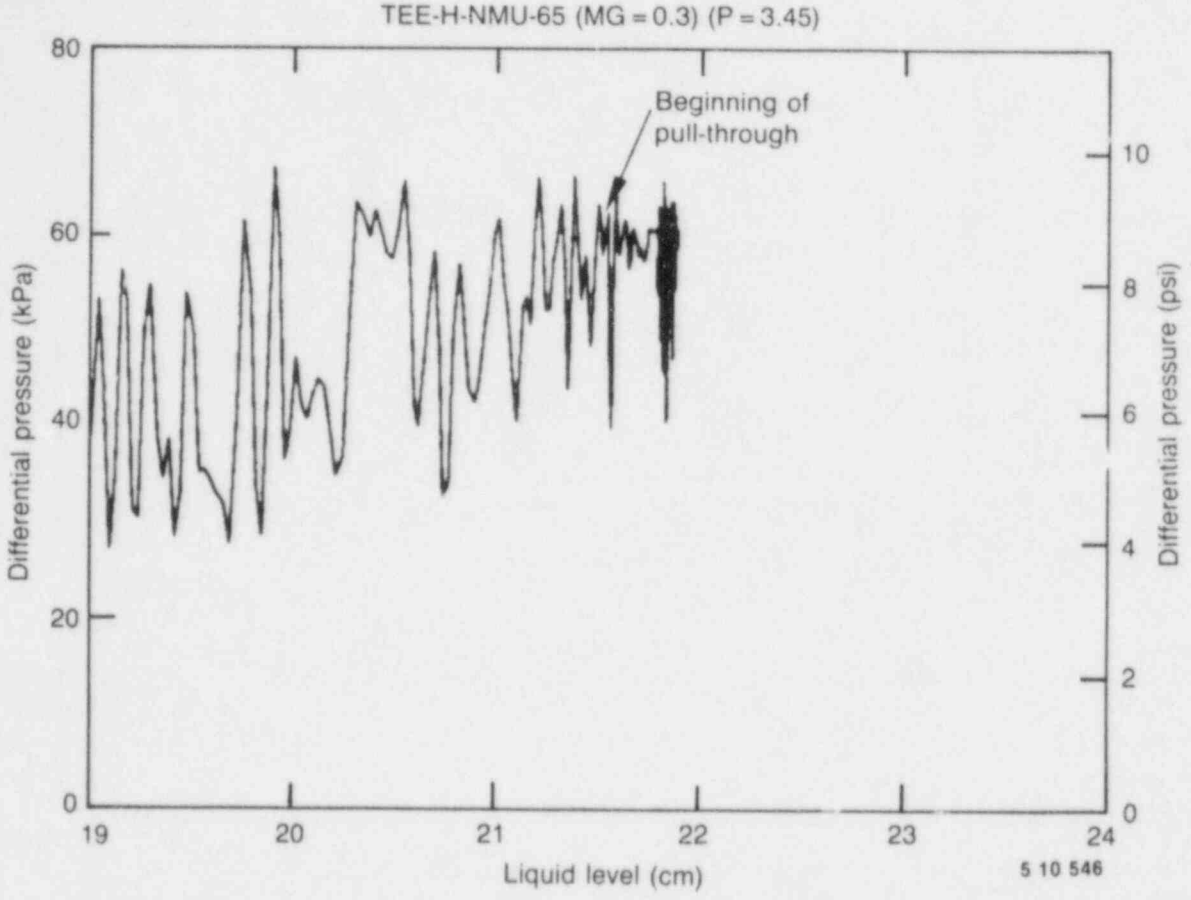

Figure 62. Example of unfiltered mainline to branchline pressure drop data, of horizontal configuration 3.45 MPa data.

Table 6. Comparison of predicted and observed levels for onsets of pull-through and entrainment for the horizontal configuration

Mainline Pressure (MPa)	Onset of Pull-Through			Onset of Entrainment			Observed Single-Phase Flow Rates (kg/s)	
	Predicted (cm)			Predicted (cm)				
	Equation (7)	Equation (10)[b]	Observed[a] (cm)	Equation (2)	Equation (9)[b]	Observed (cm)	Steam	Liquid
6.2	20.9	22.2	22.2	7.0	7.7	7.7	1.7	6.9
4.4	20.6	21.8	21.7	7.5	8.2	8.0	1.2	6.4
3.45	20.3	21.5	21.5	7.7	8.4	7.5	1.0	6.0

a. The observed onsets of vapor pull-through are based upon PDE-341, whereas the onset of liquid entrainment is based upon extrapolation of the mean flow quality versus mainline liquid level.

For the 6.2 MPa data, three transient points spanned this level and were used to determine the onset of pull-through level (a mean of 22.2 cm and a standard deviation of 0.3 cm). For the 4.4 MPa data, only a single transient run spanned the level and for the 3.45 MPa data, two transient runs were used (both resulted in the same onset level).

b. Constants used in Equations (9 and 10) are $C_e = 0.62$ and $C_p = 0.82$.

Table 7. Comparison of observed and calculated branchline flow quality with the mainline level on the centerline

Mainline Pressure (MPa)	Branchline Flow Quality at Centerline Level, X_0		C_x in Equation (11) Using X_0 from	
	Observed	Equation (12)	Data	Equation (12)
6.2	0.15	0.17	-3.4	-3.99
4.4	0.13	0.14	-3.6	-4.45
3.4	0.12	0.13	-3.8	-4.68

more useful than the transient points for comparison of branchline flow qualities to mainline liquid level. However, the transient points are of use in obtaining the level for onset of vapor pull-through by utilizing the mainline to branchline pressure drop measurement (PDE-341) as an indication of pull through.

In performing the vertical downflow tests, steam calibration of the branchline densitometers proved to be quite difficult and, in general, was not successfully achieved. Even though steam was circulated through the branchline for several minutes (limited by the catch tank capacity), apparently condensation effects in the mainline and branchline resulted in densitometer output voltages lower than the "true" steam calibration voltages. Consequently, the void fractions obtained from the branchline densitometers are greater than 1.0 for some of the data points (although still within the basic measurement uncertainty) and, therefore, their use is not recommended.

During the changeover from the horizontal to the vertical downflow configuration, the problem with the east end load cell (as discussed in Appendix I) on the catch tank was resolved and corrected. Therefore, for the vertical downflow configuration tests, the most reliable measurement of the branchline mass flow rate is that using the catch tank (MDOT-CT).

The data from the vertical downflow configuration tee/critical flow experiments are presented and discussed in the next four sections. Averaged data for steady-state portions of the data points, with constant mainline liquid levels, are provided in Tables H-10 to H-12, with initial and final conditions provided in Tables H-4 to H-6.

Vertical Downflow—6.2 MPa Data. Data averages for the steady-state portions of the vertical downflow configuration 6.2 MPa data are presented in Table H-10. Selected measurements and computed parameters are presented in Appendix E on microfiche located on the inside back cover of this report . In this section the branchline mass flow rate, flow quality, void fraction, and pressure drop as a function of mainline liquid level are presented and discussed.

The branchline mass flow rate versus mainline liquid level is presented in Figure 63 for the six transient points performed. Presented in Figure 64 is the mean and tolerance limits for these transient points and data averages for the steady-state points. Although this measurement is not a particularly good indication of the onset of pull-through, it appears that the flow rate sharply drops in the vicinity of 9-10 cm. The steady-state points indicate a linear relationship between liquid level and branchline flow rate below the onset of pull-through level.

The branchline flow quality versus mainline liquid level is presented in Figure 65 for the transient points and in Figure 66 for the mean and averaged data from the steady-state runs. This data also indicates onset of vapor pull-through level at about 9 cm. The steady-state data indicates an exponential relationship between flow quality and liquid level.

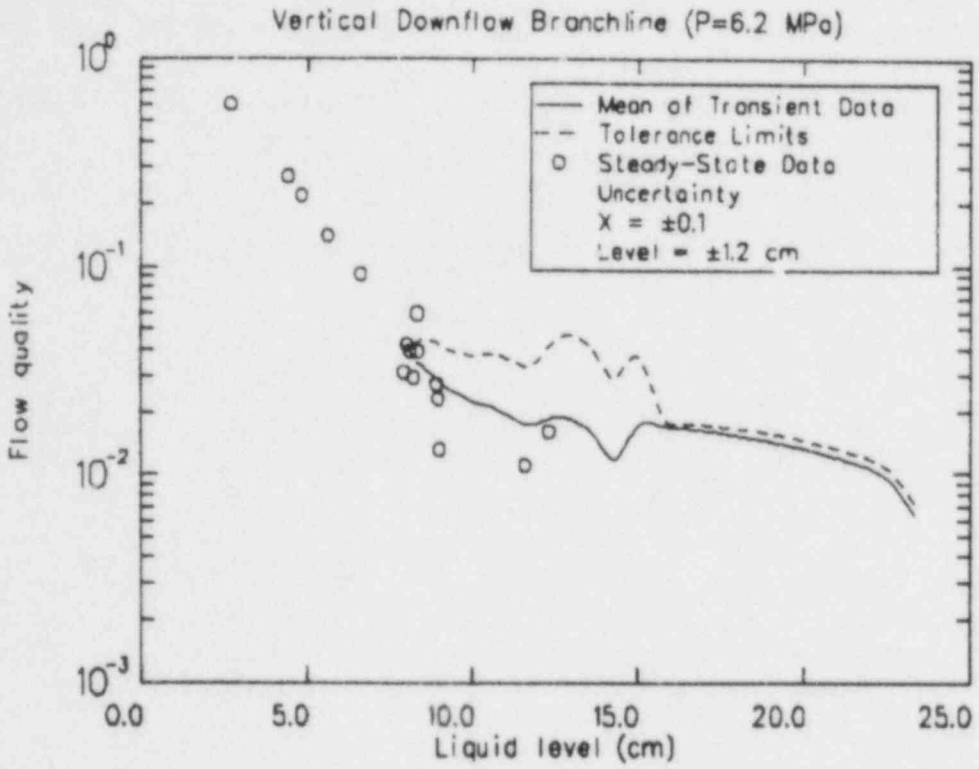

Figure 63. Transient branchline mass flow rates, of vertical downflow configuration 6.2 MPa data.

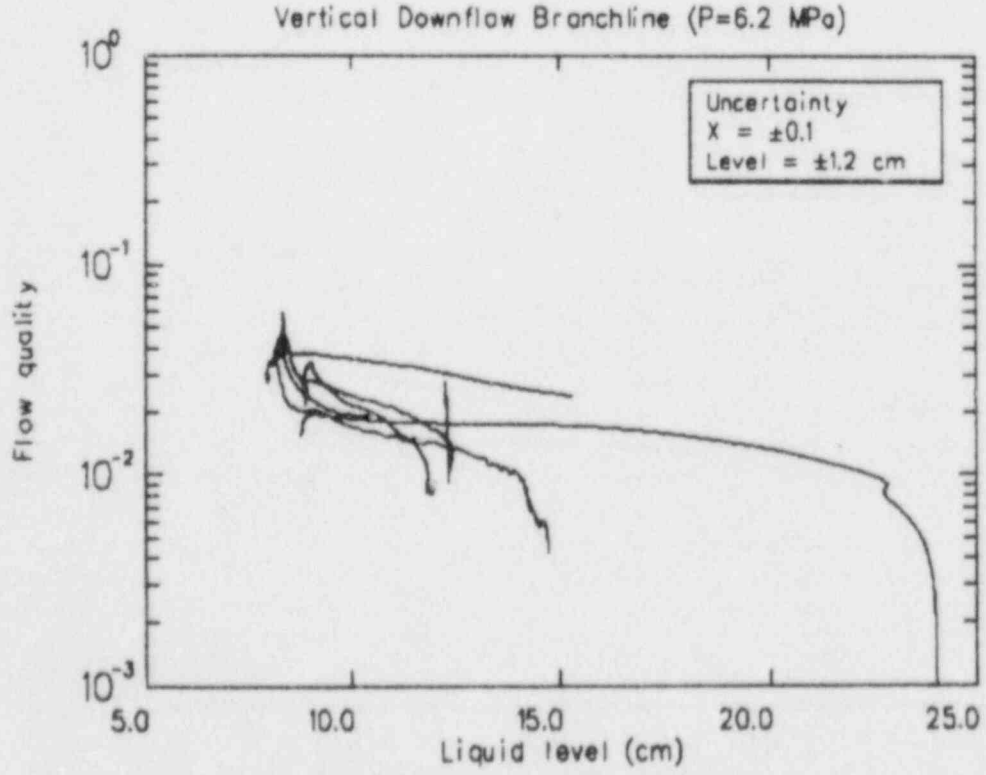

Figure 64. Mean of transient branchline mass flow rates, of vertical downflow configuration 6.2 MPa data.

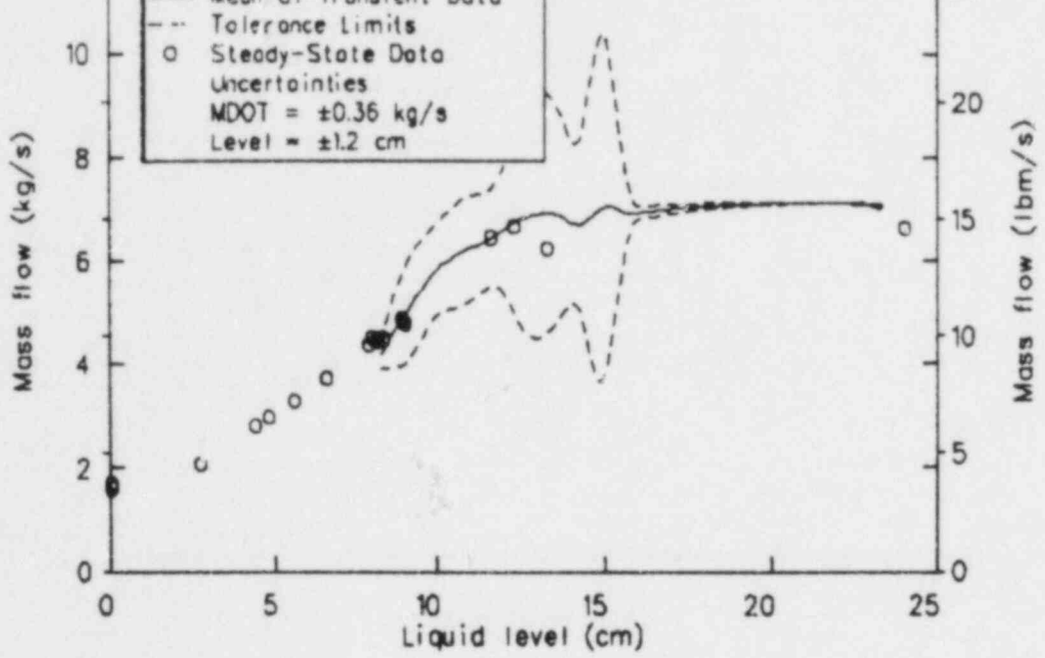

Figure 65. Transient branchline flow quality, of vertical downflow configuration 6.2 MPa data.

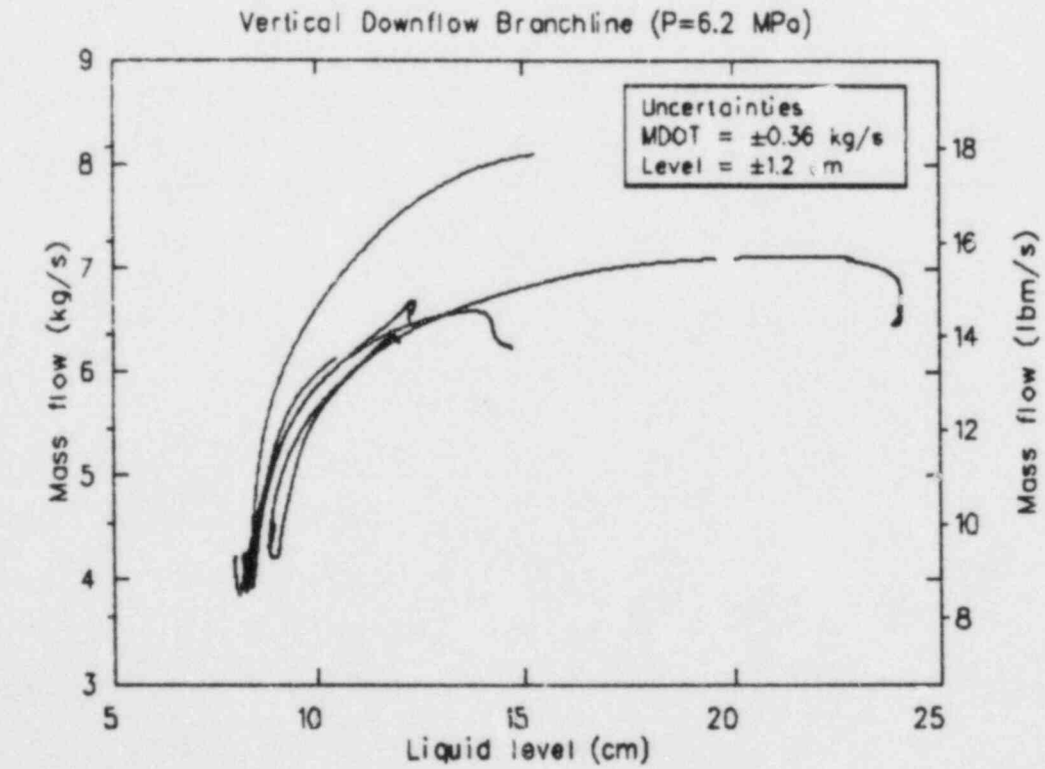

Figure 66. Mean of transient branchline flow quality, of vertical downflow configuration 6.2 MPa data.

The branchline void fraction versus mainline liquid level is presented in Figure 67 with the mean and steady-state data presented in Figure 68. There is a sharp rise in the void fraction as the level decreases below ~9 cm, with the void fraction appearing to be a constant before the onset of pull-through level. There is an apparent 0.1 offset in this data before pull-through begins, which is probably a result in electronic drift. It is however, well within the uncertainty of ±0.26.

Transient pressure drop data from mainline to branchline transient data as a function of liquid level is presented in Figure 69, with the mean and steady-state data presented in Figure 70. The signal noise level for the transient pressure drop data shows a significant increase at a level of about 9.4 cm, an indication of vapor pull-through as demonstrated in Figure 71. This measurement is perhaps the most reliable indication of the onset of pull-through of the available measurements; it is open to interpretation as to whether the increase in noise level is due to intermittent or continuous vapor pull-through. The best indication of continuous pull-through is probably the sharp drop in the magnitude of the pressure drop which occurs at about 9 cm (consistent with the other indications). In general, the relationship between the pressure drop and liquid level exhibit the same characteristics of decreasing and then increasing with decreasing liquid level, as was seen for the horizontal configuration data.

Vertical Downflow—4.4 MPa Data. Data averages for steady-state portions of the vertical downflow configuration 4.4 MPa data are presented in Table H-11. Selected measurements and calculated parameters are provided in Appendix F found on microfiche and located on the inside back cover of this report. The branchline mass flow rate, flow quality, void fraction, and pressure drop as functions of the mainline liquid level are presented in Figures 72-75 for the two transient points performed at this pressure and the steady-state data point averages. In general, observations made for the 6.2 MPa data are applicable, with the exception that the onset of intermittent pull-through level appears to be about 10.5 cm, based upon the increase in noise of PDE-341, as shown in Figure 76, with an onset of continuous pull-through occurring at about 9.3 cm, based upon the drop in magnitude of the signal.

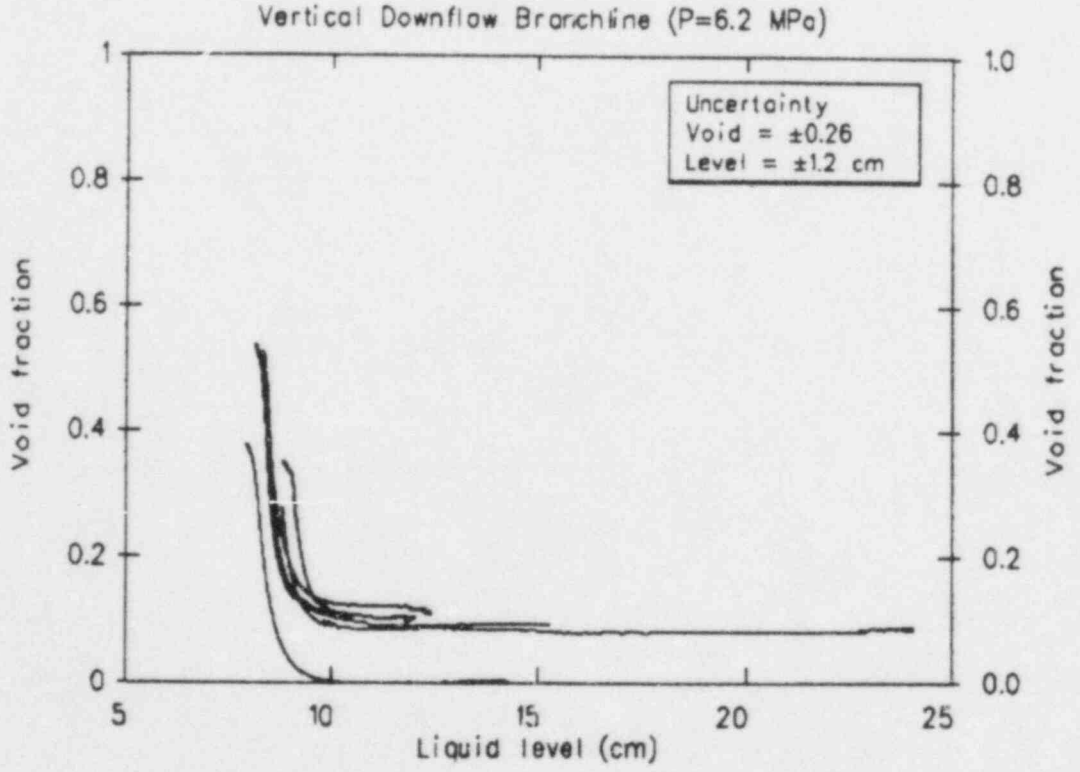

Figure 67. Transient branchline void fraction. of vertical downflow configuration 6.2 MPa data.

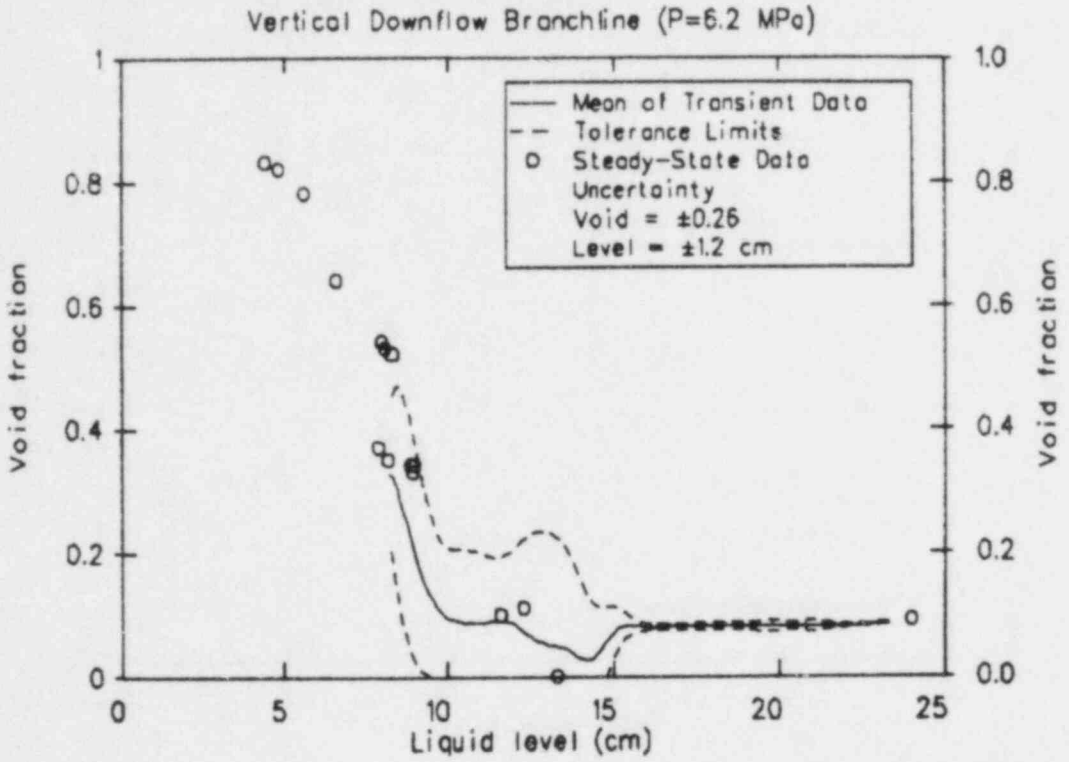

Figure 68. Mean of transient branchline void fraction, of vertical downflow configuration 6.2 MPa data.

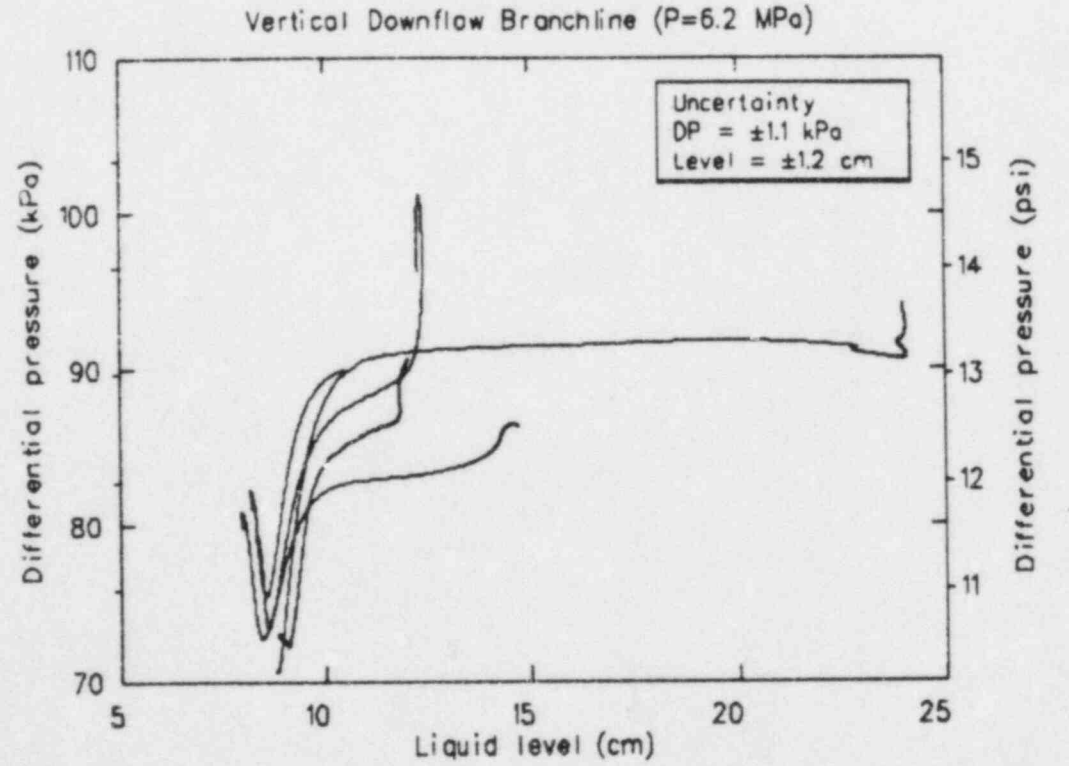

Figure 69. Transient mainline to branchline pressure drop, of vertical downflow configuration 6.2 MPa data.

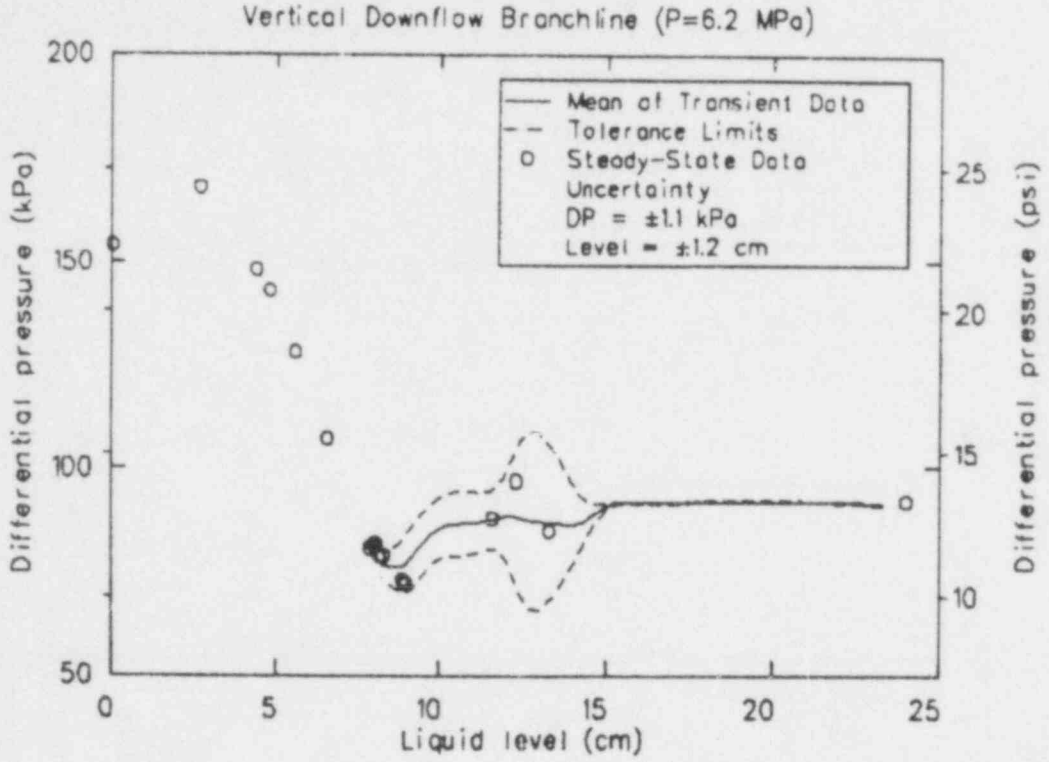

Figure 70. Mean of transient mainline to branchline pressure drop, of vertical downflow configuration 6.2 MPa data.

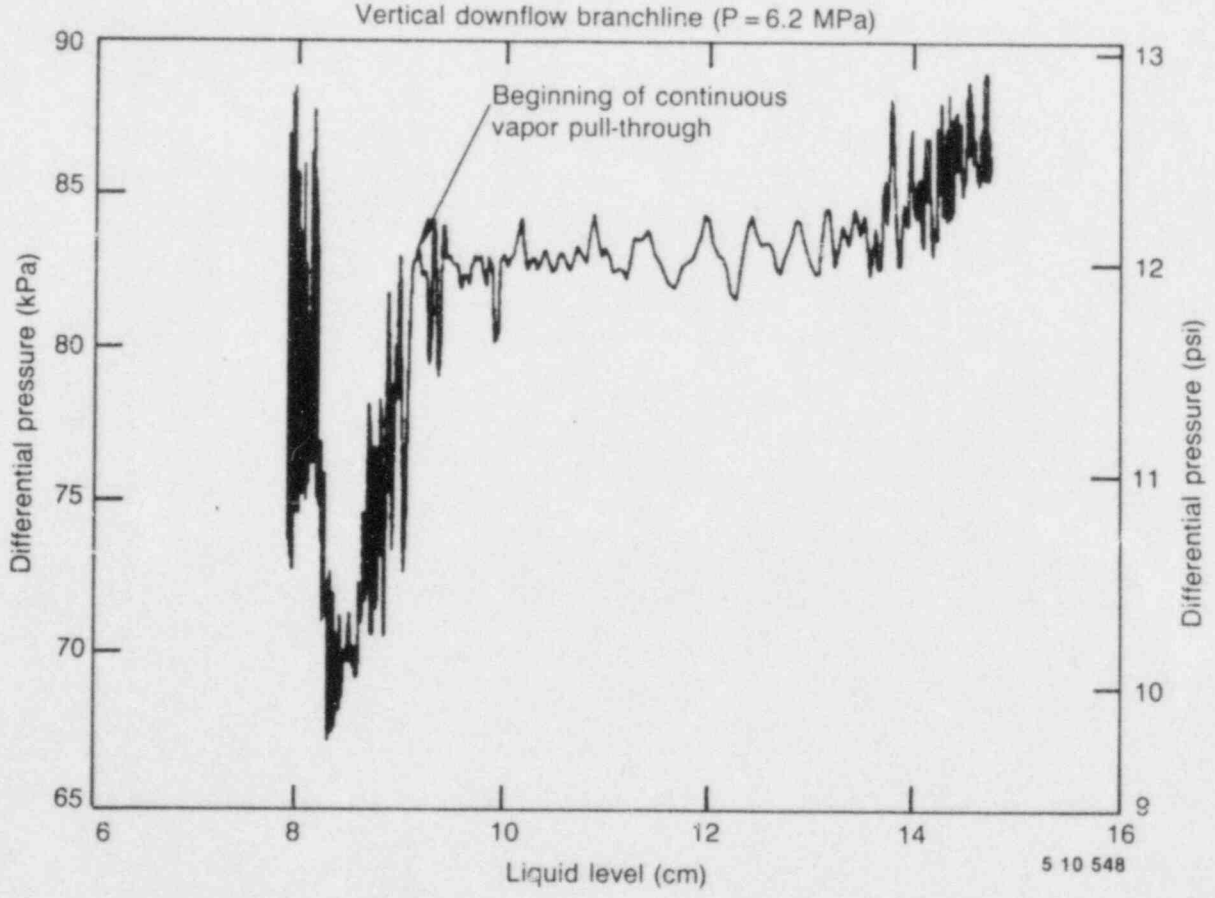

Figure 71. Example of unfiltered mainline to branchline pressure drop data, of vertical downflow configuration 6.2 MPa data.

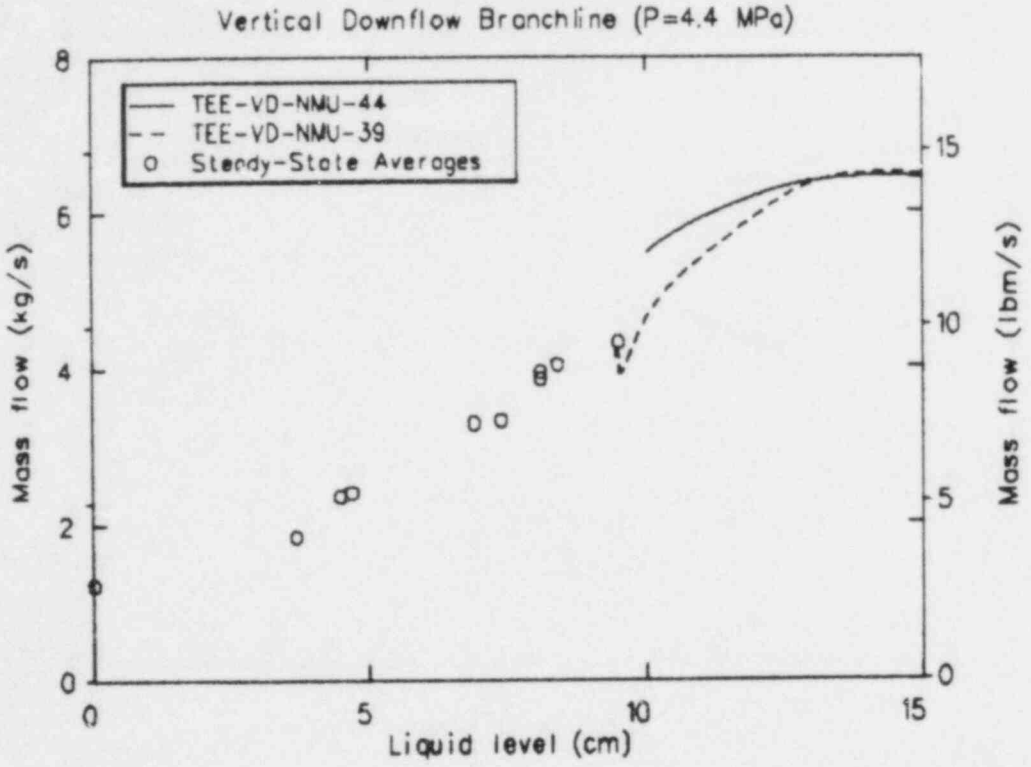

Figure 72. Mean of transient branchline mass flow rates compared with steady-state data, of vertical downflow configuration 4.4 MPa data.

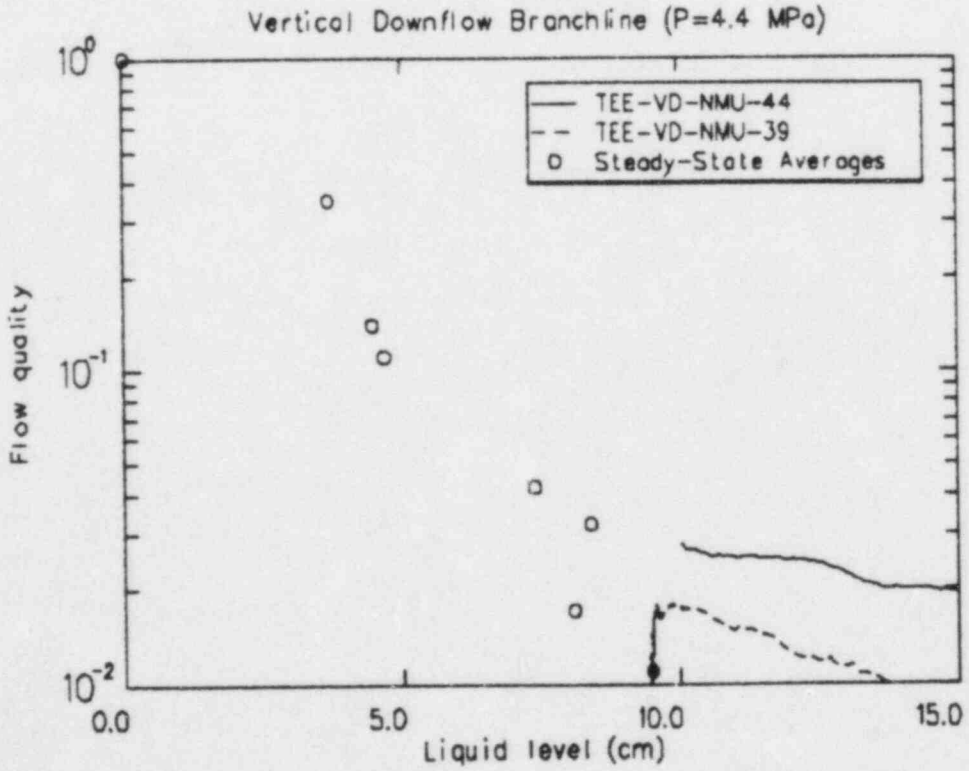

Figure 73. Mean of transient branchline flow quality compared with steady-state data, of vertical downflow configuration 4.4 MPa data.

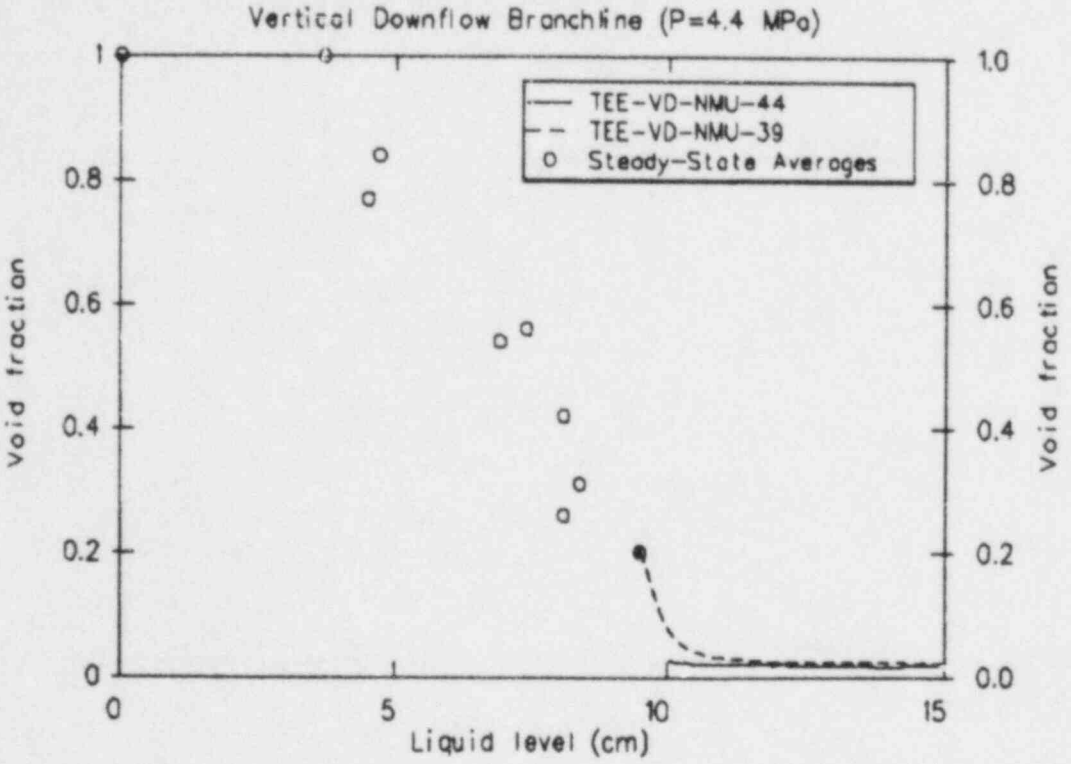

Figure 74. Mean of transient branchline void fraction compared with steady-state data, of vertical downflow configuration 4.4 MPa data.

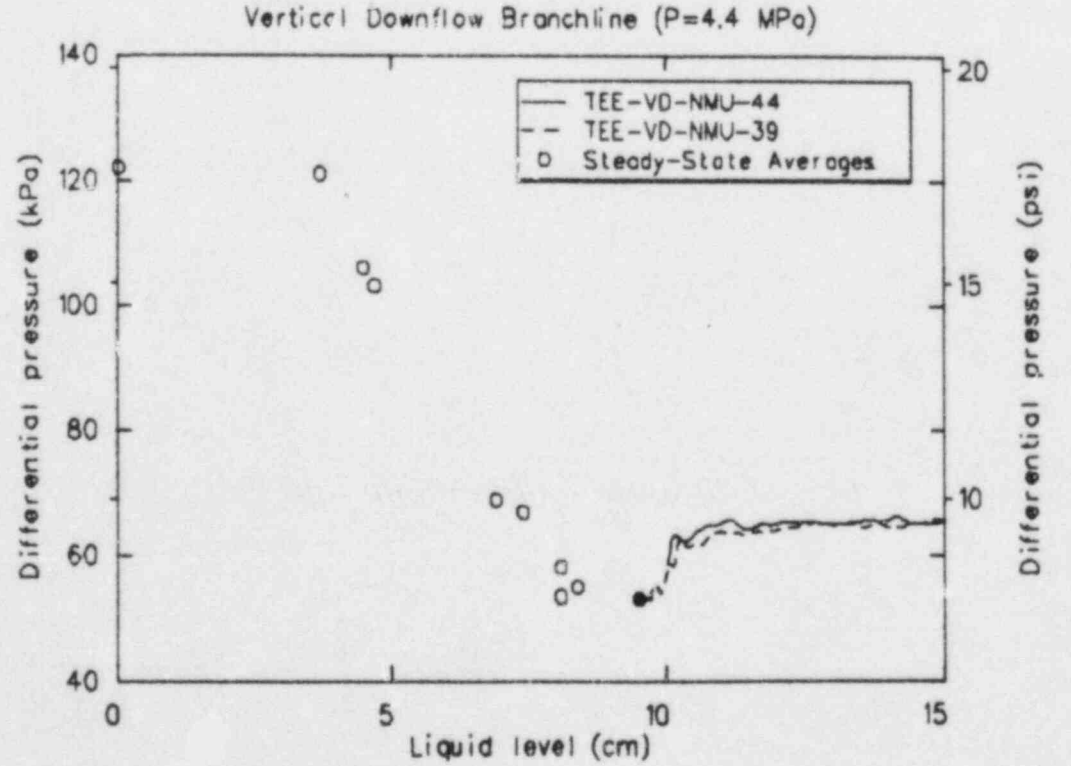

Figure 75. Mean of transient mainline to branchline pressure drop compared with steady-state data, of vertical downflow configuration 4.4 MPa data.

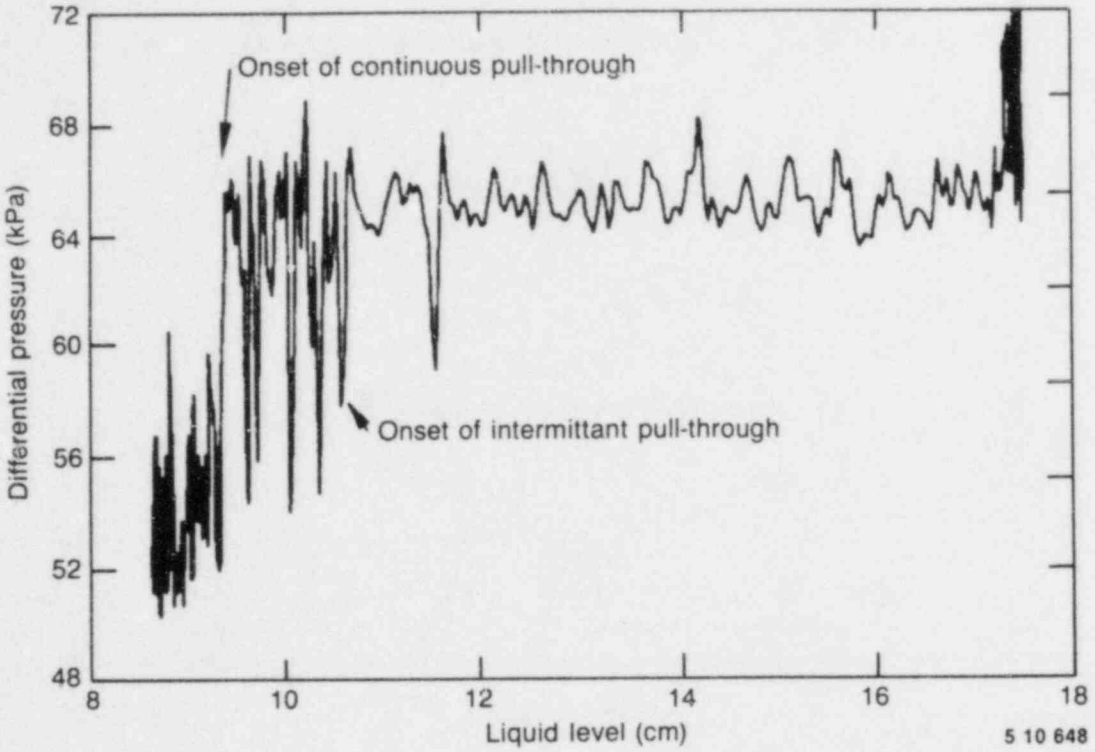

Figure 76. Example of unfiltered mainline to branchline pressure drop data, of vertical downflow configuration 4.4 MPa data.

Vertical Downflow—3.45 MPa Data. Data averages for steady-state portions of the vertical downflow configuration 3.45 MPa data are presented in Table H-12. Selected measurements and calculated parameters are provided in Appendix G found on microfiche and located on the inside back cover of this report. The branchline mass flow rate, flow quality, void fraction, and pressure drop as functions of mainline stratified liquid level are presented in Figures 77-84. These figures represent the five transient test points performed and data averages for the steady-state test points compared to the mean and tolerance limits of the transient runs. The same general observations made for 6.2 MPa data are also true for the 3.45 MPa data. The onset of intermittent vapor pull-through appears to occur at a level of ~10 cm from the increase in noise level shown in Figure 85, with continuous pull-through occurring at about 9.3 cm.

Comparison of 6.2, 4.4, and 3.45 MPa Vertical Downflow Data. Data from the three different pressures at which the vertical downflow configuration tests were performed are compared and discussed in this section. Comparisons are made using the mean of the transient test points for 6.2 and 3.45 MPa data sets and the data averages for the steady-state test points.

The branchline mass flow rates as functions of the liquid levels are presented in Figure 86. As expected, decreasing the mainline pressure resulted in a decrease in the critical flow rate out the branchline. The flow rate appears to be a linear function of liquid level from the onset of continuous pull-through (8-9.5 cm) down to a level of about 2.7 cm. At this level, the flow rates had dropped to near the all steam flow rate. Unfortunately, no data was obtained below this level[a] to verify an abrupt change in slope. The slope of the linear relationship appears to be same for the data from the three different pressures.

The flow quality for the data at the three pressures is shown in Figure 87. Although the steady-state data averages for the 6.2 and 3.45 MPa data[b]

a. The level of 2.7 cm was obtained at the minimum controllable liquid flow rate of 0.5 kg/s at 6.2 MPa.

b. The scatter in the 4.4 MPa flow quality data precludes its use in this argument.

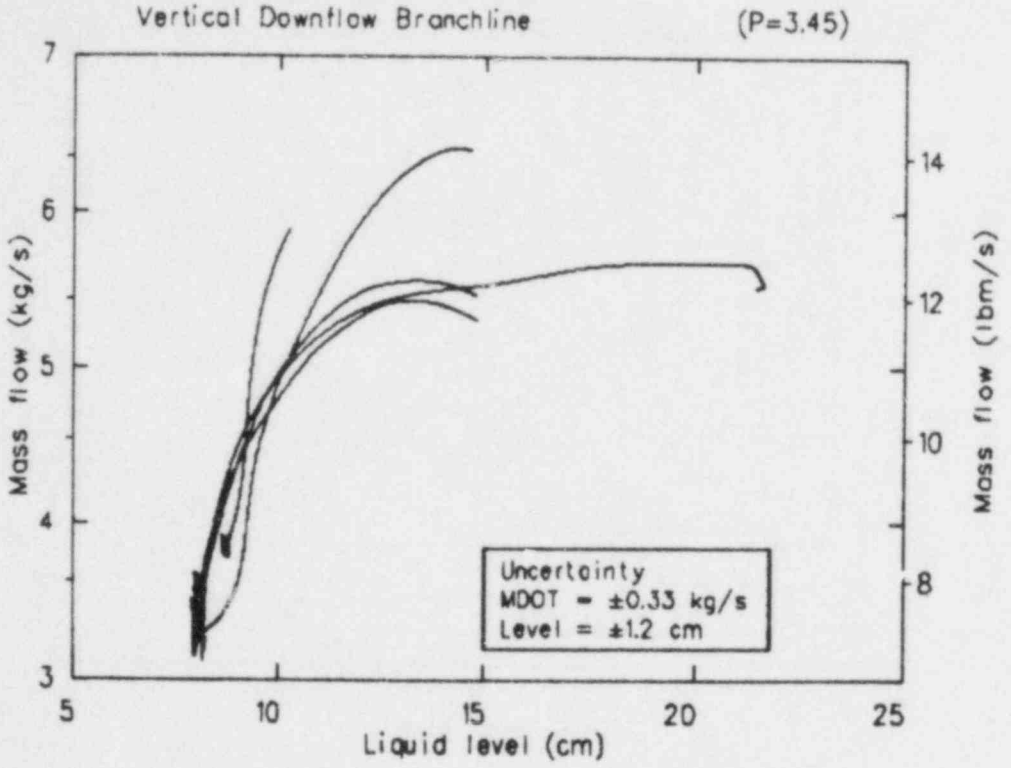

Figure 77. Transient branchline mass flow rates, of vertical downflow configuration 3.45 MPa data.

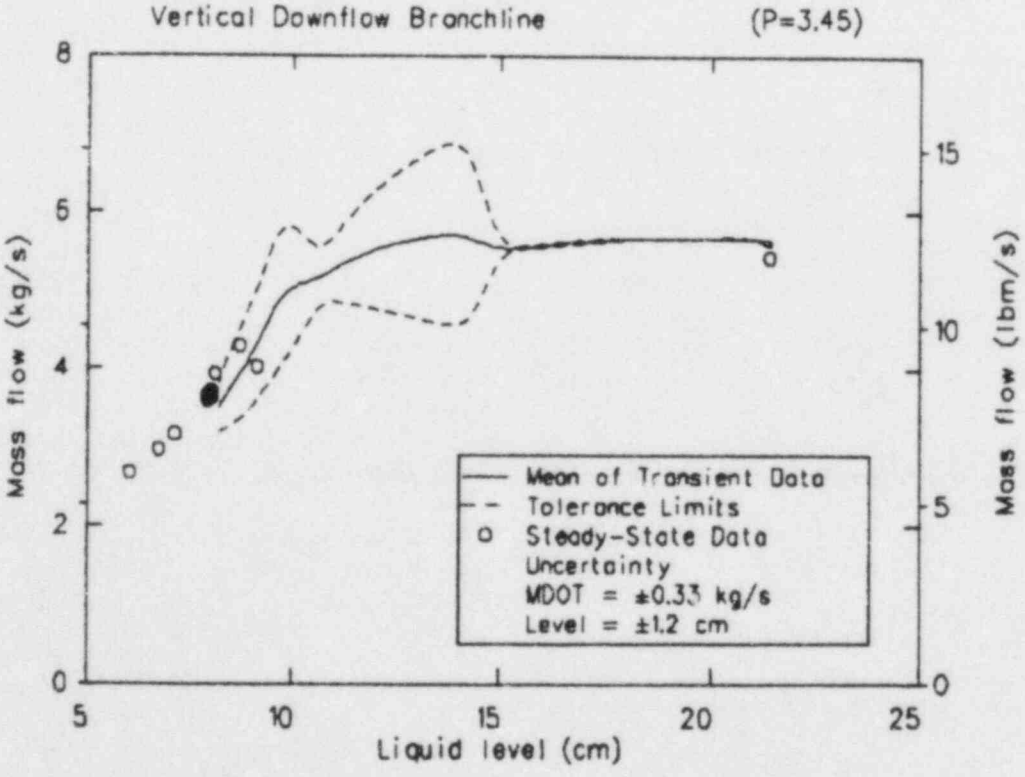

Figure 78. Mean of transient branchline mass flow rates, of vertical downflow configuration 3.45 MPa data.

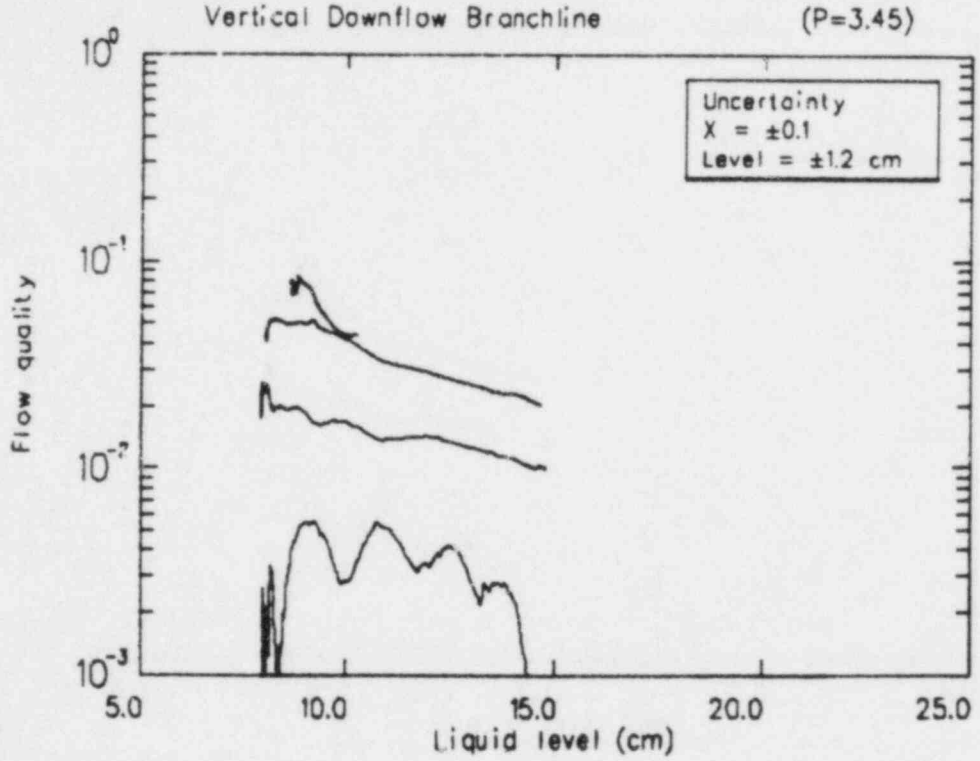

Figure 79. Transient branchline flow quality, of vertical downflow configuration 3.45 MPa data.

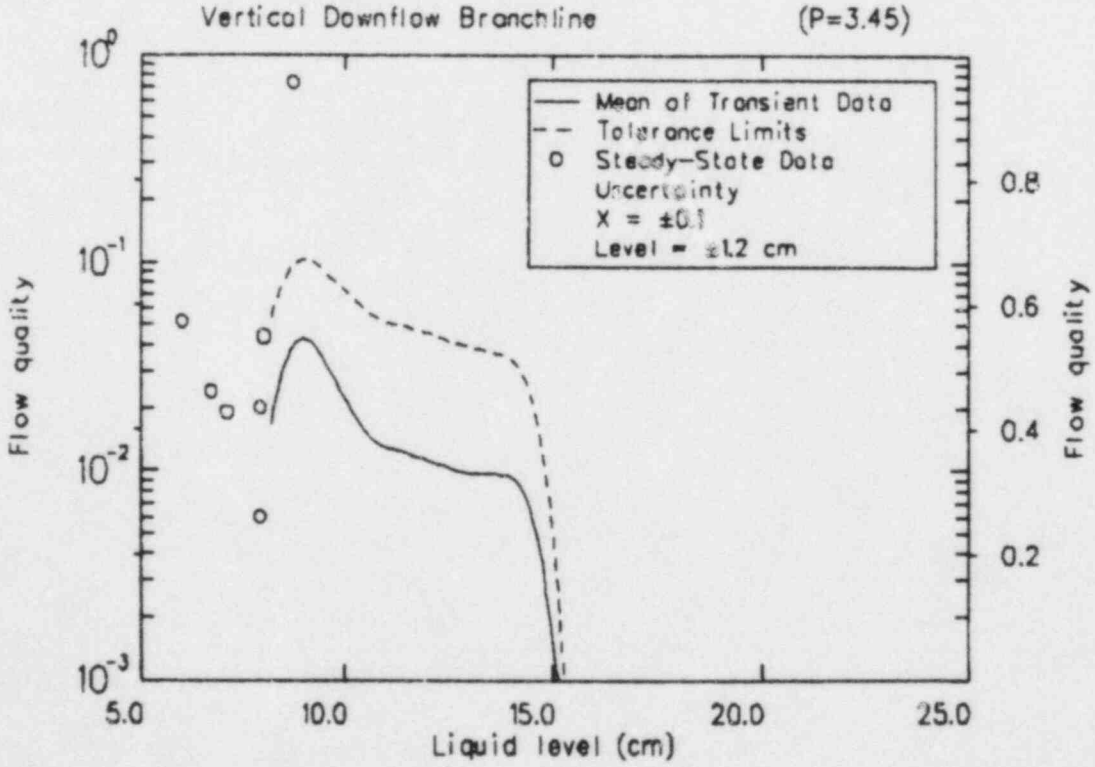

Figure 80. Mean of transient branchline flow quality, of vertical downflow configuration 3.45 MPa data.

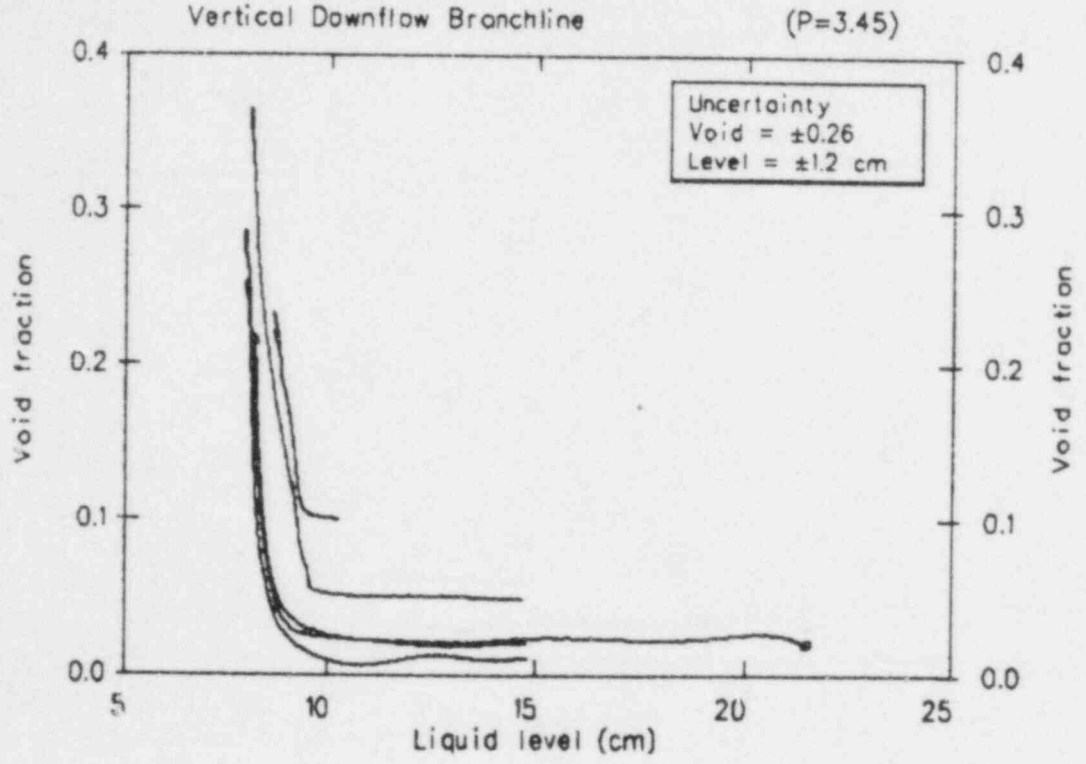

Figure 81. Transient branchline void fraction, of vertical downflow configuration 3.45 MPa data.

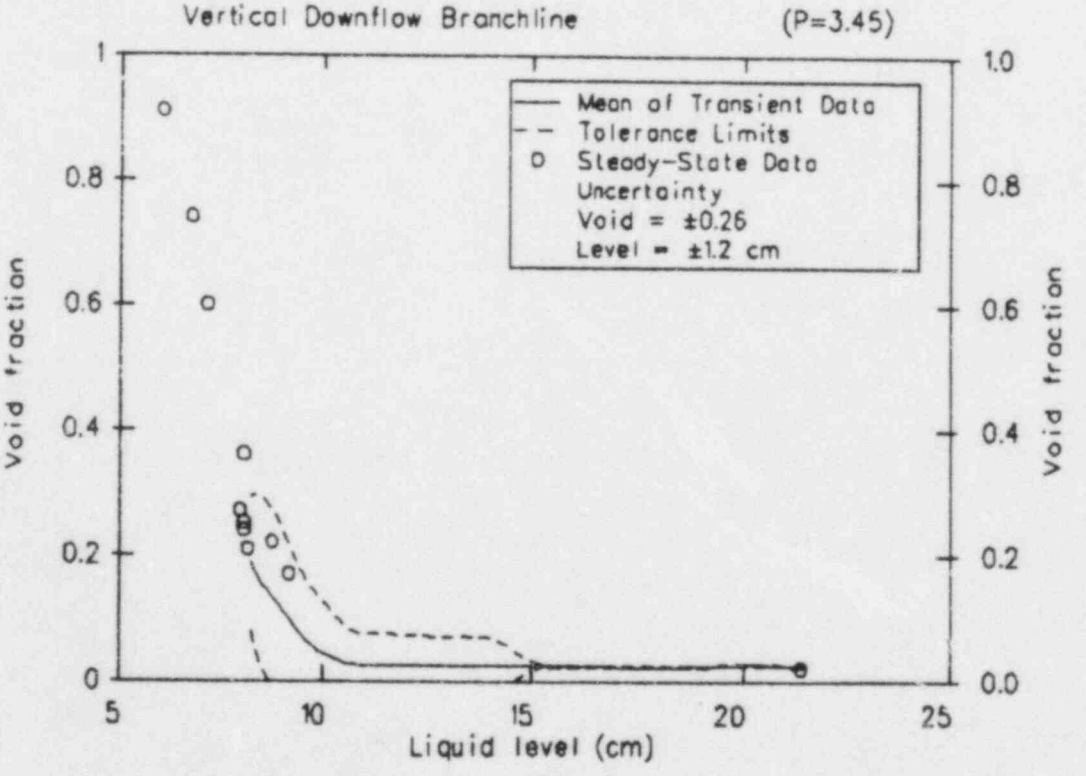

Figure 82. Mean of transient branchline void fraction, of vertical downflow configuration 3.45 MPa data.

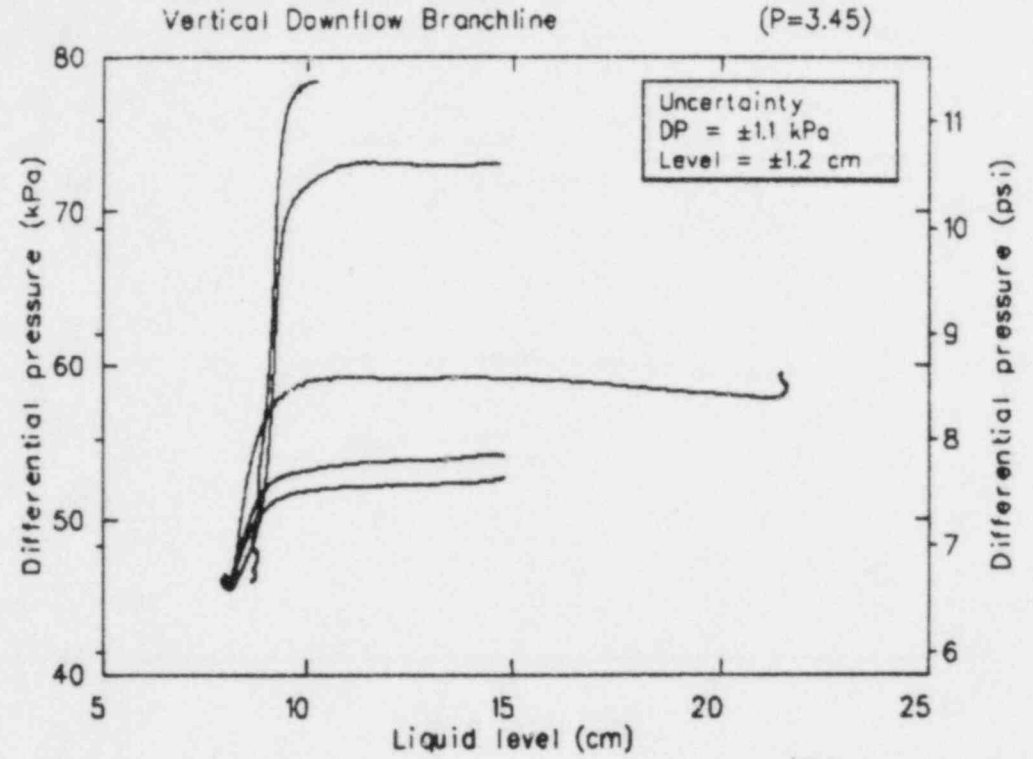

Figure 83. Transient mainline to branchline pressure drop, of vertical downflow configuration 3.45 MPa data.

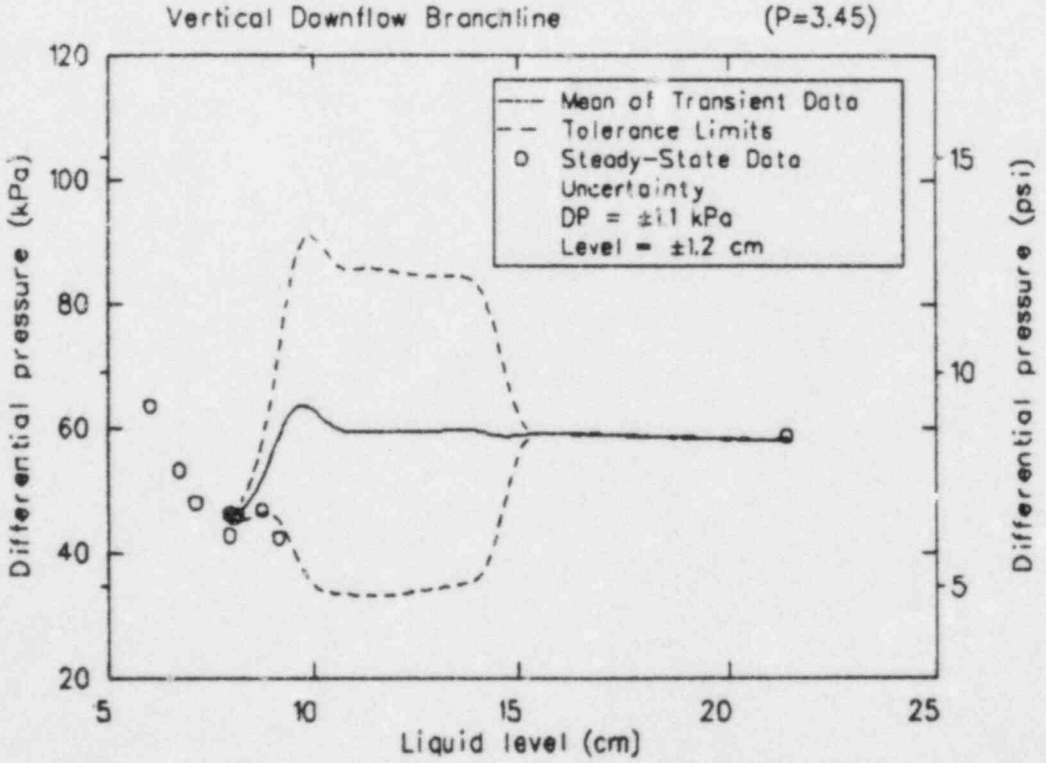

Figure 84. Mean of transient mainline to branchline pressure drop, of vertical downflow configuration 3.45 MPa data.

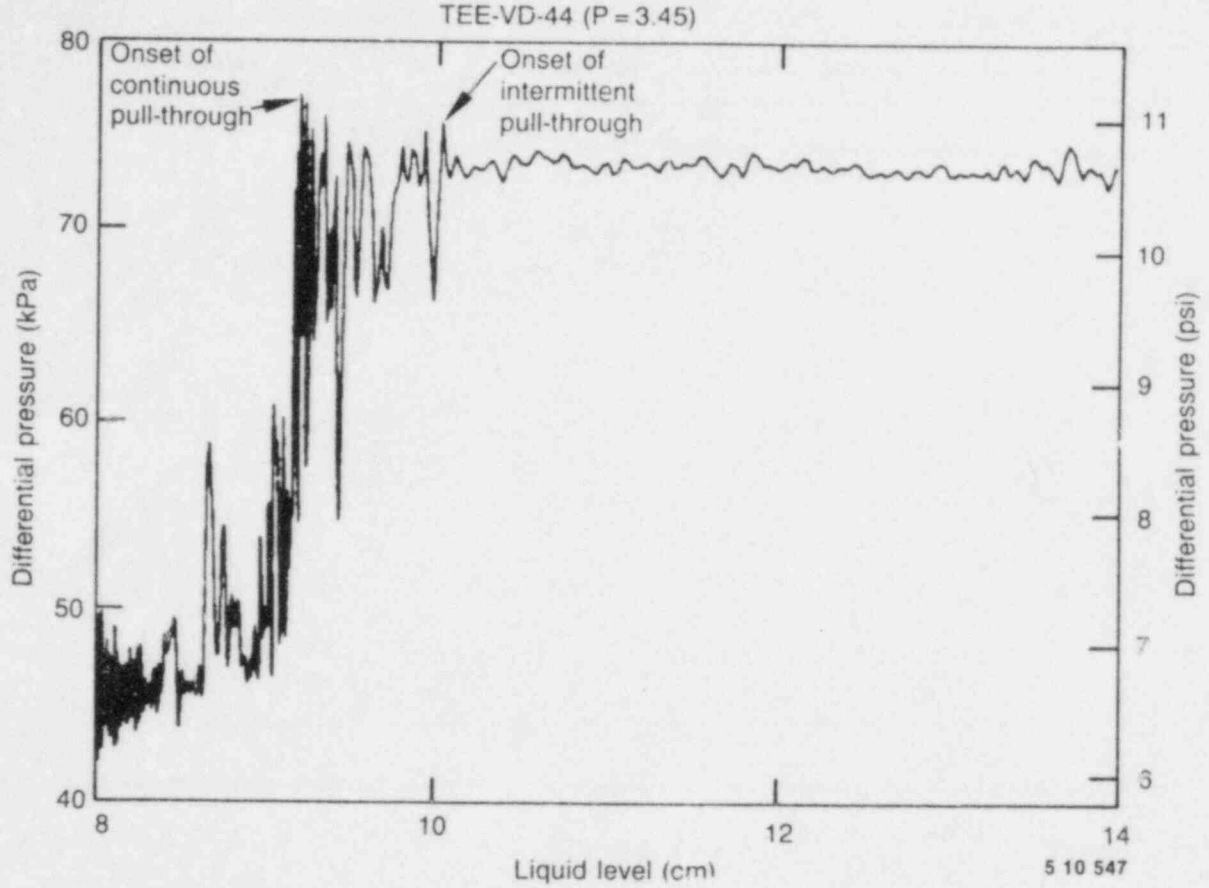

Figure 85. Example of unfiltered mainline to branchline pressure drop data, of vertical downflow configuration 3.45 MPa data.

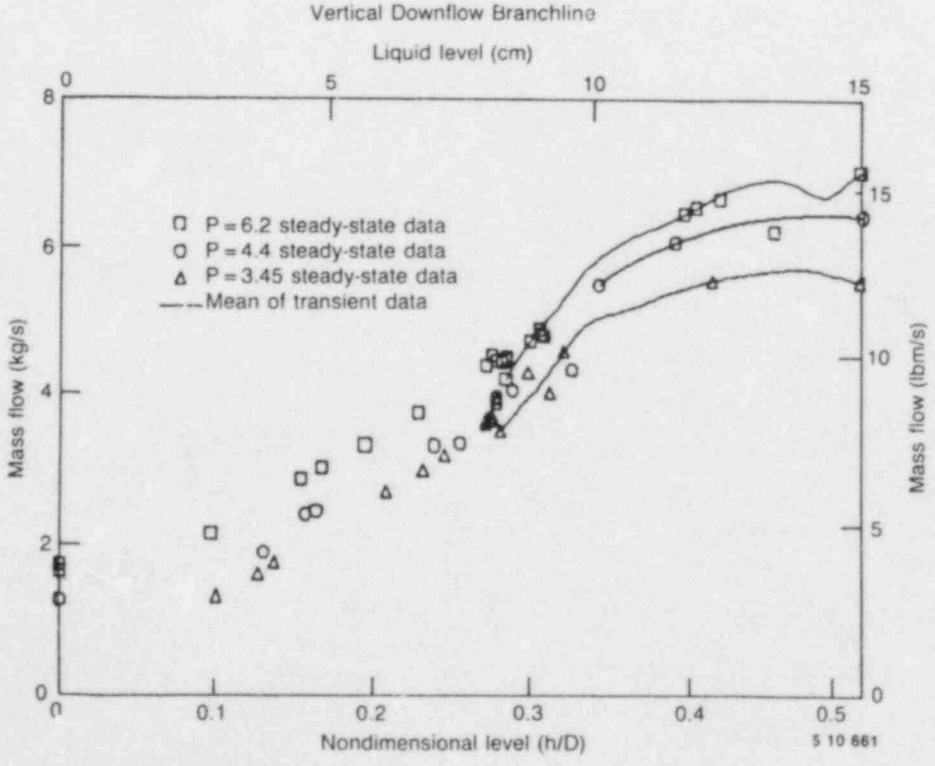

Figure 86. Comparison of steady-state and mean of transient branchline mass flow rate data for the three test pressures of vertical downflow configuration data.

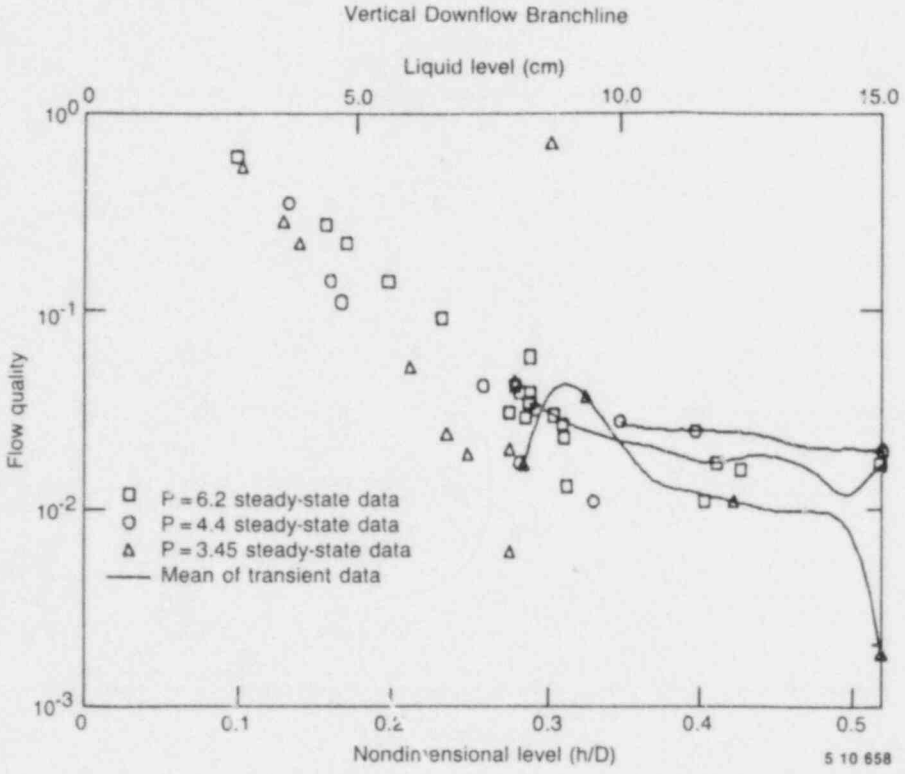

Figure 87. Comparison of steady-state and mean of transient branchline flow quality data for the three test pressures of vertical downflow configuration data.

both indicate an exponential relationship between flow quality and mainline liquid level, the slope of these relationships appear to be a function of the mainline pressure. This is contrary to the observations from the horizontal configuration data. However, since the level for onset of pull-through is a function of pressure, this observation is not surprising. An anomaly in this flow quality data is the observation that a flow quality of 1.0 would be reached at a liquid level of about 1.7 cm. This would be consistent with the observations from the branchline mass flow rate data. It is possible that there is an offset unaccounted for in the liquid level measurement. It is difficult to perceive how an offset due to the densitometer measurement could be repeated each day of testing over the two-week period in which this data was acquired.

The branchline void fraction as a function of mainline liquid level for the three different pressures is compared in Figure 88. The void fraction for the 6.2 and 4.4 MPa data approaches 1.0 in the 2-5 cm liquid level range. Obviously, for the vertical downflow configuration the void fraction covers its range of 0-1 in a small liquid level range.

The mainline to branchline pressure drop data at the three different pressures are compared in Figure 89. As expected, the magnitudes of the pressure drops decrease with decreasing pressure. All the data exhibit the same characteristic of decreasing pressure drop at the onset of pull-through, rapidly decreasing to a minimum, and then increasing to some maximum value near the all steam value.

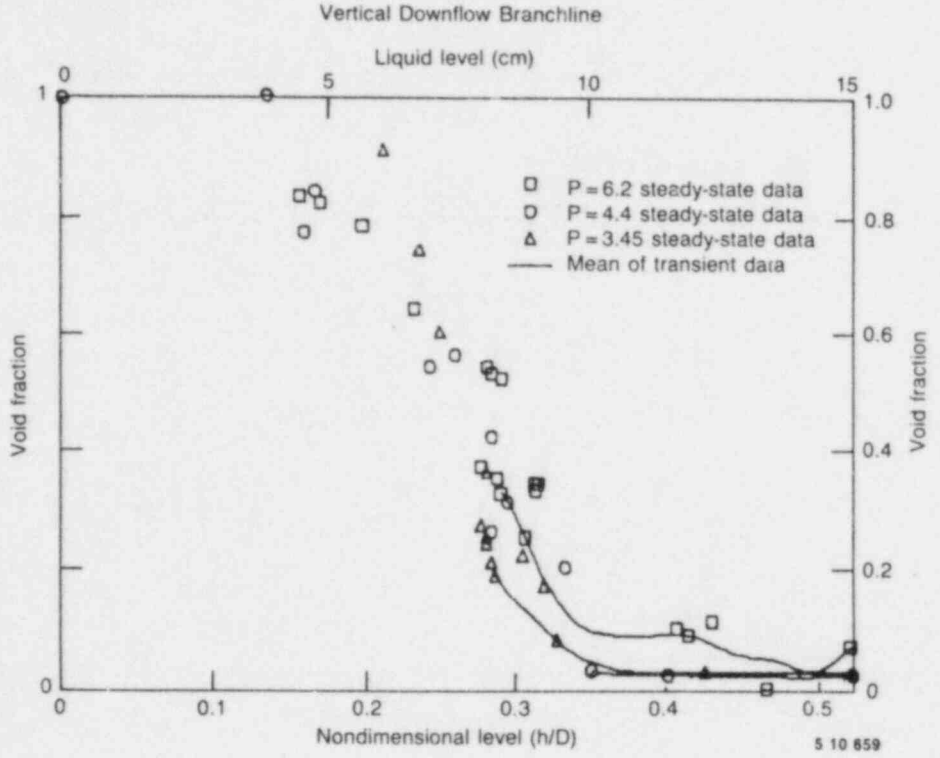

Figure 88. Comparison of steady-state and mean of transient branchline void fraction data for the three test pressures of vertical downflow configuration data.

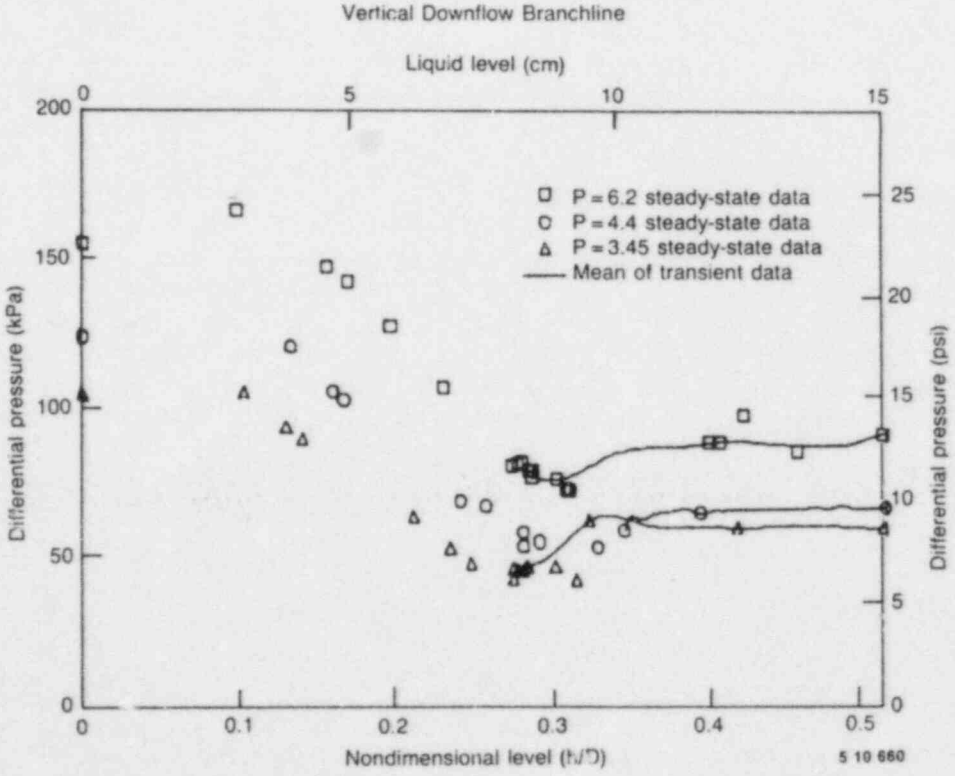

Figure 89. Comparison of steady-state and mean of transient mainline to branchline pressure drop data for the three test pressures of vertical downflow configuration data.

DATA ANALYSIS

In the following sections the data are compared to previously suggested correlations for the onset of vapor pull-through and liquid entrainment, and improvements to the correlations are suggested. Correlations for the branchline flow quality as a function of the mainline stratified liquid level are also presented.[a] The two configurations are handled in separate sections.

Horizontal Configuration

The previously presented correlation for the liquid level, above which liquid would be entrained and carried out a horizontal branchline [given in Equation (2)], can be rewritten as

$$\frac{h_e}{D} = \frac{1}{2} - \frac{C_e}{D}\left[\frac{\dot{m}_g^2}{g\rho_g(\rho_f - \rho_g)}\right]^{0.2} \qquad (9)$$

where C_e is a constant to be obtained from experimental data [equal to 0.687 in Equation (2)]. All other variables are as given in Equation (2). Similarly the correlation for onset of vapor pull-through out a horizontal branchline [presented in Equation (7)] can be rewritten as

$$\frac{h_p}{D} = \frac{1}{2} + \frac{C_p}{D}\left[\frac{\dot{m}_g^2}{g\rho_g(\rho_f - \rho_g)}\right]^{0.2} \qquad (10)$$

where C_p is a constant obtained from experimental data [which equaled 0.687 in Equation (7)].

The levels observed[b] during the tee/critical flow experiments for the onset of pull-through and entrainment are compared to the predictions of Equation (2) and (7) in Table 6. Basically, the predictions from these two equations are about 1 cm low for the 6.2 MPa data. Although this is within the measurement uncertainty of the mainline liquid level measurement, we will assume that the observed levels for onset of pull-through and entrainment are correct for the 6.2 MPa data. (The 6.2 MPa data will be used since the major emphasis in this experimental program was on high pressure data.) This results in values of the constants of Equation (9) and (10) of $C_e = 0.62$, $C_p = 0.82$. These values compare with the results reported by Smoglie[25] of $C_e = 0.69$, and $C_p = 0.75$. The onset level predictions from Equation (9) and (10) used the constants derived from the 6.2 MPa data and are also given in Table 6. The predicted onset level for both pull-through and entrainment vary less than 1 cm over the experimental pressure range (3.4-6.2 MPa). Unfortunately, the variation is not consistent as a function of pressure for the entrainment data. The results of Equation (9) show that the entrainment level decreases as the pressure increases. This is consistent with our understanding of the physical mechanisms involved with the entrainment process. Entrainment is dependent upon the momentum of the steam, which increases as the pressure increases due to increased steam density and mass flow rate into the branch. Thus, the forces for entrainment are larger at higher pressures and the entrainment process would be expected to begin at lower levels.

Previous observations of the relationship between the branchline flow quality and the mainline liquid level indicated that the flow quality is an exponential relationship between vapor pull-through and liquid entrainment levels. It is, therefore, proposed that the branchline flow quality, X, can be represented by

$$X = \begin{cases} 0 & h > h_p \\ \exp\left[C_x\left(\dfrac{h - h_e}{h_p - h_e}\right)\right] & h_e \le h \le h_p \\ 1 & h < h_e \end{cases} \qquad (11)$$

where the constant C_x is obtained from data. A reasonable level for evaluating C_x is a mainline level at the centerline of the branch, or $h = D/2$. From the 6.2 MPa data in Figure 29, $X_o = 0.15$ at $h = 14.2$ cm, which results in a C_x value of -3.4. This value is fairly constant for the data at the other two pressures ($C_x = -3.6$ at 4.4 MPa and $C_x = -3.8$ at 3.45 MPa). Smoglie[25] derived a simple model for X_o based upon a separated flow model

a. Only a limited amount of analysis has been performed in support of this data report. It was decided to analyze only the 6.2 MPa data at this time.

b. The onset level for vapor pull-through can be detected by increased noise level and decreased magnitude of the mainline to branchline pressure drop measurement (PDE-341). The onset level for liquid entrainment can best be determined by projecting the mean flow quality versus level data to a quality of one.

for the pressure drop at the branchline entrance. This model resulted in

$$X_o = \frac{1}{1 + \sqrt{\rho_f / \rho_g}} . \qquad (12)$$

However, Smoglie reported that this relation underpredicted her data by 15%, necessitating the multiplication of Equation (12) by 1.15. The centerline flow qualities given by Equation (12) for the three test pressures and the resulting C_x for Equation (11) are compared to the observed centerline flow qualities in Table 7.

Smoglie[25] presented a relationship for the branch flow quality which was a fit to air-water data, given by

$$X = X_o^{(1+C\tilde{h})} \left[1 - \frac{1}{2}\tilde{h}\,(1 + \tilde{h})\, X_o^{(1-\tilde{h})} \right]^{0.5} \qquad (13)$$

where $\tilde{h}$ is the ratio of the distance from the pipe centerline to the liquid interface for the entrainment or pull-through level. The constant, C, in Equation (13) was given as $C = 1$ for $\tilde{h} \leq 0$ and $C = (h_p - D/2)/(D/2 - h_e)$ for $\tilde{h} > 0$. The onset of entrainment and pull-through levels were given by Equations (9) and (10), using values of the constants of $C_e = 0.69$ and $C_p = 0.75$. A comparison between the 6.2 MPa data and the results of Equation (11) and Equation (13) is made in Figure 90. The results from Equation (13) are shown using values resulting from this experimental program for C_e and C_p. Both prediction methods fit the trends fairly well although, not surprisingly, the results from Equation (11) using the tabulated onset levels fit the data best. The results from Equation (13) have an advantage over Equation (11) of going to zero as the onset of pull-through level is reached. Comparing the results from Equation (11) with the 6.2 MPa data in Figure 90, we see that over most of the level range there is a very good comparison. There appears to be, however, a change in slope of the data at a level of about 16 cm which corresponds to the top of the branchline. It is not unreasonable to expect the flow quality relationship to be different for the vapor pull-through region.

One indication of the usefulness of the above correlation is its use in predicting the branchline

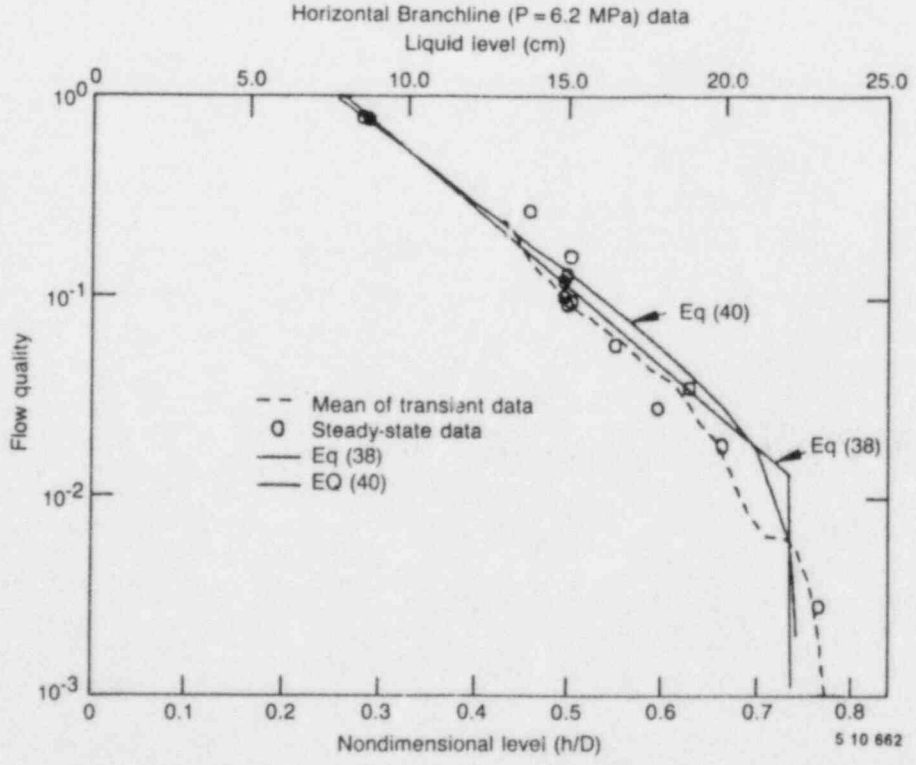

Figure 90. Comparison of branchline flow quality predictions with horizontal configuration 6.2 MPa data.

void fraction, which is a critical factor since several of the thermal-hydraulic codes (including RELAP5) use the void fraction rather than the flow quality. The void fraction, α, can be written in terms of the flow quality, assuming the two-velocity model, as

$$\alpha = \left[1 + S \frac{\rho_g}{\rho_f}\left(\frac{1}{X} - 1\right)\right]^{-1} \qquad (14)$$

where S is the slip ratio, or ratio of gas to liquid velocities. Using Equation (11) to predict to flow quality and Equation (14) to calculate the void fraction, the model results can be compared to the experimental data. This is done in Figure 91 for the cases of S = 1 and S = 2. The model correctly predicts the observed S shape of the void fraction relationship to liquid level, and the void fraction of 1.0 at the onset level for entrainment. However, the model overpredicts the void fraction for levels above the top of the branchline, approaching the level for onset of pull-through. This is partially due to the observed change in the flow quality relationship in this range and the fact that Equation (11) does not go to zero at the onset of pull-through. The results from Equation (14), using the flow quality recommended by Smoglie [Equation (13)], are also shown in Figure 91 for S = 2. In this case, results lie within the S = 1 and S = 2 range using Equation (11) and have the advantage of going to zero at the pull-through level.

Vertical Downflow Configuration

For the vertical downflow branch orientation, the level at which vapor pull-through first started was determined using the pressure drop measurement from the mainline to branchline. For this orientation, there is a concern as to whether the vapor pull-through is accomplished via a vortex or vortex-free mechanism, and whether the pull-through is continuous or intermittent. Available data (Smoglie[25]) indicates that very small velocities past the branch results in vortex-free flow behavior. Logically, intermittent vapor pull-through should be indicated by a large increase in the noise level of the mainline to branchline pressure drop measurement; continuous pull-through should also be accompanied by a sharp decrease in the magnitude of the pressure drop. Using these two observations

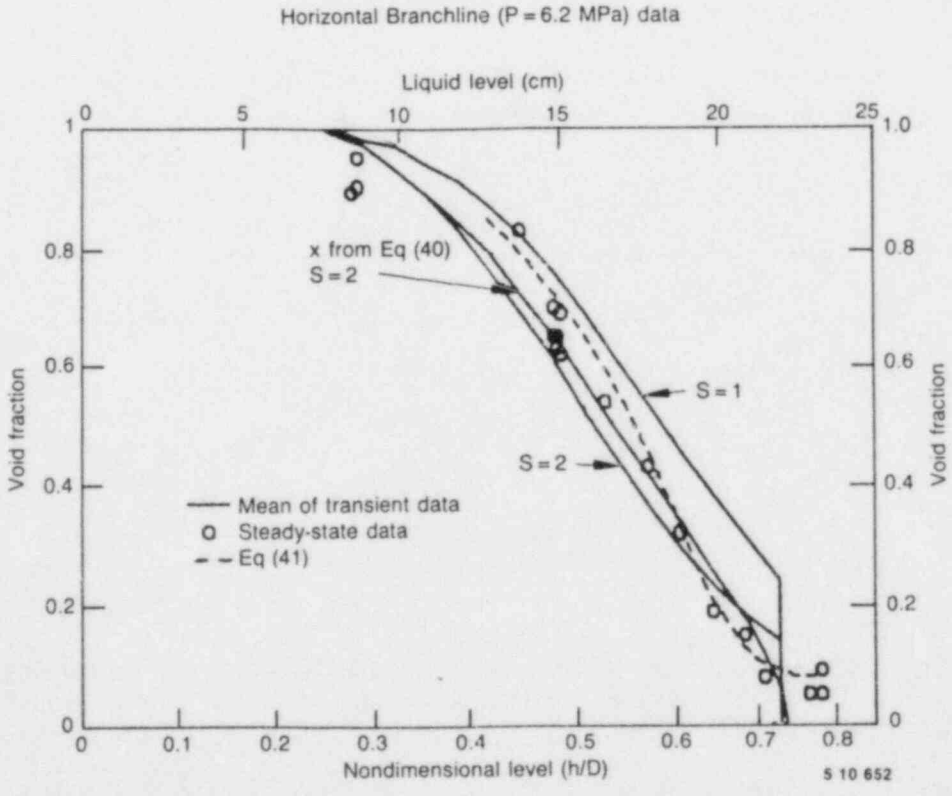

Figure 91. Comparison of branchline void fraction predictions with horizontal configuration 6.2 MPa data.

as criteria for determination of the onset of pull-through, the values given in Table 8 were obtained from the transient steam-water data such as presented in Figures 71, 76, and 85.

The correlation for the configuration originally developed by Lubin and Hurwitz[13] was for vortex-free draining from the bottom of a tank[a], and is represented by Equation (6). This equation can be rewritten as

$$h_{vp} = C_{vp}\left[\frac{\dot{m}_f^2}{g\,\rho_f\,(\rho_f - \rho_g)}\right]^{0.2} \qquad (15)$$

where

h_{vp} = the onset level for vapor pull-through (m)

C_{vp} = the constant obtained from data (nondimensional) [equal to 0.69 in Equation (6)].

a. The available data[6,7] indicates that the presence of a liquid flow past the branchline in the mainline results in a vortex-free flow.

Using the data presented in Table 8 and solving Equation (15) for C_{vp} results in C_{vp} = 0.95 - 1.07.[b] A value of 1.0 was chosen, and the results from Equation (15) are compared to predictions from Equation (6) and observed onset levels in Table 8. As expected, Equation (15) compares to the data much better than predictions from Equation (6). These steam-water data indicate that vapor pull-through occurs at a much higher level than has been previously observed from low-pressure air-water data in much smaller piping, although Smoglie reported a value of 1.17 for C_{vp} in vortex-free flow and 2.0 for vortex flow. The Smoglie value of 1.17 compares fairly well with the value of 1.0 obtained from the current experimental program.

Although the flow quality out the vertical down branch appears to be an exponential function of the mainline liquid level as it was for the horizontal branchline, the flow quality approaches 1 for a nonzero liquid level. The possibility exists that there is an approximate 2 cm bias in the level measurement from the mainline densitometer. However, there is no obvious mechanism in the

b. Solving for C_{vp} in Equation (15) using the observed onset levels for continuous pull-through results in

C_{vp} = 1.02 - 1.07 at 6.2 MPa, C_{vp} = 0.97 at 4.4 MPa, and C_{vp} = 0.95 - 1.02 at 3.4 MPa.

Table 8. Comparison of predicted and observed levels for onset of vapor pull-through in the vertical downflow configuration

Mainline Pressure (MPa)	Onset of Vapor Pull-Through (cm)				Observed Single Phase Flow Rates (kg/s)	
	Observed[a]		Predicted			
	Intermittant	Continuous	Equation (6)	Equation (15)[b]	Steam	Liquid
6.2	9.6-9.8	9.0-9.4	6.6	9.6	1.7	6.6
4.4	10.6	9.3	6.2	9.0	1.2	5.9
3.4	9.6-10.0	8.5-9.2	6.0	8.7	1.0	5.6

a. The onset of intermittent pull-through was identified by a sharp increase in the noise on the pressure drop measurement (PDE-341). The onset of continuous pull-through was identified by an abrupt drop in the level of pressure drop.

b. A value of C_{vp} = 1.0 was used.

measurement system for this type of bias, particularly over the two-week period in which this data was acquired.

Another possible mechanism is that vortex flow into the branchline coupled with steam velocities going past the branchline was sufficient to carry the liquid around the branchline and on down the mainline. This type of behavior has been previously reported[8] for a vertical upflow configuration. The vertical downflow flow quality data can be fit to a relationship of the type

$$X_v = \begin{cases} 1 & h < a \\ \exp\left[C_{vx}\left(\frac{h-a}{h_{vp}}\right)\right] & a \le h \le h_{vp} \\ 0 & h > h_{vp} \end{cases} \qquad (16)$$

where

a = the level at which $X = 1$ (cm)
= 1.7 cm

C_{vx} = a constant obtained from data (nondimensional)
= -4.7

A least squares fit to the vertical downflow steady-state data for the 6.2 MPa pressure data results in a value for C_{vx} of -4.7. The results of Equation (16) are compared to the steady-state data in Figure 92 and show a good comparison between the data and predicted results.

Smoglie[25] presented a relationship for the flow quality in this orientation as

$$X = X_o^{2.5\tilde{h}}\left[1 - \frac{1}{2}\tilde{h}\,(1+\tilde{h})\,X_o^{(1-\tilde{h})}\right]^{0.5} \qquad (17)$$

where the X_o was obtained from the horizontal analysis. The results from Equation (17), using Smoglie's constants and those obtained from this data set, are also presented in Figure 92. The results from Equation (17) do a poor job of fitting the data, although the results using this data set have the right slope. If the offset in level did not exist, then this relationship would work nicely.

Figure 93 compares the steady-state void fraction data to the prediction from Equation (13) using the flow quality predicted by Equation (16). The 6.2 MPa data is essentially bounded by the results from Equation (13) using slip ratios of 1 and 2.

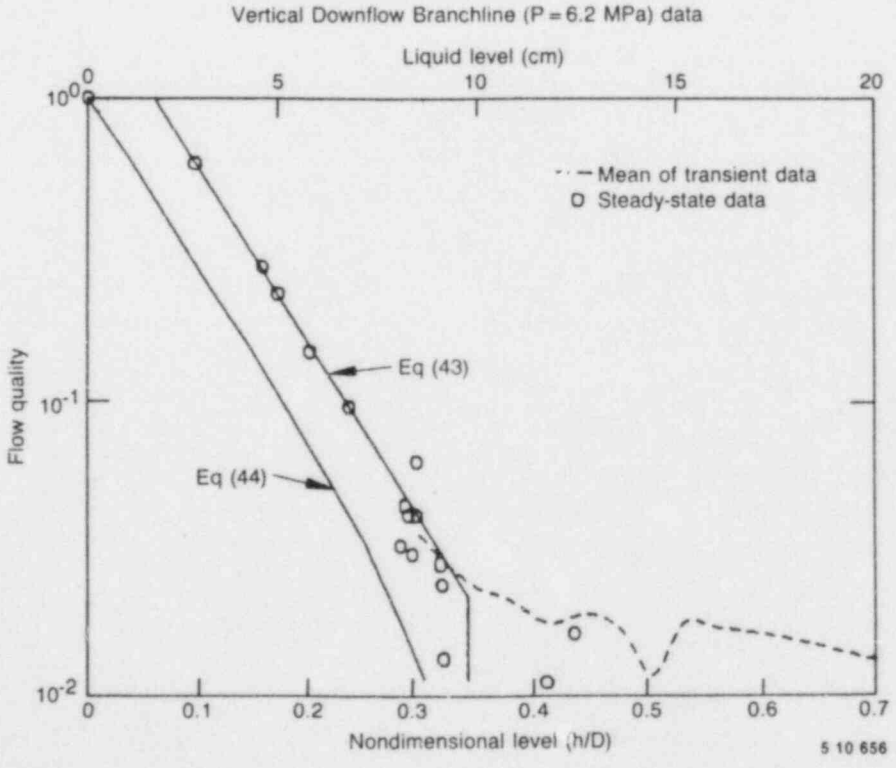

Figure 92. Comparison of branchline flow quality predictions with vertical downflow configuration 6.2 MPa data.

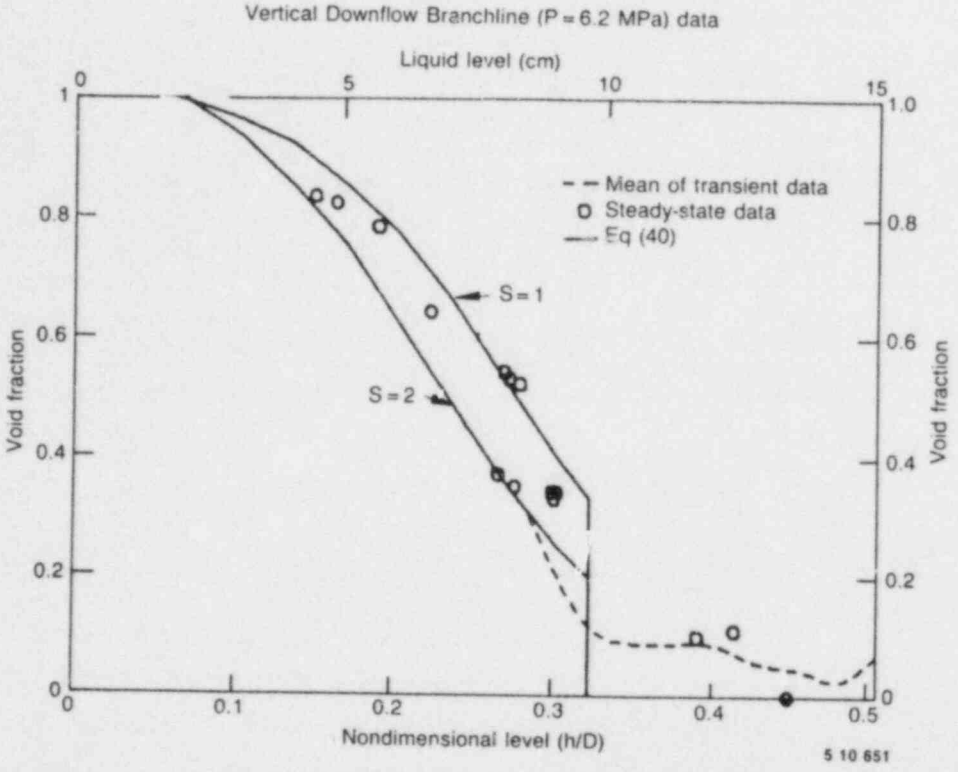

Figure 93. Comparison of branchline void fraction predictions with vertical downflow configuration 6.2 MPa data.

CONCLUSIONS

Data has been presented and discussed from a series of experiments performed to investigate the vapor pull-through and liquid entrainment phenomena with a stratified flow at a tee junction. Also discussed are the effect of these phenomena upon the mass flow rates into the branchline and the flow quality and void fraction in the branchline. In addition, data for the differential pressure from the mainline to the branchline has been presented and discussed. These experiments have expanded the existing data base from experiments performed exclusively in low pressure air/water, to include high pressure steam/water in larger pipe sizes than previously utilized. This data will be useful in determining the applicability of correlations developed in air/water and in the scalability of these correlations. The data reported was obtained for two branchline orientations, horizontal and vertical downflow, and at three different pressures 3.4, 4.4, and 6.2 MPa.

Results from these experiments confirm the forms of previously proposed correlations for predicting the mainline liquid levels at which vapor pull-through and liquid entrainment occur. However, different values for the constants used in the correlations are recommended. The data suggests that the liquid level range over which vapor pull-through and liquid entrainment occur is greater than previously reported.

For the horizontal branchline it was observed that the mass flow rate into the branchline was a linear function of the mainline liquid level (at a constant mainline pressure). However, the slope of this function changed at a level corresponding to the top of the branchline, possibly indicating that the vapor pull-through phenomena results in different fluid properties in the branchline than does the liquid entrainment phenomena. Another interpretation of this slope change involves the fact that the higher levels were obtained by reducing the mainline steam flow rate. The different steam flow rates may have resulted in different wave patterns in the mainline, thus resulting in different amounts of time-averaged vapor pull-through. Comparison of the branchline void fraction, as a function of the mainline liquid level, for the three test pressures shows equal void fractions for a level corresponding to the top of the mainline. This indicates that the best origin of a coordinate system for predicting the branchline void fraction may be the top of the branchline rather than the pipe bottom or centerline.

Flow quality data presented for the horizontal branchline indicate that the branchline flow quality is an exponential function of the mainline liquid level. A correlation for the flow quality was presented and compared to the data and the only other previously reported correlation for the branchline flow quality. Results from this correlation were used to predict the branchline void fraction, which also compared reasonably well to the data.

The data obtained for the horizontal branchline in which the mainline liquid continually changed during a test run (a transient run) compares quite well to the steady-state data obtained for constant level portions of test runs (comparison is within the tolerance limits of the transient data). This indicates that steady-state data may be used for predicting branchline properties for transient cases in which the level is slowly falling.

For the case of the vertical downflow branchline, the branchline mass flow rate at levels below the onset of vapor-pull-through appears to be a linear function of the mainline liquid level. The level at which continuous vapor pull-through begins was observed to occur at about a 50% higher level than has been previously reported. This fact is reflected in the recommended constants for the onset level of vapor pull-through in the vertical downflow branchline orientation. An anomaly observed for this configuration was that a condition of all steam flow out the branchline occurred when a small nonzero level existed in the mainline upstream of the branchline. This phenomena may have been due to an error in the level measurement or may be due to an effect of vorticity for the steam flow into the branchline, forcing the liquid away from the branchline entrance and resulting in the liquid being carried on down the mainline. This type of phenomena has been reported for the case of liquid entrainment in a vertical upflow orientation using air/water flows.

The branchline flow quality for the vertical downflow orientation was observed to follow the same type of exponential relationship as observed for the horizontal orientation. A correlation for predicting the branchline flow quality was proposed and compared favorably to the data. This

correlation was used to predict the branchline void fraction which, when compared to the data, compared quite well except at the low void fractions (less than 25%).

Further experimental work needs to be performed to further expand the data base on this subject. The effect of having the critical flow orifice located at the pipe wall as opposed to downstream in the branchline needs to be investigated. This will help to determine possible evaporation effects at the branchline entrance. Another area needing resolution is the possible vorticity effects for small liquid levels in the mainline with the vertical downflow branchline. It needs to be resolved as to whether this is a real phenomena or an artifact of the measurement system. If this is real, then a correlation relating the offset level to mainline conditions is required. Another area for further investigation is the quantification of the effect of varying mainline steam flow rates on the amount of entrainment/pull-through.

REFERENCES

1. L. T. C. Doa and J. M. Carpenter; *Experiment Data Report for LOFT Nuclear Small-Break Experiment L3-5/L3-5A*, NUREG/CR-1695, EGG-2060, November 1980.

2. K. G. Condie, *LOFT LOCE L3-5/L3-5A Results and Analysis*, paper presented at the LOFT Review Group Meeting, Idaho Falls, Idaho, November 1980.

3. C. L. Nalezny, *LOFT Two-Phase Flow Loop Design and Equipment Requirements*, ES-60215, January 23, 1979.

4. R. S. Semken, *LTSF Experiment Operating Specification for Flow Regime and Critical Flow Studies—Experiment 1*, EGG-SEMI-5913, June 1982.

5. N. Zuber, *Problems in Modeling of Small Break LOCA*, NUREG-724, October 1980.

6. C. J. Crowley and P. H. Rothe, "Flow Visualization and Break Mass Flow Measurements in Small Break Separate Effects Experiments," *Small Break Loss-of-Coolant Accident Analysis in LWRs*, EPRI WS-81-201, August 1981.

7. J. Reimann and M. Khan, *Flow Through a Small Break at the Bottom of a Large Pipe with Stratified Flow*, presented at the 2nd International Topical Meeting on Nuclear Reactor Thermal Hydraulics, Santa Barbara, CA, January 11-14, 1983.

8. J. Reimann and C. Smoglie, *Flow Through a Small Pipe at the Top of a Large Pipe with Stratified Flow*, presented at the annual meeting of the European Two-Phase Flow Group, Zurich, Switzerland, June 14-16, 1983.

9. N. Saba and R. T. Lahey, *Phase Separator Phenomena in Branch Conduits*, NUREG/CR-2590, 1982.

10. A. Craya, "Experimental Research on the Flow of Nonhomogeneous Fluids," *La Houille Blanche*, January-February 1949, pp. 56-64.

11. P. Gariel, "Experimental Research on the Flow of Nonhomogeneous Fluids," *La Houille Blanche*, January-February 1949, pp. 56-64.

12. H. Rouse, *Seven Exploratory Studies in Hydraulics*, proceedings ASChE, *82*, 1956.

13. B. Lubin and M. Hurwitz, *Vapor Pull-Through at a Tank Drain—With and Without Dielectrophoretic Baffling*, Proc. Conference Long Term Cryo-Propellant Storage in Space, NASA Marshall Space Ctr., Huntsville, Alabama, October 1966, p. 173.

14. J. L. Anderson, *Experimental Operating Specification for TPFL Tee/Critical Flow Experiments*, EGG-SEMI-6643, June 1984.

15. R. W. Hamming, *Digital Filters*, Prentice-Hall, Inc., 1977.

16. R. O. Haroldsen and K. L. Smith, *A Survey of the Data Filtering Processes Used on LOFT, Semiscale and PBF Data*, EG&G Idaho Internal Technical Report, IDS-SSD-79-11, October 1979.

17. L. K. Spink, *Principles and Practice of Flow Meter Engineering*, The Foxboro Company, 1967.

18. T. R. Meachum and J. L. Wambach, *A Comparison of Computed Density Profiles from the Transient Flow Calibration Facility, Using Three or Six Beam Measurements*, EG&G Idaho Internal Technical Report, LTR-LO-87-80-137, August 14, 1980.

19. G. D. Lassahn, *Density Profile and Mass Flow Rate Calculation Procedures*, EG&G Idaho Internal Technical Report, LTR-LO-87-80-152, March 4, 1981.

20. R. W. Golden, *Semiscale Uncertainty Report: Methodology, 1*, NUREG/CR-2459, EGG-2142, September 1982.

21. R. W. Golden, *Semiscale Uncertainty Report: Temperature, 2*, NUREG/CR-2459, to be published.

22. R. W. Golden, *Semiscale Uncertainty Report: Absolute and Differential Pressure, 3*, NUREG/CR-2459, EGG-2142, to be published.

23. R. W. Golden, *Semiscale Uncertainty Report: Force, 5*, NUREG/CR-2459, EGG-2142, to be published.

24. S. J. Kline and F. A. McClintock, "Describing Uncertainty in Single-Sample Experiments," *Mechanical Engineering*, 75, 1, January 1953, pp. 3-8.

25. C. Smoglie, *Two-Phase Flow Through Small Branches in a Horizontal Pipe with Stratified Flow*, KfK-3861, December 1984.

26. A. H. Bowker and G. J. Lieberman, *Engineering Statistics*, Prentice-Hall, Inc., 1959, pp 224-228.

27. J. Taitel and A. Dukler, "A Model for Predicting Flow Regime Transitions in Horizontal and Near Horizontal Gas-Fluid Flow," *AIChE Journal, 22*, 1976, pp. 147-155.

APPENDIX A

ENGINEERING DRAWINGS

APPENDIX A

ENGINEERING DRAWINGS

This appendix consists of engineering drawings and a tabulation of the drawings that are significant in describing the two-phase flow loop (TPFL) components. The components include reference metering sections, mainline and branchline test sections, steam separator, catch tank, flow control valves, and connecting piping. Drawings of system electronics, control systems, and support systems are not included. All drawings listed in Table A-1 are included on microfiche and are located at the end of this report.

Table A-1. Engineering drawing list

Drawing Number	Description
158990	LOFT two phase flow calibration loop piping line list
158901	LOFT two phase flow calibration loop piping plot plan
158902	THL two-phase flow calibration loop yard area—piping plans
158903	THL two-phase flow calibration loop yard area—piping section
158904	LOFT two phase flow calibration loop test cell piping plans
158905	LOFT two-phase flow calibration loop test cell piping plans
158906	LOFT two phase flow calibration loop test cell piping section
158907	THL two-phase flow calibration loop—piping details
158908	LOFT two phase flow calibration loop pipe supports
158909	THL two-phase flow calibration loop—piping details
158910	LOFT two phase flow calibration loop test cell
158911	LOFT two phase flow calibration loop structural plan elevation
411065	LOFT transient two-phase flow instrument test spool
411891	LOFT two-phase flow calibration loop steam water mixer assembly
412542	Two-phase phase flow calibration loop test section—assembly and details
415271	Two-phase flow loop 6-in. meter tube spools
416799	TPFL critical flow test installation down flow configuration
416800	LTSF critical flow test 14 in. test section filler
416801	LTSF critical flow test instrument spool
416802	LTSF critical flow test calibration valve
416803	TPFL vertical flow configuration discharge spool pieces
416804	LTSF critical flow test catch tank spool piece
416805	LTSF critical flow test modified 3 in. flange
416806	LTSF critical flow test 3 x a 1/2 reducing hub
416807	LTSF critical flow test nozzle
416808	LTSF critical flow test camera and light source flange
416809	LTSF critical glow test tank and sparger header assy
416810	LTSF critical flow test tank support
417258	THEF two-phase flow loop critical flow test orifice plates
417267	THEF two-phase flow loop critical flow test P&ID

Table A-1. (continued)

Drawing Number	Description
417956	TPFL mixing tee stratifier assembly
419369	TPFL vertical flow modification 1 1/2-in. elbow spool piece assembly
419619	LOFT two-phase flow calibration loop test cell piping plan
419620	LOFT two-phase flow calibration loop test cell piping section
6B-36518 (Peerless)	Vertical gas separator for 66-in. OD
6B-36519 (Peerless)	66-in. OD 1100 psig vertical gas separator

Table A-1. (continued)

Drawing Number	Description
417956	TPFL mixing tee stratifier assembly
419369	TPFL vertical flow modification 1 1/2-in. elbow spool piece assembly
419619	LOFT two-phase flow calibration loop test cell piping plan
419620	LOFT two-phase flow calibration loop test cell piping section
6B-36518 (Peerless)	Vertical gas separator for 66-in. OD
6B-36519 (Peerless)	66-in. OD 1100 psig vertical gas separator

APPENDIX H

TABLES OF DATA VALUES FOR STEADY-STATE CONSTANT LEVEL PORTIONS OF TEST POINTS, INCLUDING INITIAL AND FINAL CONDITIONS

Table H-1. Initial and final conditions for horizontal configuration test points (P = 6.2 MPa)

Test ID	Initial Conditions					Break Valve		Final Conditions				
		Steam Flow Levels							Steam Flow Level			
	PTS (MPa)	T/S (kg/s)	Exhaust (kg/s)	T/S (cm)	Separator (cm)	Open Time (sec)	Close Time (sec)	PTS (MPa)	T/S (kg/s)	Exhaust (kg/s)	T/S (cm)	Separator (cm)
TEE-H-NMU-(-270)	6.16	3.00	2.92	0	155.4	60	300	6.18	2.70	2.50	0	160.4
TEE-H-NMU-(-100)	6.26	3.08	3.04	0	302.3	70	430	6.26	3.05	3.08	0	305.7
TEE-H-NMU-65 (MG = 0.2)	6.18	0.21	0.35	23.9	470.0	80	310	6.19	0.22	0.22	9.6	417.6
TEE-H-NMU-65B (MG = 0.2)	6.21	0.19	0.32	23.8	492.0	75	325	6.20	0.21	0.29	18.6	432.6
TEE-H-NMU-65 (MG = 0.3)	6.21	0.30	0.41	23.3	465.9	75	250	6.21	0.29	0.34	10.1	425.7
TEE-H-NMU-65 (MG = 0.5)	6.24	0.57	0.62	21.5	476.1	70	275	6.24	0.56	0.60	10.5	425.8
TEE-H-NMU-65 (MG = 0.75)	6.20	0.71	0.76	21.0	477.4	80	330	6.20	0.71	0.72	9.7	423.0
TEE-H-NMU-65 (MG = 1.0)	6.25	0.99	0.99	19.8	476.3	70	260	6.25	0.99	1.01	12.7	430.3
TEE-H-NMU-55 (MG = 1.5)	6.27	1.42	1.37	18.7	464.6	70	290	6.27	1.42	1.44	10.3	420.4
TEE-H-NMU-65 (MG = 2.0)	6.23	1.91	1.97	17.4	479.5	80	340	6.18	1.90	1.88	10.6	425.0
TEE-H-NMU-65 (MG = 2.5)	6.21	2.49	2.50	15.7	494.7	60	320	6.21	2.49	2.48	12.9	432.5
TEE-H-NMU-55	6.18	2.93	2.86	14.1	472.9	70	310	6.19	2.94	2.86	11.2	425.5
TEE-H-NMU-43	6.18	2.87	2.73	14.3	459.2	60	290	6.26	2.94	2.83	10.3	424.9
TEE-H-NMU-24	6.28	2.96	2.95	14.2	457.9	65	355	6.30	2.96	2.91	9.6	418.0
TEE-H-NMU-24B	6.26	3.02	3.03	14.1	464.9	120	370	6.27	3.01	3.02	9.7	422.1
TEE-H-NMU-19	6.23	3.05	2.99	14.0	452.4	70	320	6.26	3.06	3.02	9.6	421.7
TEE-H-NMU-14	6.26	2.85	2.79	14.8	443.9	70	450	6.23	—	—	8.2	—
TEE-H-NMU-14R	6.32	2.83	3.13	14.3	437.4	100	460	6.28	—	—	8.2	—
TEE-H-NMU-8	6.21	2.99	2.88	12.6	433.1	65	410	—	—	—	8.6	—
TEE-H-MU-14	6.26	3.05	2.96	14.0	449.7	90	370	6.25	2.91	2.53	—	437.2
TEE-H-MU-6	6.20	3.01	2.93	8.5	420.0	155	525	6.19	2.90	2.53	—	440.3

Table H-2. Initial and final conditions for horizontal configuration test points (P = 4.4 MPa)

Test ID	Initial Conditions					Break Valve		Final Conditions				
		Steam Flow Levels							Steam Flow Level			
	PTS (MPa)	T/S (kg/s)	Exhaust (kg/s)	T/S (cm)	Separator (cm)	Open Time (sec)	Close Time (sec)	PTS (MPa)	T/S (kg/s)	Exhaust (kg/s)	T/S (cm)	Separator (cm)
TEE-H-NMU-(-100)	4.47	2.45	2.41	0	290.7	75	550	4.48	2.45	2.44	0	292.9
TEE-H-NMU-65 (MG = 0.3)	4.46	0.24	0.29	22.7	459.6	63	225	4.46	0.26	0.30	14.0	418.4
TEE-H-NMU-55 (MG = 0.5)	4.42	0.49	0.51	21.0	450.9	60	225	4.42	0.51	0.50	12.6	415.9
TEE-H-NMU-65 (MG = 1.0)	4.44	1.06	1.04	18.7	461.9	70	380	4.45	1.06	1.03	9.4	415.2
TEE-H-NMU-65 (MG = 1.5)	4.44	1.44	1.43	17.5	473.4	80	350	4.44	1.44	1.44	12.0	420.4
TEE-H-NMU-65 (MG = 2.0)	4.44	1.96	1.93	15.6	471.5	60	330	4.44	1.97	1.99	13.4	422.0
TEE-H-NMU-55	4.42	2.61	2.61	13.5	468.0	75	430	4.42	2.41	2.47	10.4	416.9
TEE-H-NMU-55B	4.46	2.40	2.45	14.2	458.1	70	460	4.45	2.40	2.46	9.3	413.3
TEE-H-NMU-65-(MG = 3.0)	4.42	2.87	2.87	12.6	478.9	60	380	4.42	2.86	2.86	12.6	429.7
TEE-H-NMU-24	4.43	2.46	2.50	14.1	440.4	65	555	4.44	2.46	2.51	9.2	408.3
TEE-H-NMU-19	4.40	2.37	2.42	14.2	452.3	70	420	4.41	2.43	2.45	9.3	413.7
TEE-H-NMU-14	4.46	2.44	2.41	14.4	442.8	60	415	4.45	2.46	2.51	9.5	413.6
TEE-H-NMU-14 (ML = 3)	4.48	2.46	2.47	13.9	425.8	60	575	4.49	2.47	2.49	7.3	414.7
TEE-H-NMU-8 (MG = 2.5)	4.52	2.39	2.29	12.0	421.2	60	525	4.56	2.42	2.41	8.7	410.9

Table H-3. Initial and final conditions for horizontal configuration test points (P = 3.45 MPa)

Test ID	Initial Conditions					Break Valve		Final Conditions				
		Steam Flow Levels							Steam Flow Level			
	PTS (MPa)	T/S (kg/s)	Exhaust (kg/s)	T/S (cm)	Separator (cm)	Open Time (sec)	Close Time (sec)	PTS (MPa)	T/S (kg/s)	Exhaust (kg/s)	T/S (cm)	Separator (cm)
TEE-H-NMU-(-100)	3.45	2.97	2.97	0	284.2	60	480	3.45	2.95	2.94	0	287.5
TEE-H-NMU-65 (MG = 0.3)	3.45	0.28	0.29	22.2	458.0	60	280	3.45	0.28	.29	12.4	415.7
TEE-H-NMU-65 (MG = 0.3) (ML = 2)	3.49	0.26	0.28	21.8	457.6	80	285	3.47	0.28	0.31	12.2	417.2
TEE-H-NMU-65 (MG = 0.5)	3.43	0.52	0.52	20.3	458.1	95	380	3.44	0.54	0.55	10.6	414.0
TEE-H-NMU-65 (MG = 1.0)	3.47	0.99	0.99	18.3	467.2	75	325	3.46	0.99	1.03	13.5	420.0
TEE-H-NMU-65 (MG = 1.6)	3.44	1.64	1.66	15.9	472.4	75	475	3.44	1.64	1.66	10.1	416.5
TEE-H-NMU-24	3.45	1.62	1.52	16.1	454.3	60	440	3.46	1.66	1.63	10.2	412.9
TEE-H-NMU-19	3.45	1.62	1.62	15.9	443.4	60	660	3.46	1.65	1.70	8.6	416.9
TEE-H-NMU-14	3.47	1.59	1.58	15.8	426.2	60	700	3.47	1.62	1.64	9.4	413.2
TEE-H-NMU-8 (ML = 3)	3.46	1.62	1.62	14.3	422.3	65	620	3.47	1.60	1.63	7.4	413.3
TEE-H-NMU-4 (ML = 2)	3.44	1.72	1.67		416.4	70	520	3.44	1.72	1.70		418.5

Table H-4. Initial and final conditions for vertical downflow configuration test points (P = 6.2 MPa)

	Initial Conditions					Break Valve		Final Conditions				
		Steam Flow Levels							Steam Flow Level			
Test ID	PTS (MPa)	T/S (kg/s)	Exhaust (kg/s)	T/S (cm)	Separator (cm)	Open Time (sec)	Close Time (sec)	PTS (MPa)	T/S (kg/s)	Exhaust (kg/s)	T/S (cm)	Separator (cm)
TEE-VD-NMU-(-100)	6.24	3.06	3.03	0.0	326.6	90	420	6.22	3.07	3.06	0.0	328.0
TEE-VD-NMU-(-100) B	6.23	3.08	3.05	0.0	310.3	70	420	6.24	3.12	3.10	0.0	314.0
TEE-VD-NMU-90	6.21	0.25	0.37	24.5	481.6	75	305	6.19	0.25	0.30	10.0	403.8
TEE-VD-NMU-44	6.23	3.02	2.99	13.6	464.3	75	275	6.22	3.18	3.20	10.1	393.9
TEE-VD-NMU-44 (MG = 2)	6.19	2.23	2.25	16.0	459.7	70	310	6.17	2.26	2.29	9.0	384.9
TEE-VD-NMU-44 (MG = 1)	6.23	0.93	0.87	21.1	445.7	90	290	6.21	1.00	0.94	9.0	387.4
TEE-VD-NMU-39	6.21	2.96	2.88	13.8	462.6	90	345	6.21	2.98	2.96	9.3	383.2
TEE-VD-NMU-34	6.28	2.96	2.96	14.0	447.6	90	350	6.26	2.98	2.98	9.2	371.7
TEE-VD-NMU-29	6.20	3.15	3.13	11.0	435.8	90	360	6.18	3.31	3.29	9.1	361.0
TEE-VD-NMU-24	6.21	3.21	3.21	10.2	428.8	75	310	6.19	3.32	3.31	10.1	356.4
TEE-VD-NMU-6	6.21	3.01	3.02	10.1	375.9	80	320	6.19	3.10	3.10	10.0	297.7
TEE-VD-NMU-5	6.22	2.96	2.96	9.3	375.1	70	290	6.20	2.97	2.97	9.2	310.6
TEE-VD-NMU-4	6.22	2.98	2.96	7.6	370.1	90	380	6.21	2.98	2.96	7.6	305.5
TEE-VD-NMU-3	6.24	3.06	3.01	6.7	380.0	80	405	6.21	3.12	3.19	6.6	318.1
TEE-VD-NMU-2	6.24	3.11	3.02	6.2	369.7	75	390	6.21	3.16	3.14	5.3	321.9
TEE-VD-NMU-1	6.20	3.20	3.15	5.7	362.4	75	340	6.21	2.99	2.91	5.3	324.5
TEE-VD-NMU-0.5	6.20	3.01	2.92	3.7	361.1	85	405	6.19	3.00	2.97	3.8	343.7

Table H-5. Initial and final conditions for vertical downflow configuration test points (P = 4.4 MPa)

	Initial Conditions					Break Valve		Final Conditions				
		Steam Flow Levels							Steam Flow Level			
Test ID	PTS (MPa)	T/S (kg/s)	Exhaust (kg/s)	T/S (cm)	Separator (cm)	Open Time (sec)	Close Time (sec)	PTS (MPa)	T/S (kg/s)	Exhaust (kg/s)	T/S (cm)	Separator (cm)
TEE-VD-NMU-(-100)	4.41	3.15	3.23	1.0	311.5	70	490	4.40	3.14	3.15	0.0	314.8
TEE-VD-NMU-90	4.45	0.30	0.37	—	479.4	90	315	4.44	0.32	0.38	—	408.7
TEE-VD-NMU-44	4.40	1.96	1.75	19.0	456.7	75	240	4.40	1.96	1.85	9.7	410.3
TEE-VD-NMU-39	4.46	2.06	2.03	18.4	437.1	110	360	4.47	2.06	2.07	10.6	368.6
TEE-VD-NMU-34	4.43	2.14	2.24	—	451.1	65	280	4.42	2.22	2.33	—	392.5
TEE-VD-NMU-29	4.48	2.02	1.94	14.7	422.5	75	270	4.49	2.02	1.98	9.7	378.0
TEE-VD-NMU-0.5	4.43	2.02	1.95	4.6	309.8	95	370	4.43	2.02	2.00	4.5	288.6
TEE-VD-NMU-1	4.46	2.06	2.12	5.5	375.9	90	370	4.45	2.07	2.13	5.5	339.9
TEE-VD-NMU-2	4.42	2.00	2.05	5.7	369.5	75	490	4.41	2.07	2.18	5.6	315.9
TEE-VD-NMU-3	4.45	2.02	2.00	8.3	352.0	105	375	4.45	2.00	1.97	8.3	296.6
TEE-VD-NMU-4	4.41	2.08	2.17	7.6	356.2	90	430	4.40	2.08	2.20	7.6	287.6
TEE-VD-NMU-5	4.45	2.06	2.07	9.2	384.8	105	375	4.45	2.06	2.07	9.1	321.0
TEE-VD-NMU-6	4.41	2.09	2.16	9.1	365.3	70	350	4.40	2.10	2.22	9.1	296.1

Table H-6. Initial and final conditions for vertical downflow configuration test points (P = 3.45 MPa)

	Initial Conditions					Break Valve		Final Conditions				
		Steam Flow Levels						Steam Flow Level				
Test ID	PTS (MPa)	T/S (kg/s)	Exhaust (kg/s)	T/S (cm)	Separator (cm)	Open Time (sec)	Close Time (sec)	PTS (MPa)	T/S (kg/s)	Exhaust (kg/s)	T/S (cm)	Separator (cm)
TEE-VD-NMU-(-100)	3.48	3.13	3.08	0	310.5	75	430	3.49	3.14	3.09	0	314.9
TEE-VD-NMU-90B	3.46	0.34	0.40	21.5	452.8	80	360	3.46	0.34	0.42	8.7	383.7
TEE-VD-NMU-44	3.45	1.61	1.45	16.1	435.3	70	290	3.44	1.61	1.49	8.9	384.2
TEE-VD-NMU-39	3.45	1.60	1.56	15.8	430.6	85	380	3.45	1.60	1.58	8.7	365.6
TEE-VD-NMU-34	3.47	1.60	1.58	15.8	430.7	90	390	3.46	1.61	1.67	8.8	359.7
TEE-VD-NMU-29	3.47	1.64	1.37	N/A	419.9	80	290	3.47	1.64	1.41	N/A	375.4
TEE-VD-NMU-24	3.47	1.60	1.57	12.0	412.2	100	400	3.47	1.60	1.65	8.8	343.7
TEE-VD-NMU-0.25	3.46	1.60	1.60	4.6	351.9	95	390	3.46	1.60	1.59	4.4	326.9
TEE-VD-NMU-0.5	3.45	1.65	1.57	3.5	380.9	90	480	3.45	1.65	1.59	3.5	367.2
TEE-VD-NMU-1	3.45	1.64	1.65	4.3	378.7	90	375	3.45	1.64	1.63	4.3	358.6
TEE-VD-NMU-2	3.47	1.64	1.63	6.8	368.8	90	345	3.47	1.64	1.62	6.8	327.4
TEE-VD-NMU-3	3.45	1.64	1.67	7.5	344.5	95	375	3.43	1.64	1.65	7.4	292.8
TEE-VD-NMU-4	3.47	1.60	1.61	7.9	345.6	110	375	3.47	1.60	1.61	7.8	293.6
TEE-VD-NMU-5	3.44	1.66	1.67	N/A	307.1	100	365	3.45	1.66	1.67	N/A	244.2
TEE-VD-NMU-6	3.45	1.66	1.68	10.4	305.0	100	380	3.45	1.66	1.70	10.4	233.0

N/A Data not available.

Table H-7. Data values for constant level portions of horizontal configuration data points (P = 6.2 MPa)

Mainline Conditions					Branchline Conditions									
								Flow Quality		Void Fraction		Pressure Drops		
Test ID	Pressure PE-302 (MPa)	Steam Flow $\dot{m}_{G\text{-}TS}$ (kg/s)	Liquid Flow $\dot{m}_{L\text{-}TS}$ (kg/s)	Liquid Level (cm)	Steam Flow $\dot{m}_{GB}$ (kg/s)	Total Flow $\dot{m}_{TB}$ (kg/s)	Catch Tank Flow $\dot{m}_{CT}$ (kg/s)	Entrance X_B	Break X_{OR}	Entrance α_B	Break α_{OR}	Entrance PDE-341 (kPa)	Break PDE-450 (MPa)	Data Averaging Time Period (sec)
TEE-H-NMU-(270)	6.15	2.99	0.12	0	1.84	1.53	1.58	1	1	—	—	112	5.21	100-160
	6.26	2.95	0.12	0	1.72	1.60	1.53	1	1	—	—	112	5.22	200-260
TEE-H-NMU-(100)	6.26	3.09	0.20	0	1.69	1.63	1.64	1	1	0.93	0.85	113	5.29	140-200
	6.26	3.09	0.19	0	1.70	1.62	1.66	1	1	0.93	0.85	113	5.29	300-360
TEE-H-NMU-65 (MG = 0.2)	6.16	0.25	5.81	23.3	0	6.88	6.80	0	0	0.05	0.08	81.1	4.46	120-140
TEE-H-NMU-65B (MG = 0.2)	6.17	0.25	6.00	23.3	0	6.79	6.82	0	0	0.09	0.06	82.5	4.45	105-165
TEE-H-NMU-65 (MG = 0.3)	6.21	0.33	6.17	22.9	0.02	6.80	6.80	0.0028	0.0019	0.05	0.08	84.2	4.47	110-135
TEE-H-NMU-65 (MG = 0.5)	6.24	0.61	6.21	21.5	0.00	6.09	6.23	0.000	0	0.08	0.11	71.3	4.66	105-150
TEE-H-NMU-65 (MG = 0.75)	6.20	0.74	6.06	20.9	0.00	5.74	5.85	2.05E-4	6.8E-5	0.15	0.12	64.9	4.72	120-180
TEE-H-NMU-65 (MG = 1.0)	6.24	1.03	6.16	19.9	0.09	5.13	5.46	0.018	0.015	0.19	0.21	58.0	4.89	110-170
TEE-H-NMU-55 (MG = 1.5)	6.27	1.46	6.02	18.9	0.16	4.55	4.84	0.035	0.030	0.32	0.21	57.0	5.02	100-160
TEE-H-NMU-65 (MG = 2.0)	6.22	1.94	6.05	17.9	0.12	4.13	4.36	0.028	0.025	0.43	0.44	61.9	5.05	150-210
TEE-H-NMU-65 (MG = 2.5)	6.20	2.53	5.79	16.6	0.23	3.82	3.94	0.061	0.058	0.54	0.52	70.5	5.06	120-180
	6.20	2.52	5.78	16.6	0.22	3.90	4.02	0.057	0.054	0.54	0.51	70.3	5.06	180-240
TEE-H-NMU-55	6.17	2.98	6.02	15.0	0.35	3.55	3.80	0.099	0.091	0.70	0.83	80.5	5.07	120-180
	6.17	2.98	6.01	15.0	0.35	3.51	3.77	0.10	0.093	0.71	0.84	80.8	5.07	180-240
TEE-H-NMU-43	6.21	2.96	6.15	15.3	0.45	3.44	3.70	0.13	0.12	0.65	0.70	80.7	5.10	120-180
TEE-H-NMU-24	6.28	2.99	5.88	15.2	0.34	3.57	3.79	0.095	0.088	0.62	0.59	81.5	5.15	100-160
TEE-H-NMU-24B	6.26	3.04	6.01	15.1	0.33	3.59	3.65	0.092	0.090	0.63	0.57	81.5	5.14	160-220
TEE-H-NMU-19	6.23	3.08	6.03	15.0	0.40	3.43	3.63	0.12	0.11	0.65	0.58	83.1	5.12	110-170
TEE-H-NMU-14	6.23	2.85	6.08	8.6	1.41	1.82	2.01	0.77	0.70	0.89	0.85	124	5.23	320-380
TEE-H-NMU-14R	6.25	2.90	5.96	8.8	1.38	1.81	1.95	0.76	0.71	0.90	0.88	125	5.26	340-400
TEE-H-NMU-8	6.21	2.97	6.08	8.8	1.39	1.83	—	—	—	0.95	0.84	124	5.22	310-370
TEE-H-MU-14	6.24	2.99	6.05	15.2	0.59	3.67	3.76	0.16	0.16	0.69	0.58	81.8	5.12	130-190
TEE-H-MU-6	6.24	2.98	6.08	13.9	0.90	3.41	3.15	0.27	0.29	0.83	0.69	98.5	5.17	200-260

Table H-8. Data values for constant level portions of horizontal configuration data points (P = 4.4 MPa)

Test ID	Mainline Conditions				Branchline Conditions									
								Flow Quality		Void Fraction		Pressure Drops		
	Pressure PE-302 (MPa)	Steam Flow $\dot{m}_{G\text{-}TS}$ (kg/s)	Liquid Flow $\dot{m}_{L\text{-}TS}$ (kg/s)	Liquid Level (cm)	Steam Flow $\dot{m}_{GB}$ (kg/s)	Total Flow $\dot{m}_{TB}$ (kg/s)	Catch Tank Flow $\dot{m}_{CT}$ (kg/s)	Entrance X_B	Break X_{OR}	Entrance α_B	Break α_{OR}	Entrance PDE-341 (kPa)	Break PDE-450 (MPa)	Data Averaging Time Period (sec)
TEE-H-NMU-(-100)	4.47	2.45	0	0	1.22	1.18	1.27	1	1	0.98	1	83.0	3.77	300-360
	4.47	2.45	0	0	1.23	1.12	1.17	1	1	0.98	1	83.0	3.77	400-460
TEE-H-NMU-65 (MG = 0.3)	4.45	0.28	6.02	22.5	0	6.36	6.42	0	0	0.04	0.04	67.9	3.03	100-140
TEE-H-NMU-55 (MG = 0.5)	4.41	0.52	6.06	20.9	0.02	5.38	5.51	0.0034	0.0026	0.07	0.10	54.4	3.16	85-120
TEE-H-NMU-65 (MG = 1.0)	4.4-	1.09	5.90	18.9	0.07	4.15	4.20	0.018	0.017	0.23	0.26	40.7	3.45	100-160
TEE-H-NMU-65 (MG = 1.5)	4.44	1.46	6.05	17.8	0.09	3.58	3.75	0.026	0.025	0.38	0.38	42.5	3.53	110-170
	4.44	1.46	6.03	17.8	0.09	3.59	3.75	0.024	0.023	0.38	0.38	42.5	3.53	200-260
TEE-H-NMU-65 (MG = 2.0)	4.44	1.99	6.05	16.3	0.15	3.02	3.23	0.048	0.045	0.56	0.53	51.4	3.59	100-160
	4.44	1.99	6.05	16.3	0.14	3.16	3.31	0.043	0.042	0.56	0.53	51.5	3.60	200-260
TEE-H-NMU-55	4.42	2.68	6.19	14.4	0.25	2.58	2.72	0.097	0.093	0.71	0.75	64.0	3.57	100-160
	4.42	2.71	6.18	14.2	0.24	2.60	2.76	0.094	0.089	0.73	0.79	65.9	3.59	300-360
TEE-H-NMU-55B	—	—	—	—	—	—	—	—	—	—	—	—	—	100-160
														200-260
TEE-H-NMU-65 (MG = 3.0)	4.42	2.85	6.10	14.0	0.27	2.55	2.63	0.11	0.10	0.73	0.65	65.7	3.62	100-160
	4.42	2.85	6.09	13.9	0.26	2.60	2.77	0.10	0.096	0.73	0.65	65.9	3.63	270-330
TEE-H-NMU-24	4.43	2.47	6.02	14.9	0.21	2.76	2.80	0.075	0.074	0.69	0.76	61.5	3.62	100-160
	4.43	2.47	6.02	9.5	0.89	1.28	1.42	0.70	0.63	0.9-	1.01	92.9	3.71	400-460
TEE-H-NMU-19	4.40	2.44	6.19	15.0	0.19	2.81	2.88	0.067	0.066	0.68	0.76	60.0	3.59	100-160
TEE-H-NMU-14	4.44	2.47	6.11	15.1	0.26	2.74	2.82	0.096	0.094	0.61	0.73	62.1	3.63	100-160
TEE-H-NMU-14 (ML = 3)	4.47	2.48	3.12	8.4	1.05	1.22	1.31	0.86	0.80	0.94	0.77	94.6	3.75	440-500
TEE-H-NMU-8	4.54	2.43	6.02	9.0	0.98	1.29	1.46	0.77	0.67	0.94	0.55	95.2	3.80	340-400
	4.55	2.43	6.00	9.0	0.98	1.38	1.53	0.72	0.64	0.94	0.55	95.3	3.81	440-500

Table H-9. Data values for constant level portions of horizontal configuration data points (P = 3.45 MPa)

	Mainline Conditions				Branchline Conditions									
								Flow Quality		Void Fraction		Pressure Drops		
Test ID	Pressure PE-302 (MPa)	Steam Flow $\dot{m}_{G\text{-}TS}$ (kg/s)	Liquid Flow $\dot{m}_{L\text{-}TS}$ (kg/s)	Liquid Level (cm)	Steam Flow $\dot{m}_{GB}$ (kg/s)	Total Flow $\dot{m}_{TB}$ (kg/s)	Catch Tank Flow $\dot{m}_{CT}$ (kg/s)	Entrance X_B	Break X_{OR}	Entrance $\bar{\alpha}_B$	Break $\bar{\alpha}_{OR}$	Entrance PDE-341 (kPa)	Break PDE-450 (MPa)	Data Averaging Time Period (sec)
TEE-H-NMU-(-100)	3.45	3.01	0	0	1.00	0.88	0.84	1	1	0.97	1	65.8	2.90	160-220
	3.45	3.01	0	0	1.00	0.93	0.90	1	1	0.97	1	65.8	2.90	360-420
TEE-H-NMU-65 (MG = 0.3)	3.49	0.30	5.98	21.9	0	5.98	6.27	0	0	—	0.01	58.8	2.2e	110-150
TEE-H-NMU-65 (MG = 0.3) (ML = 2)	3.45	0.29	2.06	21.8	0	5.58	5.71	0	0.0011	0.03	0.06	52.2	2.29	110-150
TEE-H-NMU-65 (MG = 0.5)	3.43	0.54	6.13	20.1	0.004	4.72	4.78	0.0009	0.0014	0.02	0.11	39.0	2.44	130-190
TEE-H-NMU-65 (MG = 1.0)	3.46	1.01	6.21	18.5	0.02	3.60	3.64	0.0067	0.0071	0.24	0.35	32.6	2.66	120-180
	3.46	1.01	6.21	18.5	0.005	3.60	3.70	0.0014	0.0020	0.24	0.36	32.6	2.66	180-240
TEE-H-NMU-65	3.44	1.65	6.12	16.4	0.08	2.84	2.88	0.028	0.029	0.53	0.60	40.4	2.75	160-220
	3.44	1.65	6.13	16.4	0.07	2.77	2.86	0.025	0.026	0.54	0.61	40.9	2.76	260-320
TEE-H-NMU-24	3.44	1.64	6.18	16.5	0.14	2.67	2.86	0.054	0.050	0.74	0.69	41.3	2.75	100-160
	3.44	1.65	6.17	16.4	0.13	2.51	2.88	0.051	0.045	0.75	0.69	41.2	2.76	200-260
TEE-H-NMU-19	3.45	1.65	6.30	16.0	0.14	2.61	2.59	0.054	0.056	0.64	0.62	43.3	2.77	100-160
	3.45	1.65	6.32	9.0	0.77	0.98	0.95	0.78	0.81	0.97	0.97	75.4	2.88	540-600
TEE-H-NMU-14	3.47	1.63	6.22	9.5	0.78	1.01	1.02	0.77	0.76	0.98	0.95	75.6	2.98	510-570
	3.47	1.64	6.22	9.5	0.78	0.99	1.13	0.78	0.69	0.99	0.96	75.6	2.90	610-670
TEE-H-NMU-8 (ML = 3)	3.46	1.61	2.97	8.2	0.83	0.95	0.94	0.88	0.89	0.96	0.98	75.2	2.90	510-570

Table H-10. Data values for constant level portions of vertical downflow configuration data points (P = 6.2 MPa)

Test ID	Mainline Conditions: Pressure PE-302 (MPa)	Mainline Conditions: Steam Flow $\dot{m}_{G\text{-}TS}$ (kg/s)	Mainline Conditions: Liquid Flow $\dot{m}_{L\text{-}TS}$ (kg/s)	Mainline Conditions: Liquid Level (cm)	Branchline Conditions: Steam Flow $\dot{m}_{GB}$ (kg/s)	Branchline Conditions: Total Flow $\dot{m}_{TB}$ (kg/s)	Branchline Conditions: Catch Tank Flow $\dot{m}_{CT}$ (kg/s)	Branchline Conditions: Flow Quality: Entrance X_B	Branchline Conditions: Flow Quality: Break X_{OR}	Branchline Conditions: Void Fraction: Entrance α_B	Branchline Conditions: Void Fraction: Break α_{OR}	Branchline Conditions: Pressure Drops: Entrance PDE-341 (kPa)	Branchline Conditions: Pressure Drops: Break PDE-450 (MPa)	Data Averaging Time Period (sec)
TEE-H-NMU-[illegible]-(-100)	6.23	3.09	0	0	1.62	1.62	1.69	1.0	0.96	—	—	154.0	5.20	200-260
TEE-H-NMU-[illegible]-100)	6.22	3.10	0	0	1.62	1.60	1.67	1.0	0.97	—	—	153.0	5.20	300-360
TEE-H-NMU-(-100)B	6.22	3.15	0	0	1.60	1.56	1.61	1.0	1.0	0.94	0.76	154.0	5.23	240-300
TEE-H-NMU-90	6.19	0.28	6.06	24.0	0.005	6.62	6.64	6.6E-4	5.5E-4	0.09	0.04	91.7	4.51	120-180
TEE-H-NMU-44 (MG = 1.0)	6.22	1.02	6.09	8.3	0.21	4.09	4.45	0.059	0.046	0.52	0.51	78.7	4.98	200-260
TEE-H-NMU-44 (MG = 2.0)	6.18	2.41	5.95	13.3	0.06	6.34	6.23	9.8E-3	9.5E-3	0.00	0.00	84.7	4.57	105-165
	6.17	2.31	5.94	7.9	0.12	4.10	4.37	0.031	0.028	0.37	0.32	80.6	4.95	200-260
TEE-H-NMU-44	6.22	3.11	5.96	11.6	0.07	6.26	6.44	0.011	0.011	0.10	0.08	87.8	4.58	100-160
	6.22	3.16	5.94	8.9	0.12	4.40	4.87	0.027	0.024	0.34	0.33	72.8	4.93	190-250
TEE-H-NMU-39	6.23	2.99	6.13	12.3	0.11	6.67	6.65	0.016	0.015	0.11	0.06	96.7	4.51	120-150
	6.22	3.02	6.12	8.3	0.16	4.23	4.48	0.039	0.036	0.52	0.55	78.9	4.98	240-300
TEE-H-NMU-34	6.27	3.02	6.07	8.1	0.16	4.18	4.43	0.039	0.036	0.53	0.57	81.8	5.03	200-260
TEE-H-NMU-29	6.18	3.31	5.95	8.0	0.17	4.11	4.51	0.042	0.038	0.54	0.59	81.3	4.96	180-240
TEE-H-NMU-24	6.20	3.34	5.97	9.0	0.10	4.60	4.80	0.023	0.021	0.33	0.33	72.1	4.90	150-210
TEE-H-NMU-6 (ML = 6)	6.19	3.10	6.09	9.0	0.06	4.68	4.78	0.013	0.012	0.34	0.30	71.9	4.90	180-240
TEE-H-NMU-5 (ML = 5)	6.21	2.99	5.09	8.2	0.13	4.34	4.42	0.029	0.038	0.35	0.27	78.9	4.97	150-210
TEE-H-NMU-4 (ML = 4)	6.21	3.00	4.02	6.6	0.33	3.62	3.71	0.091	0.089	0.64	0.46	107.0	5.05	180-240
TEE-H-NMU-3 (ML = 3)	6.23	3.16	3.02	5.6	0.45	3.25	3.28	0.14	0.14	0.78	0.53	128.0	5.09	200-260
TEE-H-NMU-2 (ML = 2)	6.23	3.17	2.02	4.8	0.66	2.95	2.97	0.22	0.22	0.82	0.59	143.0	5.10	180-240
TEE-H-NMU-1 (ML = 1)	6.22	3.21	1.06	4.4	0.75	2.76	2.81	0.27	0.27	0.83	0.62	148.0	5.11	180-240
TEE-H-NMU-0.5 (ML = 0.5)	6.19	3.01	0.55	2.7	1.20	2.01	2.07	0.60	0.58	1.01	0.65	168.0	5.12	200-260

Table H-1₁. Data values for constant level portions of vertical downflow configuration data points (P = 4.4 MPa)

Mainline Conditions					Branchline Conditions									
								Flow Quality		Void Fraction		Pressure Drops		
Test ID	Pressure PE-302 (MPa)	Steam Flow $\dot{m}_{G\text{-}TS}$ (kg/s)	Liquid Flow $\dot{m}_{L\text{-}TS}$ (kg/s)	Liquid Level (cm)	Steam Flow $\dot{m}_{GB}$ (kg/s)	Total Flow $\dot{m}_{TB}$ (kg/s)	Catch Tank Flow $\dot{m}_{CT}$ (kg/s)	Entrance x_B	Break x_{OR}	Entrance $\bar{\alpha}_B$	Break $\bar{\alpha}_{OR}$	Entrance PDE-341 (kPa)	Break PDE-450 (MPa)	Data Averaging Time Period (sec)
TEE-VD-NMU-(-100)	4.40	3.21	0	0.0	1.04	0.98	1.21	1	0.86	1.00	1.00	122.0	3.65	240-320
TEE-VD-NMU-90	4.44	0.33	6.03	—[a]	0.0	5.74	5.86	0.0	4.5E-4	—	—	68.1	3.10	150-210
TEE-VD-NMU-44	4.40	1.92	6.02	17.4	0.10	5.83	5.88	0.017	0.018	0.02	0.0	67.7	3.10	110-160
TEE-VD-NMU-39	4.47	2.05	6.04	9.5	0.05	4.17	4.32	0.011	0.011	0.20	0.18	53.0	3.44	240-300
TEE-VD-NMU-34	4.42	2.25	5.80	—[a]	0.0	3.78	4.42	0.0	2/3E-4	—	—	52.5	3.36	200-250
TEE-VD-NMU-29	4.48	2.00	5.94	8.4	0.12	3.69	4.04	0.032	0.030	0.31	0.29	55.0	3.53	150-210
TEE-VD-NMU-6 (ML = 6)	4.41	2.09	6.05	8.1	0.0	3.84	3.94	0.0	2.6E-4	0.26	0.33	53.4	3.42	180-240
TEE-VD-NMU-5 (ML = 5)	4.45	2.05	5.03	8.1	0.06	3.64	3.86	0.017	0.017	0.42	0.38	58.1	3.54	200-260
TEE-VD-NMU-4 (ML = 4)	4.40	2.08	4.07	6.9	0.001	3.11	3.28	4.3E-4	1.4E-3	0.54	0.56	68.8	3.51	240-300
TEE-VD-NMU-3 (ML = 3)	4.45	1.99	3.12	7.4	0.14	3.31	3.32	0.042	0.043	0.56	0.46	66.9	3.57	200-260
TEE-VD-NMU-2 (ML = 2)	4.41	2.06	1.97	4.7	0.25	2.23	2.40	0.11	0.11	0.84	0.79	103.0	3.59	240-300
TEE-VD-NMU-1 (ML = 1)	4.45	2.06	0.97	4.5	0.30	2.22	2.35	0.14	0.13	0.77	0.89	106.0	3.63	200-260
TEE-VD-NMU-0.5 (ML = 0.5)	4.43	2.01	0.54	3.7	0.63	1.80	1.83	0.35	0.35	1.0	0.74	121.0	3.66	200-260

a. Densitometer data is unavailable for this data point.

Table H-12. Data values for constant level portions of vertical downflow configuration data points (P = 3.45 MPa)

Test ID	Mainline Conditions				Branchline Conditions									
								Flow Quality		Void Fraction		Pressure Drops		
	Pressure PE-302 (MPa)	Steam Flow $\dot{m}_{G\text{-}TS}$ (kg/s)	Liquid Flow $\dot{m}_{L\text{-}TS}$ (kg/s)	Liquid Level (cm)	Steam Flow $\dot{m}_{GB}$ (kg/s)	Total Flow $\dot{m}_{TB}$ (kg/s)	Catch Tank Flow $\dot{m}_{CT}$ (kg/s)	Entrance X_B	Break X_{OR}	Entrance α_B	Break α_{OR}	Entrance PDE-341 (kPa)	Break PDE-450 (MPa)	Data Averaging Time Period (sec)
TEE-VD-NMU-90B	3.45	0.35	1.92	21.4	0.0	5.58	5.43	0.0	1.2E-3	0.02	0.08	58.5	2.34	120-180
	3.45	0.35	1.92	8.1	0.0	3.22	3.92	0.0	1.1E-3	0.21	0.06	45.9	2.61	270-330
TEE-VD-NMU-44	3.44	1.59	6.06	8.0	0.16	3.57	3.69	0.044	0.044	0.36	0.15	45.6	2.62	200-260
TEE-VD-NMU-39	3.45	1.60	1.58	7.9	0.07	3.48	3.58	0.020	0.021	0.27	0.05	46.1	2.65	240-300
TEE-VD-NMU-34	3.47	1.60	1.58	8.0	0.0	3.57	3.64	0.0	1.3E-3	0.25	0.09	45.8	2.65	240-300
TEE-VD-NMU-29	3.47	1.60	6.05	8.7	0.29	3.88	4.29	0.073	0.067	0.22	0.31	46.7	2.55	180-240
TEE-VD-NMU-24	3.47	1.59	1.91	8.0	0.0	3.61	3.66	0.0	1.3E-3	0.24	0.08	45.7	2.65	240-300
TEE-VD-NMU-6 (ML = 6)	3.45	1.65	6.00	9.1	0.0	3.95	4.02	0.0	1.3E-3	0.17	0.18	42.4	2.57	200-260
TEE-VD-NMU-5 (ML = 5)	3.44	1.65	4.87	7.9	0.023	3.65	3.65	0.006	0.008	0.27	—	42.7	2.63	200-260
TEE-VD-NMU-4 (ML = 4)	3.47	1.59	4.04	7.1	0.06	3.13	3.15	0.019	0.020	0.60	0.19	48.0	2.73	200-260
TEE-VD-NMU-3 (ML = 3)	3.44	1.64	3.03	6.7	0.07	2.96	2.96	0.024	0.026	0.74	0.20	53.1	2.73	200-260
TEE-VD-NMU-2 (ML = 2)	3.47	1.64	2.06	6.0	0.14	2.67	2.67	0.052	0.054	0.91	0.27	63.5	2.78	200-260
TEE-VD-NMU-1 (ML = 1)	3.45	1.64	0.98	3.6	0.42	1.52	1.54	0.28	0.028	—[a]	0.42	94.2	2.85	240-300
TEE-VD-NMU-0.5 (ML = 0.5)	3.45	1.64	0.52	2.8	0.65	1.20	1.23	0.54	0.53	—[a]	0.48	106.0	2.86	240-300
TEE-VD-NMU-0.25 (ML = 0.25)	3.46	1.60	0.25	3.9	0.36	1.67	1.69	0.22	0.22	—[a]	0.37	90.0	2.85	200-260

a. Invalid densitometer data.

APPENDIX I

DATA ACQUISITION AND PROCESSING

APPENDIX I

DATA ACQUISITION AND PROCESSING

The acquisition of data and posttest data processing will be discussed in this section.

Data Acquisition System

A schematic of the TPFL Data Acquisition System (DAS) is shown in Figure I-1. The TPFL DAS acquires experimental and operational test data from the two-phase flow loop test assembly. Operational test data is amplified and routed to the MODCOMP Classic Computer for calculations and display on digital panel meters, located in the control room, to provide online display of information necessary for controlling and operating the test loop.

Experimental data is routed concurrently to the Neff 620 Analog Input Subsystem for permanent recording for further data analysis. The input patch panels provide the signal programming capabilities. The narrow band digital, or Neff 620 System, provides the capability for recording up to 256 channels of analog information.

The components shown in Figure I-1 are configured to form a complete digital data acquisition system with data processing, storage, and presentation capabilities. Millivolt signals from the transducers are conditioned by the Neff 620 Series 300 signal conditioners and routed to the input patch panel. This equipment provides both constant voltage and constant current excitation for bridge type transducers. Signals from thermocouples and special signal conditioners are connected directly to the input patch panel.

Signals are patched to the desired channel on the Neff 620 Series 100 analog input subsystem where

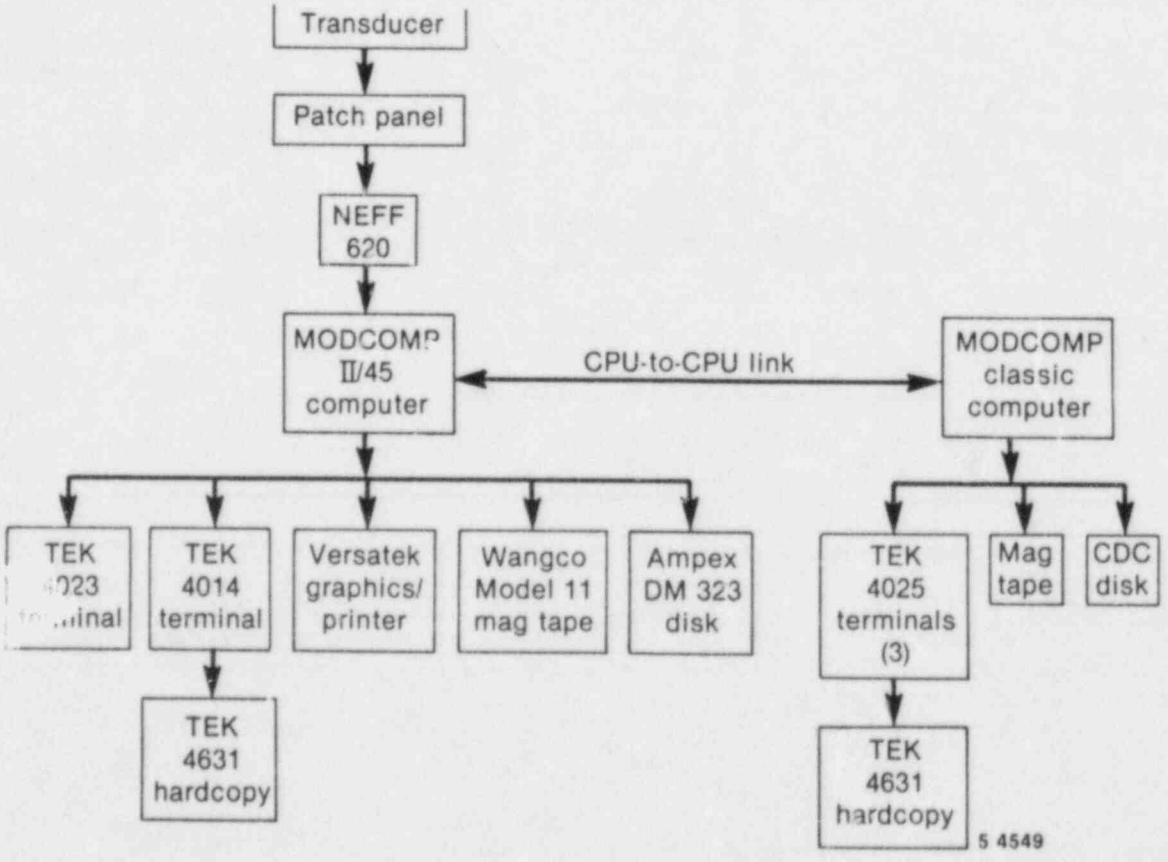

Figure I-1. Schematic of the TPFL data acquisition system.

they are amplified, filtered, time-division multiplexed, and converted from analog to digital information for subsequent storage on magnetic disc or digital tape. The MODCOMP II/45 computer is the control processor for the system and, through program instructions, manipulates and processes incoming data for storage on magnetic disc or digital tape. Program instructions are entered by the operator from the keyboard printer and refreshed CRT terminal. A storage-type CRT terminal is used to make posttest engineering unit versus time data plots of all test data.

Data for the tee/critical flow experiments was acquired at two different sample rates: 5 and 50 samples per s (sps) with two-pole antialiasing Butterworth analog filters, installed at one-fifth the sample frequency. Data acquisition was started 60 s before opening the break valve and continued for 60 s following closure of the break valve and reestablishment of steady-state conditions. Following data acquisition for a test point, data were spooled from disc to tape from transport to the Cyber computer system for subsequent processing.

Data Processing-Calculated Parameters

Following completion of testing, the data was transported and installed on the Cyber system. A schematic of the data processing on the Cyber system is shown in Figure I-2. The first step in processing was to convert the data from a MODCOMP integer format into Cyber floating point values which were then converted into SI units. The data were then filtered using a digital low pass finite impulse response (FIR) filter,[15] with a stop frequency of 0.125 Hz,[a] and the 50 sps data was decimated by 10, resulting in all channels of data having a uniform data rate of 5 Hz.[16] This data was used for calculation of various parameters of interest and were then plotted for inclusion in this report. Steady-state portions of the test points were averaged for data summaries.

The following sections present the calculated parameters and methods by which they were calculated.

Inlet Steam Mass Flow Rate. The reference inlet steam mass flow rate is measured using a calibrated orifice meter tube (3 in. schedule 80) with dual range differential pressure measurements across the orifice. The mass flow rate is calculated from

$$\dot{m}_{GI} = C_I Y \sqrt{\rho_G * DP} \qquad (I\text{-}1)$$

where

$\dot{m}_{GI}$ = the inlet steam flow rate (kg/s)

C_I = the orifice calibration coefficient (equal to 0.0797)

ρ_G = the steam phase density obtained from the pressure and saturated steam tables (kg/m^3)

DP = the measured differential pressure selected from the appropriate range transducer (kPa)

Y = the orifice compressibility[17] coefficient (nondimensional)

$= 1 - 0.402 \times 10^{-3}\ DP/P$

P = the measured pressure upstream of the orifice (MPa).

a. An exception to this procedure was the differential pressure data from mainline to branchline, which was filtered at 2.5 Hz to maintain pressure fluctuation information. This information is useful in identifying the onset of entrainment/pull-through.

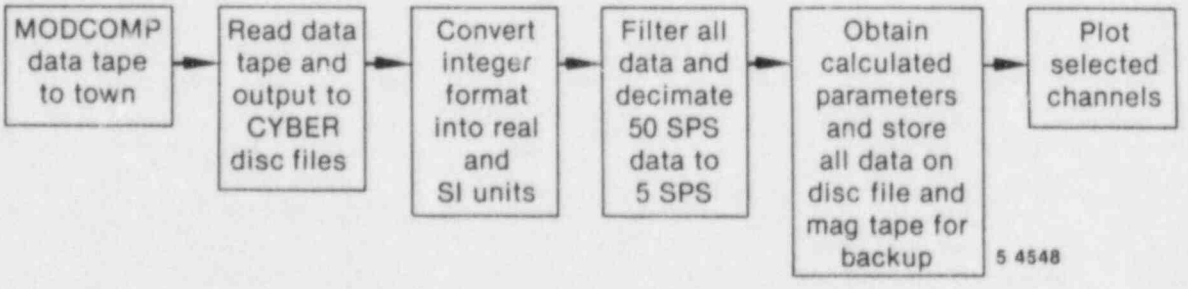

Figure I-2. Schematic of the data processing on the Cyber system.

Discharge Steam Mass Flow Rate. The mass flow rate of the steam discharged from the top of the steam separator is measured using a noncalibrated orifice[a] in the 10 in. schedule 80 discharge line, with dual range differential pressure transducers across the orifice. The mass flow is calculated from

$$\dot{m}_{GD} = C_D Y \sqrt{\rho_G * DP} \qquad (I\text{-}2)$$

where

$\dot{m}_{GD}$ = the discharge steam mass flow rate (kg/s)

C_D = the orifice calibration coefficient calculated from the A.G.A. calculation method[17] (equal to 0.0648)

Y = the orifice compressibility coefficient (nondimensional)

= $1 - 0.316 \times 10^{-3}$ DP/P.

Inlet Liquid Mass Flow Rate. The mass flow rate of the liquid into the mixing section is measured using an orifice with dual range differential pressure transducers across the orifice. The mass flow rate is calculated from

$$\dot{m}_{LI} = C_L \sqrt{\rho_L * DP} \qquad (I\text{-}3)$$

where

$\dot{m}_{LI}$ = the liquid mass flow rate (kg/s)

C_L = the orifice coefficient, obtained from liquid calibration data (equal to 0.02288)

ρ_L = the liquid density obtained from the subcooled tables using the measured temperature and pressure upstream of the orifice (kg/m^3).

Mainline Test Section Parameters. There are a number of parameters obtained for the mainline test section (the 14 in. schedule 160 pipe just upstream of the branchline entrance). These parameters include the phase densities, enthalpies, and mass flow rates. The phase densities ($\rho_{g\text{-}TS}$ and $\rho_{f\text{-}TS}$) and the steam enthalpy ($h_{g\text{-}TS}$) are obtained from the saturated steam tables using the test section pressure (PE-302). The liquid enthalpy ($h_{f\text{-}TS}$) is obtained from the subcooled steam tables using the test section pressure (PE-302) and the bottom fluid temperature measurement in the test section (TE-305). The phase mass flow rates are obtained by correcting the measured inlet flow rates for condensation effects resulting from mixing steam and water. These mass flow rates are given by

$$\dot{m}_{G\text{-}TS} = \frac{\dot{m}_{GI}(h_{gI} - h_{f\text{-}TS}) + \dot{m}_{LI}(h_{fI} - h_{f\text{-}TS})}{(h_{g\text{-}TS} - h_{f\text{-}TS})} \qquad (I\text{-}4)$$

$$\dot{m}_{L\text{-}TS} = \dot{m}_{GI} - \dot{m}_{G\text{-}TS} + \dot{m}_{LI} \qquad (I\text{-}5)$$

where

$\dot{m}_{G\text{-}TS}$ = the steam mass flow rate in the mainline test section (kg/s)

$\dot{m}_{L\text{-}TS}$ = the liquid mass flow rate in the mainline test section (kg/s)

h_{gI}, h_{fI} = the phasic enthalpies at the individual inlet measurements (J/kg).

$h_{g\text{-}TS}$, $h_{f\text{-}TS}$ = the phasic enthalpies at the mainline test section (J/kg)

The stratified liquid level in the mainline was measured two ways. The first measurement used a differential pressure transducer plumbed from top to bottom of the pipe which resulted in a direct measure of liquid level. However, voiding in the sense lines resulted in drift during a test day. The second measurement, and preferred method, was use of a six-beam gamma densitometer.[18] Each beam voltage reading was converted to a chordal average density using

$$\rho_i = \rho_g + (\rho_f - \rho_g)\frac{\ln(V_i/V_{Gi})}{\ln(V_{Li}/V_{Gi})} \qquad (I\text{-}6)$$

a. Construction of the steam separator and discharge line does not permit calibration of the measurement. In place of calibration, checks of measurement accuracy were performed using the calibrated inlet steam flow measurement, and were found to be within the combined measurement uncertainty (see tables of initial conditions).

where

ρ_i = the i^{th} beam chordal average density (kg/m^3)

V_i = The i^{th} beam voltage reading (volts)

V_{Li}, V_{Gi} = the all liquid and all steam calibration voltages for beam i (volts)

ρ_f, ρ_g = the liquid and steam phase densities at calibration conditions (kg/m^3).

The resulting six density readings were used as input to a program[19] which calculated the stratified liquid level in the mainline.

Catch Tank Parameters. The catch tank measurement system has been previously described. The primary parameter of interest from the catch tank is the total two-phase mass flow rate through the branchline and the critical flow nozzle. A secondary parameter of interest is a calculation of the break flow quality obtained from a thermodynamic balance of the catch tank.

The mass flow rate into the catch tank is obtained by differentiating the total fluid weight obtained from the load cells.[a]

The differentiation routine used performed a sliding linear least squares fit to the data over a 301 data point window. Since the data sample rate was 5 samples per s, the resulting differentiation was over a sliding 60 s time frame centered on each data point. (To start the differentiation routine, the first data point was used as the first 151 data points.)

The thermodynamic balance to obtain break flow quality used the mass flow rate (described previously) and the fluid enthalpy obtained from the fluid temperature measured in the catch tank. The flow obtained thus is given by[b]

$$X_{CT} = \frac{(h_{f\text{-}CT}) - (h_{f\text{-}OR}) + \left(\frac{dh_{f\text{-}CT}}{dt}\right)\left(\frac{\dot{m}_{CT}}{M_{CT}}\right)}{(h_{g\text{-}OR}) - (h_{f\text{-}OR})} \qquad (I\text{-}7)$$

where

X_{CT} = the flow quality obtained from the catch tank (nondimensional)

$h_{f\text{-}CT}$ = the liquid enthalpy, in the catch tank (J/kg)

$h_{f\text{-}OR}$, $h_{g\text{-}OR}$ = the phasic enthalpies just upstream of the break orifice (critical flow nozzle) in the branchline (J/kg)

$\frac{dh_{f\text{-}CT}}{dt}$ = the differential of the liquid enthalpy in the catch tank (J/kg-s)

M_{CT} = the total liquid mass in the catch tank (kg)

$\dot{m}_{CT}$ = the mass flow rate into the catch tank (kg/s).

Branchline Parameters. Parameters for the 1-1/2 in. schedule 160 branchline are calculated for two locations: the entrance using the mainline conditions and just upstream of the break orifice using the measured pressure and density at that location.

At the entrance to the branchline the individual phase mass flow rates are obtained from system mass and energy balances. The steam flow rate into the branch is obtained from the difference in the steam flow rates upsteam of the branch and discharged from the steam separator, with storage in the separator accounted for; thus

$$\dot{m}_{GB} = \dot{m}_{G\text{-}TS} - \dot{m}_{GD} - \rho_{g\text{-}TS} A_{ss} \frac{dL}{dt} \qquad (I\text{-}8)$$

---

a. For the horizontal configuration testing, the east end load cell had a short in the electronics which invalidated the data for that cell. Using the west end load cell (LD-LC-1), in conjunction with cold fill liquid calibration data, the total catch tank fluid weight was obtained by multiplying the west end load cell data by 2.06.

For the vertical downflow configuration, the load cell problems were corrected and total weight was obtained by summing the data from the two load cells.

b. This derivation assumes negligible time response between the flow through the orifice and arrival at the catch tank.

where

$\dot{m}_{GB}$ = the branchline steam flow rate (kg/s)

$\dot{m}_{G\text{-}TS}$ = the mainline test section steam flow rate (kg/s)

$\dot{m}_{GD}$ = the steam separator discharge flow rate (kg/s)

A_{ss} = the cross sectional area of the steam separator tank (equal to 1.916 m^2)

$\frac{dL}{dt}$ = the rate of change of the steam separator level obtained from differentiating the liquid level measurement (m/s).

The liquid mass flow rate into the branchline is obtained from a system mass balance utilizing the steam separator tank liquid level and the mainline void fraction obtained from the 6-beam densitometer. This mass flow rate is calculated from

$$\dot{m}_{LB} = \rho_{f\text{-}TS} A_{ss} \frac{dL}{dt} + L_{TS} A_{TS} \frac{d\alpha_L}{dt} \qquad \text{(I-9)}$$

where

$\dot{m}_{LB}$ = the liquid mass flow rate into the branchline (kg/s)

L_{TS} = the length of the mainline from the mixing tee into the steam separator (equal to 8.5 m)

A_{TS} = the mainline flow area (equal to 0.0633 m^2)

$\frac{d\alpha_L}{dt}$ = the rate of change of the mainline liquid area fraction (s^{-1}).

The steam mass flow rate into the branch is adjusted to account for evaporation due to pressure drop from the mainline to upstream of the break orifice. This is accomplished using

$$\dot{m}_{G\text{-}OR} = \frac{\dot{m}_{GB}(h_{g\text{-}TS} - h_{f\text{-}OR}) + \dot{m}_{LB}(h_{f\text{-}TS} - h_{f\text{-}OR})}{h_{fg\text{-}OR}} \qquad \text{(I-10)}$$

where

$\dot{m}_{G\text{-}OR}$ = the steam flow rate upstream of the orifice (kg/s)

$h_{f\text{-}OR}$, $h_{fg\text{-}OR}$ = the liquid enthalpy and heat of vaporization upstream of the orifice (J/kg).

This adjustment is a small fraction of the branch steam flow rate.

Two different branchline flow qualities are calculated: one at the entrance to the branchline and one just upstream of the orifice. The major difference is in the total mass flow rate used in the calculation. The entrance flow quality, X_B, uses the sum of steam and liquid flows from a system mass balance, whereas the orifice flow quality, X_{OR}, uses the total mass flow obtained from the catch tank. These flow qualities are given by

$$X_B = \frac{\dot{m}_{GB}}{\dot{m}_{GB} + \dot{m}_{LB}} . \qquad \text{(I-11)}$$

$$X_{OR} = \frac{\dot{m}_{G\text{-}OR}}{\dot{m}_{CT}} . \qquad \text{(I-12)}$$

The branchline had two densitometers mounted on the pipe, one (a 2-beam densitometer) about 10 diameters downstream of the branchline entrance, and the second (a single diametrical vertical beam) mounted about 5 diameters upstream of the orifice. The individual beams were converted into chordal densities using Equation (I-6). These densities were then used to calculate the void fractions at these locations. The two-beam data were used as input to a densitometer fitting routine[19] which output an area averaged density. Investigation of the routine revealed that the fit always defaulted to a homogeneous density. Therefore, the void fractions can be written as

$$\alpha_B = \frac{\rho_f - \frac{1}{2}(\rho_{3A} + \rho_{3B})}{\rho_f - \rho_g} \qquad \text{(I-13)}$$

$$\alpha_{OR} = \frac{\rho_f - \rho_1}{\rho_f - \rho_g} \qquad \text{(I-14)}$$

where

α_B = the void fraction at the 2-beam branchline densitometer (nondimensional)

α_{OR} = the line average void fraction from the single-beam branchline densitometer (nondimensional)

ρ_{3A}, ρ_{3B} = the individual density readings from the two-beam densitometer, channel ID's DE-3A and DE-3B (kg/m^3)

ρ_1 = the single-beam density reading, channel ID DE-1-1 (kg/m^3)

ρ_f, ρ_g = the phase densities in the branchline (kg/m^3).

APPENDIX J

MEASUREMENTS UNCERTAINTIES

APPENDIX J

MEASUREMENTS UNCERTAINTIES

Usefulness of data is a direct function of how accurate the data is and how well that accuracy (or inversely the uncertainty) is known. In this section, the uncertainties for the basic measurements (temperatures, pressures, differential pressures, and load cells) are presented. These uncertainties are obtained from a series of uncertainty documents generated by the WRRTP (References 20, 21, 22, 23) primarily to document uncertainties for the Semiscale program. The International Standards Organization's (ISO) draft standard, "Fluid Flow Measurement Uncertainty" (ISO TC30 SC 9), is the basis of the method used in the WRRTP documents to determine uncertainties. In addition to the basic measurement uncertainties, the uncertainties in all calculated parameters (such as mass flow rates calculated from an orifice) are presented. The method used for combining individual uncertainties for calculated parameters is the root-sum-square (RSS) method, originally proposed by Kline and McClintock.[24] All quoted uncertainties are at the 95% confidence level. Derivation of these uncertainties is presented in the following sections.

Basic Measurement Uncertainties

The basic measurements are considered to be temperatures, pressures, differential pressures (DPs) and load cells. Quoted uncertainties are from the transducer through the data system and include all uncertainties introduced by the transducer calibration, signal conditioning, and the data system. A summary of the basic uncertainties is provided in Table J-1. The measurement uncertainty in the fluid temperatures (using Type K thermocouples) is considered to be ± 2.2 K.[21]

Uncertainties in the pressure and differential pressure measurements are quoted[22] in terms of percent of full scale. For the absolute pressure

Table J-1. Summary of uncertainties in basic measurements

Measurement Type	Range	Uncertainty (at 95% Confidence Level)
Fluid temperatures	300-585 K	2.2 K
Absolute pressures	0-6.9 MPa	0.02 MPa
Differential pressures	0-12.5 kPa	0.07 kPa
Differential pressures	0-24.8 kPa	0.14 kPa
Differential pressures	0-124.4 kPa	0.71 kPa
Differential pressures	0-172.4 kPa	0.98 kPa
Differential pressures	0-199 kPa	1.1 kPa
Differential pressures	0-6.89 MPa	0.039 MPa
Load cells	0-5000 kg	11 kg
Liquid levels	0-77 cm 0-743 cm	3 cm 15 cm

transducer this value is 0.29% of full scale. For DP measurements this value is 0.57% of full scale and does not include the possible effects of a partially voided sense line, which was assumed corrected prior to the test point or posttest, using the no flow data averages. For the load cell measurements, the quoted[23] uncertainty is 0.24% of full scale.

Uncertainties in Calculated Parameters

Calculated parameters are those parameters that have their basis in one or more basic measurements. Examples are thermodynamic properties (phase densities and enthalpies) and mass flow rates calculated from the measurements at an orifice. The method used in the root-sum-square method is given by

$$\Delta R = \left[\sum_{i=1}^{N}\left(\frac{\partial R}{\partial V_i}\,\Delta V_i\right)^2\right]^{1/2} \qquad \text{(J-1)}$$

where

R = the calculated result

V_i = i^{th} independent variable

ΔR, ΔVi = absolute uncertainty in the result and the independent i^{th} variable, respectively.

This method was applied to each of the calculated parameters in the following sections. A summary of the uncertainties in the calculated parameters is provided in Table J-2.

Thermodynamic Properties. The thermodynamic properties of the individual phases are obtained from a set of computer steam tables. The properties are determined by using the measured temperature and pressure for subcooled liquid (the liquid inlet flow measurement) and the pressure for saturated locations (inlet steam flow and test section, mainline and branchline fluid properties). Since a simple equation for these properties is not readily available, Equation (J-1) cannot be used. Instead, the uncertainties in the temperatures and pressures were used to give the maximum deviation in the thermodynamic properties. This should result in a confidence level greater than 95%. Results of this procedure are given in Table J-3.

Mass Flow Rate from Orifices. The mass flow rate using an orifice is calculated from

$$\dot{m} = C\,Y\sqrt{\rho * DP} \qquad \text{(J-2)}$$

where

C = the orifice calibration coefficient obtained from liquid calibration data (for the TPFL test facility)

Y = the orifice compressibility factor for gas flow (equal to 1 for liquid)

ρ = the phase density upstream of the orifice

DP = the differential pressure across the orifice.

The calculated parameter uncertainty equation, Equation (J-1), can be applied to Equation (J-2) resulting in

$$\frac{\Delta\dot{m}}{\dot{m}} = \left[\left(\frac{\Delta C}{C}\right)^2 + \left(\frac{\Delta Y}{Y}\right)^2 + \frac{1}{4}\left(\frac{\Delta\rho}{\rho}\right)^2 + \frac{1}{4}\left(\frac{\Delta DP}{DP}\right)^2\right]^{1/2} \qquad \text{(J-3)}$$

where the Δ's indicate the absolute uncertainty in each of the individual uncertainty components. The uncertainty values presented in Table J-2 were obtained by using the uncertainty values given in Tables J-1 and J-3 and using an uncertainty in the orifice calibration coefficient of 1% for calibrated orifices and 2% for uncalibrated orifices.[a]

Catch Tank Parameters. The purpose of the catch tank was to collect the two-phase mixture from the simulated break (branchline), condense the steam, and weigh the total discharge. The catch tank was suspended from two load cells and was open to the atmosphere. A 5-thermocouple rake was mounted in the tank to provide a vertical temperature profile. From this data, it was determined that the fluid temperature in the liquid was uniform due to extremely good thermal mixing. Therefore, the centerline thermocouple was used to obtain the subcooled liquid enthalpy.

a. This is an estimate of the uncertainties based upon experience.

Table J-2. Summary of uncertainties for calculated parameters

Identification	Description	Nominal Uncertainty
MDOT-LIQ, INLET	Inlet liquid flow rate	0.07 kg/s
MDOT-STM, INLET	Inlet steam flow rate	0.047 kg/s
MDOT-LIQ-T/S	Mainline liquid flow rate	0.07 kg/s
MDOT-STM-T/S	Mainline steam flow rate	0.05 kg/s
MDOT-STM-BRANCH	Branchline steam flow rate	0.08 kg/s
MDOT-TOT-BRANCH	Branchline total flow rate from mass balance	0.33 kg/s
MDOT-CT	Branchline total flow rate from catch tank	0.36 kg/s
MDOT-STM, DISCH	Exhaust steam flow rate	0.06 kg/s
STRAT LIQ HT-T/S	Mainline stratified liquid height	1.2 cm
VOID-BRANCH	Branchline void fraction-entrance	0.26
VOID-BREAK	Branchline void fraction-upstream of break orifice	0.26
BRANCH FLOW QUAL	Branchline flow quality at entrance-from system mass balance	0.10
BREAK FLOW QUAL	Flow quality upstream of critical flow nozzle from catch tank flow rate and steam flow rates	0.10
CT-FLOW QUAL	Branchline flow quality from thermodynamic balance of the catch tank	0.33

Table J-3. Uncertainties in thermodynamic properties

$\Delta\rho_g$	=	± 0.1 kg/m^3
$\Delta\rho_f$	=	± 0.4 kg/m^3 (saturation)
	=	± 4.0 kg/m^3 (subcooled)
Δh_g	=	± 0.0003 J/kg
Δh_f	=	± 0.004 J/kg
ΔT_{sat}	=	± 0.3 K

The two parameters of interest from the catch tank are the mass flow rate into the catch tank from the branchline and the flow quality in the branchline upstream of the critical flow nozzle. The mass flow rate is obtained by differentiating the sum of the load cells data and the flow quality is obtained from a thermodynamic balance on the fluid in the catch tank.

The method for calculating the uncertainty in the mass flow rate is not covered in the WRRTF uncertainty documents, nor is the method to obtain it obvious. As such, it was decided to specify the uncertainty to be the uncertainty in the sum of the load cell data divided by the averaging time period

of the least squares differentiation routine. The routine performed a sliding linear least square fit over 301 data points. Using this number of data points and the sample rate (5 samples per second), the averaging time period is 60 s. The uncertainty for the sum of the load cells[23] is 0.24% of full scale, or 21.8 kg. This results in an uncertainty in the catch tank mass flow rate of

$$\Delta \dot{m}_{CT} = \frac{21.8\ kg}{60\ s} = 0.36\ kg/s \quad .$$

Another possible way of estimating the uncertainty is to compare the calculated mass flow rate into the catch tank (the branchline flow rate) with the single-phase branchline steam flow rate calculated from the difference of the inlet and exit steam flow rates for an all steam test point. This method results in an uncertainty of 0.20 kg/s.

The flow quality upstream of the critical flow nozzle, based upon the catch tank thermodynamic balance, is given by Equation (I-7). Applying Equation (J-1) to Equation (14) results in an uncertainty in the flow quality of

$$\Delta X_{CT} = \left[\left(\frac{\Delta \dot{h}_{f\text{-}CT}}{h_{fg\text{-}OR}} \frac{M_{CT}}{\dot{m}_{CT}}\right)^2 + \left(\frac{\dot{h}_{f\text{-}CT}}{h_{fg\text{-}OR}} \frac{M_{CT}}{\dot{m}_{CT}} \frac{\Delta \dot{m}_{CT}}{\dot{m}_{CT}}\right)^2 + \left(\frac{\Delta h_{f\text{-}CT}}{h_{fg\text{-}OR}}\right)^2 + \left(\frac{\Delta h_{f\text{-}OR}}{h_{fg\text{-}OR}}\right)^2 + \left(\frac{\Delta h_{fg\text{-}OR}}{h_{fg\text{-}OR}} X\right)^2 + \left(\frac{\dot{h}_{f\text{-}CT}}{h_{fg\text{-}OR}} \frac{\Delta M_{CT}}{\dot{m}_{CT}}\right)^2\right]^{1/2} \qquad (J\text{-}4)$$

where the first two terms are the only significant contributions to the uncertainty. The rate of change of the catch tank liquid enthalpy, $h_{f\text{-}CT}$, is obtained by the same differentiation process as the catch tank mass flow rate. Using the same logic for the uncertainty results in a value of ±155 J/kg-s for $\Delta h_{f\text{-}CT}$, where the major uncertainty contribution is from the uncertainty in the fluid temperature (±2.2 K).

Evaluating Equation (J-4) for two test cases results in $\Delta X_{CT} = \pm 0.51$ for $X_{CT} = 1$ and $\Delta X_{CT} = \pm 0.15$ for $X_{CT} = 0.1$. For the purposes of reporting a single value, the average of the two extremes (0.33) will be used.

Branchline Parameters. The calculated parameters for the branchline are steam and liquid flow rates, void fractions, and flow qualities. The uncertainties for these parameters are discussed next.

Branchline Steam Flow. Branchline steam flow is calculated using Equation (I-8). Applying the uncertainty Equation (J-1) to this equation results in

$$\Delta \dot{m}_{GB} = \left[\left(\Delta \dot{m}_{G\text{-}TS}\right)^2 + \left(\Delta \dot{m}_{GD}\right)^2 + \left(\Delta \dot{m}_{GS}\right)^2\right]^{1/2} \qquad (J\text{-}5)$$

where the steam storage term, $\Delta \dot{m}_{GS}$, is given by

$$\Delta \dot{m}_{GS} = \left[\left(\frac{\Delta \rho_{g\text{-}TS}}{\rho_{g\text{-}TS}}\right)^2 + \left(\frac{\Delta A_{ss}}{A_{ss}}\right)^2 + \left(\frac{\Delta \dot{L}}{\dot{L}}\right)^2\right]^{1/2} \dot{m}_{GS} \quad . \qquad (J\text{-}6)$$

Evaluating $\Delta \dot{m}_{GS}$ for the maximum observed rate of level change at 6.2 MPa of $\dot{L} = 0.4$ cm/s ($\Delta \dot{L} = 0.17$ cm/s, $\Delta A/A = 0.0005$, $\Delta \rho / \rho = 0.003$) results in a value for $\Delta \dot{m}_{GS}$ of ±0.004 kg/s. Using this value, and results from Table J-2, in Equation (J-5) gives an uncertainty in the branchline steam flow rate of ±0.079 kg/s.

The entrance branchline steam flow is adjusted for phase change due to the pressure drop from the mainline to the orifice using Equation (I-10) to obtain the orifice steam flow rate. Applying Equation (J-1) to Equation (I-10) gives

$$\Delta \dot{m}_{G\text{-}OR} = \left[\left(\frac{h_{g\text{-}TS} - h_{f\text{-}OR}}{h_{fg\text{-}OR}} \Delta \dot{m}_{GB}\right)^2\right.$$

$$+\left(\frac{h_{f\text{-}TS} - h_{f\text{-}OR}}{h_{fg\text{-}OR}}\,\Delta\dot{m}_{LB}\right)^2\Bigg]^{1/2} \qquad \text{(J-7)}$$

where the insignificant terms due to uncertainties in the phasic enthalpies have been dropped. Evaluation of Equation (J-7) for a typical case ($\Delta\dot{m}_{LB}$ is evaluated in the next section) results in $\Delta\dot{m}_{G\text{-}OR}$ = 0.079 kg/s, where almost the entire uncertainty is from the uncertainty in branchline steam flow rate.

Branchline Liquid Flow. Branchline liquid flow is calculated from a system mass balance, Equation (I-9), utilizing the test section and separator tank level changes. Applying the uncertainty equation, Equation (J-1), to Equation (I-10) gives the uncertainty in the liquid flow into the branch as

$$\Delta\dot{m}_{LB} = \Big[(\rho_{f\text{-}TS}\, A_{ss}\, \Delta\dot{L})^2 + (\rho_{f\text{-}TS}\, A_{TS}\, \Delta\alpha_{TS})^2\Big]^{1/2} \qquad \text{(J-8)}$$

where the terms due to uncertainties in phase density, areas and lengths (insignificant contributions to the total uncertainty), have been disregarded. Using the same logic for the rate of change of mainline void fraction as for the catch tank mass flow rate (see section on mainline parameters for $\Delta\dot{\alpha}_{TS}$), $\Delta\dot{\alpha}_{TS}$ = 0.00052 . Evaluating Equation (J-8) for a typical data point results in $\Delta\dot{m}_{LB}$ = 0.32 kg/s, where the two uncertainties provide nearly equal contributions.

Branchline Void Fractions. Branchline void fractions are obtained from reduction of the data from the two branchline densitometers as described in Section I. The uncertainty in densitometer readings has not been covered in the WRRTP uncertainty documents. The uncertainties for these measurements are derived below.

For the purpose of the uncertainty analysis, the void fraction can be obtained from Equation (I-6) (assuming that the densitometer was calibrated at hot conditions) as

$$\alpha = \frac{\ln (V_i/V_G)}{\ln (V_L/V_G)} \,. \qquad \text{(J-9)}$$

Applying Equation (J-1) results in

$$\Delta\alpha = \left\{\left(\frac{\Delta V}{V}\right)^2 + \left[(1\text{-}\alpha)\,\frac{\Delta V_F}{V_F}\right]^2 + \left(\alpha\,\frac{\Delta V_G}{V_G}\right)^2\right\}^{1/2} . \qquad \text{(J-10)}$$

This equation results in a nonconstant, nonlinear uncertainty for a single-beam over the void fraction range. However, using a linear uncertainty provides a conservative estimate of the uncertainty and is the method that will be used. First, however, the uncertainty in the individual voltages must be obtained. There are two principle contributions to the uncertainty in the voltage: the data system (including the signal conditioning electronics) and the statistical functions due to the radiation source. The Semiscale uncertainty documents state that the uncertainty due to the data system is 0.22% of full scale. The uncertainty due to the statistical function is a function of the count rate and the standard deviation (or time constant) of the densitometer ratemeter. The ratemeter manual states that the count rate standard deviation (with the meter switch set at, 1%) is given by

$$\sigma_{CR} = [0.01 * (FS * CR)]^{1/2} \,.$$

The uncertainty in the voltage reading (at 95% level) can therefore be given as

$$\frac{\Delta V}{V} = 0.02\left(\frac{10}{V}\right)^{1/2} + 0.0022\,\frac{10}{V} \,. \qquad \text{(J-11)}$$

Equation (J-10) can be reduced, for the two end points, to

$$\Delta\alpha_G = \frac{\sqrt{2}}{\ln (V_L/V_G)}\,\frac{\Delta V_G}{V_G} \,. \qquad \text{(J-12a)}$$

$$\Delta\alpha_L = \frac{\sqrt{2}}{\ln (V_L/V_G)}\,\frac{\Delta V_L}{V_L} \,. \qquad \text{(J-12b)}$$

Equation (J-12) has been evaluated for typical calibration voltage readings in Table J-4.

Branchline Flow Qualities. Branchline flow qualities are obtained from Equations (I-11) and (I-12).

Table J-4. Uncertainties in void fractions obtained from densitometers

Densitometer Channel ID	Location	Typical Calibration Coefficients		Uncertainties		
		Steam (volts)	Liquid (volts)	$\alpha = 1$	$\alpha = 0$	$\alpha = 1/2$
DE-1-1	Branchline-orifice	4.19	3.41	0.25	0.28	0.26
DE-3A	Branchline—	9.70	8.70	0.29	0.31	0.30
DE-3B	Entrance	9.52	8.10	0.20	0.22	0.21
DE-1A	Mainline—	9.35	1.86	0.02	0.05	0.04
DE-1B	Upstream of	9.57	1.65	0.02	0.05	0.03
DE-1C	branch	9.80	3.31	0.03	0.05	0.04
DE-2A		9.90	2.06	0.02	0.05	0.03
DE-2B		9.67	1.64	0.02	0.05	0.03
DE-2C		9.74	3.18	0.03	0.05	0.04

Applying Equation (J-1) to these equations gives the uncertainties as

$$\Delta X_B = \left(2 * \Delta \dot{m}_{GB}^2 + \Delta \dot{m}_{LB}^2\right)^{\frac{1}{2}} + (\dot{m}_{GB} + \dot{m}_{LB}) \quad . \tag{J-13}$$

$$\Delta X_{OR} = \left(\Delta \dot{m}_{G\text{-}OR}^2 + \Delta \dot{m}_{CT}^2\right)^{\frac{1}{2}} + (\dot{m}_{CT}) \quad . \tag{J-14}$$

Evaluating these expressions, using the previously obtained uncertainties, results in

$\Delta X_B = 0.19$ @$X_B = 1$

$\Delta X_B = 0.10$ @$X_B = 0.1$

$\Delta X_{OR} = 0.23$ @$X_{OR} = 1.0$

$\Delta X_{OR} = 0.16$ @$X_{OR} = 0.1$.

The uncertainty values at a flow quality of one are unreasonable due to inclusion of the liquid flow uncertainty. Therefore, for the purpose of reporting a single uncertainty, the average of the two values is used.

Mainline Parameters. The calculated parameters of interest for the mainline are phasic mass flow rates, densities from the densitometers, and the stratified liquid level obtained from the mainline 6-beam densitometer. Since the mainline phasic mass flow rates are obtained from the inlet flow rates corrected for mixing effects, and uncertainties due to accounting for mixing effects are insignificant, the uncertainties in the mainline phasic mass flow rates are the same as the uncertainties for the inlet flow rates.

The uncertainty in the stratified liquid level from the 6-beam densitometer is a function of the uncertainty of the individual beam densities. These uncertainties were calculated as given in the Branchline Liquid Flow Section in this appendix and are listed in Table J-4. A least squares fit to the data is used to obtain the stratified liquid level from the 6-beam readings. A conservative estimate of the uncertainty in the stratified liquid level, based upon the two diametrical densitometer beams which have major weights in the fit, is ± 1.2 cm.

Using this same logic for the mainline void fraction, the uncertainty is 0.03. The rate of change of the mainline void fraction is used in the storage terms of the system mass balance and is obtained from differentiating the mainline void fraction. Using the same procedure as previously used with differentiated parameters, the uncertainty is given as $\Delta\dot{\alpha}_{TS} = 0.03/60\ s = 0.00052\ S^{-1}$.

NRC FORM 335 (2-84) NRCM 1102, 3201, 3202

U.S. NUCLEAR REGULATORY COMMISSION

BIBLIOGRAPHIC DATA SHEET

SEE INSTRUCTIONS ON THE REVERSE

1. REPORT NUMBER (Assigned by TIDC, add Vol. No., if any)
NUREG/CR-4164
EGG-2377

2. TITLE AND SUBTITLE
DATA REPORT FOR THE TPFL TEE/CRITICAL FLOW EXPERIMENTS

3. LEAVE BLANK

4. DATE REPORT COMPLETED
MONTH: November YEAR: 1985

5. AUTHOR(S)
James L. Anderson and William A. Owca

6. DATE REPORT ISSUED
MONTH: November YEAR: 1985

7. PERFORMING ORGANIZATION NAME AND MAILING ADDRESS (Include Zip Code)
EG&G Idaho, Inc.
P.O. Box 1625
Idaho Falls, Idaho 83415

8. PROJECT/TASK/WORK UNIT NUMBER

9. FIN OR GRANT NUMBER
FIN No. A6320

10. SPONSORING ORGANIZATION NAME AND MAILING ADDRESS (Include Zip Code)
U.S. Nuclear Regulatory Commission
Division of Accident Evaluation
Office of Nuclear Regulatory Research
Washington, D.C. 20555

11a. TYPE OF REPORT
Formal

b. PERIOD COVERED (Inclusive dates)

12. SUPPLEMENTARY NOTES

13. ABSTRACT (200 words or less)

A series of experiments have been performed investigating the phenomena of liquid entrainment and vapor pull-through at a tee junction between a horizontal pipe and a small branchline. These experiments were performed under conditions of stratified steam-water flow at 3.4, 4.4, and 6.2 MPa in the 28.4 cm diameter mainline, and critical flow through a nozzle installed in the branchline. Two orientations of the branchline were investigated: horizontal and vertical downflow. This report documents the experimental program, presents the data obtained, and discusses correlations for predicting the levels at which the onset of vapor pull-through and liquid entrainment occur and correlations for predicting the flow quality into the branchline.

14. DOCUMENT ANALYSIS a. KEYWORDS/DESCRIPTORS

b. IDENTIFIERS/OPEN ENDED TERMS

15. AVAILABILITY STATEMENT
Unlimited

16. SECURITY CLASSIFICATION
(This page) Unclassified
(This report) Unclassified

17. NUMBER OF PAGES

18. PRICE

EG&G Idaho
P.O. Box 1625
Idaho Falls, Idaho
83415